Placental Vascular Development in Pregnancies Complicated by Maternal Diabetes

A thesis submitted to The University of Manchester for the degree of
Doctor of Philosophy
in the Faculty of Biology, Medicine and Health

2021

MATINA B. HAKIM
School of Medical Sciences

Table of Contents

LIST OF FIGURES **5**

LIST OF TABLES **8**

LIST OF ABBREVIATIONS **9**

ABSTRACT **11**

DECLARATION **13**

COPYRIGHT STATEMENT **14**

ABOUT THE AUTHOR **15**

ACKNOWLEDGEMENTS **16**

DEDICATION **17**

1 CHAPTER ONE: INTRODUCTION **18**

1.1 OVERVIEW 19
1.1.1 Maternal Diabetes 20
1.1.2 Diabetes Associated Complications: Increased risk of Morbidity and Mortality for Fetus 21
1.1.3 Diabetic Complications and Vascular Development 26
1.2 HUMAN PLACENTA 31
1.2.1 Fetoplacental Vasculature 32
1.2.2 Altered fetoplacental vasculature in pregnancies complicated by diabetes 36
1.2.3 Evidence for abnormal placental microvasculature in diabetes 36
1.3 THE NORMAL DEVELOPMENT OF THE PLACENTA AND PLACENTAL VASCULATURE 46
1.3.1 Placenta Vascular Formation 47
1.3.1.1 Vasculogenesis 48
1.3.1.2 Angiogenesis 49
1.3.2 Regulators of Placental Vasculature development: Angiogenic Growth factors: 52
1.3.2.1 Vascular Endothelial Growth Factor (VEGF) 54
1.3.2.1.1 PIGF 54
1.3.2.1.2 VEGF Receptors 56
1.3.2.2 Fibroblast growth factor family 58
1.3.2.3 Angiopoietin 58
1.3.2.4 PDGF 59
1.3.2.5 TGFB 60
1.3.3 Abnormal angiogenesis in diabetes: regulatory factors 61
1.3.3.1 Altered Angiogenic factors in maternal diabetes and consequences for aberrant fetoplacental vasculature and or vascular dysfunction 64
1.3.3.2 Hyperglycaemia 67
1.3.3.3 Hyperinsulinaemia 71
1.3.3.4 Advanced Glycation End products (AGEs) 73
1.3.3.5 Oxidative Stress 73
1.3.3.6 Inflammation 74
1.3.3.7 Obesity 75
1.4 EARLY PREGNANCY AND THE NEED FOR EARLY INTERVENTION 77
1.5 TREATMENT, CONTROL AND IMPLICATIONS 78
1.5.1 Insulin 79
1.5.2 Metformin 79
1.6 SUMMARY 81
1.7 HYPOTHESIS 83
1.7.1 Aims 83

2 CHAPTER TWO: GENERAL METHODS SECTION **84**

2.1 SUBJECTS 85
2.1.1 Biobank sample recruitment and collection 85
2.1.2 Velocity sample recruitment and collection 85
2.2 DEMOGRAPHIC, CLINICAL AND GROSS PLACENTAL EXAMINATION DETAILS OF SUBJECTS 86
2.3 FETOPLACENTAL VASCULAR CORROSION CASTING 88

2.3.1 Micro CT Image acquisition and processing 90
2.3.2 Image Analysis 91
2.4 IN VITRO MODEL OF ANGIOGENESIS 93
2.4.1 Culture of Human Umbilical Vein Endothelial Cells (HUVECs) to assess effects of glucose, insulin and metformin on angiogenesis in vitro 93
2.4.2 Pilot studies to determine optimum cell plating density, time of cellular network formation and effect of VEGF 93
2.4.3 Imaging of HUVECs to assess cellular network formation 95
2.4.4 Effects of glucose, insulin and metformin on cellular mesh network formation by HUVECs in vitro 96

3 CHAPTER THREE: VASCULAR CORROSION CASTING REVEALS ALTERED PLACENTAL VASCULAR STRUCTURE IN PREGNANCIES COMPLICATED BY MATERNAL DIABETES 97

3.1 BACKGROUND 98
3.2 AIMS 99
3.3 MATERIALS AND METHODS 100
3.4 STATISTICAL ANALYSES 101
3.5 PLACENTAL CASTS DATA PROCESSING 102
3.5.1 Vascular Casts vessel biometry outputs 102
3.5.2 Examination of extent of resin penetration into vessel walls 103
3.5.3 Synthesis of Data Output 107
3.5.4 Mode of Data Presentation 111
3.5.5 Maternal demographics and placental features of samples studied 113
3.6 RESULTS: MEASUREMENTS OF VASCULAR MORPHOLOGY 115
3.6.1 Vessel segments in normal and pregestational diabetes casts presented in both outputs 115
3.6.2 Vessel length alterations observed in pregestational diabetes 121
3.6.3 Decreased vascular volume in casts from pregestational diabetes pregnancies 124
3.6.4 Summary 128
3.7 PLACENTAL VASCULAR DEVELOPMENT ASSOCIATIONS TO MATERNAL GLYCAEMIC CONTROL IN PREGNANCIES COMPLICATED BY PRE-GESTATIONAL DIABETES. 129
3.7.1 Demographic and clinical details of study participants 129
3.7.2 Shorter vessel length observed in poor diabetes control clinical group 132
3.7.3 Vascular volume alterations in both pathological clinical groups of maternal glycaemic control 136
3.7.4 Summary 140
3.8 PLACENTAL VASCULAR DEVELOPMENT ASSOCIATIONS TO MATERNAL (PIGF) LEVELS IN PREGNANCIES COMPLICATED BY PREGESTATIONAL DIABETES. 141
3.8.1 Demographic and clinical details of study participants 143
3.8.2 Vessel length discrepancies in lower PIGF profile group in pregestational diabetes 144
3.8.3 Vascular volume alterations in PIGF profile groups in pregestational diabetes 148
3.8.4 Summary 152
3.9 DISCUSSION 153
3.9.1 Unreported differences were observed in the vasculature of placentas from normal and pregestational diabetes complicated pregnancies. 155
3.9.2 Alterations were observed in the vasculature of placentas from normal and maternal glycaemic control groups in pregestational diabetes complicated pregnancies 155
3.9.3 Discrepancies in vasculature of placentas associated with lower PIGF levels in pregnancies complicated by pregestational diabetes. 158
3.9.4 Strengths and limitations of study 159
3.9.5 Chapter 3 Overall Summary 161

4 CHAPTER FOUR: IN VITRO EXAMINATION OF THE EFFECTS OF HYPERGLYCAEMIA, INSULIN AND METFORMIN ON PLACENTAL ANGIOGENESIS 162

4.1 BACKGROUND 163
4.1.1 Diabetes and Angiogenesis 163
4.1.1.1 Glucose and Angiogenesis 164
4.1.2 Insulin and Angiogenesis 165
4.1.3 Metformin and Angiogenesis 166
4.2 HYPOTHESIS 167

4.3 Materials and Methods 167
4.3.1 Maternal Plasma glucose concentrations in diabetes 167
4.3.2 Effects of glucose, insulin and metformin on cellular network formation by HUVECs in vitro 168
4.3.3 Effect of glucose concentration on HUVEC cellular networks 168
4.3.4 Effect of fluctuating glucose concentration on HUVEC cellular networks 169
4.3.5 Effect of glucose +/- insulin and metformin on HUVEC cellular networks 169
4.3.6 Live Bio-imaging system 170
4.4 Analysis of HUVEC cellular networks 170
4.4.1 Cellular network formation Analysis 173
4.4.2 Statistical Analysis 174
4.5 Results 174
4.5.1 The effect of glucose concentration on HUVEC cellular networks 174
4.5.2 Effect of fluctuating glucose concentrations on HUVEC cellular networks 180
4.5.3 Effect of glucose +/- insulin and metformin on HUVEC cellular networks 189
4.6 Discussion 195
4.6.1 Angiogenesis cellular network formation Assays 196
4.6.6.1 Significance of HUVEC cellular network variables quantified by Image J 197
4.6.2 Exposure to high glucose concentrations impair cellular network formation in vitro model of angiogenesis. 198
4.6.3 Effects of fluctuation in glucose concentrations on angiogenesis; can glycaemic control rescue effects of impaired angiogenesis? 200
4.6.4 Effects of varying glucose concentrations, insulin and metformin on endothelial cells behaviour 203
4.6.5 Strength and Study Limitations 208
4.6.6 Summary 210

5 CHAPTER FIVE: GENERAL DISCUSSION 212

5.1 Overview 213
5.2 Reduced measured vascular volume at term in women with pregestational diabetes compared with normal pregnancy 214
5.2.1 Are vascular structure differences between normal and pregestational diabetes pregnancies related to maternal glycaemic control and/or growth factors? 216
5.2.2 Placenta growth factor: marker for aberrant fetoplacental vascular development? 217
5.3 The role of Insulin and Metformin on placental angiogenesis 219
5.4 Conclusion 223
5.5 Recommendations for future work 225

BIBLIOGRAPHY 230

APPENDICES 253

Appendix 1: Velocity Study Protocol 254
Appendix 2: Avizo Micro-CT Data Analysis Protocol 261
Appendix 2(I): R code Protocol for Cast Data Analysis 275
Appendix 3: Chapter 3 Results: Binned size numbers data presentation 279
Appendix 3(I): Vascular Vessel length in normal and pregestational diabetes 279
Appendix 3(II): Vascular volume in normal and pregestational diabetes 281
Appendix 3(III): Vascular Vessel length in normal and maternal glycaemic control groups in pregestational diabetes 283
Appendix 3(IV): Vascular volume in normal and maternal glycaemic control groups in pregestational diabetes 285
Appendix 3(V): Vascular vessel length in PIGF profile groups in pregestational diabetes 287
Appendix 3(VI): Vascular volume in PIGF profile groups in pregestational diabetes 289
Appendix 3(VII): Measured vascular volume and Uterine artery Doppler measurements in pregestational diabetes 291
Appendix 4(I): Angiogenesis Analyzer Protocol (Carpentier ,2012 Image J Plugin) 293
Appendix 4(II): Angiogenesis Pilot Experiments Results 295

Word Count: 73550

List of Figures

Chapter 1

Figure 1.1 Temporal trends in obstetric outcomes in diabetes 24
Figure 1.2 Classification of blood vessels in systemic circulation and corresponding vessels in fetoplacental vasculature. Adapted from Pearson Education, 2017 [34] 28
Figure 1.3 The interplay among abnormalities of angiogenesis in various tissues and the development of chronic diabetic complications. 29
Figure 1.4 Illustration of Anthropometry of fetoplacental vasculature 33
Figure 1.5 Gross Anatomy of human term placenta 35
Figure 1.6 Schematic representation of normal term villous tree and disorders of villous maturation. 37
Figure 1.7 Histology of normal term placenta compared to disorders of villous maturation. 38
Figure 1.8 Structural differences of normal placental terminal villi and pathological forms of villi in diabetic placenta. 40
Figure 1.9 Three-dimensional reconstruction of villous capillary bed in normal pregnancy and pre-gestational diabetes. 41
Figure 1.10 Histological features of first trimester placenta vs term placenta villi. 47
Figure 1.11 Schematic representation of the sequential regulation of vasculogenesis and angiogenesis during human placental development. 49
Figure 1.12 3D Patterns of villous development and cross section of three classes of term villi. 51
Figure 1.13 Structural model of human placental growth factor (PIGF)-1, VEGF-A and VEGF-B. 56
Figure 1.14 Schematic of VEGF family molecules and their receptor interactions, signalling and functions. 57
Figure 1.15 Image of Normal retina and Diabetic retinopathy 62
Figure 1.16 Scheme to show summary of mechanisms proposed to link maternal hyperglycaemia to abnormal fetoplacental angiogenesis. 68
Figure 1.17 Scheme to show summary of mechanisms proposed to link fetal hyperinsulinaemia to abnormal fetoplacental angiogenesis. 72
Figure 1.18 Scheme to summarise mechanisms that could link maternal diabetes to abnormal fetoplacental vascular development, placental dysfunction and fetal growth disorders. 76
Figure 1.19 Placental development and windows of metabolic insults in maternal diabetes 77

Chapter 2

Figure 2.1 Schematic diagram of placental vascular corrosion casting method (numbered steps illustrating different stages during the casting processes) 89
Figure 2.2 The principle of micro-CT imaging 91
Figure 2.3 Diagram with snapshots of components of Image processing 92
Figure 2.4 Pictorial representation of Angiogenesis Assay method 94
Figure 2.5 Schematic to show images taken of human umbilical vein endothelial cells in vitro to assess the formation of cellular networks 95

Chapter 3

Figure 3.1 Imaged and Analysed placental vascular corrosion cast 103
Figure 3.2 Example of cast with and without artefacts on vessel walls 104
Figure 3.3 The level of methacrylate resin outside vessels in arterial casts with artefacts and without artefacts. 105
Figure 3.4 The level of methacrylate resin outside smaller vessels in venous cast. 106
Figure 3.5: Illustration of anatomy of fetoplacental vasculature 107

Figure 3.6 Snapshot of data synthesis protocol....108
Figure 3.7 Diagrams illustrating modes of data presentation 111
Figure 3.8 Number of Vessel segments in radius bins in normal and pregestational diabetes casts. 116
Figure 3.9 Mean number of vessel segments in arterial and venous casts from clinical groups demonstrated in different modes of data presentation (radius size bins and binned size numbers)....117
Figure 3.10 Relationship between vascular placenta volume, gestation and birthweight 119
Figure 3.11 Relationship between maximum measured vascular volume and birthweight z-score 120
Figure 3.12 The length of arteries and veins in normal and pregestational diabetes casts 122
Figure 3.13 The total length of arteries and veins in normal and pregestational diabetes casts...123
Figure 3.14 The mean volume of arteries and veins in normal and pregestational diabetes casts. 125
Figure 3.15 The total volume of arteries and veins in normal and pregestational diabetes casts in radius size bins. 127
Figure 3.16 The chord length of arteries and veins in normal and maternal glycaemic status groups in pregestational diabetes casts. 133
Figure 3.17 The total length of arteries and veins in normal and maternal glycaemic status groups in pregestational diabetes casts 134
Figure 3.18 The mean volume of arteries and veins in normal and maternal glycaemic status groups in pregestational diabetes casts. 137
Figure 3.19 The total volume of arteries and veins in normal and maternal glycaemic status groups in pregestational diabetes casts. 138
Figure 3.20 The PIGF profiles women with pregestational diabetes over the course of pregnancy in categories of trimester....142
Figure 3.21 The length of arteries and veins in maternal PIGF profile groups in pregestational diabetes casts....145
Figure 3.22 The total length of arteries and veins in maternal PIGF profile groups in pregestational diabetes casts....146
Figure 3.23 The mean volume of arteries and veins in maternal PIGF profile groups in pregestational diabetes casts. 149
Figure 3.24 The total volume of arteries and veins in maternal PIGF profile groups in pregestational diabetes casts. 150

Chapter 4

Figure 4.1 Diagram to show variables measured to assess cellular networks formed by human umbilical endothelial cells in vitro 172
Figure 4.2 Example Image J Plugin Analysis....173
Figure 4.3 Representative images to show the effect of medium glucose concentration on HUVEC cellular networks after 18h of culture. 175
Figure 4.4 Effect of medium glucose concentration on variables of cellular networks formed by HUVECs....176
Figure 4.5 Effect of medium glucose concentration on the sum of variables of cellular networks formed by HUVECs....178
Figure 4.6 Representative live images to illustrate the effect of medium glucose concentration on the time course of development of HUVEC cellular networks. 179
Figure 4.7 Representative live bio images of HUVEC cellular networks formed in response to changing medium glucose concentration every 4h: control experiment with 5mM glucose 181
Figure 4.8 Representative live bio images of HUVEC cellular networks formed in response to changing glucose concentration every 4 h: control experiment with 18mM glucose 182
Figure 4.9 Representative live bio images of HUVEC cellular networks formed in response to

changing glucose concentration every 4 h: experiment with 5mM glucose to 18mM fluctuating glucose concentrations....183
Figure 4.10 The effects of fluctuating glucose concentration(5mM-18mM) on HUVEC cellular network....184
Figure 4.11 Representative live bio images of HUVEC cellular networks formed in response to changing medium glucose concentration every 4 h: control experiment with 25mM glucose 185
Figure 4.12 Representative live bio images of HUVEC cellular networks formed in response to changing glucose concentration every 4 h: experiment with 5mM glucose to 25mM fluctuating glucose concentrations....186
Figure 4.13 The effects of fluctuating glucose concentration(5mM-25mM) on HUVEC cellular network....187
Figure 4.14 Summarised representative live bio images of HUVEC cellular networks formed in response to medium, high and changing glucose concentrations 188
Figure 4.15 Effects of insulin +/- metformin on cellular networks formed by HUVEC cells maintained in 5mM glucose 190
Figure 4.16 Effects of insulin +/- metformin on cellular networks formed by HUVEC cells maintained in 18mM glucose 191
Figure 4.17 Effects of insulin +/- metformin on cellular networks formed by HUVEC cells maintained in 25mM glucose 192
Figure 4.18 Effects of insulin +/- metformin on cellular network meshes, segments and branches, formed by HUVECs maintained in 5mM, 18mM or 25mM glucose....193
Figure 4.19 Effects of insulin +/- metformin on cellular network master segments, and master junctions, formed by HUVECs maintained in 5mM, 18mM or 25mM glucose....194
Figure 4.20 Putative mechanisms of action of metformin in pregnancy....207

Appendix 3(ii)

Figure A3.0.1 The length of arteries and veins in normal and pregestational diabetes casts.....279
Figure A3.0.2 The total length of arteries and veins in normal and pregestational diabetes casts. 280
Figure A3.0.3 The mean vascular volume of arteries and veins in normal and pregestational diabetes casts....281
Figure A3.0.4 The total vascular volume of arteries and veins in normal and pregestational diabetes casts....282
Figure A3.0.5 The length of arteries and veins in normal and maternal glycaemic status groups in pregestational diabetes casts. 283
Figure A3.0.6 The total length of arteries and veins in normal and maternal glycaemic status groups in pregestational diabetes casts. 284
Figure A3.0.7 The mean vascular volume of arteries and veins in normal and maternal glycaemic status groups in pregestational diabetes casts....285
Figure A3.0.8 The total vascular volume of arteries and veins in normal and maternal glycaemic status groups in pregestational diabetes casts....286
Figure A3.0.9 The length of arteries and veins in maternal PIGF profile groups in pregestational diabetes casts....287
Figure A3.0.10 The total length of arteries and veins in maternal PIGF profile groups in pregestational diabetes casts. 288
Figure A3.0.11 The mean vascular volume of arteries and veins in maternal PIGF profile groups in pregestational diabetes casts. 289
Figure A3.0.12 The total vascular volume of arteries and veins in maternal PIGF profile groups in pregestational diabetes casts. 290
Figure A3.0.13 The distribution of measured maximum vascular volume per placenta weight ratio of venous and arterial placental casts with Uterine Doppler measurements from

Pregestational diabetes pregnancies. 291
Figure A3.0.14 The distribution of measured maximum vascular volume per placenta weight ratio of venous and arterial placental casts with Umbilical Doppler measurements from pregestational diabetes pregnancies. 292

Appendix 4(ii)

Figure A.4.0.15 Seeding densities of HUVECs on basement membrane substrate 296
Figure A4.0.16 In vitro effects of VEGF concentrations on HUVECs 298

List of tables

Chapter 1

Table 1.1 Summary of Adverse pregnancy outcomes reported in diabetes pregnancies characterised by maternal diabetes 25
Table 1.2 Summary of Angiogenesis Alterations in Various Diabetic Organs and Tissues 30
Table 1.3 Summary of Gross and Histopathologic Placental Findings in maternal diabetes....45
Table 1.4 Angiogenic factors and receptors , their function and location in the placenta 52
Table 1.5 Altered expression and levels of proangiogenic factors in different types of maternal diabetes....65

Chapter 2

Table 2.1 Demographic, clinical and placental examination details of maternal and fetal donor participants. 87

Chapter 3

Table 3.1 Vascular corrosion cast measured vessel radius and diameter output with corresponding physiological level dimensions....109
Table 3.2 Avizo software measured variables and presented metrics 110
Table 3.3 Exemplary outline of measure radius bins in different output modes of presentation .112
Table 3.4 Demographic, clinical and placental examination details of study....114
Table 3.5 Demographic and clinical details of study participants 131
Table 3.6 Demographic and clinical details of study participants 143

Chapter 4

Table 4.1 Angiogenesis Analyzer measured data variables and their definitions 171

List of Abbreviations

AGA	Appropriate for Gestational Age
AGEs	Advanced Glycation End products
Ang	Angiopoietin
BMI	Body mass index
CD31	Cluster of differentiation 31
DAB	3,3’-diaminobenzidine
DMEM	Dulbecco's modified Eagle's medium
DMSO	Dimethyl sulfoxide
ECM	Extracellular matrix
EBM-2	Endothelial basal medium-2
EGM-2	Endothelial growth medium-2
EGM-MV	Endothelial growth medium-microvascular
eNOS	Endothelial nitric oxide synthase
FBS	Fetal bovine serum
FGF	Fibroblast growth factor
FGR	Fetal growth restriction
FM	Fetal macrosomia
GDM	Gestational diabetes mellitus
GTT	Glucose tolerance test
HAPO	Hyperglycaemia and adverse pregnancy outcome
H&E	Haematoxylin and eosin
HIF	Hypoxia inducible factor
HMEC	Human mammary epithelial cells
HPAEC	Human placental artery endothelial cells
HPVEC	Human placental vein endothelial cells
HUVEC	Human umbilical vein endothelial cells
IBR	Individualised birth weight ratio
IL-8	Interleukin 8
IGF1	Insulin- like growth factors 1
IGF2	Insulin- like growth factors 2
IGF-IR	IGF-I receptor

IGF1Rα	IGF-I receptor alpha subunit
IGF2R	IGF-II receptor
IRS1	Insulin receptor substrate 1
IRS2	Insulin receptor substrate 2
KOH	Potassium hydroxide
LGA	Large for gestational age
MAPK	Mitogen-activated protein kinase
Micro-CT	Micro-computed tomography
NBF	Neutral buffered formalin
NO	Nitric oxide
NOX	NADH oxidase gene
PA	Placenta Area
PBS	Phosphate buffered saline
PE	Pre-eclampsia
PDGF	Platelet derived growth factor
PlGF	Placental growth factor
PKC	Protein Kinase C
ROS	Reactive oxygen species
SGA	Small for gestational age
T1DM	Type 1 diabetes mellitus
T2DM	Type 2 diabetes mellitus
TNF-α	Tumour necrosis factor alpha
VEGF	Vascular endothelial growth factor
VEGFR	Vascular endothelial growth factor receptor
WHO	World Health Organisation

Abstract

Diabetes in pregnancy is associated with an increased frequency of placental pathology and abnormalities in fetal growth. Placental development is a vital component in perinatal survival and consequently delivery of a healthy infant. However, the relationship between maternal diabetes and poor perinatal outcome remains poorly understood with knowledge gaps in the underlying mechanisms that directly influence placental development in a diabetic environment such that the fetus is at increased risk of placental dysfunction in late pregnancy.

The current study sought to characterise structural changes in placentas at term from pregnancies complicated by maternal diabetes in relation to fetal outcome, maternal glycaemic control and maternal levels of angiogenic factors (PlGF). This thesis tested the hypotheses that placental network structure would be different in pregestational diabetes compared to normal pregnancy and that other components of the diabetic environment *in utero* in early pregnancy may influence placental vascular development.

The experiments in this study involved the use of vascular corrosion casting of chorionic plate arteries and veins to quantify assessment of placental vascular networks. Vascular casts were scanned using Micro-CT imaging and software (Avizo 9.40) to generate quantifiable characteristics of the placental vasculature in both normal and pregestational diabetes pregnancies. Following this, key artery and vein network biometric outputs from Micro-CT imaging were related to birthweight, maternal glycaemic control (HbA1c measurement in first and last trimester) and maternal serum PlGF concentration measured at early, mid and late trimesters during pregnancy in women with diabetes.

In addition, studies were conducted using a well-established *in vitro* model of angiogenesis, to investigate the effects of elevated glucose concentration with and without insulin and metformin on network formation. Images of cellular networks were analysed using the ImageJ software with an angiogenesis analyser extension.

Fetoplacental artery and venous network structures at delivery were significantly different in pregnancies complicated by pregestational diabetes with decreased length of vessels and reduced vascular volume observed in diabetes. The implications of these vasculature alterations of the placenta on its function were not investigated. Hyperglycaemia might be related to the observations of reduction in arterial volume as poor maternal glycaemic control contributed to reduced arterial and venous vascular volume in diabetes, but venous

vascular volume was also reduced in women with good glycaemic control. Reduced vascular volumes in pregestational diabetes were not related to low maternal serum PlGF concentration in the third trimester. The ability of HUVECs to form cellular network structure was inhibited under high glucose environment (hyperglycaemia). Fluctuating level of glucose concentrations also affected endothelial cell behaviour by hindering their ability to form cellular mesh network structures even after switching back to normoglycaemic conditions. In the presence of metformin and pathophysiological concentrations of insulin, HUVECs maintained in medium containing high glucose concentration appeared improved in network formation. This thesis provides compelling evidence indicating that hyperglycaemia and/or other components of the diabetic environment affect fetoplacental vascular development as observed in altered placenta structure at term. Therapies involving metformin provide a promising start to development of tailored clinical interventions for treatment of aberrant fetal growth in maternal diabetes. Future work will investigate mechanisms that underlie structural changes using *in vitro* models and the implications of altered placenta structure on function.

Declaration

No portion of the work referred to in this thesis has been submitted in support of an application for another degree or qualification of this or any other university or other institute of learning.

Copyright Statement

i. The author of this thesis (including any appendices and/or schedules to this thesis) owns certain copyright or related rights in it (the "Copyright") and s/he has given the University of Manchester certain rights to use such Copyright, including for administrative purposes.

ii. Copies of this thesis, either in full or in extracts and whether in hard or electronic copy, may be made **only** in accordance with the Copyright, Designs and Patents Act 1988 (as amended) and regulations issued under it or, where appropriate, in accordance with licensing agreements which the University has from time to time. This page must form part of any such copies made.

iii. The ownership of certain Copyright, patents, designs, trademarks and other intellectual property (the "Intellectual Property") and any reproductions of copyright works in the thesis, for example graphs and tables ("Reproductions"), which may be described in this thesis, may not be owned by the author and may be owned by third parties. Such Intellectual Property and Reproductions cannot and must not be made available for use without the prior written permission of the owner(s) of the relevant Intellectual Property and/or Reproductions.

iv. Further information on the conditions under which disclosure, publication and commercialisation of this thesis, the Copyright and any Intellectual Property and/or Reproductions described in it may take place is available in the University IP Policy (see http://documents.manchester.ac.uk/DocuInfo.aspx?DocID=2442 0), in any relevant Thesis restriction declarations deposited in the University Library, the University Library's regulations (see http://www.library.manchester.ac.uk/about/regulations/) and in the University's policy on Presentation of Theses.

About the Author

Matina has previously studied an undergraduate degree in Biomedical Science at Liverpool John Moores University and studied a Master's of Research degree in Biomedical science and Translational Medicine at the University of Liverpool.

The research project for the master's degree involved exploring the relationship between obesity and increased risks of developing endometrial cancers and the use of extracellular vesicles(exosomes) as potential targets for therapy delivery.

(I) Conference Presentations

Hakim,M., Aplin,J.D., Greenwood,S.,Lowe,T.,and Myers,J.E. (2018) Increased Placental Venous Vessel Diameters In Pre-Gestational Diabetes .International Federation of Placenta Association, 2018 Tokyo, Japan (Poster)

Hakim,M., Aplin,J.D., Greenwood,S., Lowe,T., and Myers,J.E. (2018) Placental Vascular development in pregnancies complicated by maternal diabetes. The University of Manchester Postgraduate Summer Research Showcase 2018, Manchester, UK (Poster).

(II)Travel Grants

The University of Manchester Harold Fox Travel Grants, 2018

British Society for Developmental Biology: The Company of Biologists Travel Award, 2018

Acknowledgements

For having the opportunity to learn from wonderful scientists throughout my programme, I would like to thank my supervisors Prof. Jenny Myers, Prof. John Aplin and Dr. Susan Greenwood.

To Prof. Myers, thank you for offering me the opportunity to conduct such an amazing project under your supervision and your continuous support throughout my studies as well as providing an enriching research experience with your vast clinical and statistical knowledge.

I would like to thank Prof. John Aplin for his contributions, rendering his expertise to this project and all past and present members of the Aplin Laboratory group for useful lab meetings that inspired me throughout my studies and contributed to my academic development.

To Dr. Susan Greenwood, I am most grateful for the supervision, support, insightful discussions, pastoral care, invaluable advice throughout my study and all your patient efforts in spearing me on to complete this programme in the face of challenges even after your retirement! I cannot thank you enough.

I would also like to Dr. Tristan Lowe for training on Micro CT imaging and analysis and Dr. Julia Behnsen for her unwavering support at the Henry Mosley X-ray Imaging Facility.

I would like to express my special appreciation and thanks to my colleagues and staff of the Maternal and Fetal Health Research group for their valuable input and suggestions on all aspects of my research during my time at the department. I would also like to thank research midwives Giovanna Bernatavicius and Heather Glossop for recruiting participants for the Velocity study and Jess Morecroft for recruiting Biobank control participants for this project and all the staff at the St Mary's Hospital who participated in the research. A huge thank you to all of the women who have kindly donated their tissue and placentas-post-delivery for this work and hence making my research possible. Finally, my undue thanks goes to Tommy's Baby Charity for funding this project.

Last, but by no means least, I would like to thank my family and express my sincere gratitude to my parents Mr and Mrs Mohamed, Mr and Mrs Hakim, my siblings, friends, mentors and educators for their unflinching support, love and encouragement over the years. To Wewura, thank you for your love, sacrifices and support through this journey. Indeed, which of the favours of my Lord will I deny, All praise belongs to Him.

Dedication

This thesis is dedicated to my late father Hakim Dauda, for providing an inspirational canvass of life and an environment that instilled in me right from an early age all the boundless opportunities and possibilities.

1 Chapter One: Introduction

1.1 Overview

Globally 20 million or 16% of live births had some form of hyperglycaemia in pregnancy in 2019. The International Diabetes Federation suggests that 1 in 6 (16.8%) pregnancies are affected by diabetes. Of this number, 13.6% are affected by pregestational diabetes – a number which is likely to increase in future in line with the increasing prevalence of diabetes in the non-pregnant population. Diabetic women are at increased risk of poor pregnancy outcome, defined as babies too small (Fetal growth restriction, FGR) or too large (fetal overgrowth, LGA). Both these growth disorders increase risk of mortality, neonatal/infant morbidity and poor health in adult life. It has been widely documented that in pregnancies complicated by maternal diabetes there is a fourfold increased risk of stillbirth.

Fetal growth depends on appropriate development and function of the placenta and placental dysfunction underlies growth disorders in pregnancy pathologies. However, the relationship between maternal diabetes and poor perinatal outcome remains poorly understood with knowledge gaps in the underlying mechanisms that directly influence placental development in a diabetic environment such that the fetus is at increased risk of placental dysfunction in late pregnancy. There is a need for a clearer understanding of placental disease in maternal diabetes, in particular how it relates to stillbirth and the disparate outcomes of fetal growth restriction and fetal overgrowth, and the features of maternal diabetes in early gestation that underlie placental dysfunction.

The prevalence of diabetic vasculopathies in non-pregnant individuals is widely reported, with organ specific increased/inadequate angiogenesis contributing to the clinical complications. In pregnancy, fetoplacental blood vessel development is vital for adequate blood flow between the fetus and placenta essential to facilitate delivery of oxygen and nutrients to the developing fetus. Studies on altered fetoplacental vasculature development in maternal diabetes focus on small calibre blood vessels with differences in the morphology highlighted in increased villous immaturity and hyper vascularisation of the fetoplacental microvasculature, the site of nutrient exchange, in maternal diabetes implying abnormal (increased/altered) angiogenesis. The flow of blood to/from these vessels is determined by larger arteries and veins that branch from/diverge on the umbilical cord respectively but it is not known whether development of these vessels is altered in maternal diabetes and whether this relates to fetal outcome, maternal glycaemic control

or maternal angiogenic factors. Key features of maternal diabetes such as maternal glycaemic status, pro-angiogenic growth factors, fetal hyperinsulinemia or maternal treatment with metformin could be instrumental in regulating and initiating changes in micro-and macro vascular development.

In this study, casts were made of placental arteries and veins to compare vascular networks in normal pregnancies and in women with pregestational diabetes and key metrics related to birthweight, maternal glucose control and maternal plasma PlGF. To investigate potential mechanisms underlying dysregulated fetoplacental microvascular angiogenesis in maternal diabetes, an *in vitro* angiogenesis assay was used to assess the effects of glucose, insulin and metformin on the formation of cellular networks. This thesis will test the influence of components of the diabetic environment *in utero* on placental vascular development.

1.1.1 Maternal Diabetes

Over the years, the prevalence of diabetes has increased globally and the age of onset has shifted down a generation to people of working age and more recently adolescents [1-3]. In 2015 it was estimated that about 415 million people were living with diabetes worldwide, a number which is expected to increase to almost half a billion by 2030 [4]. The global prevalence of diabetes among adults over 18 years of age has risen from 4.7% in 1980 to 8.5% in 2014 [4]. In 2019, there were an estimated 223 million women (20-79 years) living with diabetes. This number is projected to increase to 343 million by 2045 [5]. As a result, more women of reproductive age have diabetes and more pregnancies are complicated by diabetes.

Diabetes type 1 (T1 DM) is an autoimmune disorder characterized by deficient insulin production as a result of destruction of pancreatic β-cells and requires daily administration of insulin [1]. In terms of maternal diabetes, this type is prevalent in women younger than 30 years of age who usually have a family history of autoimmune diseases [1]. On the other hand, Type 2 diabetes (T2 DM) results from ineffective use of insulin by cells and tissues [1]. This type accounts for the majority of diabetes worldwide and is largely the result of excess body weight and physical inactivity [1]. In pregnancy, type 2 diabetes occurs usually in obese women of 30 years of age or older diagnosed with inadequate insulin secretion or

increased tissue resistance to insulin [1]. The symptoms of these two presentations of diabetes are quite similar but in type 2 diabetes symptoms are often less marked leading to late diagnosis of the disease when complications and symptoms have already manifested [2].

Gestational diabetes (GDM), which accounts for over 86% of pregnancies complicated by diabetes, is defined by the World Health Organisation (WHO) as 'carbohydrate intolerance resulting in hyperglycaemia of variable severity with onset or first recognition during pregnancy' [2]. According to the latest WHO recommendation the screening for GDM should be performed universally with the standard 75g OGTT (oral glucose tolerance test) evaluating only the 2-hour blood glucose values or together with the fasting ones. The reference ranges are 4.0 to 6.0 mmol/L (72 to 108 mg/dL) when fasting and up to 7.8 mmol/L (140 mg/dL) 2 hours after eating [2].The relationship between diabetes and complications that arise in pregnancy is poorly understood.

Globally, there are over 60 million women of reproductive age with diabetes [5]. In the UK, approximately 700,000 women give birth in England and Wales each year, and up to 5% of these women have either pre-existing diabetes or gestational diabetes. It is estimated that 87.5% have gestational diabetes, 7.5% have type 1 diabetes and the remaining 5% have type 2 diabetes [6]. The likelihood of serious complications of pregnancy such as stillbirth, pre-eclampsia, fetal growth restriction, fetal macrosomia and fetal malformations is heightened in women with diabetes [7, 8]. Abnormalities of fetal growth and development in pregnancies affected by the different types of diabetes have been associated with an increased frequency of placental pathology.

1.1.2 Diabetes Associated Complications: Increased risk of Morbidity and Mortality for Fetus

Maternal complications of diabetes in pregnancy include pre-eclampsia, preterm labour, polyhydramnios, increased rates of operative delivery and increased infective morbidity [9, 10]. The principle complications encountered in third trimester are fetal macrosomia and intrauterine fetal demise; birth of a macrosomic baby can result in shoulder dystocia, birth trauma, brachial plexus injury [9, 10]. Diabetes is more common in obese women (particularly GDM) and maternal obesity is becoming increasingly prevalent. The Confidential Enquiry into Maternal and Child Enquiries (CMACE) Obesity in Pregnancy

national project reported the UK prevalence of women with a known BMI ≥ 35 (Class II and Class III obesity) at any point in pregnancy, who give birth ≥ 24+0 weeks' gestation, is 4.99%. This translated into approximately 38,478 maternities each year in the UK. The prevalence of women with a pregnancy BMI ≥ 40 (Class III obesity) in the UK is 2.01%, while super-morbid obesity (BMI ≥ 50) affects 0.19% of all women giving birth [11]. Obesity per se is associated with increased risk of stillbirth with FGR(fetal growth restriction) and delivery of an overgrown baby(Large for Gestational Age LGA); effects which are exacerbated in maternal diabetes [10]. Obesity is the most potent risk factor for Type 2 diabetes and accounts for 80–85 per cent of the overall risk of developing Type 2 diabetes which underlies the current global spread of the condition [5].

Similarly, pregnancies characterised by pre-existing diabetes are also associated with considerably increased rates of adverse obstetric and perinatal outcomes as shown in data from population-based studies [8, 12-14]. Studies have demonstrated associations with perinatal and post neonatal mortality and diabetes in pregnancy. A population based birth linked cohort study revealed that pregestational diabetes (PGDM) may increase the risk of perinatal death to a much greater extent when comparing First Nations versus non-Indigenous populations. PGDM was associated with an increased risk of perinatal death to a much greater extent in First Nations (RR=5.08[95% CI 2.99 to 8.62], p<0.001; absolute risk (AR)=21.6 [8.6–34.6] per 1000) than in non-Indigenous populations (RR=1.76[1.17, 2.66], p=0.003; AR=4.2[0.2, 8.1] per 1000). PGDM was associated with an increased risk of post neonatal death in non-Indigenous (RR=3.46[1.71, 6.99], p<0.001; AR=2.4[0.1, 4.8] per 1000) but not First Nations (RR=1.16[0.28, 4.77], p=0.35) infants [15]. However, as the study was a large population study (over 250,000 participants from 1996-2010) there was a lack of data on glycaemic control in diabetic pregnancies. Other studies have also highlighted a consistent relationship observed between diabetes mellitus subtype and obstetric outcomes, with women with T1 DM having the highest rate of intervention and the highest rates of adverse perinatal outcomes followed by women with T2 DM and women with GDM. The rate of neonatal morbidity ranged from 8.7% in women without diabetes mellitus to 11.0%, 17.4%, and 24.1% in women with GDM , T2DM, T1DM, respectively (P < 0.001) [16] as seen in **Figure 1.1**. Reports of stratified analysis by gestational age have also shown infants of mothers with diabetes have a significantly higher risk of mortality at 26 weeks' gestation and mortality or severe morbidity at 31 weeks' gestation than infants of mothers without diabetes [14]. Evaluation of neonatal and

maternal morbidity in mothers with gestational diabetes also revealed an increased risk of delivery by C-section, preterm birth, macrosomia at birth and neonatal hypoglycaemia [13]. Reports on trends in incidence, obstetric interventions, and pregnancy outcomes have also highlighted that pregestational diabetes and gestational diabetes incidence have increased significantly over time in a population based study of diabetes during pregnancy in Spain (2009–2015). Differences in the prevalence of comorbidities, obstetric risk factors, and the rate of adverse obstetric outcomes among women with different types of diabetes were found. Women with T2DM were more likely to have obstetric comorbidity (70.12%) than those with GDM (60.28%), T1DM (59.45%), and no diabetes (41.82%). Previous caesarean delivery, preeclampsia, smoking, hypertension, and obesity were the most prevalent risk factors in all types of diabetes. Women with T1DM had more severe maternal morbidity (RR 1.97; 95% CI1.70–2.29) and neonatal morbidity (preterm birth, RR 3.32; 95% CI 3.14–3.51, and fetal overgrowth, RR 8.05; 95% CI 7.41–8.75) [17]. However again in this large study, clinical data regarding diabetes control and treatments, as well as indications for obstetric intervention were not collected.

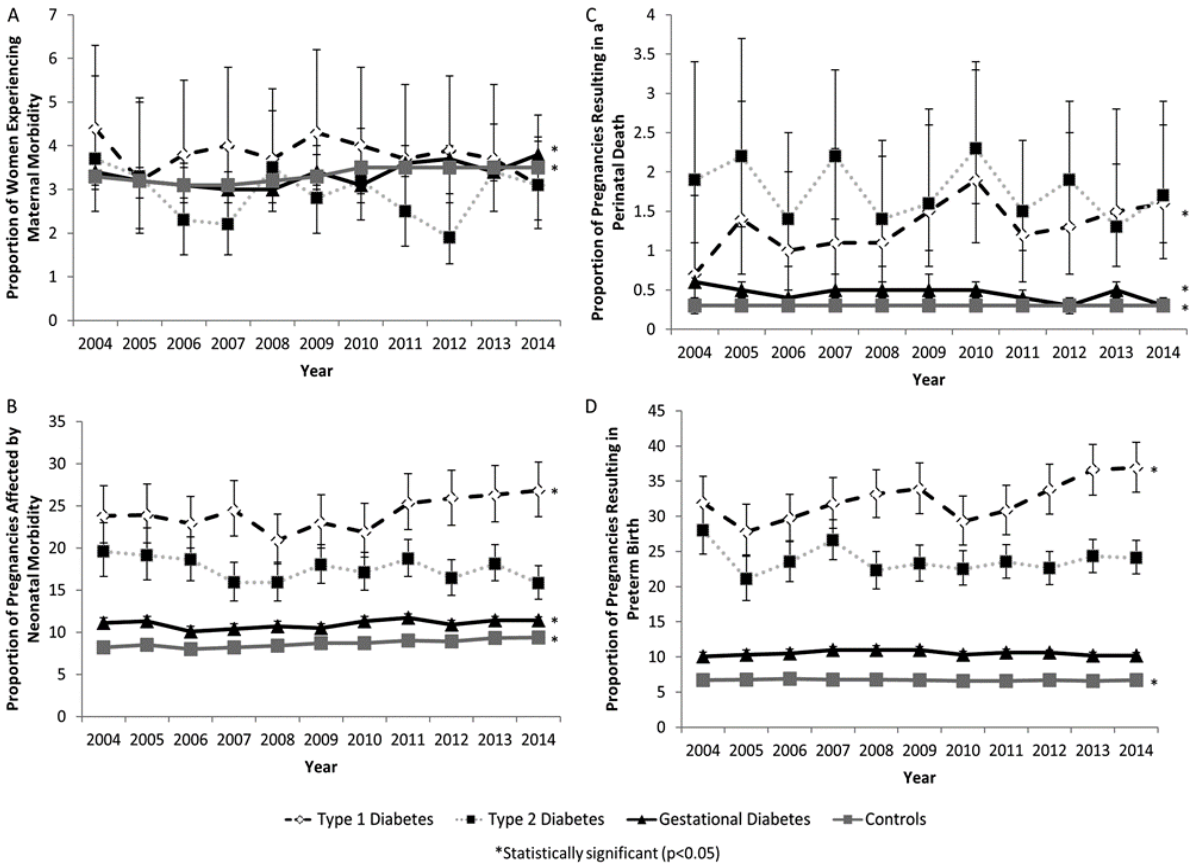

Figure 1.1 Temporal trends in obstetric outcomes in diabetes
Graphs show proportion of pregnancies resulting in A, maternal morbidity; B, neonatal morbidity; C, perinatal death; D, preterm birth) among pregnancies in women with type 1, type 2, and gestational diabetes mellitus compared with women without diabetes mellitus (Canada, excluding Quebec, 2004 to 2015). Graph image from Metcalfe et al.(2017) [16].

The major measures and outcomes reported in publications included in-hospital mortality, perinatal death (stillbirth), neonatal death [died in the first 28 days after birth]) and post neonatal death (died between 28 and 364 days after birth). Other outcomes and morbidities reported included; birth defects, preterm (<37 completed weeks of gestation), small for gestational age (SGA, <10th percentile in birth weight for sex and gestational age,) large for gestational age (LGA, > 90th percentile), macrosomia, hypoglycaemia, hypocalcaemia, hypomagnesaemia, respiratory distress, congenital malformations, and hyperbillirubinaemia as summarised in **Table 1.1**.

Table 1.1 Summary of Adverse pregnancy outcomes reported in diabetes pregnancies characterised by maternal diabetes

Adverse Outcomes	Pregnancy with T1DM	Pregnancy with T2DM	Pregnancy with GDM
Perinatal Mortality Still birth	✓	✓	✓
Neonatal Mortality	✓	✓	✓
Post neonatal death	✓	✓	✓
Macrosomia	✓	✓	✓
FGR	✓	✓	✓
SGA	✓	✓	✓
LGA	✓	✓	✓
Respiratory Distress syndrome	✓	✓	✓
Intraventricular Haemorrhage grade 3-4	✓	✓	✓
Shoulder dystocia	✓	✓	✓
Hypoglycaemia Hypomagnesaemia Hyperbillirubinaemia	✓	✓	✓
BPD (bronchopulmonary dysplasia) cPVL (cystic periventricular leukomalacia) NEC (necrotizing enterocolitis)	✓	✓	✓
Stillbirth	✓	✓	✓

The table summarises adverse pregnancy outcomes reported in pregnancies complicated by diabetes. Data represents summary of adverse pregnancy outcomes;✓ reported ,T1DM-type 1 diabetes, T2DM-type 2 diabetes, GDM gestational diabetes mellitus , FGR-fetal growth restriction, SGA – small for gestational age, LGA large for gestational age, RDS-respiratory distress syndrome newborn, cPVL(cystic periventricular leukomalacia) NEC-necrotizing enterocolitis, BPD-bronchopulmonary dysplasia [8, 17-23].

The summary shown in **Table 1.1** suggests that the rates of adverse pregnancy outcomes are increased in pregnancies complicated with diabetes compared to normal pregnancies with significant difference reported between subtypes of diabetes in studies mentioned above. This places a considerable burden on healthcare systems in managing increasing number of pregnancies complicated by obesity and diabetes as a result of complications to mother and fetus with these morbidities. However, there still remains inadequate understanding of the mechanisms that account for the range of these poor fetal outcomes that are evident in pregnancies characterised by maternal diabetes. Poor control of maternal hyperglycaemia has been linked to increased incidence of fetal macrosomia in diabetes [24]; however even with treatment and management of hyperglycaemia [25], there is still a higher incidence of fetal macrosomia and other poor fetal outcomes compared to non-complicated pregnancies [26]. There is therefore a pressing need for understanding the aetiology of fetal macrosomia and other adverse complications associated with infants exposed to the diabetic milieu during pregnancies. Diabetes in the non-pregnant population is associated with vascular pathology including altered vascular development and function; it is probable that diabetes could affect the development and function of blood vessels in the placenta in pregnancy. Experimental animal studies have highlighted the importance of the regulation of angiogenesis and vasodilatation of the uterine and placental vessels as the two key mechanisms that increase placental blood flow during late gestation, which is paramount for normal fetal growth and development [27-29]. Abnormalities in placental function/development are therefore likely to underlie these adverse fetal outcomes associated with maternal diabetes outlined in **Table 1.1**. It is also widely reported in diabetes in the non-pregnant population that vascular complications make up majority of the pathologies.

1.1.3 Diabetic Complications and Vascular Development

The abnormalities in the vasculature that are evident in diabetic non-pregnant individuals, and the underlying causes/pathogenesis, could also be true of the placental vasculature in maternal diabetes. Understanding the hallmarks of vascular development complications in the non-pregnant diabetic population can give a better understanding of how the diabetic environment affects placental development. Vasculature remodelling occurs constantly in the human body to adapt to physiologic and pathologic conditions. This phenomenon is

characterised by angiogenesis, which refers to the formation of new blood vessels from pre-existing ones , neovascularisation which refers to the formation of blood vessels in previously avascular areas or newly formed tissues [30] and arteriogenesis which refers to the formation of new arteries by remodelling of pre-existing vessels, mainly stimulated by hemodynamic forces [31]. The remodelling of the vasculature i.e. growth and regression is important to allow the supply of oxygen and nutrients to all cells throughout the body.

The circulatory system conducts the supply of oxygen and nutrients to cells throughout the body via macrovasculature and microvasculature. The macrovasculature is composed of arteries and veins, large capacity vessels responsible for transporting blood rapidly toward or away from organs as shown in **Figure 1.2**. The macrovasculature is made up of large conduit vessels involved in macrocirculation. The microvasculature consists of three types of small vessels: arterioles, capillaries, and venules. These microvessels form a network that regulates local blood perfusion and conducts blood–tissue exchange (**Figure 1.2**). The microvasculature is defined as vessels that are 10-200 µm in diameter involved in microcirculation.

In the fetoplacental circulation, deoxygenated blood is delivered to the placenta via two umbilical arteries. These arteries branch into large chorionic vessels which feed 60 – 100 individual villous trees. The villous trees themselves branch dichotomously for several generations before feeding several parallel capillary conduit pathways, which provide the site for placental gas exchange. The function of large conduit arteries is to supply blood to the resistance arteries. Resistance arteries regulate blood flow to optimise nutrient exchange by sheer stress, metabolites and endocrine factors whereas venules/veins as capacitance vessels take the oxygenated blood (and nutrient rich blood) to the fetus and thus regulation of venous return is important in supporting fetal growth [32, 33].

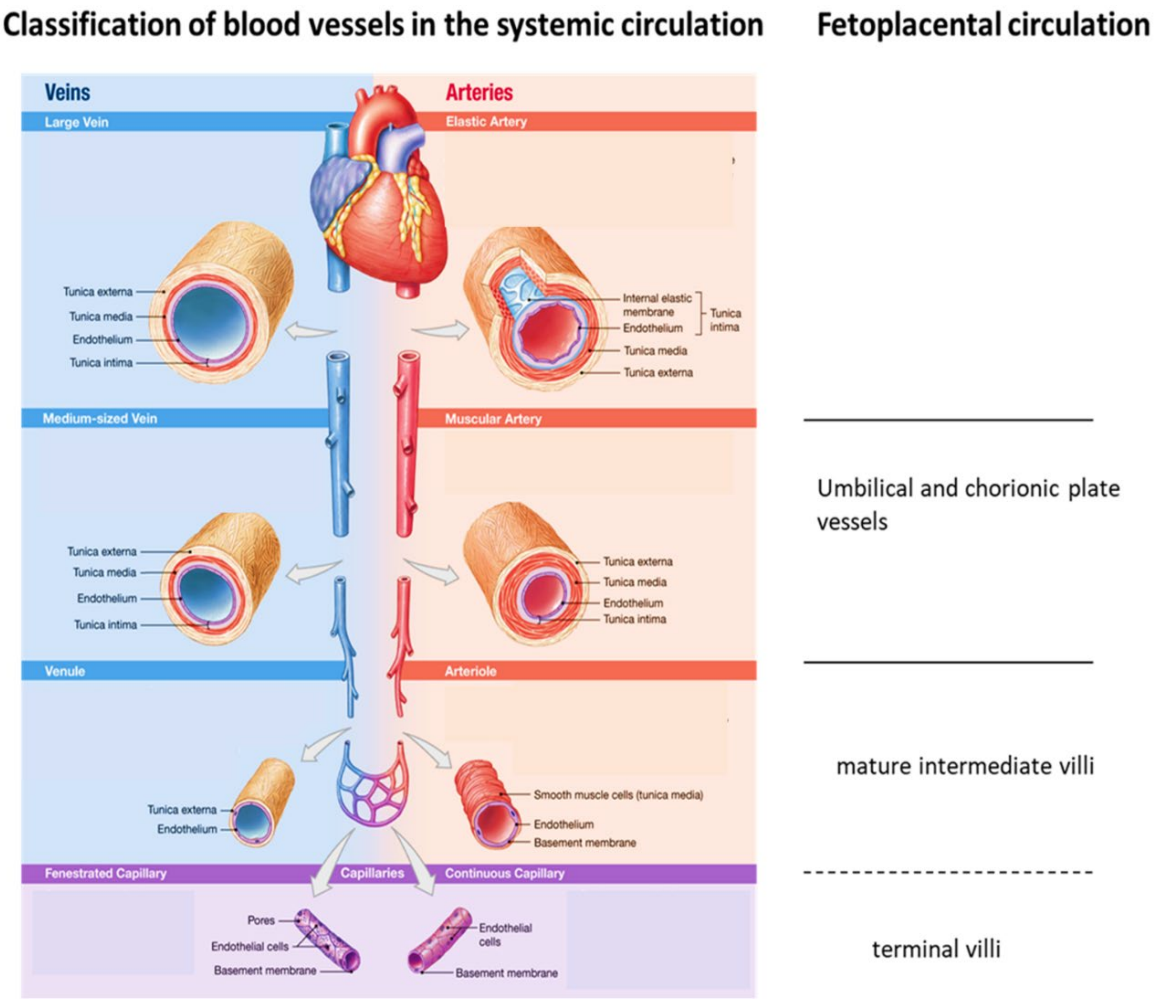

Figure 1.2 Classification of blood vessels in systemic circulation and corresponding vessels in fetoplacental vasculature. Adapted from Pearson Education, 2017 [34].

Excessive or defective angiogenic responses is dire to the homeostasis of the body and can lead to pathologic states [35]. Diabetes mellitus has been associated with excesses or defects in angiogenic processes known as the "diabetic paradox" shown in **Figure 1.3**, observed in various tissues and organs [36], where there is a hyper-proliferation of the vessels in some tissues (e.g. retina), but insufficient vascularisation in ischemic limbs and myocardium in diabetes mellitus are also associated with tissue specific responses. The reasons why some tissues undergo increased vascularisation and proliferative angiogenesis but in other tissues angiogenic responses fail is poorly understood.

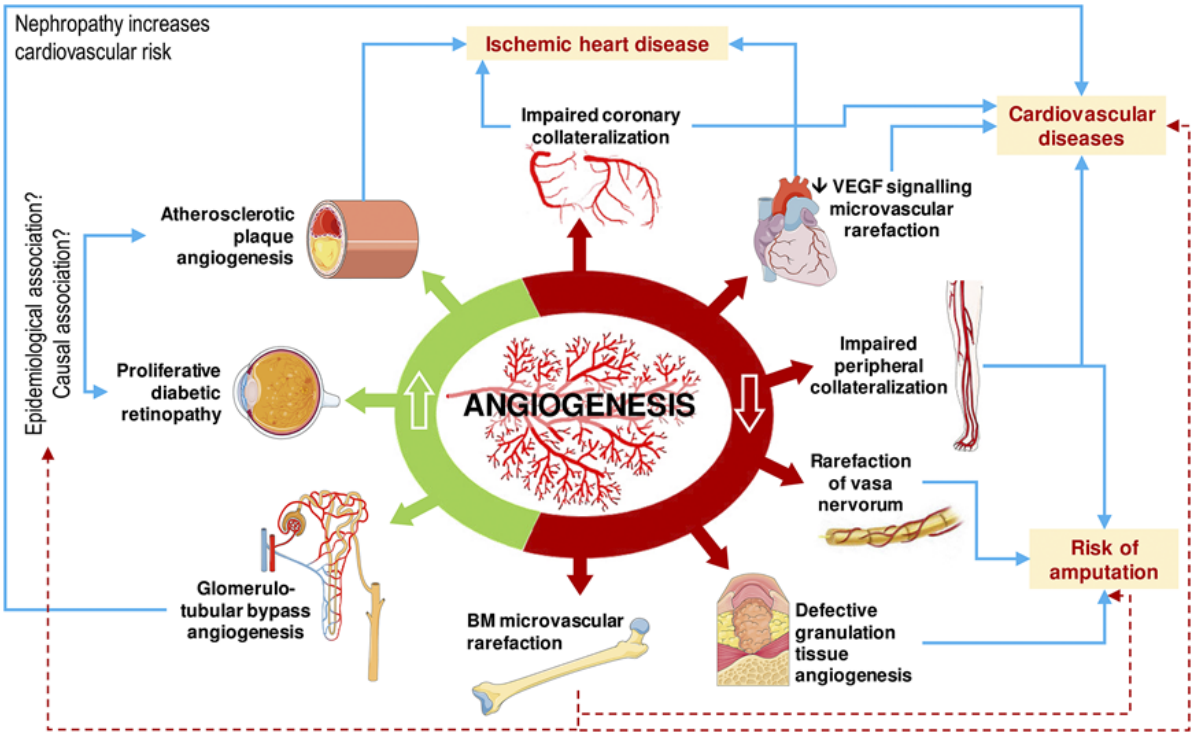

Figure 1.3 The interplay among abnormalities of angiogenesis in various tissues and the development of chronic diabetic complications.
VEGF= (vascular endothelial growth factor) Green-excessive, Red-defective. Image taken from Fadini et al. (2019) [36].

These diabetic complications are characterised under (organ dependent) altered angiogenesis (microvasculature) and formation of anastomoses or collaterals (macrovasculature) in retina, heart, kidneys, nerves. Microvascular complications include retinopathy, nephropathy and neuropathy. Macrovascular complications include cardiovascular diseases, cerebrovascular diseases and peripheral vascular diseases as outlined in **Table 1.2**.

Table 1.2 Summary of Angiogenesis Alterations in Various Diabetic Organs and Tissues

Organ/Tissue	Angiogenesis Alterations	Clinical Consequences	
		Microvasculature	**Macrovasculature**
Eye	Retinal angiogenesis	Diabetic retinopathy	
	Macular involvement	Diabetic macular oedema	
	Choroidal angiogenesis	Neovascular glaucoma	
Kidney	Early angiogenesis connecting glomeruli with tubule	Glomerular hemodynamic dysfunction	
	Late impairment of peritubular angiogenesis	Fibrosis	
Nerves	Depletion of vasa nervorum	Reduced conduction velocity (neuropathy)	
Heart	Impaired VEGF signalling	Microvascular rarefaction	Cardiovascular diseases Angina Myocardial infarction
	Defective coronary collateralisation		Coronary Heart disease
Brain	Defective coronary collateralisation		Cerebrovascular disease; Stroke, TIA
Peripheral circulation	Impaired collateralisation		Worse clinical course of atherosclerosis obliterans Peripheral artery disease (PAD)
Skin	Impaired wound bed angiogenesis	Delayed wound healing	
Lung	Reduction in microvascular density	Diabetic lung disease	
Bone marrow	Microvascular rarefaction	Impaired stem cell mobilisation and worse course of transplantation	
Adipose tissue	Impaired angiogenesis during adipose expansion	Adipose hypoxia, inflammation, and insulin resistance	
Islets	Impaired angiogenic support	α-Cell/β-cell dysfunction	
		Worse islet transplant outcomes	

-Data in table demonstrate the multisystem and multiorgan extensive alterations of angiogenesis associated with diabetes and how they can contribute to disease onset, progression, and complications from Fadini et al. (2019) [36].

These clinical complications outlined in **Table 1.2** support a relationship between diabetes and the incidence and progression of microvascular and macro vascular complications such as diabetic retinopathy, nephropathy and peripheral vascular complications. With the above compelling evidence on multisystem and multiorgan vascular complications as major pathology associated with diabetes in the non- pregnant population, it is expected that angiogenesis abnormalities are present in essentially all organs and tissues of patients with diabetes. Therefore, it is probable that these complications could arise in the placenta and the examination of the placenta vasculature could identify causes of fetal growth abnormalities in pregnancies complicated by maternal diabetes.

1.2 Human Placenta

The human placenta is a specialised organ instrumental to the development of the fetus [37]. It acts as the organ for nutrient and oxygen exchange and a selective permeability barrier between the mother and growing embryo [37]. The human placenta can be structurally viewed as a large fetal micro vascular bed, with fetal capillaries lying within the stroma of the placental villous tree in close proximity to overlying syncytiotrophoblast (STB) which is directly bathed in maternal blood flowing from the maternal spiral arteries; it is this arrangement that permits efficient exchange of solutes and gases between the maternal and fetal circulations without intermingling of the two as shown in **Figure 1.4** [37]. However, its exposure to maternal circulation renders it particularly vulnerable to any aberrant circulatory factors that may be present [38]. The normal formation, growth and function of this organ is tightly regulated for effective exchange of nutrients, respiratory gases and fetal metabolic wastes between mother and fetus in a circulatory system that includes the maternal, fetal and placental unit [30].

1.2.1 Fetoplacental Vasculature

In the human placenta, there are two anatomically separate vascular systems namely the maternal-placental (uteroplacental) and the fetoplacental systems. The arteries in the feto-placental system convey deoxygenated blood and waste products from the fetus to the villi while oxygenated blood is conveyed by the veins from the villi to the fetus as described in **Figure 1.4**. Nutrient and gaseous exchange occurs between maternal and fetal blood in the capillaries within the terminal villi (categorised under microvasculature by definition of <150µm of vessel diameter) where exchange occurs. The uteroplacental arteries adapt in early pregnancy to become low resistance high flow vessels to facilitate the delivery of maternal blood into the intervillous space bathing the fetal villous tree [39]. Fetoplacental vessels (and the overlying trophoblast layer) are capable of responding to vasoactive agents, growth factors, oxygen, glucose and nutrients in maternal blood (if they cross the placenta i.e. the STB) with compensatory mechanisms; alterations in transporter systems, increased/decreased angiogenesis and chorionic villous branching are all evidences of this [40], [41-46]. The exchange of nutrients occurs in the terminal parts of the villous tree, by STB bathed directly in maternal blood, with the efficiency of nutrient exchange being dependent on the structure/function of the fetoplacental vasculature.

The placenta is composed of several layers of cells acting as a barrier for the diffusion (simple or facilitated) of substances between the maternal and fetal circulatory systems. The placenta has been characterized as “a lipid membrane that permits bidirectional transfer of substances between maternal and fetal compartments”[47]. In humans, the placental barrier consists of the trophoblastic epithelium, covering the villi, the chorionic connective tissue, and the fetal capillary endothelium[48]. The average thickness of the barrier varies from the first trimester (20–30 µm) to the third trimester (2–4 µm)[49]. At term the average exchange area is approximately 11m^2 and the placental blood flow rate is approximately 450 mL/min [50]. The intensity of the passage of substances across the placenta is an important function and is inversely proportional to the thickness of placental membranes and other placental transfer factors that influence transport across placenta : uteroplacental and umbilical blood flow, pH of the blood, placental permeability (passive or active transport system), placental maturity over gestation period (size, surface area, and thickness), lipid-protein content of membranes, placental metabolism, plasma protein binding, lipid solubility, and other physicochemical properties[47].

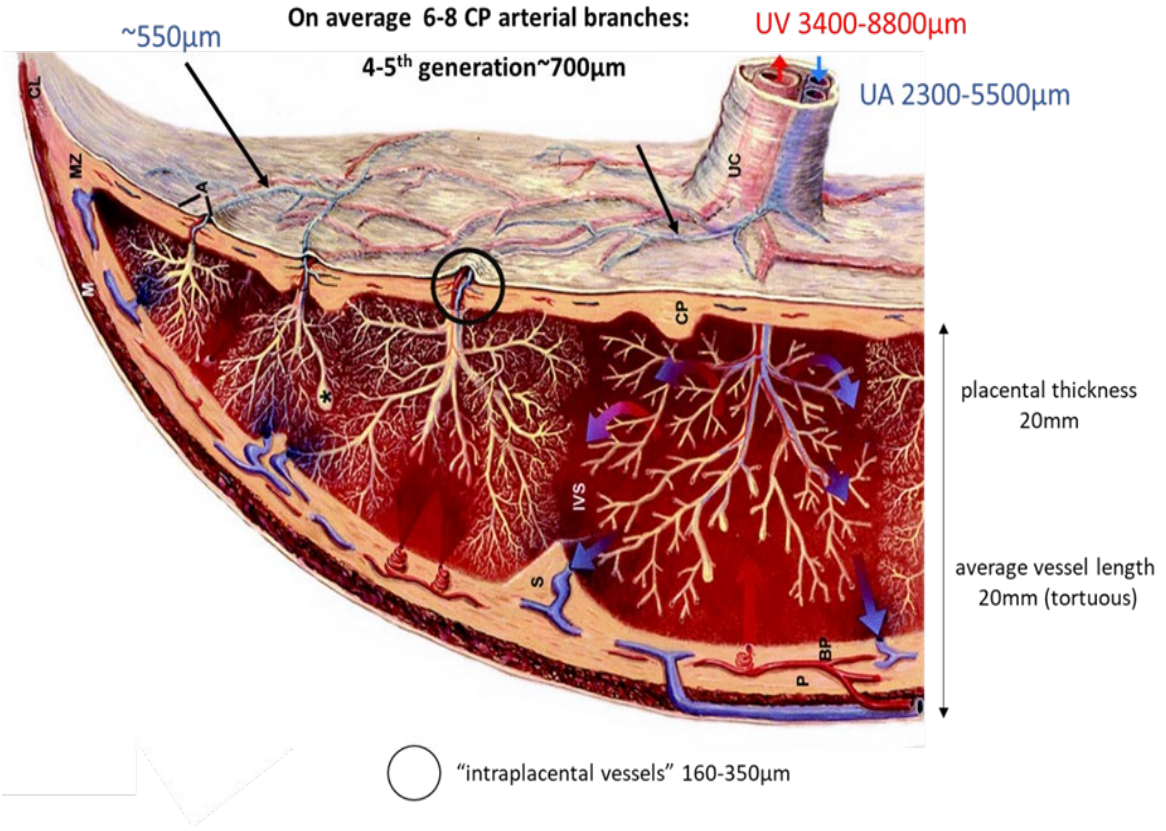

Figure 1.4 Illustration of Anthropometry of fetoplacental vasculature

Image showing the fetoplacental vasculature branching network of arteries and veins and information of diameter of vessels on vascular beds. The umbilical arteries (UA) and vein (UV) branch off at the insertion in the placenta into 6–8 generations that traverse over the whole chorionic plate (CP). In the chorionic plate of a mature placenta, the arteries usually overlay the veins. The chorionic vessels are relatively large (>350µm) and much smaller vessels (<350µm) branch off this network at almost right angles and penetrate into the placenta toward the maternal side to constitute the Intraplacental vessels (IP). The IP vessels give rise to the villous trees (<150µm) that are the essential structures involved in material exchange between mother and fetus. Image reproduced from Benirschke et al.(2012) and Gordon et al. (2007)[37] [51, 52].

The umbilical cord stems from the connecting stalk which connects the early placenta to the embryo. A mature umbilical cord comprises of three blood vessels; two arteries and one vein, surrounded by a loose connective tissue called Wharton's jelly throughout its length. The two umbilical arteries are usually connected within the umbilical cord, at or near its insertion point on the placenta, by the Hyrtl's anastomosis (within about 3 - 5cm above)[53] [54]. Branches of each of the three umbilical vessels form a distinct tree-like network of vessels. Because of the Hyrtl's anastomosis, the two arterial trees are connected and may collectively be seen as the "arterial tree" (though they are separable). Typically, arteries cross over veins on the chorionic plate [33], however there are no anastomoses between the chorionic networks with the exception of certain pathological situations (twin-twin transfusion syndrome). From the point of insertion of the umbilical cord on the placenta, the umbilical vessels release and branch across the surface of the chorionic plate and are now referred to as chorionic plate vessels i.e. chorionic plate arteries and chorionic plate veins that can be categorized under the macrovasculature by definition of vessels >300μm. The chorionic plate veins all converge onto the single umbilical vein and hence the direction of blood flow in these veins is towards the umbilical vein at the cord insertion point. These vessels branch all the way into the placental core until they reach the bases of the stem villi.

In regards to a central cord insertion (**Figure 1.5**), the distance to the chorionic plate margin is only one half of the placenta diameter and a dichotomous branching pattern may be the easiest way to traverse most of the chorionic plate with a minimal number of generations. A few monopodial ramifications coming off the first and second dichotomous branches ensure perfusion of the areas in between. Studies have highlighted the fact that the organisation of the chorionic vasculature is consistent, not random, and dependent on the umbilical cord insertion, but they could not explain the physiological reasons [37, 44].

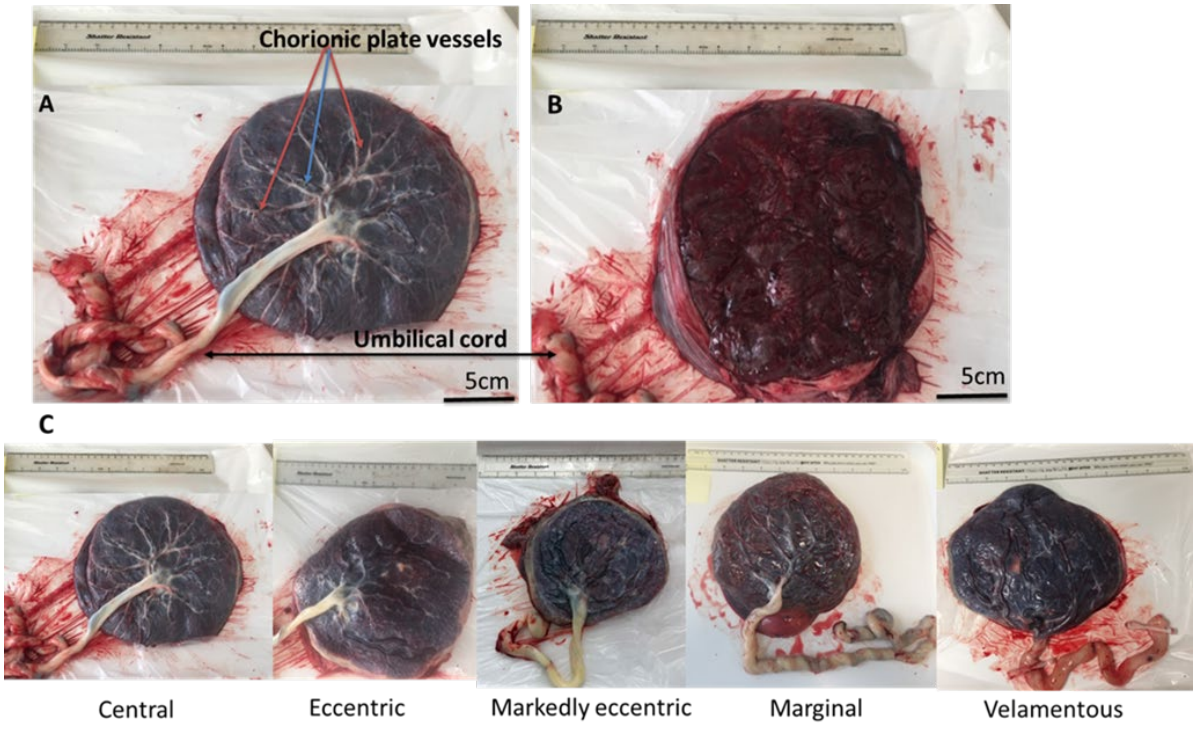

Figure 1.5 Gross Anatomy of human term placenta

Images show the maternal and fetal surfaces of the human placenta at term and examples of different types of cord insertion. The normal human placenta at term is usually a round to oval disk-like organ and has a maternal unit opposite to a fetal unit. **(A)** The fetal surface consists of the umbilical cord and the chorionic plate, over which the umbilical arteries and veins successively branch and are termed (**red arrows**) chorionic plate veins and (**blue arrows**) chorionic plate arteries. **(B)** The decidua covers the maternal surface and the placenta contains 15 – 20 lobules also known as cotyledons which are separated by visible grooves divided by septa. At term, the mature human placenta measures about 22cm in diameter, ~2.5cm thick and weighs 450– 600g [55] **(C)** In normal pregnancy the umbilical cord inserts into the centre of the placenta (central insertion) or slightly off-centre (eccentric insertion). However, sometimes the cord inserts within 2 cm of the placenta edge, called a marginal cord insertion (MCI), or not into the placenta at all which is called a velamentous cord insertion (VCI) [56].

In a 2017 meta-analysis [56] , normal cord insertion was reported to occur about 90% of the time. However, sometimes marginal cord insertion (MCI) or velamentous cord insertion (VCI) cases occur, where the umbilical cord inserts into the membranes of the amniotic sac and unprotected blood vessels run through the membranes before reaching the placenta edge. When the umbilical cord is supported by very little or no placental tissue, the risk of blood vessel abruption becomes much greater. A review on abnormal cord insertions

reported that MCIs and VCIs are considered abnormal cord insertions and occur about 7% and 1% of the time, respectively [56] . They occur more frequently in multiples pregnancies and are associated with spontaneous abortion, preterm labour, small for gestational age(SGA) infants, vasa previa, emergency caesarean, and other adverse outcomes [56]. Investigations looking at cord insertion in diabetes in relation to poor outcome may well be important as presumably cord insertion will have a major influence on the pattern pf blood vessel branching on the chorionic plate.

1.2.2 Altered fetoplacental vasculature in pregnancies complicated by diabetes

Early studies on altered fetoplacental vasculature in maternal diabetes focussed on small calibre blood vessels and mainly reported histological findings [57]. More recently, other methods such as stereology and whole organ casting have been employed in examination of the fetoplacental vasculature [58]. Results have differed among studies, which could potentially reflect differences in the type of diabetes, the glycaemic control of study participants, or the study methodology/approaches to assess fetoplacental vascular development. Alternatively, these inconsistencies in findings may represent different biologic adaptations to distinct metabolic complications of the disease.

1.2.3 Evidence for abnormal placental microvasculature in diabetes

There are variations in placental abnormalities reported in maternal diabetes studies. Placental villous immaturity has been reported in both pre-gestational and gestational diabetes [59-61]. Placental villous immaturity, also referred to as distal villous immaturity (DVI), is defined as “a placental phenotype characterized by enlarged distal villi with excessive stroma, hypercellular villous trophoblast, paucity of vasculosyncytial membranes, and a decreased fetoplacental weight ratio” [61]. It is largely observed in term or near-term placentas and is associated with specific maternal conditions including impaired glucose tolerance, obesity, and excessive pregnancy weight gain [62]. Other descriptions of disorders of villous maturation have been described in classifications of delayed maturation, maturation arrest, and accelerated maturation as shown in **Figure 1.6** and **Figure 1.7**.

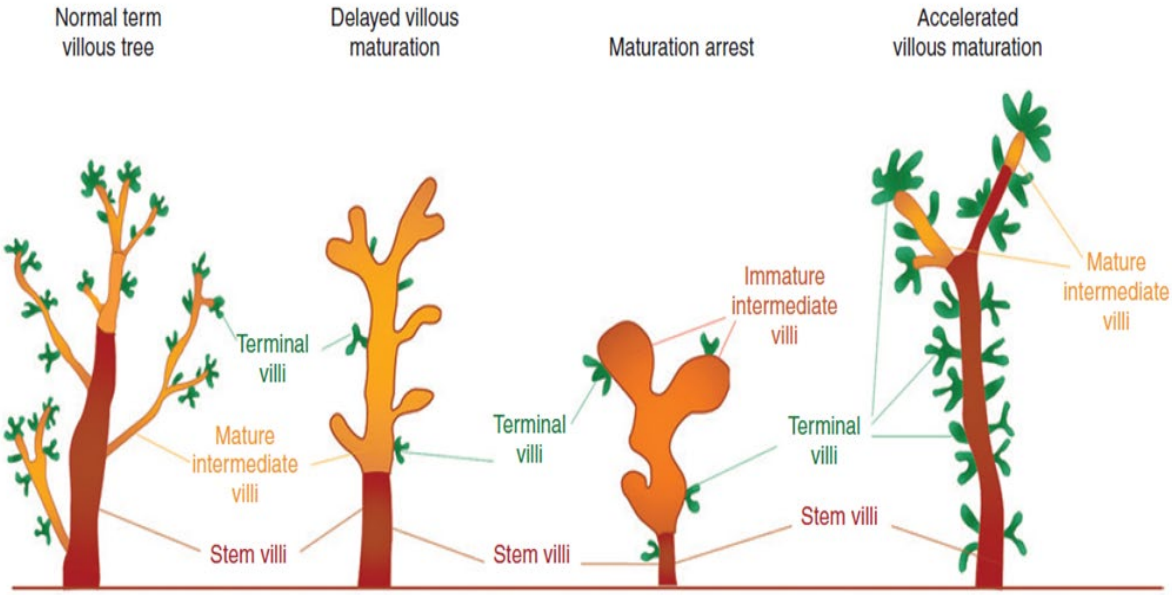

Figure 1.6 Schematic representation of normal term villous tree and disorders of villous maturation.

Brown: trunk of a tree depicting stem villi; **orange**: intermediate trunk of a tree depicting immature intermediate villi; **yellow**: branches of a tree depicting mature intermediate villi; and **green**: leaves of a tree depicting terminal villi. At term, the villous tree is constituted by terminal villi, mature intermediate villi, stem villi, and even mesenchymal villi [88] (0–5%; not depicted here). Delayed villous maturation is characterized by medium-sized intermediate villi of peripheral mature type along with stem villi. The villi display reticular stroma, centralized vessels, and diminished vasculo-syncytial membranes. Maturation arrest is characterized by the predominance of immature intermediate villi displaying primitive mesenchymal, embryonic, and loose reticular stroma with Hofbauer cells, few capillaries, considerably reduced vasculosyncytial membranes, and diminished intervillous space. Accelerated villous maturation is characterized by hypermature, hypoplastic, and slender terminal villi resembling the histology of term villi with considerably increased intervillous space. Image taken from Jaiman et al. (2020) [63].

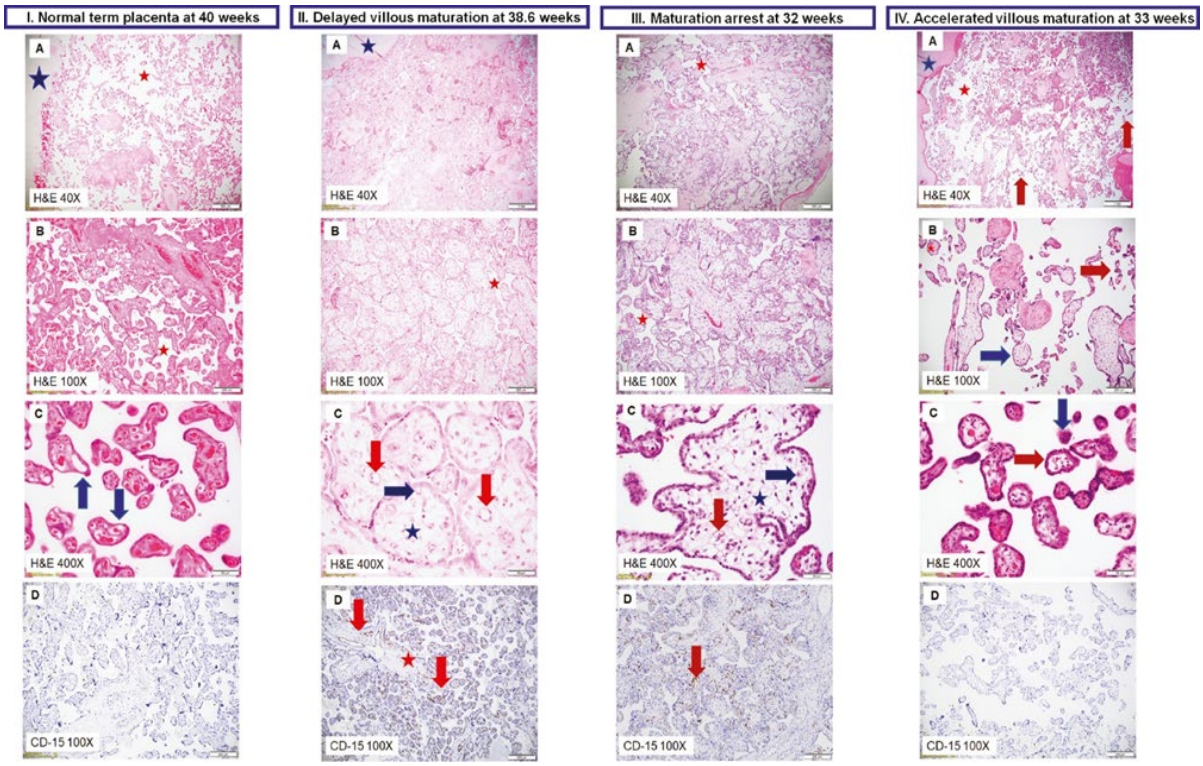

Figure 1.7 Histology of normal term placenta compared to disorders of villous maturation.
Panels showing – normal term placenta (40 weeks) (I); – delayed villous maturation (38.6 weeks) (II); – maturation arrest (32 weeks) (III); IV – accelerated villous maturation (33 weeks). (A), (B) and (C) display H&E-stained sections at 40, 100, and 400× magnifications, respectively. (D) shows Immunohistochemistry of CD15-stained sections at 100× magnification. Images from (Jaiman et al. 2020) [63]

Another pathologic description of altered fetoplacental vasculature in diabetes is distal villous hypoplasia [64, 65]. This is described as a form of placental villous maldevelopment that is characterized by a sparse, poorly developed distal villous tree with abnormally shaped, elongated, slender villi and widening of the intervillous space. This placental pathology is associated with significant intrauterine growth restriction and adverse consequences for the fetus such as neurodevelopmental delay and adult cardiovascular disease [64, 66, 67]. A systemic review concluded that increased villous immaturity [66, 68-70], increased volume and surface area of parenchymal tissue, defined as the intervillous space, the trophoblast layer, and fetal capillaries of both the peripheral and stem villi [71-73] were the placental abnormalities most consistently reported in diabetes. Furthermore, studies have reported increased parenchymal volumes, on average 12% larger than placentas from normoglycaemic controls, but a decrease in non-parenchymal

tissue defined as the chorionic and decidual plates, fetoplacental vessels of diameter greater than 0.1 cm, and intercotyledonary septa [71-75] in women with well-controlled T1DM compared to normoglycaemic controls [71].

A study conducted by Mayhew et al (2002) reported increased measures of fetoplacental angiogenesis by comparing capillary volume, surface area and length in T1DM. This study concluded that the characterized changes in angiogenesis occurred exclusively via longitudinal growth without a change in the cross-sectional calibre or shape of the capillaries, compared to controls in placentas affected with maternal T1DM despite adequate glycated haemoglobin levels [46]. Conversely, Jirkovska et al. (2012) reported increased branching angiogenesis, hypovascular and hypervascular villi in diabetic placentas in addition to changed structure of villous stroma (**Figure 1.8**) and enhanced capillary surface areas in terminal villi of placentas affected by maternal T1DM with good glycaemic control [76, 77].

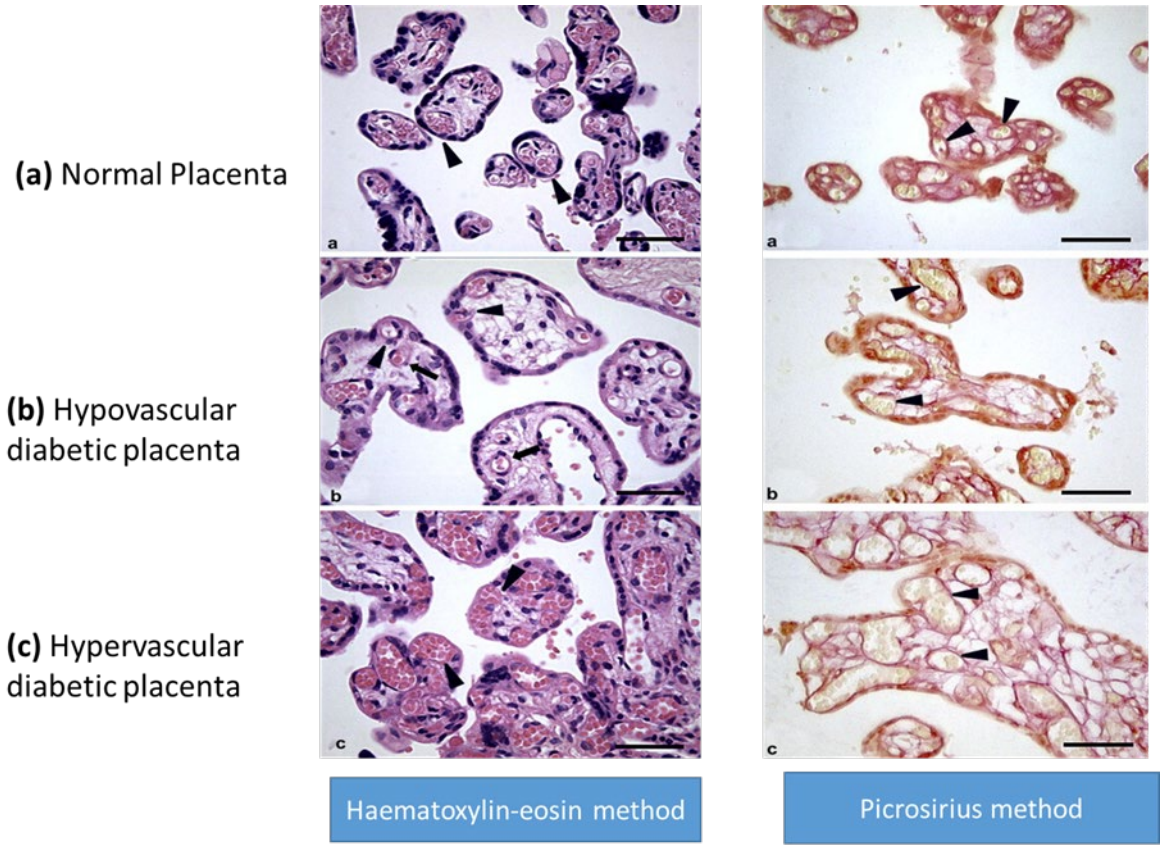

Figure 1.8 Structural differences of normal placental terminal villi and pathological forms of villi in diabetic placenta.

Villi of normal placenta (a) are smaller than pathological villi of diabetic placenta, their capillaries form with villous syncytiotrophoblast vasculosyncytial membranes (arrowheads). Larger hypovascular villi (b) display small-diameter capillaries predominantly in a tight relationship to the trophoblast (arrowheads), but some of them lie distant from the trophoblast (arrows). Unlike normal villi the stroma resembles sparse network. In large hypervascular villi (c) numerous and large capillary profiles dominate the structure (arrowheads), and only small part of villous stroma is observable. Bars = 100 µm. Placental villi stained with the picrosirius method display occurrence of collagen in the villous stroma. Capillaries in villi of normal placenta (a) have more intense coloured layer around their outer surface corresponding to the presence of collagen fibres mantle (arrowheads), and the collagen meshwork in the stroma is dense. The collagen mantle surrounding capillaries (arrowheads) looks thinner and the collagen meshwork enclosing stromal channels seems to be variously arranged in both forms of pathological villi (b,c). Bars = 100 µm. Images taken from Jirkovská et al. (2012) [77].

This conflict in findings results from the different approaches used in these studies and classification methods used in analysing the findings. Mayhew (2002) used a design based stereological analysis which provides 3D properties from histologic sections such as volume surface, area and diameters. This method determines these parameters independent of 3D

structural (topological) properties i.e. the differences found in volumes of tissue using stereology does not provide information on 3D structural changes. Therefore, identical stereologic volumes could be associated with different 3D structures. However, the Jirkovska study (2012) involved methods of immunohistochemistry, confocal microscopy, topological schemes and 3D reconstruction, as shown in **Figure 1.9**, for quantitative assessment of capillary branching pattern.

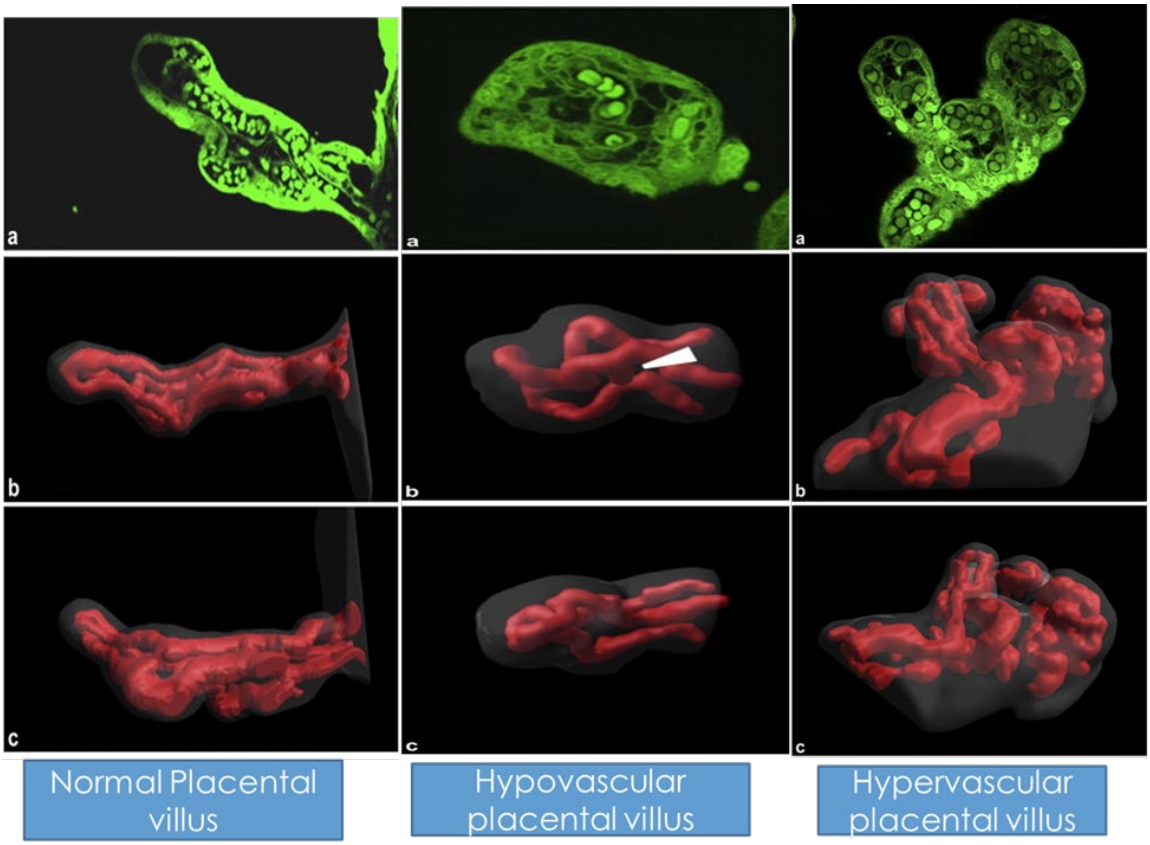

Figure 1.9 Three-dimensional reconstruction of villous capillary bed in normal pregnancy and pre-gestational diabetes.

One section from the source stack of serial optical sections (a) and two projections of reconstructed capillaries (b, c) show that terminal villus of a normal placenta is long and slender, and its branching capillaries have almost parallel arrangement. The three-dimensional reconstruction of the villous capillary bed in a hypovascular placental villus from a pregestational diabetic shows one section from the source stack of serial optical sections (a) and two projections of reconstructed capillaries (b, c). In the hypovascular villus thin capillaries are located in more voluminous stroma (a). Capillary branches are distant each to other and their course is wavy. The arrowhead indicates a capillary bud. The right-hand panel shows a three-dimensional reconstruction of a villous capillary bed in a hypervascular villus from pregestational diabetes pregnancy. One section from the source stack of serial optical sections demonstrates numerous and large capillary profiles (a) and two projections of reconstructed capillaries show extremely wavy course and irregular diameter of capillaries (b, c). Images taken from Jirkovská et al. (2012) [77].

In common with Jirkovska et al (2012), other studies have also reported an increase in the number of capillaries per terminal villi in women with T1DM. Teasdale (1983) studied 10 placentas of diabetic women. The women in Teasdale's study were classified as having diabetes Class B (White 1978), that is onset of diabetes after age 20 years but present less than 10 years and requiring insulin therapy. Five of the placentas of diabetics in Teasdale's study were from pregnancies where the babies were large for gestational age; the placentas of these babies were heavier than those of a control group, mainly due to a significant accumulation of non-parenchyma and only a moderate increase in parenchymal tissue. None had any history of smoking, or any other complications of pregnancy, and they all reported excellent maternal plasma glucose control during pregnancy. These differences may be partly explained by Teasdale's definition of parenchyma which does not include villous connective tissue [71, 72, 78], and GDM [79, 80]. Bjork & Persson (1984) performed morphometric assessment on villi from different parts of the cotyledon in placentas from 13 insulin-dependent diabetic women and compared the results with those from placentas of 10 non-diabetics. Experimental measurements were made on unfixed villi and the results expressed in arbitrary units. They found that the organisation of the cotyledon, of increasing villous length and surface area towards the periphery, was not present in the placentas of diabetics. In the diabetic women, placental villi were of equal length throughout the cotyledon and although the average villous length did not differ from that of the control group, the average surface area was greater. They concluded that the increase in villous surface area observed was due to increased branching of peripheral villi in the diabetic group [81].

One contributor to the lack of consistency in description of placental vasculature in pregestational diabetes could be the absence of a simple, comprehensive, and widely accepted classification system with reproducible grading of placenta phenotypes. A recent validation experiment on the classifications of villous types [82] suggested that researchers aiming to quantify placental structure could not solely rely on routine histological section analysis. The study involved two groups of morphologists (Group 1 consisted of 3 standard morphologists who were not experts in placental morphology and group 2 consisted of 3 expert morphologists with long- standing experience in placental microscopic anatomy and pathology). These groups were given a total collection of 165 photographs of villous sections for villous types (terminal villi, intermediate villi, stem villi) to be classified

histologically by assessment of the terminal distance and stromal core of the villi using a formalized task description. The results from this study demonstrated that inter-rater variability was high and indicated substantial observer influence on the classification of the different villous types. Cross-match of villous types with the predetermined positions of villous branches of villous trees revealed substantial mismatch between the classifications of villous types. There were no histopathological findings examined in the study.

This study by Haeussner et al. (2015) alludes to the fact that discrepancies in the classification of placental lesions could be observer dependent highlighting the need for a widely accepted classification system and the use of more advanced techniques to provide an objective quantitative assessment of fetoplacental vascular development [82]. It is therefore important to be wary of some of the pitfalls associated with classification of placenta pathology.

In contrast to the small diameter vessels (microvasculature), less is known about diabetes impacts on the development of the macrovasculature and whether there are changes in the vascular networks of the larger calibre vessels in pregestational diabetes. Studies report mainly on macrovascular diseases complications with insufficient detail on changes or impact on structure of large calibre chorionic plate vessels. Abnormalities in larger calibre blood vessel development have been reported in fetal growth restriction, showing longer venous and shorter arterial vasculature in FGR placentas [58]. Previous investigations have also demonstrated the presence of fewer chorionic plate arteries and sparse capillaries in FGR placentas [83].

In summary, the weight of evidence and highlights of reviews on placenta pathology in maternal diabetes suggests that placentas from pregnancies complicated by maternal diabetes may display increases in branching and non-branching angiogenesis, that pregestational diabetes promotes enhanced angiogenesis and that villous immaturity in diabetes is often associated with increased placental weight or poor glycaemic control; however, significant variability in study characteristics prevents quantitative meta-analysis. Differences in the morphology of the placental microvasculature in type 1 and type 2 diabetes compared to normal pregnancy are likely to be secondary to altered angiogenesis. Although the majority of publications report increased villous immaturity and hyper vascularisation of the fetoplacental microvasculature in diabetes, this has not always been

related to maternal glycaemic control or pregnancy outcome as shown in the summary **Table 1.3**. In addition, there is very little information on pathologies of the larger calibre arteries and veins of the chorionic plate of the fetoplacental vasculature in maternal diabetes.

Table 1.3 Summary of Gross and Histopathologic Placental Findings in maternal diabetes

Placental pathology	Pregestational diabetes		Gestational diabetes
	Type 1 diabetes	Type 2 diabetes	
Growth/weight	- Increased placental weight compared to healthy controls [43, 66, 84, 85]		- Increased placental weight [75, 86, 87]
Degree of villous maturity	- Increased frequency of immature villi compared to healthy controls [57, 60, 66, 69]		- Increased frequency of immature villi [88, 89]
Measures of angiogenesis	- Increased number of capillaries in terminal villi compared to healthy controls [90] [76] - Greater combined length of fetal capillaries compared to healthy controls - Increased mean number of redundant connections per terminal villi compared to healthy controls [77]		- Increased mean number of redundant connections per terminal villi compared to healthy controls [46, 77, 78, 91]
Volume and surface areas of parenchymal tissue (contains the structure or compartments that are strictly concerned in metabolic exchanges between mother and fetus)	- Increased volume of parenchymal tissue compared to healthy controls [70-72, 74]		- Increased volume of parenchymal tissue compared to healthy controls [78]
Primary vascular and secondary vascular lesions	- Increased incidence of nucleated fetal red blood cells, fibrinoid necrosis, villous immaturity, and chorangiosis compared to healthy controls [66]		- Increased incidence of fibrinoid necrosis [88] and chorangiosis [89]

Table summarises findings on placental histopathology in diabetes.

The inconsistencies and gaps in published data highlight the potential need of advantages of using an unbiased quantitative approach to assess placental arterial and venous structure particularly investigations focusing on the impact of diabetes on large calibre chorionic plate vessels in relation to maternal glucose status and fetal outcomes.

The use of approaches such as vascular casting could also offer advantages to examination of the fetoplacental vasculature as vascular casting enables the study of the vascular pattern of normal or pathological tissue providing details of the three-dimensional anatomic arrangement of the vascular replica. Vascular corrosion casting in combination with Micro-CT imaging have been reported to enable quantification of fetoplacental vasculature (mainly chorionic plate vessels >150μm) on a holistic level [58].

The above abnormalities in placental blood vessels in diabetes, could point to aberrant angiogenesis. The vascular development of the placenta plays a very important role in adequate fetoplacental blood flow to optimise nutrient delivery to the fetus and transfer of fetal metabolites to mother by placental syncytiotrophoblast (**Figure 1.10**). This process is reliant on the appropriate development of fetoplacental blood vessels from early pregnancy to term by vasculogenesis and angiogenesis.

1.3 The normal development of the placenta and placental vasculature

In pregnancy, placental development begins with implantation of the conceptus and the differentiation of the trophectoderm to form the pre-villous trophoblast around seventh day post conception [37]. Placental trophoblast develops from the trophectoderm while the embryoblast forms the embryo and the extraembryonic mesoderm, amnion and umbilical cord, which connects the embryo to the placenta.

The primary villi consist of a network of columns and floating villi interwoven with a precursory intervillous space. Then a subsequent invasion of the primary villi by mesenchymal cells pushes the trophoblast to the periphery forming the secondary villi. At this point the placental vasculature begins to develop. The primitive development of the vasculature is driven by the differentiation of the mesenchyme into angioblast stem cells, which are precursory to the placenta endothelium [44] .

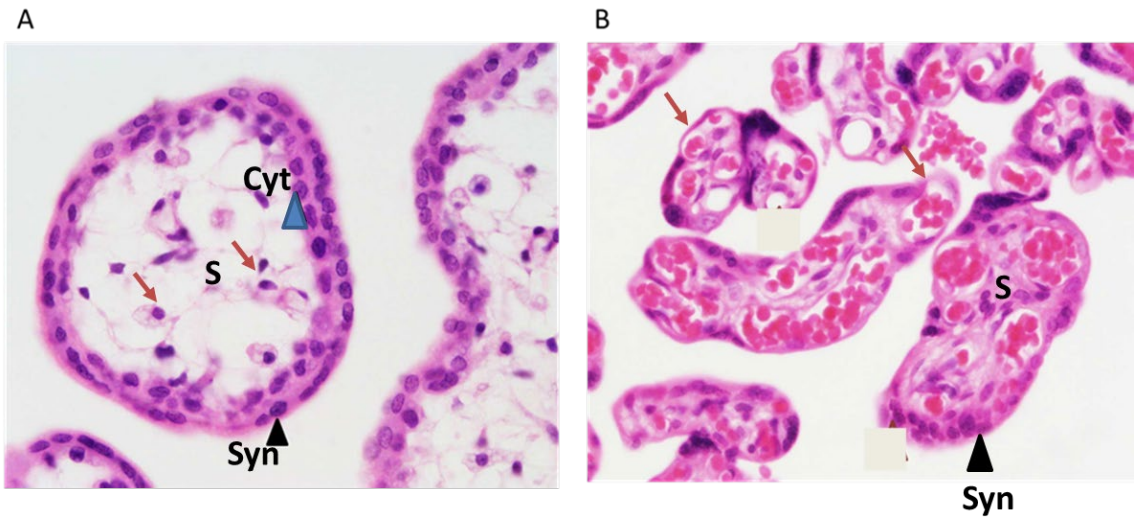

Figure 1.10 Histological features of first trimester placenta vs term placenta villi. Haematoxylin and eosin-stained cross- sections of (**A**) first trimester human Placental Villi and **(B)** human term placental villi. Black arrow-Syn, syncytiotrophoblast; blue arrow-Cyt, cytotrophoblast; S, stroma, red arrows point to Hofbauer cells in (**A**) and blood vessels in (**B**). (**A**): Villi in cross-section. Villi are cover in shell of syncytiotrophoblast and some cytotrophoblast cells. Villi core contains mainly mesenchyme cells. The structure, as well as the histological features of the human placenta varies with gestational age. (**B**): Surface layer of villi now lack cytotrophoblast cell layer and now are covered with only a syncytiotrophoblast layer (shell). Syncytiotrophoblast layer is variable in thickness from a thin cytoplasmic layer to regions of clumped nuclei. Villi core mainly occupied by fetal capillaries and larger blood vessels, with only a small amount of connective tissue. Fetal red blood cells now appear to the earlier distinctive nuclei. Images from (Hill, M.A. 2021, Embryology Placental villi).

1.3.1 Placenta Vascular Formation

Two distinct processes are responsible for giving rise to blood vessels. Vasculogenesis is defined as the differentiation of precursor cells (angioblasts) into endothelial cells and the *de novo* formation of a primitive vascular network, whereas angiogenesis is defined as the growth of new capillaries from pre-existing blood vessels (**Figure 1.11**) [30]. During development of the placenta vasculature, primitive (primary) villi form from proliferation of trabeculae into the intervillous space around the 13th day post conception(dpc) [92]. The villi at this stage only consist of two trophoblast cell layers; cytotrophoblast core surrounded by a layer of syncytiotrophoblast. In the next few days, extra-embryonic mesenchyme from the chorionic plate invades the cytotrophoblast cell layer, transforming the villi into secondary villi. Mesenchymal cells invade the cytotrophoblast which initiates

the process of vascularisation within the villi. Mesenchyme-derived macrophages expressing angiogenic growth factors initiate vasculogenesis at around 20 days post conception [37]. Placental blood vessels begin to form in the villi at this stage, where they are now referred to as tertiary villous mesenchyme/mesenchymal villi.

1.3.1.1 Vasculogenesis

The beginning of vasculogenesis is evident in the placenta at around 20 days post conception, progenitor cells then begin the process of forming the endothelial lining of the developing capillaries. The placenta becomes vascularised by formation of capillaries within the villi [37]. The process of *de novo* vascular formation begins with the formation of the endothelial progenitor cells called angioblasts as seen in the extraembryonic mesoderm allantois [44, 93]. This is as a result of differentiation events from pluripotent mesodermal stem cells to progenitor haemangiogenic stem cells, haemangioblasts, angioblasts and finally endothelial cells as seen in **Figure 1.11** [27]. When formed, endothelial cells proliferate, migrate and interact with one another, aligning into tubes which subsequently become surrounded by supporting structures such as pericytes, smooth muscle, basement membrane to form continuous vascular networks [94]. This process continues until 32 days post conception when the vessels connect to the fetal circulation via the connecting stalk which later becomes the umbilical cord. Mesenchymal villi are slender, comprising of abundant Langhans cells, early vessels and under-developed stroma. Subsequently, they differentiate either into immature or mature intermediate villi [39]. By the 5th week post conception, the fetal vessels meet and merge with the locally formed villous vessels establishing the complete feto-placental vasculature [37].

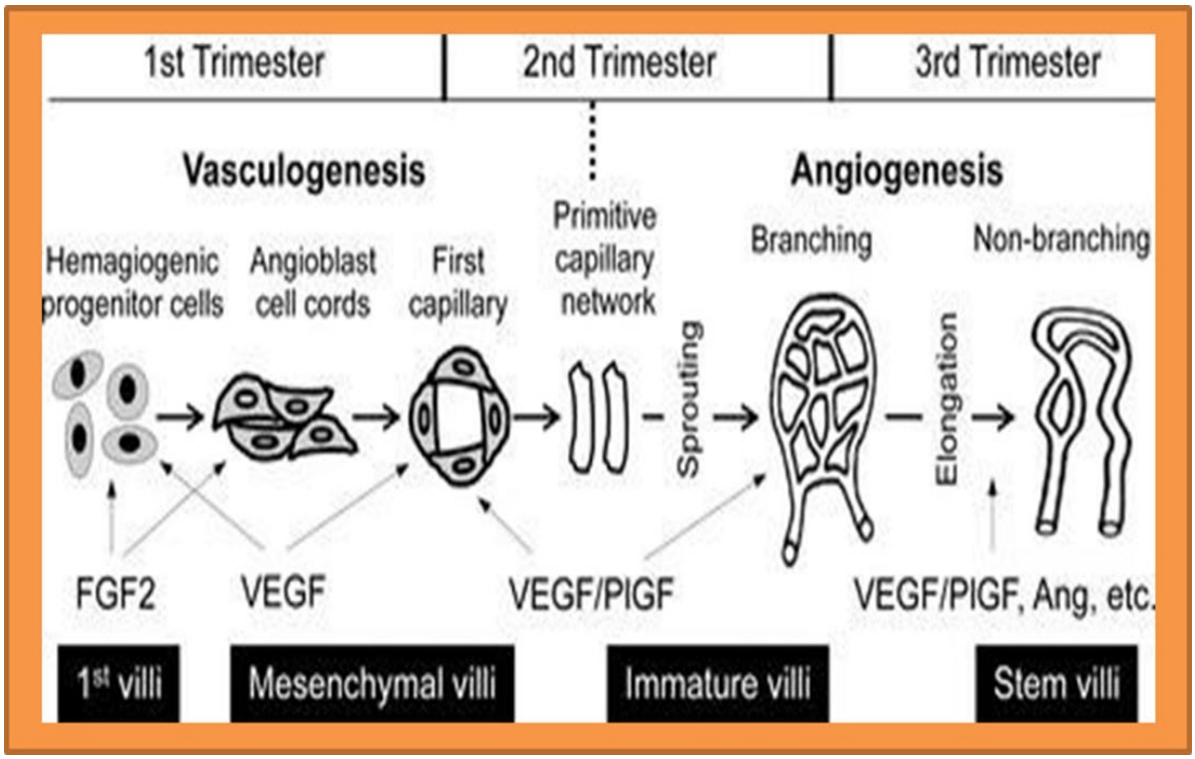

Figure 1.11 Schematic representation of the sequential regulation of vasculogenesis and angiogenesis during human placental development.
As illustrated in the diagram different growth factors influence vasculogenesis / angiogenesis throughout gestation outlined in detail in section **1.4.1.2** Taken from Chen and Zhen (2013) [27].

1.3.1.2 Angiogenesis

During pregnancy extensive angiogenesis occurs in both maternal and fetal placenta tissues [93]. Two different forms of angiogenesis: branching (the formation of new vessels by sprouting) and non-branching (the formation of capillary loops through elongation) have been observed in the placenta in the last third of pregnancy (**Figure 1.11**) [32, 95]. The initial branching angiogenesis occurs prior to 24 weeks post conception and onwards till term non- branching angiogenesis occurs [95].

As erythrocytes are detected, the process of vascularisation switches mainly to sprouting and non-sprouting angiogenesis within the placental villi, although some vasculogenesis is still taking place until late first trimester and early second trimester [96]. Endothelial cells from pre-existing vessels migrate, and sprout to form new ones, filling up the expanding immature intermediate villi [97]. Each immature intermediate villus consists of stroma, abundant macrophages and a dense capillary network [92, 98]. Distal immature

intermediate villi revert into their parent (mesenchymal villi) to sustain their generation, while proximal ones progressively transform into stem villi. Centrally located capillaries within the fibrous stroma of the stem villi, differentiate into arterioles and venules while peripheral ones regress [92].

At this stage the developing embryo receives nutrients via vitelline circulation from the yolk sac as the placental circulation remains inactive. The yolk sac is an extraembryonic membrane attached to the ventral surface of the embryo [99]. By 24 weeks, reversion of distal immature intermediate villi to mesenchymal villi stops and mesenchymal villi switch to production of mature intermediate villi while residual immature intermediate villi are incessantly converted into stem villi. Histologically, mature intermediate villi possess straight elongated capillaries [92]. These capillaries grow longer than the mature intermediate villi and subsequently form loops which further develop into highly vascularised grape-like gas-exchanging structures – the terminal villi [44, 92] as seen in **Figure 1.12**. Within the terminal villi, vessels continue to grow by the multi-stage process of non-sprouting/non-branching angiogenesis. In the third trimester, terminal villi formation by non-branching angiogenesis increases (**Figure 1.11**), causing a massive increase in the surface area available for materno-fetal exchange to about $13m^2$ at term, with up to 25% of the entire fetoplacental blood volume being within the terminal villous capillaries [100].This process of vessel development, as well as maturation of intermediate villi and development of new terminal villi, continues during the third trimester till term [55].

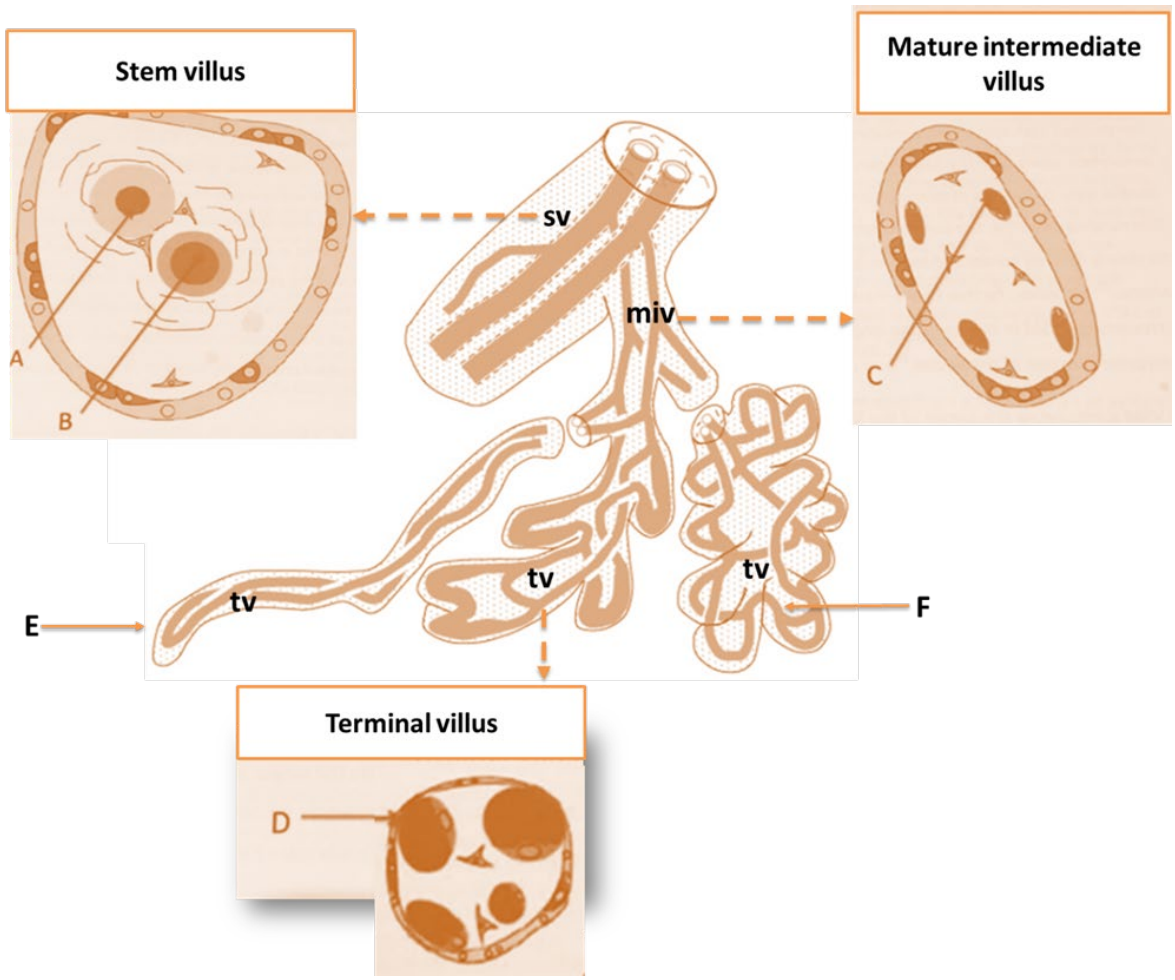

Figure 1.12 3D Patterns of villous development and cross section of three classes of term villi.

The 3 distinct classes of villi within the architecture of term placenta and 3D structure of vascular systems within the villus. SV; largest villi are the stem villi located internally, next to the inner surface of the chorionic plate and range between 150 -1000> microns in luminal diameter **A:** central placental artery of SV with thick vascular smooth muscle surrounding lumen **B:** central placental vein of SV with thin vascular smooth muscle surrounding lumen. MIV; the stem villi branch into slender intermediate villi measuring 60 – 100µm in diameter, these contain a very loose stroma and slender small calibre arterioles and venules (the post-capillary venules) with poorly defined or absent muscular walls. Arteriole and venule sizes are widely variable; the smallest ones measure 20 – 40µm in diameter **C**: small longitudinal capillaries of the MIV. TV; the intermediate villi branch into numerous terminal villi. These are grape-like terminal branches of the villous tree measuring 30 – 80µm containing a loose stroma rich in highly coiled capillaries. Their mean diameter ranges between 12 – 14µm, and they are characterised by areas of focal dilatation (sinusoids) measuring up to 50µm in diameter. **D**: the vasculo-syncytial membrane of the TV with thin layer of overlaying syncytiocytotrophoblast**. (E-F**):TV of the MIV from term placenta with varying degrees of vascularisation. **E**:abnormal development (excessive non-branching angiogenesis).**F**: abnormal development (excessive branching angiogenesis)[44, 94, 101]. Adapted from Charnock-Jones et al. (2003).

1.3.2 Regulators of Placental Vasculature development: Angiogenic Growth factors:

The key processes of vasculogenesis and angiogenesis are regulated by different growth factors considered in detail below [30, 93, 95, 102, 103].

Table 1.4A : Angiogenic factors and receptors, their function and location in the placenta

Angiogenic Factors and Receptors	Function	Placental Site	Ref.
VEGF-A	Regulate placental vasculogenesis and angiogenesis in paracrine and/or autocrine manners	Trophoblast, Hofbauer cells, vascular smooth muscle	[94, 104]
VEGF-B	Specific function in placenta development has not been defined.	None detected	[94]
VEGF-C	Mediates angiogenesis in the placenta. facilitate immune tolerance of human uterine NK cells at the maternal-fetal interface	Decidual natural killer cells	[94, 105]
VEGF-D	Lymphangiogenesis	None detected	[94] [106]
PlGF	Stimulates angiogenesis to control trophoblast growth and differentiation	Trophoblast	[94, 104, 106]
FGF-1 **FGF-2**	promote endothelial cell proliferation and vasculogenesis.	Trophoblast and vascular smooth muscle	[94, 107, 108]
Ang-1	Maintains vessel integrity and plays a role in the later stages of vascular remodelling	Villous trophoblast and perivascular cells	[94]
Ang-2	Functions to loosen cell-cell interactions and allow access to angiogenic inducers such as VEGF	Villous trophoblast	[94]
PDGF	Stimulates growth and migration of endothelial cells. Recruitment of pericytes required for stabilisation and maturation of blood vessels	Villous stroma	[109]
TGFβ	Inhibition of proliferation and invasiveness extravillous trophoblasts, and stimulation of differentiation by inducing multinucleated cell formation	Syncytiotrophobl-ast cells of the placental villi	[110, 111]

Table 1.4B: **Angiogenic factor receptors, their function and location in the placenta**

Angiogenic Factor receptors	Function	Placental Site	Ref.
VEGFR-1 (flt-1)	Vasculogenesis Angiogenesis	Villous endothelial cells and trophoblast	[94]
VEGFR-2 (kdr):	Vasculogenesis Angiogenesis	Villous endothelial cells	[94]
VEGFR-3 (flt-4)	Lymphangiogenesis	Trophoblast	[94]
Soluble VEGFR-1 (sflt-1)	sFlt-1 inhibits angiogenesis regulating blood vessel growth through reduction of free VEGF and PlGF concentrations.	Trophoblast	[94]
FGFR1	Activate signal transduction pathways, such as the MAPK cascade, and stimulate mitogenesis, differentiation, and cell migration	Villous stroma	[112]
FGFR2		Villous stroma and cytotrophoblast	[112, 113]
FGFR3		Villous stroma and cytotrophoblast	[112]
FGFR4		Villous stroma	[112]
Tie-1	Promote growth and migration during placental development. Activates signaling pathways to initiate angiogenesis Regulation of vascular smooth muscle cell recruitment.	Villous endothelial cells and trophoblast Syncytiotrophobl-ast	[94]
Tie-2		Syncytiotrophoblast and cytotrophoblast	
PDGFRα (PDGFRA) and -Rβ (PDGFRB)	Regulate trophoblast proliferation in the human placenta.	Syncytiotroph-oblast and cytotrophoblast	[114]
TGFβR I		Microvillus membrane, syncytiotroph-oblast, and cytotrophoblast	[110, 111, 115]
TGFβR II		Syncytiotroph-oblast	[111, 115]
TGFβR III		Expressed in the decidua	[110]
TGFβR IV		Microvillus membrane	[111]

[Tables adapted from (Charnock-Jones et al. 2004)]

1.3.2.1 Vascular Endothelial Growth Factor (VEGF)

The VEGF family of growth factors, originally known as vascular permeability factor (VPF),[116] includes important signalling proteins involved in both vasculogenesis and angiogenesis throughout gestation. The VEGF family consists of five members in mammals: VEGF-A, placenta growth factor (PlGF), VEGF-B, VEGF-C and VEGF-D (**Table 1.4A**). All members of the VEGF family stimulate cellular responses by binding to tyrosine kinase receptors (the VEGFRs) shown in **Figure 1.13** on cell surfaces, causing them to dimerize and become activated through transphosphorylation, although to different sites, times, and extents. VEGF-A, VEGF-C and placenta growth factor (PlGF) are all expressed in different sites within the human placenta. VEGF-A is expressed in trophoblast, macrophages and vascular smooth muscle cells and stimulates endothelial expression of proteases such as urokinase-type and tissue-type plasminogen activators and interstitial collagenase that break down extracellular matrix and release endothelial cells from anchorage, allowing them to migrate and proliferate. [94, 104]. During normal pregnancy, human placental VEGF expression increases with gestational age. VEGF has been shown to regulate all steps of the angiogenesis process as shown in **Figure 1.11** [27].

1.3.2.1.1 PlGF

PlGF is an angiogenic factor of the VEGF family, discovered by Maglione et al. in 1991 [117]. PlGF and its receptor VEGFR-1 (flt-1), are expressed in trophoblast [94]. PlGF functions to control trophoblast growth and differentiation. The secretion of PlGF by trophoblast cells has been reported to be the signal that initiates and coordinates vascularisation in the decidual and placenta during early embryogenesis [118]. Studies have reported PlGF stimulates angiogenesis by moving VEGF from the VEGFR-1, hence increasing the fraction of VEGF available to activate VEGFR-2 (**Figure 1.14**). Alternatively, PlGF may also stimulate angiogenesis by transmitting intracellular signals through VEGFR-1. Angiogenic functions of PlGF include; binding to VEGFR-1 in endothelial cells which facilitates VEGF binding and activation of VEGFR-2; recruitment of monocytes/macrophages to promote vessel growth; and mobilizing hematopoietic progenitor cells from bone marrow [119]. In the placenta , placental growth factor (PlGF) is critically important for the formation of the placental capillary network via sprouting and elongation (**Figure 1.11**) with the development of the

villous tree. PlGF and VEGF-A are also known to form a PlGF/VEGF heterodimer which is a highly potent endothelial mitogen [73]. The synergism between VEGF and PlGF is hypothesized to contribute to both physiological angiogenic processes and pathological plasma extravasation [119]. The synergism between PlGF and VEGF is specific; PlGF deficiency is reported to impair the cell response to VEGF [120].

Carmeliet et al. (2001), reported that in PlGF −/− cells, VEGF only induced endothelial migration by 25%, proliferation by 40% and survival by 7% compared to PlGF +/+ endothelial cells [120]. Additionally, high concentrations of PlGF alone did not affect the response of wild-type endothelial cells to VEGF, because these cells already produced sufficient PlGF. However, at low doses, PlGF dose-dependently restored the impaired VEGF-response in PlGF −/− endothelial cells. This suggests that, PlGF though ineffective alone, amplifies the VEGF response by activating VEGFR-1 [120]. Levels of PlGF concentrations in maternal serum rise during pregnancy, peaking at the end of mid trimester of pregnancy. Low levels of PlGF concentrations during pregnancy are associated with pregnancy complications including recognized later-life cardiovascular risk [121]. A growing body of evidence also point to (PlGF), measurable in the maternal circulation, as a maternal serum biomarker for placenta disease [122-125].

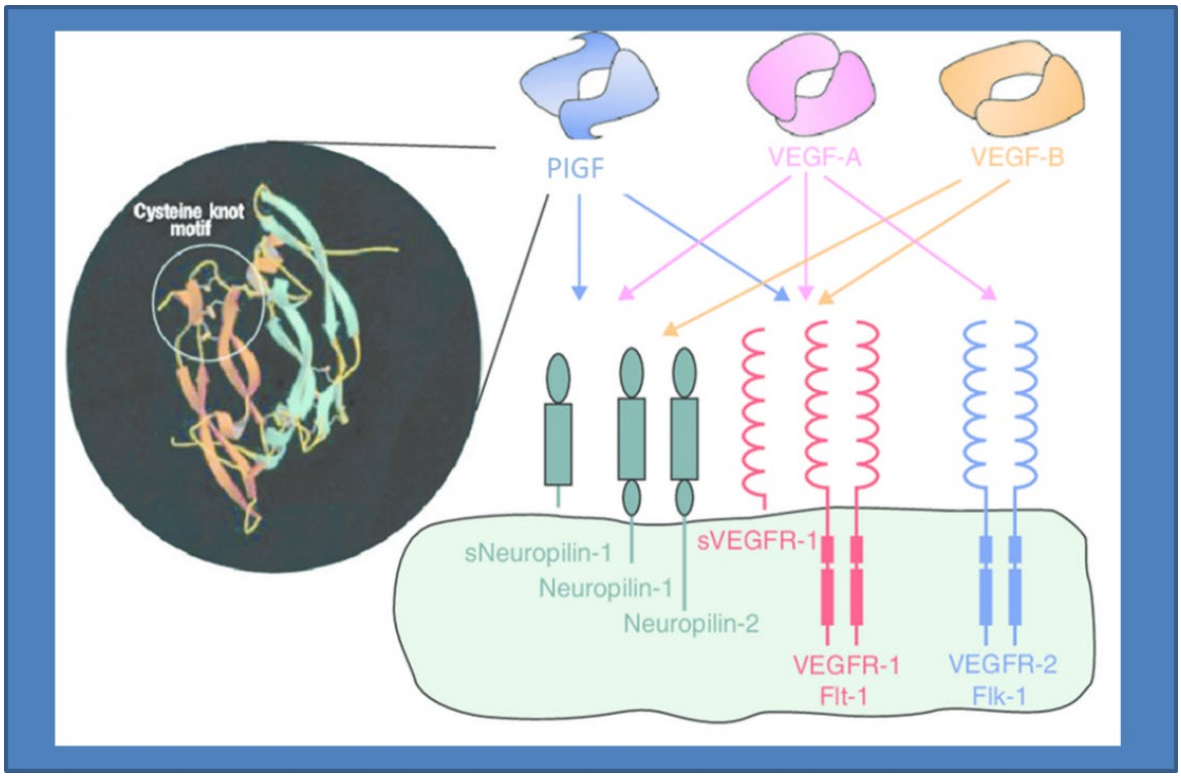

Figure 1.13 Structural model of human placental growth factor (PIGF)-1, VEGF-A and VEGF-B.

Schematic representation of the binding of homodimers of PlGF, vascular endothelial growth factor (VEGF)-A, and VEGF- B to their respective receptors. Adapted from Nguyen et al. (2016) [126].

1.3.2.1.2 VEGF Receptors

VEGFRs are typical tyrosine kinase receptors (TKRs) carrying an extracellular domain for ligand binding, a transmembrane domain, and a cytoplasmic domain, including a tyrosine kinase domain. The overall structure of VEGFRs is similar to that of the PDGFR family members; however, these 2 receptor families have clear differences: the PDGFR extracellular domain contains 5 immunoglobulin (Ig)–like domains, whereas VEGFRs bear 7 Ig-like domains. The biological functions of VEGF polypeptides are mediated upon binding to type III receptor tyrosine kinases (RTKs), VEGFR-1 (Flt-1), VEGFR-2 (KDR/Flk-1) and VEGFR-3 (Flt-4) [127]. They consist of seven extracellular immunoglobulin (Ig)-like domains, a transmembrane (TM) domain, a regulatory juxtamembrane domain, an intracellular tyrosine kinase domain interrupted by a short peptide, the kinase insert domain, followed by a sequence carrying several tyrosine residues involved in recruiting downstream signalling molecules [128]. These receptors are expressed on the cell surface of many bone-marrow-derived cells such as hematopoietic cells , macrophages and endothelial cells, on

some malignant cells [129] and on vascular smooth muscle cells (VSMCs) [130] . In the placenta , VEGF receptors are expressed in villous endothelial cells and trophoblast (**Table 1.4B**) and play a role in angiogenesis i.e. regulating blood vessel growth through reduction of free VEGF and PlGF concentrations. VEGF-A and its receptors VEGFR-1 and VEGFR-2 play major roles in physiological as well as pathological angiogenesis, including tumour angiogenesis. VEGF-C/D and their receptor VEGFR-3 can regulate angiogenesis at early embryogenesis but mostly function as critical regulators of Lymphangiogenesis [127, 131]. VEGF-A has a variety of functions, including pro-angiogenic activity, vascular permeability activity, and the stimulation of cell migration in macrophage lineage and endothelial cells. Furthermore, under pathological conditions, synergism between PlGF and VEGF-A has been shown to contribute to angiogenesis [120].

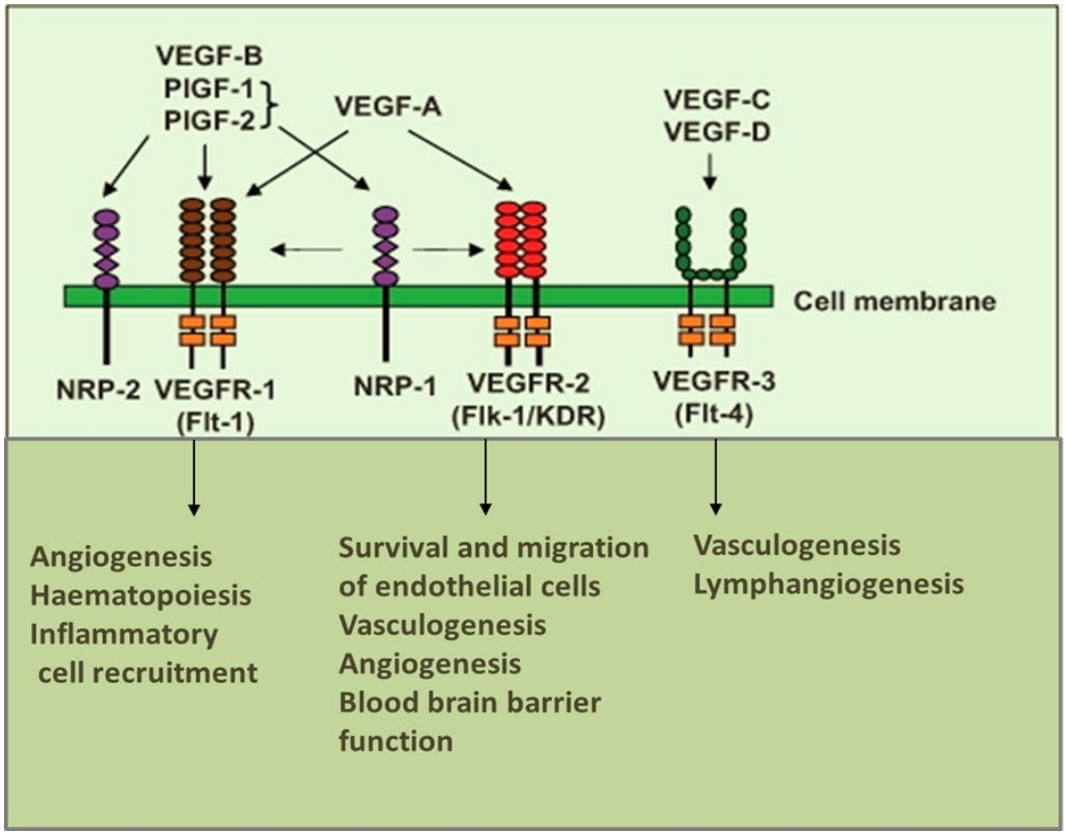

Figure 1.14 Schematic of VEGF family molecules and their receptor interactions, signalling and functions.

VEGF-A binds to both VEGFR-1 and VEGFR-2. VEGF-B, PlGF-1 and -2 bind to VEGFR-1. VEGF-C and VEGF-D bind to VEGFR3. PlGF-1 and -2 also bind to neuropilin 1 and 2 (NRP-1 and NRP-2). Activation of VEGFR-1, VEGFR-2, and VEGFR-3 leads to autophosphorylation and coupling to the intracellular signal transducer and induce vasculogenesis, angiogenesis, and lymphangiogenesis, respectively. Adapted from Wang and Zhao, (2010) [119]

1.3.2.2 Fibroblast growth factor family

The fibroblast growth factors (FGF) are a family of cell signalling proteins that are involved in a wide variety of processes, most notably as crucial elements for normal development. These growth factors generally act as systemic or locally circulating molecules of extracellular origin that activate cell surface receptors [132]. In humans, 22 members of the FGF family have been identified, all of which are structurally related signalling molecules [132, 133]. Members FGF1 through FGF10 all bind fibroblast growth factor receptors (FGFRs). FGF1 is also known as acidic fibroblast growth factor, and FGF2 is also known as basic fibroblast growth factor. The mammalian fibroblast growth factor receptor family has 4 members, FGFR1, FGFR2, FGFR3, and FGFR4 (**Table 1.4B**). The FGFRs consist of three extracellular immunoglobulin-type domains (D1-D3), a single-span trans-membrane domain and an intracellular split tyrosine kinase domain. FGF-1 and -2 are co-localised in first trimester cytotrophoblast cells and extravillous trophoblast and in the endothelial cells and smooth muscle cells of placental vessels by term (**Table 1.4A**). In the placenta, FGF2 regulates the formation of angioblasts along with the formation of the first mesenchymal villi as shown in **Figure 1.11** [107, 108, 134].

1.3.2.3 Angiopoietin

Angiopoietin is part of the vascular growth factors family with roles in embryonic and postnatal angiogenesis. The angiopoietin (Ang) family of growth factors includes four members, all of which bind to the endothelial receptor tyrosine kinase Tie2 [135, 136]. Two of the Angs, Ang-1 and Ang-4, activate the Tie2 receptor, whereas Ang-2 and Ang-3 inhibit Ang-1-induced Tie2 phosphorylation. Angiopoietin signalling most directly corresponds with angiogenesis; angiogenesis proceeds through sprouting, endothelial cell migration, proliferation, and vessel destabilisation and stabilisation [137]. Ang-1 and Ang-2, are expressed in the placenta [138]. Ang-1 is expressed in the villous trophoblast and perivascular cells while Ang-2 is expressed solely in the villous trophoblast (**Table 1.4A**). They are responsible for assembling and disassembling the endothelial lining of blood vessels [139]. Angiopoietins are involved in upregulation to facilitate the expansion of placental vascular network during the third trimester [27]. Ang-1 induces vessel maturation. Ang-2 cooperates with other angiogenic factors in the induction of sprouting angiogenesis. Ang-2 appears to antagonize Ang-1 function by preventing its binding to Tie-

2 receptors. Tie-1 heterodimerizes with Tie-2 and antagonizes Ang-1-mediated vessel maturation. Angiopoietin-1 is critical for vessel maturation, adhesion, migration, and survival. Angiopoietin-2, on the other hand, promotes cell death and disrupts vascularisation [140]. However, when it is in conjunction with vascular endothelial growth factors, it has been reported it can promote neo-vascularisation [120, 137].

1.3.2.4 PDGF

Platelet-derived growth factor (PDGF) is also a member of growth factors that regulate cell growth and division. In particular, PDGF plays a significant role in blood vessel formation, the growth of blood vessels from already-existing blood vessel tissue [104, 131]. Platelet-derived growth factor is a dimeric glycoprotein that can be composed of two A subunit (PDGF-AA), two B subunits (PDGF-BB), or one of each (PDGF-AB). There are five different isoforms of PDGF that activate cellular response through two different receptors. The known ligands include; PDGF-AA (PDGFA), -BB (PDGFB), -CC (PDGFC), and -DD (PDGFD), and -AB (a PDGFA and PDGFB heterodimer). The ligands interact with the two tyrosine kinase receptor monomers, PDGFRα (PDGFRA) and -Rβ (PDGFRB) The PDGF family also includes a few other members of the family, including the VEGF sub-family [137, 141]. PDGF binds to the PDGFR ligand binding pocket located within the second and third immunoglobulin domains. Upon activation by PDGF, these receptors dimerize. The auto-phosphorylation of several sites on their cytosolic domains, which serve to mediate binding of cofactors then subsequently activate signal transduction. PDGF plays a role in embryonic development, cell proliferation, cell migration, and angiogenesis [142]. In the human placenta, PDGF is expressed in the villous stroma [109]. It induces angiogenesis by signalling via two receptors (α and β) to stimulate growth and migration of endothelial cells. In addition, PDGF is involved in recruitment of pericytes required for stabilisation and maturation of blood vessels [143-145].

1.3.2.5 TGFB

Transforming growth factor beta (TGFβ) is one of the growth factors that have been reported to play significant roles in both vasculogenesis and angiogenesis and is therefore essential for development and homeostasis of the vascular system. TGFβ drives vascular responses via its binding to a TGFβ receptor complex formed by type I and type II receptors, as well as type III co-receptors present on both endothelial and mural cells [146]. The transforming growth factor beta (TGF-beta) has been reported as a vital regulator of placental development and functions; TGF-beta exerts several modulatory effects on trophoblast cells, such as inhibition of proliferation and invasiveness, and stimulation of differentiation by inducing multinucleated cell formation in the placenta [147] [148].

In summary, studies have shown that throughout gestation, placental expressions of angiogenic factors mentioned above and in **Table 1.4** play significant roles in regulating angiogenesis (**Figure 1.11**) and contributing to increased efficiency in coordinating development of the vascular system via sprouting and elongation in the placental villi as shown in **Figure 1.11** [27]**.** Experimental animal studies have also highlighted the importance of the regulation of angiogenesis and vasodilatation of the uterine and placental vessels as the two key mechanisms that increase placental blood flow during late gestation, which is paramount for normal fetal growth and development [28, 29]. Reports suggest that most regulatory growth factors and cytokines of placental vasculogenesis and angiogenesis such as vascular endothelial growth factor (VEGF), fibroblast growth factor (FGF-2), angiopoietins, placental growth factor (PlGF), tumour necrosis factor-α (TNF-α), interleukin 8 (IL-8) and insulin- like growth factors 1 and 2 (IGF1, IGF2) outlined in **Table 1.5** are altered in maternal diabetes mellitus [95]. These reports suggest that the diabetic environment alters the expression and levels of these angiogenic factors affecting their roles and function in vasculogenesis and angiogenesis. Insulin and IGFs are implicated in the regulation of fetal and placental growth and development. IGF1 and IGF2 are synthesized in placental mesenchymal cells, such as macrophages and endothelial cells, with little change throughout gestation. However, while IGF1 is present in the trophoblast compartment at all gestational stages, IGF2 is not found in the syncytiotrophoblast and its expression in villous and extravillous cytotrophoblast in the first trimester becomes undetectable at term of gestation [149].

1.3.3 Abnormal angiogenesis in diabetes: regulatory factors

The effects of diabetes on the macrovasculature in relation to larger calibre vessels remains poorly reported. Diabetes predispose individuals to the development of macrovascular complications of diabetes through complex molecular pathways that involve hyperglycaemia and insulin resistance [150]. Macrovascular complications of diabetes are affect the coronary arteries, peripheral arteries, and cerebrovasculature [150]. Early macrovascular disease is associated with atherosclerotic plaque in the vasculature supplying blood to the heart, brain, limbs, and other organs. Late stages of macrovascular disease involve complete obstruction of these vessels, which can increase the risks of myocardial infarction (MI), stroke, claudication, and gangrene [151]. Although macrovascular disease in diabetes is multifactorial, the common recipient of injury reported in the literature is the vascular endothelium via impairing the ability of the vasculature to vasodilate through inhibition of the nitric oxide (NO) pathway [152].

As discussed earlier, diabetes mellitus has been associated with abnormalities in angiogenic processes (excesses or defects) with both contributing to critical features of chronic diabetic vascular complications that result in severe clinical consequences [36]. For example, diabetic retinopathy (**Figure 1.15**), a secondary microvascular complication of diabetes mellitus, is attributed to two major retinal problems that cause the majority of the diabetes related vision loss: diabetic macular oedema and complications from abnormal retinal blood vessel growth characterised by pathologic ocular angiogenesis [153].

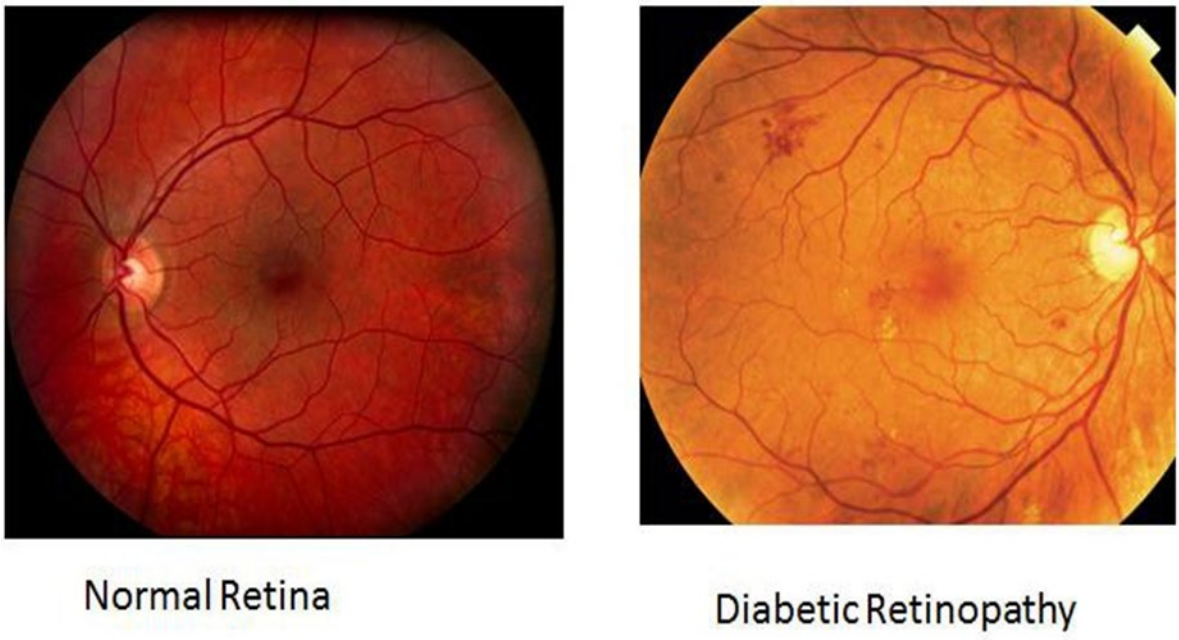

Figure 1.15 Image of Normal retina and Diabetic retinopathy
Normal Retina: The fovea (the dark red spot in the centre), the healthy pink retinal colour, and normal blood vessels surrounding it without any bleeding. Background Diabetic Retinopathy: The red spots of bleeding and yellow spots of cholesterol leakage throughout the retina with increased neovascularisation (abnormal blood vessel growth). (Taken from © 2017, Eye Physicians of North Houston) [154].

Diabetic retinopathy can be classified into two stages: nonproliferative and proliferative. Secondary to angiogenesis, it has been reported that increased retinal blood flow plays a key role in the progression of diabetic retinopathy [153]. Understanding the role of hyperglycaemia seems to be the most critical factor in regulating retinal blood flow, as increased levels of blood glucose are thought to have a structural and physiological effect on retinal capillaries causing them to be both functionally and anatomically incompetent. However, studies have shown that high blood glucose induces hypoxia in retinal tissues, thus leading to the production of VEGF-A (vascular endothelial growth factor protein). The main mechanism is through hypoxia and AGEs (advanced glycosylation products); AGEs correlate with prolonged hyperglycaemia and produce ROS (reactive oxygen species) and ROS increases VEGF expression. Hypoxia also induces HIF-1α (hypoxia inducible factor), which stimulates production of VEGF and VEGF receptors. VEGF leads to mitogenic effect

and proteolysis of basement membrane that is the first stage of angiogenic process and causes proliferative diabetic retinopathy [155]. Hypoxia is a key regulator of VEGF induced ocular neovascularisation. A study reported 69 of 136 samples of ocular fluid from patients with diabetic retinopathy contained detectable levels of VEGF and concentrations were higher in those patients with signs of retinal disease [156]. These findings suggest that the balance between VEGF and angiogenic inhibitors may determine the proliferation of angiogenesis in diabetic retinopathy [153]. Therapies with anti-VEGF agents such as ranibizumab and bevacizumab shows that VEGF through several mechanisms play a role in the pathogenesis of diabetic macular oedema [157, 158]. Early studies have also reported increased expression of placenta growth factor in proliferative diabetic retinopathy. Specimens from patients with either proliferative diabetic retinopathy or macular hole observed that PIGF immunoreactivity was intensely localized to the endothelial and perivascular regions of newly formed blood vessels of excised fibrovascular preretinal membranes. Intense localisation of PIGF protein was also observed in superficial retinal vessels in diabetic retinae adjacent to neovascular preretinal membranes. Localisation of PIGF was weak or absent in diabetic retinae that showed no evidence of neovascular proliferation. PIGF protein was also absent in normal retinae suggesting an implicate role for PIGF in the pathogenesis of proliferative diabetic retinopathy [159].

Similarly, in diabetic nephropathy there is evidence that excess and abnormal angiogenesis occurs early in diabetic kidney disease (DKD) [160]. In both human and experimental animal studies, abnormal capillaries were observed to contribute to glomerular hypertrophy, forming anastomoses with peritubular capillaries [161, 162]. VEGF-A overexpression induced by hyperglycaemia and shear stress in DKD was also reported as a compensatory attempt to reduce intraglomerular pressure, as newly formed vessels were often found to bypass the glomerulus connecting to peritubular capillaries [36]. In addition to VEGF-A, an imbalance of angiopoietin-1 and angiopoietin-2 was also reportedly associated with abnormal regulation of angiogenesis in DKD [163]. A recent review on angiogenic abnormalities [36] associated with diabetes suggest that mechanisms influencing angiogenesis in diabetes include defective responses to hypoxia and proangiogenic factors, impaired NO signalling, shortage of proangiogenic cells, and loss of pericytes. The findings also suggest that exposure to high glucose directly affects angiogenic and or vasculogenic processes.

1.3.3.1 Altered Angiogenic factors in maternal diabetes and consequences for aberrant fetoplacental vasculature and or vascular dysfunction

Pregestational diabetes and gestational diabetes are associated with altered expression/levels of angiogenic factors (**Table 1.4**) which could modulate vasculogenesis and angiogenesis in the fetoplacental vasculature depending on the onset of the disease [77, 164-169]. Reports suggest that most regulatory growth factors and cytokines of placental vasculogenesis and angiogenesis such as vascular endothelial growth factor (VEGF), fibroblast growth factor (FGF-2), angiopoietins, placental growth factor (PlGF), tumour necrosis factor-α (TNF-α), interleukin 8 (IL-8) and insulin- like growth factors 1 and 2 (IGF1, IGF2) are altered in maternal diabetes mellitus as summarised below in **Table 1.5**.

Table 1.5 Altered expression and levels of proangiogenic factors in different types of maternal diabetes

Angiogenic Factors	Type of Diabetes	Placenta	Cord
VEGF	GDM T1DM	↓protein [170] =mRNA [171]	↓[89] ↓[165]
PIGF	GDM T1DM	↓protein [170] =mRNA [171]	↓[89] ↓[165]
FGF	GDM T1DM	↑mRNA and protein [172] ↑mRNA and protein [173, 174] ↑protein[175] =mRNA [171]	↑[172],[166] ↑[166]
Angiopoietin	GDM T1DM	↓protein [176] =mRNA [171]	
PDGF	GDM	↑mRNA[177]	
TFGβ			
Erythropoietin	GDM T1DM		↑[178] [89]] ↑[178, 179]
IL6	GDM T1DM	↑mRNA [180]	↓[29]
TNF-α	GDM	↑protein [181] ↑mRNA [176] =mRNA [180]	=[182] ↓[29]
Insulin	GDM T1DM		↑[183-186] ↑[[85, 179, 184]
IGF1	GDM	=mRNA [172] ↓mRNA [176]	↑[172, 187, 188]
	T1DM		=[85]
	IDDM		↑[189]
	T2DM		=[187]
	D	=mRNA [190]	↑[190]
IGF2	GDM	↑mRNA [176]	↑[169] =[188]
	IDDM		↑[169, 189]
	D	=mRNA [190] ↓peptide [190]	↑[190]

↑ indicates elevated levels, ↓ indicates reduced levels, and = indicates unchanged levels

in diabetes. GDM: gestational diabetes mellitus; T1D: type 1 diabetes; T2D: type 2 diabetes; IDDM: insulin dependent diabetes mellitus without further classification; D: diabetes without further classification. Data from Cvitic et al.,2014 [149].

The evidence provided in a review also concludes on the premise that, as dissecting the molecular regulators of the different tissue-specific alterations of angiogenesis and vasculogenesis remains a tasking challenge in devising new therapeutic approaches, glycaemic control remains the most realistic therapeutic strategy to normalize angiogenesis in diabetes [36]. It is also hypothesized that there could be an intersection between micro and macro vascular complications, in which microvascular complications distinctly precede macrovascular complications. However, whether complications in both vessel types progress simultaneously still remains elusive [151].

Studies have attempted to elucidate the underlying causes of abnormalities in fetal growth caused by maternal diabetes and their direct/indirect effects on altering angiogenic factors important in regulating placental vasculature development.

Placental blood flow determines the transport of flow-limited substances such as oxygen and glucose [191, 192]. Efficient uteroplacental and fetoplacental circulation is crucial for the maintenance of physiological fetal growth. Abnormalities of placental blood flow have been associated with adverse fetal outcomes in disorders such as preeclampsia, intrauterine fetal growth restriction, and poorly controlled pregestational diabetes mellitus [193-195]. A study on uteroplacental blood flow index in the diabetic pregnant women, reported that the maternal-placental blood flow index was reduced 35% to 45% compared to that in healthy women. The blood flow index tended to be further impaired in those diabetic women who had higher blood glucose values [196]. In addition, some placentas from pregnancies complicated by type 1 diabetes have shown fibrinoid necrosis and atherosis in their decidual bed, as observed in preeclampsia [197]. There is a relationship between the severity of this pathology and abnormal uterine arcuate artery systolic/ diastolic ratios in type 1 diabetic patients [198]. Pietryga et al. (2005) demonstrated significantly increased uterine artery vascular impedance in pregnant women with type 1 diabetes with vasculopathies. Abnormal uterine artery Doppler was related to pregestational vasculopathies and adverse perinatal outcomes. This study's results also suggested that, the uterine arteries affected in women with clinical signs of pregestational

vasculopathies may influence placental perfusion and fetal well-being [199]. This could also suggest that impairment of uteroplacental circulation is a primary pathology in the placentas of women with severe vasculopathies and changes in the umbilical artery may occur later as an adaptation to reduced uteroplacental perfusion [200, 201]. Changes in maternal placental blood vessels during the course of pregnancy under the influence of hyperglycaemia have been considered as characteristic for microangiopathic diabetic [202]. Thickening of basement membranes, proliferation of endothelial cells, and disarrangement in perivascular space with increase of collagen, proteoglycans, and glycosaminoglycans are reported characteristic vessel changes as a consequence of hyperglycaemia [203].

Another hypothesis to account for abnormalities in fetal growth associated with diabetes was proposed by Pedersen (1967). The hypothesis stated that "maternal hyperglycaemia results in fetal hyperglycaemia and, hence, in hypertrophy of fetal islet tissue with insulin-hypersecretion. This again means a greater fetal utilisation of glucose. This phenomenon will explain several abnormal structure and changes found in the newborn" [204]. This hypothesis focuses on trophoblast delivery of glucose to the fetus. However, maternal hyperglycaemia, or fluctuating glucose levels modulates vascular development and may directly influence or possibly affect placental vascular permeability and function.

1.3.3.2 Hyperglycaemia

Hyperglycaemia is defined as an excessive amount of glucose circulating in the blood plasma (has been defined by the World Health Organisation as blood glucose levels greater than 7.0 mmol/L (126 mg/dl) when fasting and blood glucose levels greater than 11.0 mmol/L (200 mg/dl) 2 hours after meals) [5]. Studies on the placenta in diabetes (GDM and T1DM), have shown reduced and unchanged levels of proangiogenic factor VEGF expression respectively as highlighted in **Table 1.5** [170, 171]. However, hyperglycaemia has been reported to affect regulation of angiogenesis by inducing expression of inhibitory genes to promote neovascularisation via increased production of reactive oxygen species (ROS) and production of advanced glycation end products (AGEs) (**Figure 1.16**) leading to increase in VEGF mRNA expression and has direct effects by acting as pro-constrictor, proangiogenic, pro-permeability and pro- inflammatory agent [205]. Molecular pathways

such as the Protein Kinase C (PKC) pathway are also affected by high glucose. Animal studies have also reported that, the rise in blood glucose causes a de-novo synthesis of diacylglycerol in various tissues in the rat, which in turn causes an increase in the production of PKC [40, 88, 89, 206-208]. This increase in PKC production triggers the increased release of several growth factors such as VEGF that contribute to altered placental angiogenesis [41, 208-211].

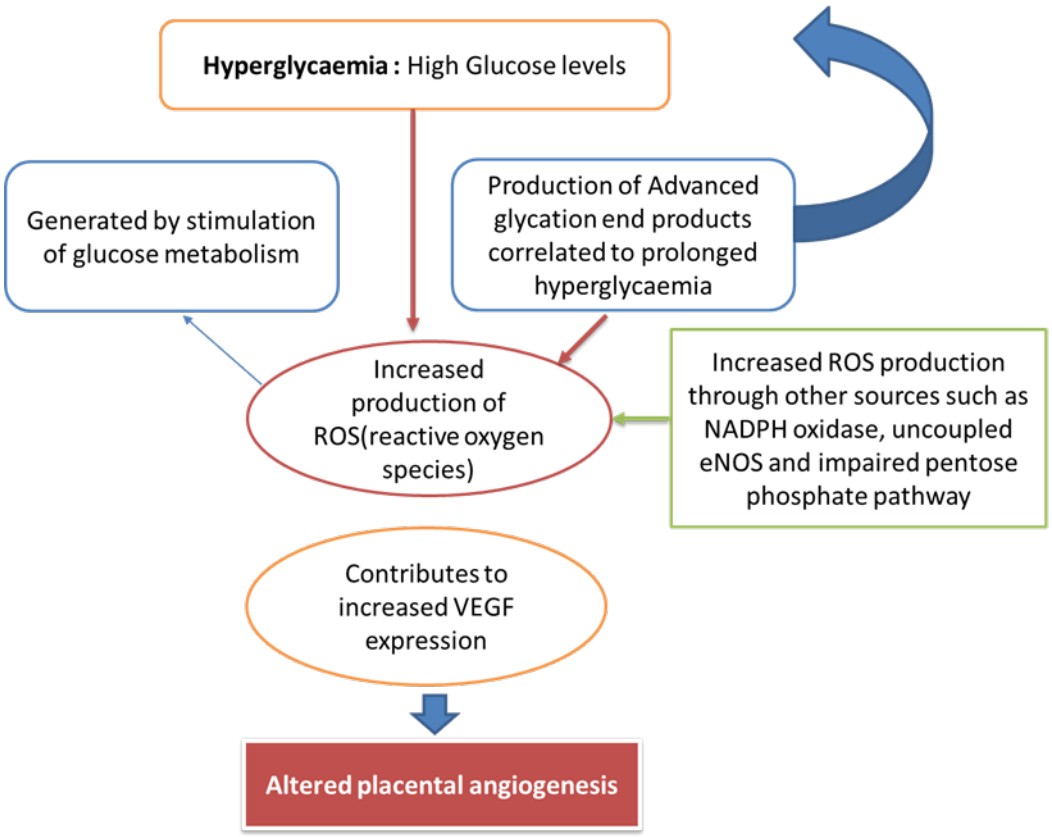

Figure 1.16 Scheme to show summary of mechanisms proposed to link maternal hyperglycaemia to abnormal fetoplacental angiogenesis.
Schematic diagram summarising effects of hyperglycaemia in contributing to altered angiogenesis via increased production of ROS in response to other factors such as formation of advanced glycation end products (AGE's) and its role in altered expression of growth factors (VEGF) that may influence placenta development (angiogenesis) and function.

While maternal insulin does not cross the placenta [212-214], maternal glucose freely passes to the fetus along its concentration gradient and stimulates secretion of insulin from the fetal pancreas. Fetal growth directly depends on the nutrients crossing the placenta.

Glucose serves as the primary source of energy for metabolism and growth of fetoplacental tissues. Glucose crosses the placenta and is transported by facilitated-diffusion glucose transporters, based on the concentration-dependent kinetics [215]. A sodium-independent transport system for D-glucose has been identified in the microvillous (apical) and basal plasma membrane of the syncytiotrophoblast The transport system has a high capacity and is saturable only at maternal concentrations ≥20mmol/L [216]. Several glucose transporters have been identified in the human term placenta (GLUT-1, GLUT-3, GLUT-4,GLUT-8, GLUT-12) [215, 217-219]. GLUT-1 and GLUT-8 are ubiquitously expressed in all cells of the human placenta. GLUT-1 is the predominant transporter on the trophoblast, with a 3:1 asymmetric distribution between the microvillous and basal membrane [219] and accounts for glucose uptake into the trophoblast and subsequent transfer to the fetus. GLUT-3 as well as the insulin-sensitive glucose transporters GLUT-4 and GLUT-12 are predominantly located on the fetal aspect of the placenta (i.e. endothelial cells and stroma), where they may facilitate glucose uptake from the fetal circulation [220, 221].

Glucose transport in the placenta is regulated by the extracellular (maternal) glucose concentration and GLUT expression and activity in the microvillous membrane (glucose uptake) and basal membrane (glucose delivery) [222]. Glucose uptake into fetal tissues is regulated by glucose transporters that increase or decrease in response to both acute and chronic changes in fetal glucose concentration and conditions of intrauterine growth restriction[223]. Acevedo et al. (2005) demonstrated that insulin and nitric oxide (NO) stimulate glucose uptake in human placenta and suggested that both potential regulators of glucose transport use different signalling pathways[224]. GLUT-I is regulated by ambient glucose levels.

Hyperglycaemia reduces GLUT-1 transcript and protein levels (SI) and translocates GLUT-1 from the surface to intracellular sites [225], resulting in a loss of functional GLUT-L on the

trophoblast surface. This loss of GLUT-1 at the cell surface alters glucose uptake. The GLUT-1 response to hyperglycaemia is found at term but nor in the first trimester [226]. Insulin is essential for regulating intracellular and plasma levels of glucose in peripheral tissues, such as adipose tissue, skeletal muscle, and liver, via mechanisms that include Akt/PKB and mitogen-activated kinase (MAPK) pathways. The activation of the insulin signalling pathway in the placenta is associated with control of cell survival, differentiation, proliferation, and metabolism of primarily amino acids, and, in a gestational age-specific manner, to the transfer of glucose[213]. In the first trimester of pregnancy, placental glucose transfer is enhanced by insulin; while during the third trimester glucose uptake is not regulated by insulin [227].

Thus, maternal hyperglycaemia subjects the fetus to a state of hyperinsulinemia and hyperglycaemia, thought to be the major contributing factor for adverse perinatal outcomes associated with maternal diabetes [149]. However, despite good glycaemic control some pregnant women with diabetes of any classification GDM, type 1 or type 2, deliver large or macrosomic fetuses [228]. This questions whether the Pedersen hypothesis reflects the whole story. The role of hyperglycaemia in pregnancies complicated by diabetes present one possible explanation for the range of complications observed in diabetes. Studies have shown that the principle complication of fetal macrosomia as a consequence of pathological changes observed in placentas from pregnancies complicated by diabetes cannot be fully accounted for by maternal hyperglycaemia. For example, the incidence of fetal macrosomia in a non-selected prospective nationwide cohort of 289 Type I diabetic women with good glycaemic control (i.e. mean HbA(1c) <or=7.0%) was as high as 48.8%, with 26.6% of infants weighing more than 97.7th percentile [228]. The Pedersen hypothesis also does not account for other disparate outcomes such and FGR and stillbirths reported in maternal diabetes.

1.3.3.3 Hyperinsulinaemia

Hyperinsulinaemia has been suggested as contributing to altering placental angiogenic factors and thus altered placental vascular development and dysfunction. Hyperinsulinaemia is defined as elevated circulating insulin in relationship to its usual level relative to blood glucose. Studies have suggested that fetal insulin is involved in the control of placental angiogenesis and permeability of the vasculature as evidence points to the enhancement of VEGF protein expression and secretion by insulin (**Figure 1.17**) [149, 229, 230]. This may explain excessive placental vascularisation in conditions of fetal macrosomia [231]. Clinical trials have shown that acute intensive insulin therapy exacerbates diabetic blood retinal barrier breakdown via activation of the hypoxia inducible factor-1alpha (HIF-1α)/VEGF pathway and is accountable for blindness [230]. Retinal HIF-1α levels increase as a result of intensive insulin therapy and this promotes HIF-1α translocation into the nucleus, which in turn increases VEGF mRNA expression and protein synthesis via the PI3-kinase and mitogen activated protein kinase (MAPK) pathways. Activation of PI3-kinase/Akt can upregulate the expression of HIF-1α, which in turn increases VEGF expression through a direct interaction with the VEGF promoter [211, 230]. Elevated fetal insulin could modulate fetoplacental vascular development in maternal diabetes because receptors are expressed on fetoplacental endothelium. Insulin and IGF receptors are expressed on distinct placental surface cell types, specifically in the mesenchymal cells such as macrophages and endothelial cells, with minimal changes throughout gestation [229].

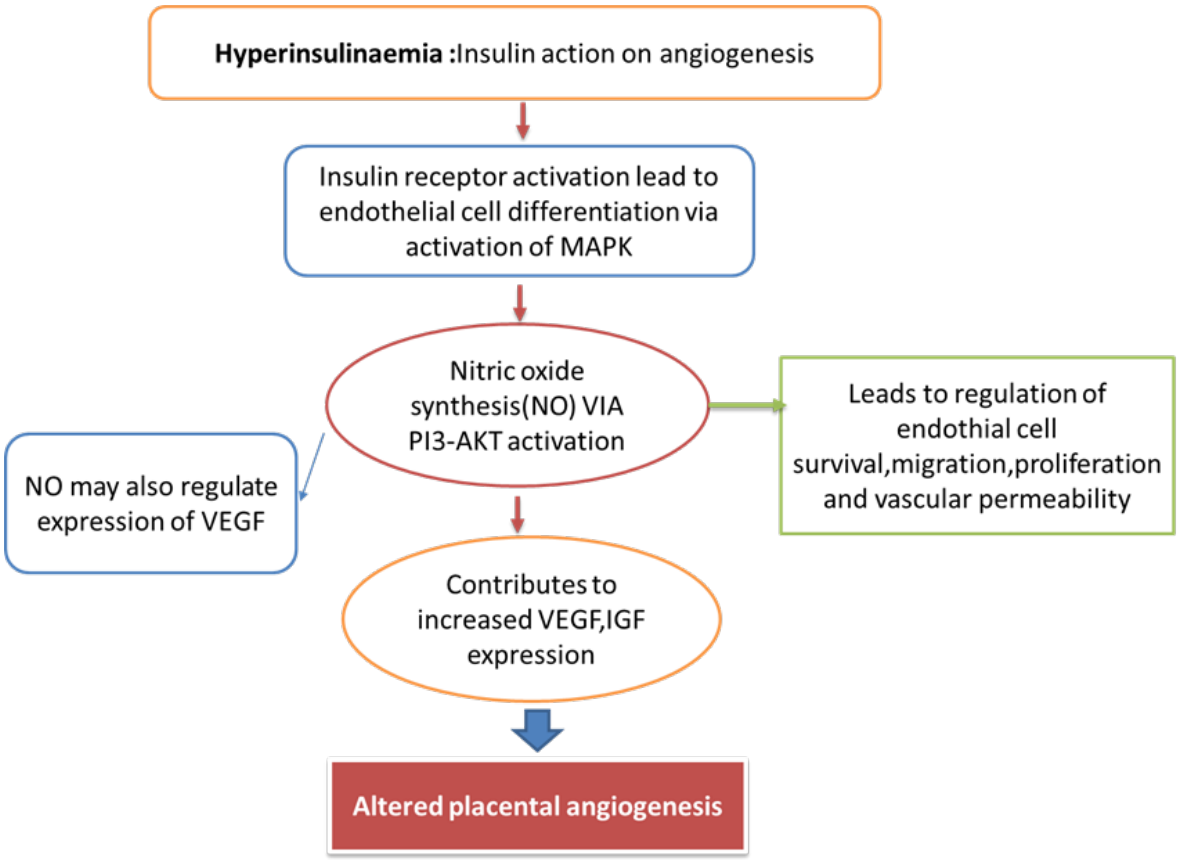

Figure 1.17 Scheme to show summary of mechanisms proposed to link fetal hyperinsulinaemia to abnormal fetoplacental angiogenesis.

Schematic representation demonstrating how fetal hyperinsulinaemia could impact on fetoplacental angiogenesis through effects on nitric oxide activation and altered expression of growth factors. Insulin receptor activation stimulates endothelial cell differentiation via activation of mitogen activated protein kinase (MAPK) pathways. This activates nitric oxide synthesis via activation of PI3-kinase/Akt. This can upregulate the expression of HIF-1α, which in turn increases VEGF expression and possibly altered placental angiogenesis [231].

1.3.3.4 Advanced Glycation End products (AGEs)

There is growing evidence on the effects of advanced glycation end products (AGEs) on the expression of key receptors in endocrine regulation of placental development. AGEs are biochemical end products of non-enzymatic glycosylation in diabetic patients with poor glycaemic control [232]. The formation of these products has been shown to play significant roles in the pathogenesis of microvascular complications of diabetes via formation of cross-links between endogenous molecules such as lipids and nucleic acids in the basement membrane of the extracellular matrix and by engaging the receptor for advanced glycation end products (RAGE) [233]. The activation of RAGE by AGEs causes upregulation of the transcription factor nuclear factor-kappaB and its target genes. AGEs in the basement membrane inhibit monocyte migration. Monocytes/macrophages are the major players in collateral formation. Studies have shown that VEGF-dependent monocyte function is severely impaired in diabetic patients [234]. AGEs in diabetes cause defective VEGF signalling including inactivation of the VEGF receptor, FLK-1, which affects endothelial growth and migration, monocyte, and EPC recruitment. AGE-bound RAGE increases endothelial permeability to macromolecules and blocks nitric oxide activity in the endothelium resulting in impairment in angiogenesis [233, 235] [236].

1.3.3.5 Oxidative Stress

Oxidative stress is another factor that may contribute to the proinflammatory environment of diabetes and affect angiogenesis. There is increased expression of markers of chronic oxidative stress such as 8-isoprostane, increased activity of superoxide dismutase and glutathione peroxidase, or elevated levels of malondialdehyde (MDA) in placentas from pregnancies complicated by diabetes [233, 237]. The effects of oxidative stress on angiogenesis has been well documented in pathologies such as TDM2 [35]. As with the other hyperglycaemia-induced mechanisms, high glucose levels and AGEs formation leads to the generation of excess ROS via multiple mechanisms including increased flux through the polyol and hexosamine pathways and protein kinase C (PKC) activation. Pathological angiogenesis is initiated by demands for oxygen resulting in a hypoxia/reoxygenation cycle, which, in turn promotes the formation of reactive oxygen species(ROS). ROS stimulates the induction of VEGF expression in various cell types, such as endothelial cells, smooth muscle

cells, and macrophages [35] [238]. However, the increased levels of ROS impair endothelial function by depleting NO availability and causing oxidative damage to cellular DNA, lipids and proteins [239]. Studies show indices of oxidative damage are elevated in maternal, placental and fetal tissues from maternal diabetes pregnancies [89, 240, 241]. For example, studies of placental tissue extracted from GDM pregnancies also reported higher protein carbonyl content, a marker of protein oxidation, and exhibited greater release of 8-isoprostane, an indicator of lipid peroxidation [237]. *In vitro* studies have also demonstrated that high glucose treatment in cultured isolated endothelial colony forming cells from cord blood of normal pregnancy reproduced the abnormal proliferative and migratory properties observed in GDM-derived cells [242]. Similarly, *in vitro* high glucose exposure increased markers of oxidative stress and enzymatic sources of ROS in HUVECs collected from normal pregnancy [243] [244].

1.3.3.6 Inflammation

In many pathologies, it has been established that oxidative stress induced angiogenesis and inflammation are intimately related [245, 246]. Oxidative stress is coupled with heightened inflammation, as there is a high degree of intersection between redox and inflammatory signalling pathways. Through activation of redox sensitive transcription factors, ROS regulate the gene expression of several pro-inflammatory molecules including cytokines, cell adhesion molecules (CAM), and Cox-2, a major mediator of vascular inflammation. Indeed, amplification of pregnancy-induced immune activation is common to GDM pregnancies. Increased circulating concentrations of pro-inflammatory cytokines including tumour necrosis factor-α (TNF-α), interleukin-6 (IL-6) and monocyte chemoattractant protein-1 (MCP-1) have been reported in women diagnosed with GDM (**Table 1.5**). Inflammatory cells release proangiogenic growth factors, including vascular endothelial growth factor (VEGF) [247, 248], which facilitate neovascularisation. Newly formed blood vessels enhance inflammatory cell recruitment, thereby promoting chronic inflammation, which is a key hallmark in complications of diabetes [245].

During normal pregnancy, each trimester is associated with a distinctive pattern of placental cytokine expression necessary for the various stages of placentation [229]. This tightly regulated balance in placental expression of pro-inflammatory and anti-inflammatory mediators is disrupted in maternal diabetes, as demonstrated by studies

showing altered cytokine production (**Table 1.5**). The findings suggest that the placenta serves as a barrier to limit exposure of pro-inflammatory signalling molecules derived from the placenta or maternal tissues to the fetus [222]. *In vitro* studies on HUVECs observed pro-inflammatory phenotype in HUVECs collected from GDM pregnancies, which was marked by heightened monocyte adhesion and increased CAM levels after cells were treated with TNF-α [249]. HUVECs from normal pregnancies exposed to intermittent high glucose were observed to increase expression of CAMs, intercellular adhesion molecule-1 (ICAM), vascular cell adhesion molecule 1 (VCAM-1) and E-selectin [250].

These metabolic disorders mentioned above that have been reported as mechanisms underlying altered angiogenesis, abnormal placenta vasculature and potential contributors to adverse fetal outcome in maternal diabetes, are common to maternal obesity. Maternal obesity is present in the majority of maternal diabetes cases specifically GDM and has also been independently reported to predict fetal macrosomia [25].

1.3.3.7 Obesity

Currently, it has been widely documented that there is an association between increased incidence of obesity and pregnancies complicated by maternal diabetes especially increasing incidence of type 2 diabetes. The majority of women of reproductive age with pre-existing diabetes now consist of women with type-2 rather than type-1 diabetes [251]. Obesity presents metabolic symptoms both in pregnancy and the non-pregnant population which involves an inflammatory milieu, where macrophages in the adipose tissue produce cytokines that affect post receptor insulin signalling which results in increased insulin resistance [252]. Pregnancy itself is an inflammatory condition, very possibly initiated to allow immuno-tolerance of the fetus by the mother [253]. Therefore, heightened inflammation has become an important factor in understanding the mechanisms that characterize increased insulin resistance in pregnancies [25]. Research studies continue to explore some of the unknown mechanisms that underpin diabetic complications in the non-pregnant population and their contribution (**Figure 1.18**) to altered fetoplacental vascular development in pregnancies complicated by maternal diabetes.

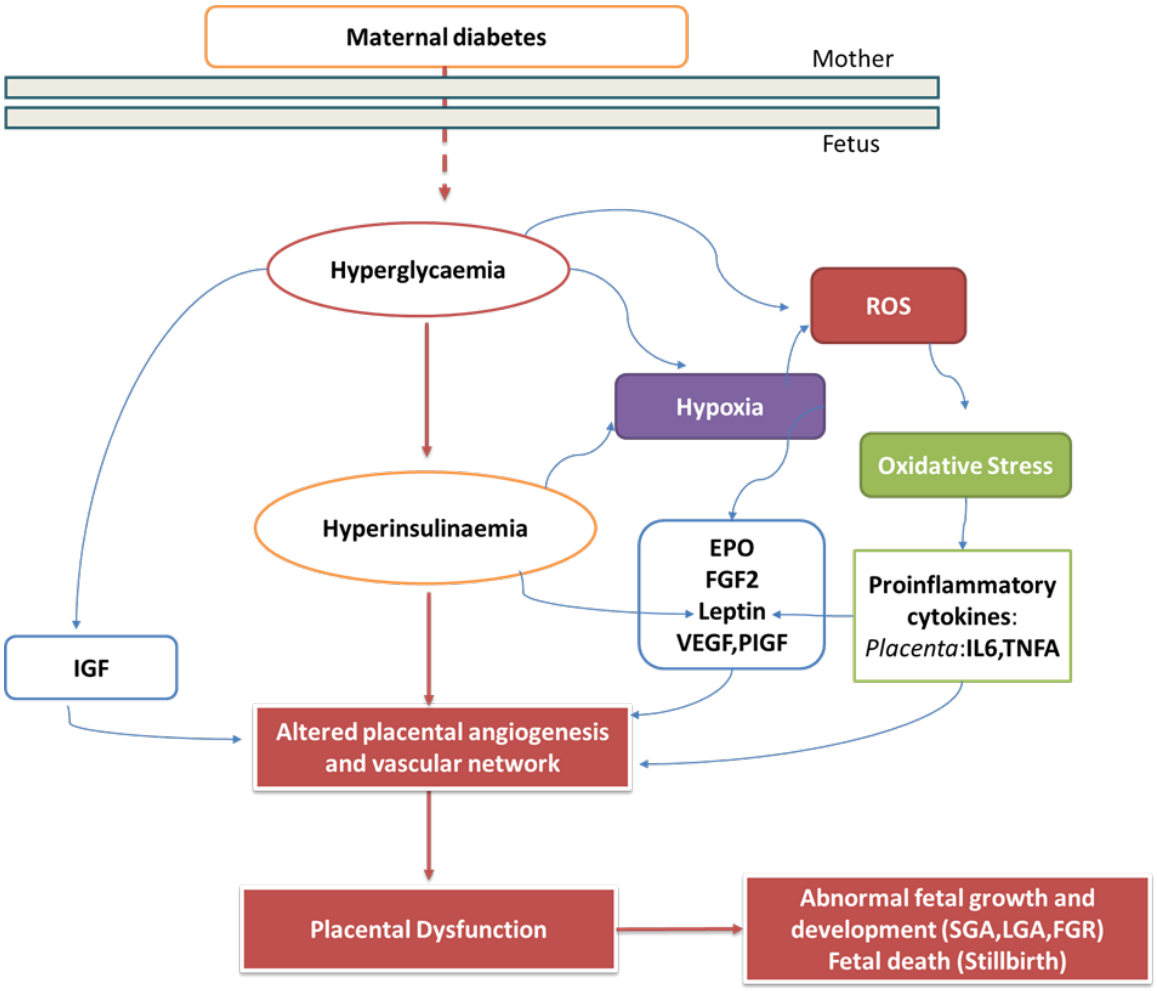

Figure 1.18 Scheme to summarise mechanisms that could link maternal diabetes to abnormal fetoplacental vascular development, placental dysfunction and fetal growth disorders.

Schematic representation of hypothesis that takes into consideration the factors in a diabetic environment *in utero* such as hyperglycaemia, hyperinsulinemia and other external factors that might arise in response to this environment (oxidative stress, inflammation and hypoxia).The schematic describes their roles in altered expression of growth factors that may induce metabolic, hormonal, and inflammatory changes that lead to placental hypervascularisation or influence the development and function of placenta. The resultant adverse outcomes that might lead to long term health implications are also highlighted. Factors such as Leptin are regulated by multiple aspects of the fetal diabetic environment. In pregnancies complicated by maternal diabetes mellitus, placental leptin production and fetal plasma leptin is increased. TNF-α and IL6 upregulate leptin expression in trophoblasts *in vitro* [254]. EPO also involved in regulation of angiogenesis during embryonic development, mitogenesis, and stimulation of circulating endothelial progenitor cells. Adapted from Cvitic et al. 2014 [149].

The schematic in **Figure 1.18** illustrates the complexity of factors that could contribute to altered fetoplacental vascular network formation/angiogenesis in situ in maternal diabetes. The mechanisms proposed in **Figure 1.18** could be further modulated in utero by diabetes pharmacological treatment metformin discussed in section **1.5**.

1.4 Early Pregnancy and the need for early intervention

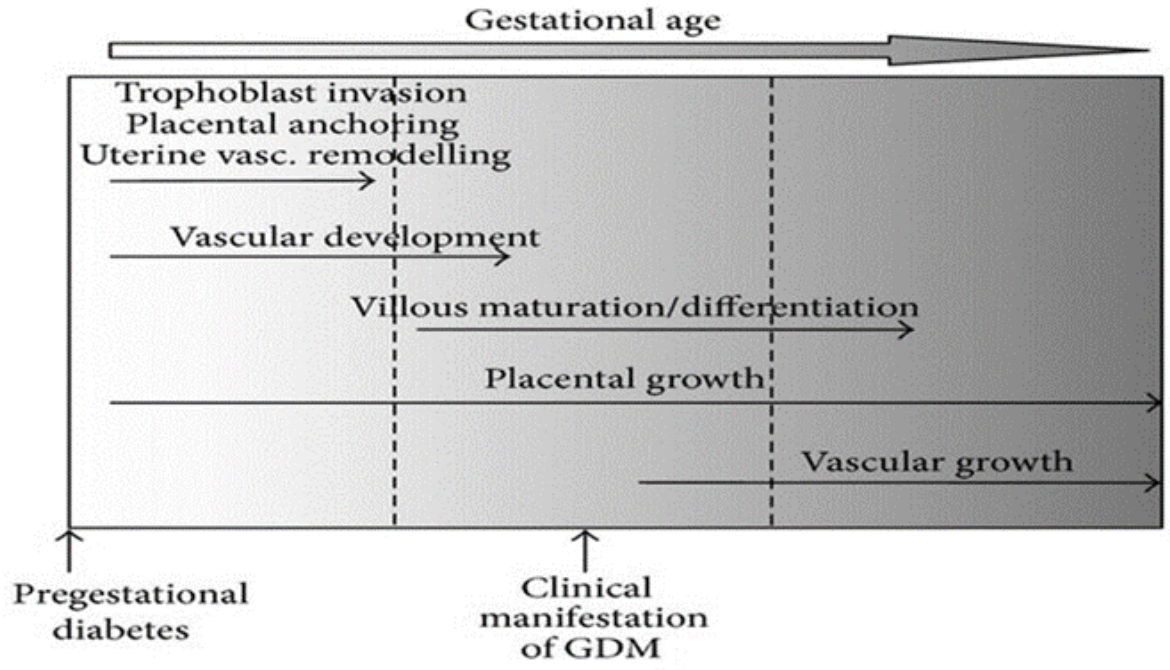

Figure 1.19 Placental development and windows of metabolic insults in maternal diabetes
Schematic representation of specific windows of placental development susceptible to metabolic insults of pregestational and gestational diabetes, respectively. Taken from Cvitic et al. (2014) [149].

The effects of factors that characterise diabetic complications on the early processes in vasculogenesis and angiogenesis is unclear hence further studies are required to highlight the specific impact of these factors (i.e. hyperglycaemia, hyperinsulinaemia, oxidative stress etc.) in placenta development in the first trimester. The placenta is reported to be sensitive to the hyperglycaemic milieu and responds with adaptive changes in the structure

and function of the trophoblasts [255]. In rat the most vulnerable time for the fetus is in early pregnancy, when just three injections of high glucose in early pregnancy caused an increase in fetal weight at term [256]. Similarly, placentomegaly and fetal macrosomia at the end of gestation is a distinct feature of many diabetic pregnancies which also indicates that there is a period of accelerated placental growth in these pregnancies as seen in placental growth in diabetic rats [257]. This observation may also support or parallel reported findings on the biphasic growth pattern of the fetus in T1DM pregnancies [258]. Subsequently, observations on the fetoplacental vasculature made at delivery will reflect earlier events in vessel development, but most of these observations have not yet been related to factors such as fetal growth velocity, umbilical blood flow velocity, maternal serum concentrations of placental derived growth factors in early pregnancy and importantly longitudinal glycaemic control. Determining whether altered fetoplacental vascular structure at term is related to fetal growth, maternal serum biomarkers and glycaemic control earlier in pregnancy could lead to the development of targeted interventions in the first trimester to restore normal fetal growth.

1.5 Treatment, Control and Implications

There is no known preventive measure against pregestational diabetes Type 1 and insulin is administered in management of the disease. Type 2 diabetes, which accounts for the majority of cases [4] can sometimes be prevented or delayed, with assertive lifestyle choices such as healthy diets, physical activity to maintain healthy body weight and avoidance of key risk factors such as smoking [2]. There is international consensus over the importance of tight glucose control before conception and throughout pregnancy to optimise pregnancy outcomes. Given that early pregnancy is a time of enhanced insulin sensitivity, it is important to have good glycaemic control throughout pregnancy. The situation rapidly reverses by approximately 16 weeks as insulin resistance increases exponentially during the second and early third trimesters [149]. The insulin requirement levels off toward the end of the third trimester with placental aging. A rapid reduction in insulin requirements can indicate the development of placental insufficiency [239]. In normal pregnancies and women with normal pancreatic function, insulin production is sufficient to meet the challenge of this physiological insulin resistance and to maintain normal glucose levels [149]. However, in women with diabetes, hyperglycaemia occurs if

treatment is not adjusted appropriately. A recent Cochrane systematic review was not able to recommend any specific insulin regimen over another for the treatment of diabetes in pregnancy [259]. Insulin therapy and medications such as metformin are used in management of pregnancies characterised by maternal diabetes.

1.5.1 Insulin

Although developing evidence supports the use of glyburide or metformin in the management of pregestational and gestational diabetes, many guidelines continue to recommend insulin as the first-line therapy. In pregnancy, this could in part be as a result of safety data indicating clinically insignificant amounts of human insulin that cross the placenta [6, 260]. The physiology of pregnancy requires frequent titration of insulin to match changing requirements and underscores the importance of daily and frequent self-monitoring of blood glucose. Due to the complexity of insulin management in pregnancy, referral to a specialized centre offering team-based care is usually recommended [261].

Evidence from clinical trials demonstrated that insulin compared with usual prenatal care in the management of GDM resulted in decreased numbers of births associated with shoulder dystocia, macrosomia, and preeclampsia [262] .

1.5.2 Metformin

Although in diabetes, many pathways and mechanisms that underlie altered vasculature are involved in ROS-induced endothelial dysfunction, few effective antioxidant approaches have achieved clinical success. Traditional antioxidant therapy has been reported to be inefficient at alleviating oxidative stress during diabetes [263]. Metformin, a biguanide compound, exerts its clinical effect by both reducing hepatic glucose output and by increasing insulin sensitivity [264]. This results in a decreased glucose level without an associated high risk of either hypoglycaemia or weight gain[265, 266]. These characteristics have established metformin as an ideal first-line treatment for individuals with type 2 diabetes and, hypothetically, a particularly attractive drug for use in pregnancy. Evidence shows that metformin, a blood sugar lowering agonist, decreased fetal mortality in type 2 diabetes [3, 6]. Studies also showed that metformin improved vascular endothelial functions and insulin sensitivity in patients with type 2 diabetes [267] and also decreased

expression of VCAM-1, E-selectin and PAI-1, which was not related to changes in glycaemic control [268].Likewise, other clinical studies also demonstrated the endothelial protective effects of metformin in patients with diabetes with findings that reported decreased weight, BMI, systolic blood pressure, and fasting plasma glucose, and improved lipid profile. Endothelium-dependent forearm blood flow (FBF) responses were also improved [269].

Conversely, there are studies that report metformin has no significant effects on endothelium in patients with type 2 diabetes in the non-pregnant population [270]. The UK Prospective Diabetes Study demonstrated that although monotherapy with metformin and also sulfonylureas or insulin can achieve good glycaemic control initially, sustained control with these agents fails in 50% of patients after three years [271].

In addition, whereas insulin crosses placenta very sparingly if at all, metformin is known to cross the placenta, and its use in pregnancy has been limited by concerns regarding potential adverse effects on both the mother and the fetus [272]. There is controversy over the value of metformin as a treatment for dysregulated angiogenesis in type 2 diabetes in non –pregnant individuals [273]. This highlights the potential need for multiple therapies which target different aspects of diabetic abnormalities to protect vascular function and obtain adequate long-term glycaemic control.

Overall, the beneficial effects of metformin have been summarised as follows; direct reduction of insulin resistance in type 2 diabetes, antioxidant effects in both types of diabetes, which ultimately increases NO bioavailability, and direct effects on vascular endothelial and smooth muscle cells causing vasorelaxation [267]. All of these effects are reported to subsequently improve endothelial dysfunction in diabetes. A recent review also reports metformin can promote or inhibit angiogenesis [273]. Insulin and metformin could alter trophoblast production/secretion of angiogenic factors. The potential effects of insulin +/- metformin and high/fluctuating (unstable) glucose levels on the processes of angiogenesis have yet to be determined.

1.6 Summary

It has been widely documented that in pregnancies complicated by maternal diabetes there is a corresponding increase in incidence rates of complications and adverse fetal outcomes (SGA, LGA, fetal macrosomia and stillbirth) [13, 14, 23]. This places a considerable burden on healthcare systems in managing the increasing number of pregnancies complicated by obesity and diabetes. However, the relationship between maternal diabetes and poor perinatal outcome remains poorly understood with knowledge gaps in the underlying mechanisms that directly influence placental development in a diabetic environment such that the fetus is at increased risk of placental dysfunction in late pregnancy. The vascular development of the placenta plays a very important role in adequate fetoplacental blood flow to optimise nutrient delivery to the fetus and transfer of fetal metabolites to mother by placental syncytiotrophoblast. This process is reliant on the appropriate development of fetoplacental blood vessels from early pregnancy to term by vasculogenesis and angiogenesis [30, 94, 95, 274].

Diabetes in the non-pregnant population is associated with vascular pathology including altered vascular development and function. Diabetes mellitus has been associated with abnormalities in angiogenic processes (excesses or defects) with both contributing to critical features of chronic diabetic vascular complications in the microvasculature and "macrovasculature" [36, 275]. The processes of vasculogenesis and angiogenesis are regulated by different growth factors such as VEGF, PIGF, insulin/IGF system, which are essential to the process of vascular development [27, 30]. In diabetes, vascular complications that result in severe clinical consequences such diabetic retinopathy, diabetic neuropathy, diabetic nephropathy, impaired wound healing have been associated with altered angiogenic factors [35, 276]. By analogy similar mechanisms could underlie altered development and function of blood vessels in the placenta in pregnancies complicated by maternal diabetes. Previous studies and investigations were hampered by small sample numbers and sizes, insufficient clinical characterisation and monitoring and the lack of a holistic, full organ approach to characterisation of the vascular anatomy of the placenta in diabetes.

In contrast to the microvasculature, there is very little information on the impact of maternal diabetes on network formation by the larger calibre arteries and veins of the chorionic plate, responsible for delivery of blood to and from the vessels that regulate blood flow at the sites of maternal-fetal nutrient exchange. Furthermore, it is not known whether vascular networks at term are related to fetal outcome, or to maternal glycaemic control or maternal circulating angiogenic factors earlier in diabetic pregnancy. It is also important to determine the potential for interactions between the maternal and fetal environment in regulating angiogenesis in maternal diabetes (i.e. maternal hyperglycaemia alone and in conjunction with fetal hyperinsulinemia) and whether these effects are modulated by maternal therapy (e.g. metformin). Identifying factors that underlie altered placental vascularity in pregnancies complicated by diabetes and relating longitudinal changes in maternal glycaemia to vascular structure of placenta at term and fetal outcome may point to potential areas for more appropriate interventions

Currently, therapeutic measures for management of diabetes in pregnancy have failed to make impact on reducing poor pregnancy outcomes such as fetal growth restriction (FGR), large for gestational age (LGA), macrosomia and stillbirth [264, 271, 277-279]. This suggests that these measures are not addressing the underlying pathology and/or are missing specific windows of therapeutic benefit during pregnancy. This highlights the need for therapies which target different aspects/manifestations of diabetic abnormalities to protect vascular function while maintaining adequate long-term glycaemic control.

Determining relationships between fetoplacental vascular networks, fetal outcome, maternal glucose control and maternal serum levels of angiogenic factors could improve understanding of the origins of these disparate poor pregnancy outcomes in diabetes and facilitate targeted and timely interventions in the future.

1.7 Hypothesis

The overarching hypothesis for this study is that in maternal diabetes, hyperglycaemia and/or other components of the diabetic environment *in utero* in early pregnancy may influence placental vascular development increasing risk of placental dysfunction, aberrant fetal growth and stillbirth in late pregnancy.

1.7.1 Aims

The study had three main research aims:

1. To determine whether there are differences in placental macrovascular networks at term in women with pregestational diabetes compared with normal pregnancy
2. To determine whether metrics of the placental macrovascular network at term are related to fetal growth, maternal glycaemic control and maternal plasma PIGF concentrations in women with pregestational diabetes
3. To determine whether hyperglycaemia +/-insulin and metformin have potential to regulate fetoplacental angiogenesis using human umbilical vein endothelial cells *in vitro*

For Aim 1, vascular corrosion casting of chorionic plate arteries and veins (150-2000µm) was used to assess placental vascular networks. Vascular casts were scanned using Micro-CT imaging, reconstructed into a three-dimensional virtual object and analysed with segmentation and skeletonisation software (Avizo 9.40) to generate quantifiable characteristics of the placental vasculature.

For Aim 2, key artery and vein network biometric outputs from Micro-CT imaging were related to birthweight, maternal glycaemic control (HbA1c measurement in first and last trimester) and maternal serum PlGF concentration measured at early, mid and late trimesters during pregnancy in diabetic women.

For Aim 3, a well-established *in vitro* model of angiogenesis, based on the ability of endothelial cells to form network structures when plated on an extracellular matrix support, was used to investigate the effects of elevated glucose concentration with and without insulin and metformin on network formation. Images of networks were taken under a light microscope (Olympus BX41) and Qcapture Image Pro® Plus 7.0 (Media Cybernetics) and cellular mesh network variables analysed using the ImageJ software with an angiogenesis analyser extension. The specific aims of each study are elaborated in detail in their corresponding chapter.

2 Chapter Two: General Methods Section

2.1 Subjects

This project focused on 2 groups of women: (1) women from the VELOCITY study with pre-gestational diabetes and women from the term tissue bank having normal pregnancy (2). Women with gestational diabetes from the term tissue bank were also recruited, their placentas were not analysed in this project.

2.1.1 Biobank sample recruitment and collection

All placenta tissues from normal pregnancies and gestational diabetes were obtained from women who delivered at St. Mary's Hospital, Manchester, United Kingdom, under Biobank ethical approval (REC 08/H1010/55). Informed consent was obtained prior to delivery and normal placentas were collected within 40- 60 minutes of delivery.

Referral criteria: Women having normal pregnancy at term >35 weeks
Exclusion criteria: Pregnancies complicated by FGR (fetal growth restriction), PE (Preeclampsia), Non singleton, Women unable to provide written informed consent and women who signed up for stem cell collection post-delivery (Anthony Nolan).

Data: Maternal age, height and weight ethnicity, smoking status, parity, mode of delivery, gestational age at delivery were recorded and body mass index was (Kg/m^2) calculated. Pregnancy outcome data were also recorded (birthweight, Individualised birthweight ratio, fetal sex and mode of delivery).

2.1.2 Velocity sample recruitment and collection

Velocity is a cohort observational study of 250 women with pregestational diabetes over the course of 5 years (commenced September 2016) and evaluates fetal growth velocity in pregnancies complicated by maternal diabetes. Over a 5-year period, women were recruited at <20 weeks gestation with pre-existing diabetes (criteria included in **Appendix 1***)* and seen subsequently at 4 weekly visits. Multiparous women, women unable to provide written informed consent and women under 16 years of age were excluded from recruitment. Maternal age, height and weight, ethnicity, smoking status, parity, mode of delivery, gestational age at delivery were recorded and body mass index was (Kg/m^2) calculated. Uteroplacental Doppler assessments, fetal biometry, placental volume and 3D fractional thigh measurements were also collected. Maternal serum HbA1c (first and last

trimester measurements) and maternal plasma PlGF levels were recorded (23,33,36 weeks; early, mid, late trimester). Continuous glucose monitoring was also conducted at 3 times points (10-16, 22-26, 30-34 weeks) and a diary of daily activity recorded. Vascular assessments, maternal blood and urine collections, pregnancy outcome data, collection of cord blood and skinfold thickness of infants at 28weeks was also taken. The detailed protocols are presented in **Appendix 1**. Placentas of women in the velocity study were collected within 40 – 80 minutes of delivery.

2.2 Demographic, clinical and gross placental examination details of subjects

The demographic and clinical details of the women and babies whose placentas were collected in total across the duration of this project including samples collected and stored for histological analysis are shown in **Table 2.1.** Statistical analysis using Mann Whitney U test demonstrated that gestational age, individualised birthweight ratio, mode of delivery and fetal sex were significantly different between women with normal pregnancies and women with pregnancies complicated by diabetes**.** Median gestational age was 273(261-295) days and 259 (217-280) days $p< 0.00001$ for the normal and pregestational diabetes pregnancy groups respectively. Median individualised birthweight ratio was 41.5(6-100) and 69 (2-100), $p=0.0067$ for the normal and pregestational diabetes groups respectively. In mode of delivery ($p=0.0359$), 1 out of 30 women within the control group having normal pregnancy had vaginal births (3.3%) and 29 out of 30 delivered via caesarean-section (96.7%). On the other hand, 18 out of 72 women with pregnancies complicated by pregestational diabetes had vaginal births (25.0%) and 54 out of 72 delivered via caesarean-section (75.0%). Fetal sex outcome for control group was 20 (66.7%) males and 10 (33.3%) females. Fetal sex outcome was 32(44.4%) males and 40 (55.6%) females, ($p=0.0392$).

Demographic details of sub-groups of women whose placentas were utilised in this project in specific studies are shown where appropriate in Chapter 3. Statistical analysis demonstrated that there were differences between the two groups from which samples were used in this project and these differences are outlined in the corresponding chapter (Chapter 3).

Table 2.1 Demographic, clinical and placental examination details of maternal and fetal donor participants.

Demographic data	Normal Pregnancies (n=30)	Pregestational diabetes Pregnancies (n =72)	*p* value
Ethnicity			
-White	20(66.7%)	32(44.4%)	
-Black	0(0.0%)	8(11.1%)	
-Asian	7(23.3%)	18(25.0%)	
-Mixed	0(0.0%)	5(6.9%)	
-Other	3(10.0%)	9(12.5%)	
Maternal age, years	34(26-48)	31(24-44)	0.39358
Maternal BMI, Kg/m^2	32.2(19.7-59.4)	28.6(20.6- 47.4)	0.1814
Gestational age at delivery, (days)	273(261-295)	259.7(217-280)	**<0.00001**
Parity			0.4965
-0	6(25%)	12(17.7%)	
-1 >	24(75%)	60(83.3%)	
Birth weight, g	3300(2780-4390)	3144(2107-4640)	0.1423
Placenta weight, g	537(375-781)	601(448.5-905)	0.28774
IBR, centile	41.5(6-100)	69(2-100)	**0.0067**
Smoking, number (%)	6/30(20.0%)	2/72 (2.8%)	0.1378
Mode of delivery, number (%)			
Vaginal	1/30(3.3%)	18/72(25.0%)	**0.0359**
Caesarean section	29/30(96.7.%)	54/72(75.0%)	
Fetal Sex			**0.0392**
Male:	20(66.7%)	32(44.4%)	
Female:	10(33.3%)	40(55.6%)	

Demographic data of all the placentas collected during this project. Values represent median and interquartile range (IQR) in parenthesis, or number with percentage in parenthesis. p-value obtained from Mann Whitney U test, $p < 0.05$ is the chosen level of significance. BMI, IBR represent body mass index and individualised birth weight ratio respectively.

2.3 Fetoplacental vascular corrosion casting

To compare fetoplacental vascular structure at term in women having normal pregnancy and pre-gestational diabetes, vascular corrosion casting was used. Vascular corrosion casts as shown in **Figure 2.1**, enables the study of the vascular pattern of normal or pathological tissues. The methods of casting and analysis of casts were followed according to published methods [58, 83]. The placenta was weighed after collection and then fetal membranes and excess umbilical cord length were trimmed off each placenta and weighed separately. Photographs were taken of the fetal and maternal sides of each placenta against a white tray background and rule for scale. Images were uploaded on to Image Pro Plus software (Media Cybernetics Inc, USA) and the software computed the surface area for each placenta based on a tracing of the placental disc outline.

The fetoplacental vasculature was perfused with a radiopaque methyl methacrylate-based casting material [Batson's No.17, Anatomical Corrosion Kit (Polysciences Inc, Germany)] as described in published corrosion casting protocols as outlined in the following steps [58, 83, 280, 281]. The cord was clamped after delivery to ensure the dilation of the vessels even before placentas were photographed on both sides. To prepare venous vascular casts, the umbilical vein was cannulated within the cord, while for arterial casts, one of the umbilical arteries was cannulated (ahead of the Hyrtl's anastomosis, about 5cm before cord insertion) using a 20G cannula held in place with a suture. The two umbilical arteries are connected by the Hyrtl's anastomosis near the cord insertion in most human placentas [53, 54]. Cannulation of one of the arteries ahead of the anastomosis allowed flow of casting material into both arteries. The placenta was transferred to a fume hood and cannulated vessels were infused with about 20ml of 5000iu/L heparin in phosphate buffered saline (PBS) to prevent intravascular coagulation as reported in protocols. Casting polymer mixture was prepared according to Batson's Kit protocol as shown in **Figure 2.1** step 1. & 2. and manually injected via the cannula and syringe. The vessels were filled until back pressure prevented any further injection. The cannula was closed and the cord clamped below the point of cannulation, to ensure no leakage of the polymer. The placenta was placed on a polythene sheet on ice to lower the temperature, allowing polymerisation to occur at a more uniform rate overnight as reported [58] in a Class II microbiological safety cabinet (MSC). After 24hrs, the whole cast placenta was submerged in 500ml of 20% w/v

potassium hydroxide (KOH; Fisher Scientific, Lutterworth, UK) within a gasket- sealed tub in a water bath at 40°C in the safety cabinet. The KOH solution was changed at 6h intervals continuously until the tissue around the cast was completely corroded. Corroded solution was safely disposed and the solution was then replaced with distilled water for a similar 6h routine to rinse off any excess KOH solution. At the end of the process, the rinsed cast were air dried under a fume hood, photographed and stored under HTA guidelines till they were scanned.

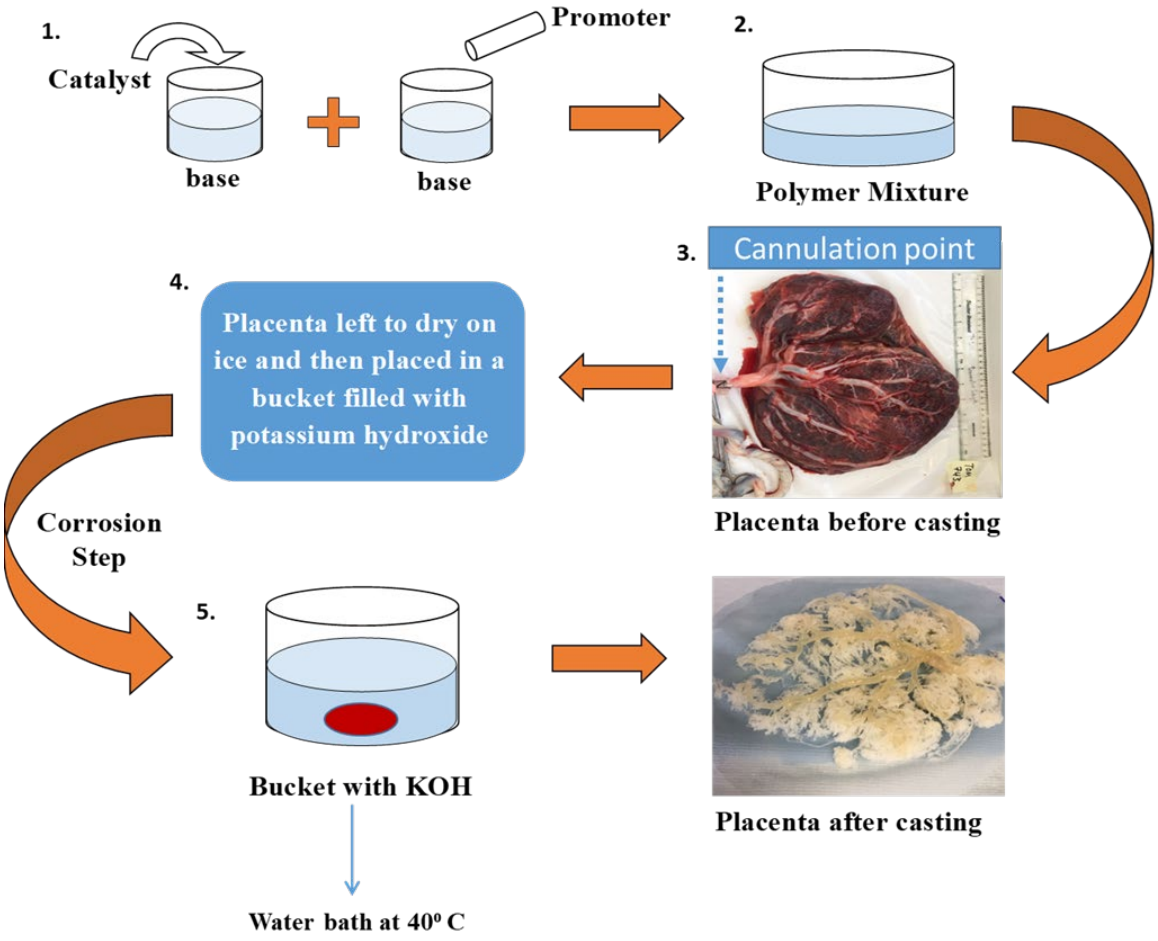

Figure 2.1 Schematic diagram of placental vascular corrosion casting method (numbered steps illustrating different stages during the casting processes)

2.3.1 Micro CT Image acquisition and processing

The methods of image processing and analysis of casts as described in published literature were used [58, 83]. A high resolution micro-CT machine (Nikon metris XTH225, Nikon Metrology NV) was used in acquiring 3D datasets from placenta casts scanned as shown in **Figure 2.2**. The machine was fitted with a 225/320keV x-ray CT source, a rotating stage and a 2000 x 2000 Perkin Elmer detector, controlled by Nikon's Inspect-X software. The cast was put on the rotating stage over 360^{o} at angular increments of 5^{o} around the vertical axis and positioned via homing to get the whole cast within the field of view.

The scan was performed with an x-ray source tube emitting x-rays from a microfocus in cone beam geometry geo at 42keV x-ray energy. The maximum magnification and exposure time varied depending on each specimen's circumference, which had to be within the cone beam of irradiation. Each scan generated about 3000- 6000 slice views for each cast using a step scan. An application (Inspect-X, CT Agent, Metris, UK) was used to receive CT scan slice data and volumes of files were transferred and reconstructed via synchronising reconstruction software (CT Pro 2.0, Metris, UK).

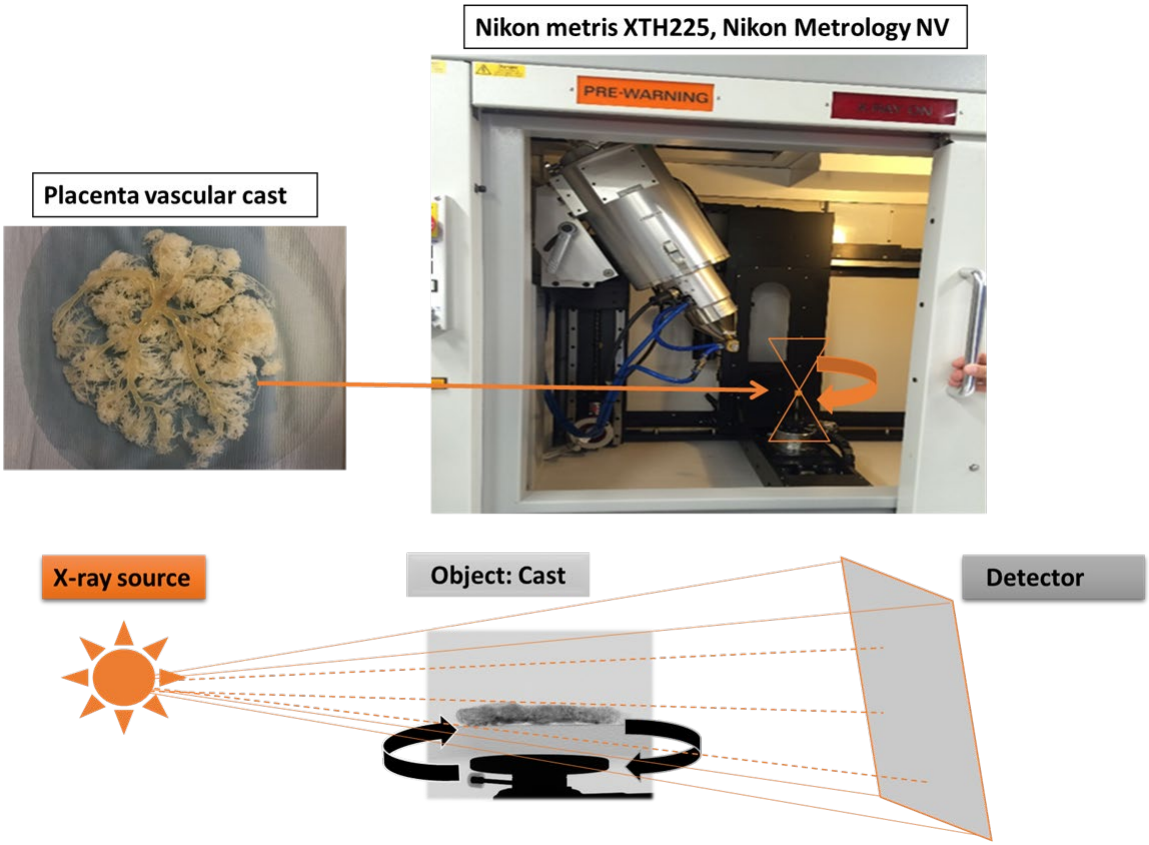

Figure 2.2 The principle of micro-CT imaging
The orange area in Nikon XTH225 represents mounting stage where casts are placed. X-ray source depicted as displayed is positioned opposite detector with rotating stage in the middle (object: cast). The source emits x-rays in cone beam geometry through the cast which is rotated over 360^{o} to generate numerous slices of radiographs in the XY, XZ and YZ planes.

2.3.2 Image Analysis

Following 3D reconstruction of the CT projections into a single volume 3D virtual object on CT Pro, a MATLAB (MathWorks, Massachusetts, USA) algorithm was used to export the data into. hx and .tiff format compatible with volume rendering in Avizo (Avizo 8.0, FEI Visualisation Sciences Group, Konrad-Zuse-Zentrum fur Informationstechnik Berlin (ZIB) and FEI, SAS) analysis software shown in **Figure 2.3**. Each 3D dataset was volume-rendered in Avizo. Background noise was removed from the image using the 'orthoslice' tool and colour map adjustments.

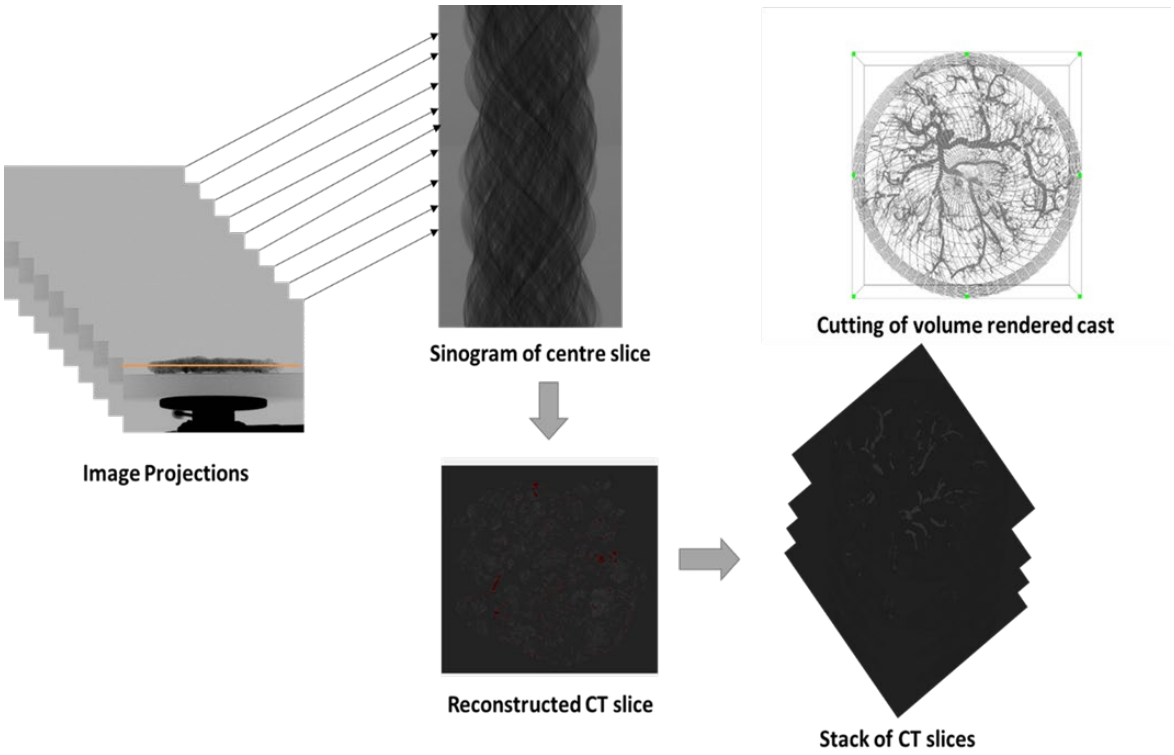

Figure 2.3 Diagram with snapshots of components of Image processing
Each cast produces about 4000-6000 image projections depending on size. Slices of scan shown with representative sonogram of centre slice which is detected in reconstruction software to determine slice thickness and increments. Reconstructed slices are stacked in an 8-bit tiff. Volume file containing single slices. Reconstructed slices are then uploaded on to (Avizo 8.0, FEI Visualisation) software and volume rendered into 3D skeletonised image of cast.

The vessels in each sub volume were segmented using the 'image segmentation' tool on Avizo. Segmented vessels were skeletonised, rendering them in different colours based on their diameter as shown in **Figure 3.1**. In Avizo, nodes along the path of each vessel were recognized as a site of branching and/or any deviation of the vessel from a straight path. The nodes separated the vessels into various segments, from which measurements of morphological parameters including vessel length, diameter, volume and tortuosity were derived. Data obtained were added together for further analysis outlined in the corresponding chapter (Chapter 3).

2.4 *In vitro* model of angiogenesis

2.4.1 Culture of Human Umbilical Vein Endothelial Cells (HUVECs) to assess effects of glucose, insulin and metformin on angiogenesis *in vitro*

Potential effects of glucose concentration, insulin and metformin on modulating fetoplacental angiogenesis were assessed using an *in vitro* model of cellular network formation by HUVECs [282, 283]. All *in vitro* experiments were performed in a sterile microbiological safety cabinet (BSC). HUVECs were obtained from Lonza (UK). Frozen cells were thawed on ice and the cells were maintained in culture flasks in EBM basal medium (LONZA CC-3121) supplemented with EGM-MV SingleQuot Kit Suppl. & Growth Factors (CC-4143) and FGF2 (10ng/ml) or VascuLife® endothelial basal medium (Lifeline Cell Technology LL-0005) and FGF2 (10ng/ml) and passaged when 70% confluent. Cells were used for experiments at passage number 5.

2.4.2 Pilot studies to determine optimum cell plating density, time of cellular network formation and effect of VEGF

Growth factor-reduced BD Matrigel Product (#356230) from the freezer (−20 °C) was thawed on ice. During the thawing process a 96 well culture plate (Corning Inc, USA) was also placed on ice in B.S.C. 15µl of thawed matrigel was then added to each well of a 96 well plate and the plate incubated for 30–60 min at 37°C (21% O_2, 5% CO_2, 37°C) to allow the gel to solidify as illustrated in **Figure 2.4**. The flask of cells was washed thrice with phosphate buffered saline solution without $Ca^{2+/}Mg^{2+}$ (HBSS; Invitrogen) and trypsinised (Trypsin-EDTA; Lonza, catalogue number CC-5012) for few minutes to detach the cells (2ml trypsin per 75cm^2 flask, 1ml trypsin per 25cm^2 flask). Serum-containing media [Dulbecco's modified Eagle's medium (DMEM; Lonza) or VascuLife® endothelial basal medium (Lifeline Cell Technology LL-0005) and FGF2 (10ng/ml) with fetal bovine serum (FBS; Lonza)] was added to neutralise trypsin. Cells were spun down for 10 minutes at 1000rpm and the pellet re-suspended in 1ml of medium. After the cells were passaged, they were counted in a haemocytometer, then plated onto matrigel-coated wells at 5,000, 10,000, 15,000 and 20,000 per well (**Figure A3.0.14**). Cells were cultured in control medium (no VEGF), medium with VEGF (Human Recombinant VEGF 165) at 100pg/ml, to reproduce the concentration in umbilical cord blood [284-286] and high VEGF at 6.67ng/ml (positive control) (**Figure A4.0.16**). The high concentration was chosen because it is the EC_{50} concentration for

maximum vasodilation of the fetoplacental vasculature in the perfused placenta [287]. The cells were then observed at 6h, 12h, 18h and 24h for cellular mesh network formation. In these pilot studies, cellular mesh network formation was assessed qualitatively from captured images.

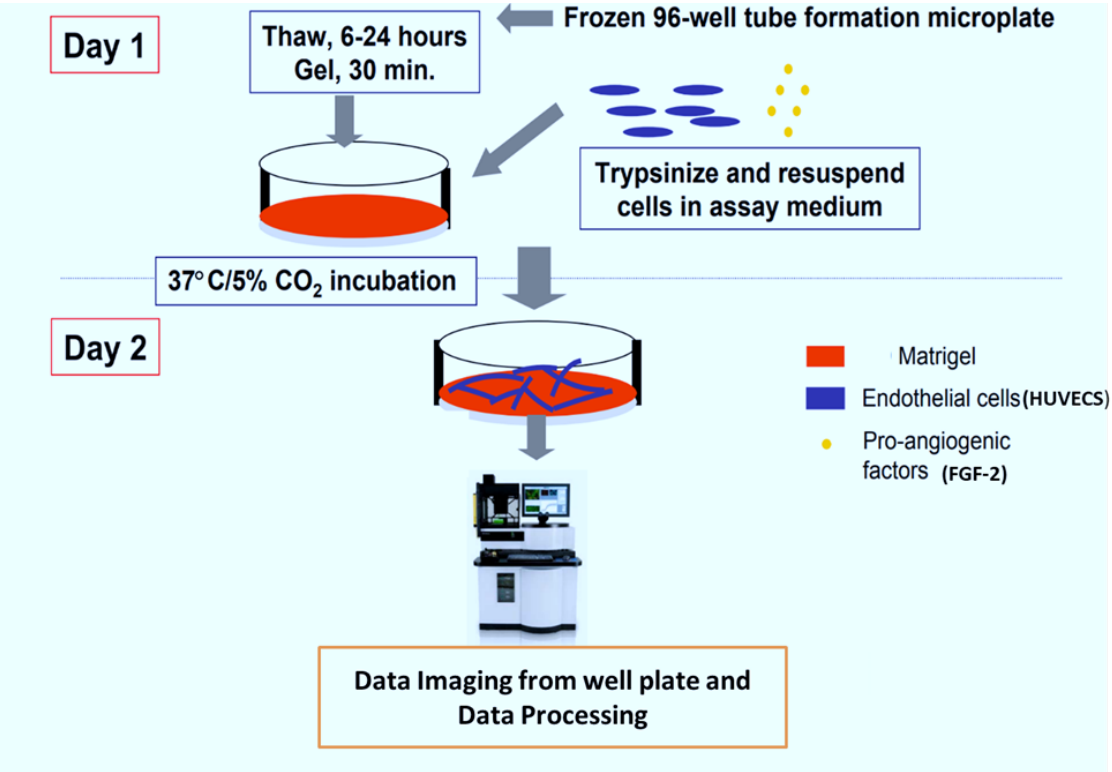

Figure 2.4 Pictorial representation of Angiogenesis Assay method
The cells were cultured in flasks in EBM Basal medium (LONZA CC-3121) supplemented with EGM-MV SingleQuot Kit Suppl. & Growth Factors (CC- 4143) and FGF2 (10ng/ml) and passaged when 70% confluent. Growth factor-reduced BD Matrigel Product (#356230) from the freezer (−20 °C) was used as the matrix substrate. Cells were then plated in respective densities and incubated and imaged at different time points. Image adapted from Wu et al.,2004[An Automated Endothelial Cell Tube Formation Assay System for the Screening of Angiogenesis Stimulatory and Inhibitory Molecule, BD Biosciences Discovery Labware, Bedford, MA 01730;]

2.4.3 Imaging of HUVECs to assess cellular network formation

Following plating, the cells were observed at 6h, 12h, 18h and 24h for cellular network formation and imaged under an inverted light microscope with 4× objective (final magnification x40). 4 Images per well were taken in clockwise direction under a light microscope (Olympus BX41) and Qcapture Image Pro® Plus 7.0 (Media Cybernetics) as shown in **Figure 2.5**.

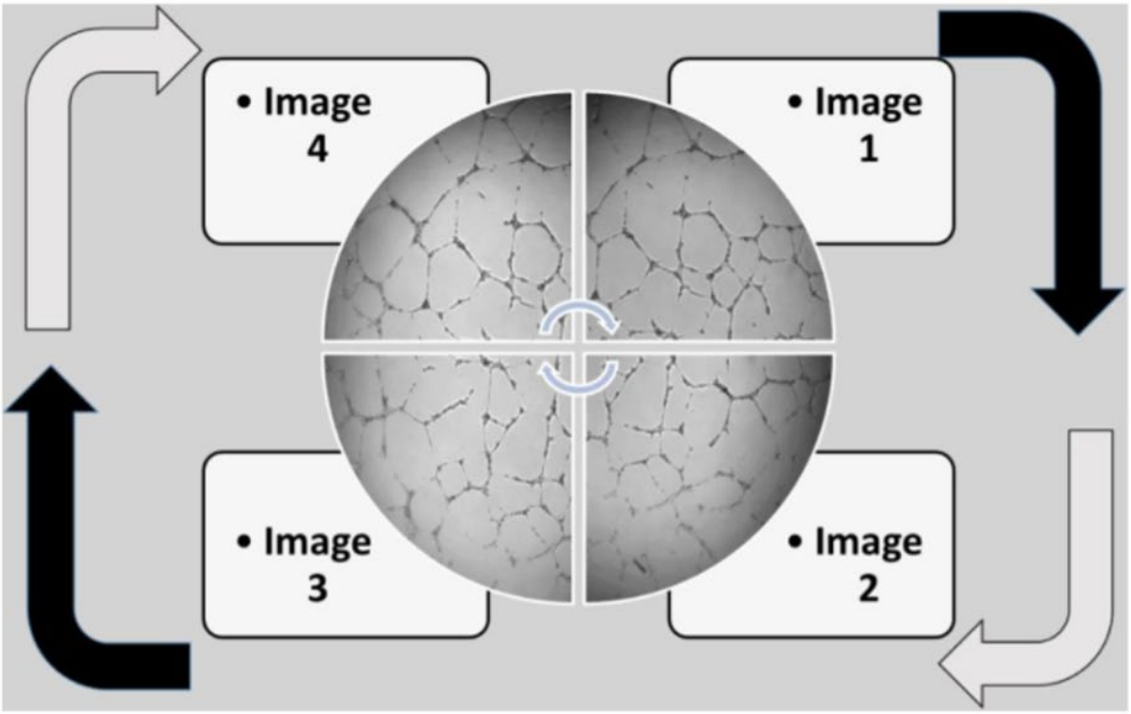

Figure 2.5 Schematic to show images taken of human umbilical vein endothelial cells *in vitro* to assess the formation of cellular networks

Images were taken in clockwise direction and collated on PowerPoint for observational purposes. Images used to assess the cellular network formation in response to plating density and time (**Figure A.4.0.15**), and the effects of VEGF used as a positive control (**Figure A4.0.16**) are shown in the **Appendix 4**. From these pilot studies a plating density of 15000 cells per well, and time period of 18h, were considered optimal for the subsequent studies of the effects of glucose, insulin and metformin on cellular network formation by HUVECs.

2.4.4 Effects of glucose, insulin and metformin on cellular mesh network formation by HUVECs *in vitro*

Informed by the pilot studies, experiments were performed on HUVECs, maintained as described above, and plated at 15000 cells per well. Cells were cultured in media containing a range of glucose concentrations (7 -25mM) +/- metformin or insulin to investigate the effects of glucose in combination with insulin at physiological concentrations and metformin at therapeutically relevant concentrations. The cells were then observed at different time intervals on a live bio- imaging system and images were taken at various time intervals for quantification of the cellular network formation using ImageJ software with an angiogenesis analyser extension. The experimental protocols for these studies, the image capture system and analyses of network formation are described in full in corresponding chapter sections (Chapter 4).

3 Chapter Three: Vascular Corrosion Casting Reveals Altered Placental Vascular Structure in Pregnancies Complicated by Maternal Diabetes

3.1 Background

Placental development is a vital process in pregnancy required for sustaining healthy pregnancy journeys and normal fetal development. Vasculogenesis and angiogenesis in the placenta during pregnancy maintain sufficient supply, transfer and exchange of nutrients between mother and fetus. Any disruption of these key mechanisms (vasculogenesis and angiogenesis) or alterations in the *in utero* environment can increase the risk of a number of complications that can affect both fetal growth and maternal health. Diabetes in the non-pregnant population is associated with vascular pathology including altered vascular development and function[36]. Therefore, it is probable that diabetes could affect the development and function of blood vessels in the placenta during pregnancy. However, this relationship remains poorly understood with knowledge gaps in the underlying mechanisms that directly influence placental development in a diabetic environment *in utero* such that the fetus is at increased risk of placental dysfunction in late pregnancy and hence increasing the risk of poor pregnancy outcomes which include fetal growth restrictions (FGR), macrosomia and stillbirth.

There have not been enough studies conducted on the fetal regulation of placenta vasculature, which will give a greater insight in to the relationship between glycaemic control and placental development in diabetic pregnancies. The lack of clinical evidence on altered vasculature at different stages of diabetic pregnancies makes it even more difficult to single out key intervention studies.

Histological studies have demonstrated that diabetes in pregnancy is associated with an increased incidence of placental pathology and consequently abnormalities in fetal growth as highlighted extensively in section (**1.2.2** and **1.2.3**). In addition to the lack of consistency in reports of pathologic placental lesions. Furthermore, variations in vascularity of samples from different regions of the placenta sampled in histology pose difficulties in interpretations extended to the entire placental vascular morphology.

In addition, reports in the literature on alterations in fetoplacental microvasculature in diabetes have not always related findings to maternal glycaemic control or pregnancy outcome. The inconsistencies and gaps in published data highlight the potential need of advantages of using a comprehensive quantitative approach to assess fetoplacental vasculature in diabetes relating to maternal glucose status, other circulating factors and fetal outcome. Levels of PlGF concentrations in maternal serum rise during pregnancy,

peaking at the end of mid trimester of pregnancy. Low levels of PlGF concentrations during pregnancy have been associated with pregnancy complications including recognized later-life cardiovascular risk [121]. A growing body of evidence in the literature also point to (PlGF), measurable in the maternal circulation, as a maternal serum biomarker for placenta disease [122-125].

Previous work in our laboratory has compared the placenta vasculature between normal and growth restricted pregnancies using casting and Micro- CT [83]. This approach was able to demonstrate hitherto unknown differences in arterial and venous vascular structure of placentas [58]. Micro-CT scanning technique provides details of the three-dimensional anatomic arrangement of the vascular replica to enable quantification of fetoplacental microvasculature on a holistic level and 3-D Microscopy will show records of topology, hierarchy and quantitative data such as diameters, length and volume of placental peripheral villous trees providing a better representation of the placenta's entire vascularity.

3.2 Aims

The aims of the study in this chapter were split into two parts:

1. To determine whether there are differences in placental macrovascular networks at term in women with pregestational diabetes compared with normal pregnancy.

2. To determine whether metrics of the placental macrovascular network at term are related to fetal growth velocity, maternal glycaemic control and maternal plasma PIGF concentrations in women with pregestational diabetes.

The aim of the first part of the study was addressed using a combination of corrosion casting and micro computed tomography (micro-CT) imaging to achieve a full account of placental vascular morphology. To our knowledge the technique has yet to be used in the study of the human placental vascular tree in pregnancies complicated by pregestational diabetes. Having performed micro-CT on vessel casts derived from human placentas, the arterial and venous vessel networks in placentas from uncomplicated pregnancies and pregnancies complicated by pregestational diabetes were compared.

The aim of the second part of the study was addressed by relating measurements of vessel network to maternal glycaemic control during pregnancy and to PIGF levels during pregnancy.

3.3 Materials and methods

Data Collection: This project focused on 2 groups of women: (1) women from the VELOCITY study with pre-gestational diabetes and women from the term tissue bank having normal pregnancy (2). Women with pre-existing diabetes were recruited at <20 weeks. Detailed information was collected from women participating in the velocity study throughout their pregnancy. Demographic data including maternal age, ethnicity, parity, maternal height and weight was collected. HbA1c measurements, uteroplacental assessments, fetal biometry, placental volume, and 3D fractional thigh measurements were also collected. Continuous glucose monitoring was conducted at 3 times points (10-16, 22-26, 30-34 weeks) and a diary of daily activity recorded together with vascular assessments, maternal blood and urine collections, pregnancy outcome data, collection of cord blood and skinfold thickness of infants at 28weeks and the placenta was collected within 40 – 60 minutes of delivery as outlined in detailed in chapter 2 (Appendix 1).

Haemoglobin A1c (HbA1c) Measurements: starting in the first trimester, HbA1c was measured during Velocity study participant's prenatal visits, as a part of their standard clinical care during pregnancy for all women with pre-existing type 1 or 2 diabetes. For the present analysis, we evaluated information on the first prenatal HbA1c (first) and the HbA1c closest(last) to delivery to determine glycaemic control during pregnancy. This measure was evaluated continuously, as well as dichotomized into groups with overall good control (most measurements <48 mmol/mol) versus overall poor control (most measurements ≥48 mmol/mol). For women with measurements either side of 48 over pregnancy, the mid pregnancy HbA1C was considered to decide group allocation. Diabetes group allocation was done before any analysis of the placental casts

PlGF Measurements: For assay performance, maternal samples were frozen at –80°C and thawed once. We analysed ethylenediaminetetraacetic acid(EDTA) plasma for free PlGF using Alere Triage PlGF fluorescence Immunoassay systems with the Alere Triage Meter® (Alere San Diego, California). These assays involved addition of several drops of plasma sample anticoagulated using EDTA to the sample port on the test device. Once added, the specimen reacts with fluorescent antibody conjugates and flows through the test device by capillary action. The test device was then inserted in to Alere Triage Meter ® and analysis is based on the amount of fluorescence the meter detects within the measurement zone. The results are displayed on the screen and recorded. The PlGF upper limit was 5000 pg/mL with measurable range of 12-3000pg/mL. Values below 12pg/mL were recorded as < 12pg/mL and values above the measurable range were reported as > 3000pg/Ml. The PlGF assays were performed in one batch with triplicates for accuracy and standardisation. Measurements were taken for 3 different time points during pregnancy (16,28,33 weeks)

Casting and Micro CT Imaging: To compare fetoplacental vascular structure at term in women having normal pregnancy and pre-gestational diabetes, Batson's Anatomical corrosion kit radiopaque methyl methacrylate-based casting material was used to produce venous and arterial casts of placentas from normal pregnancies (n=17) and pregnancies complicated by pre-gestational diabetes (n=33) at term as detailed in chapter 2. Casts were scanned in a Nikon metris XTH225, reconstructed into a three-dimensional virtual object and segmentation and skeletonisation software (Avizo 9.40) used to generate the number of vessel segments, length of vessel segments (via measurement of chord length) diameter of vessels (via radius measurement) as well as total length and total volume of vessel segments.

3.4 Statistical Analyses

Statistical analyses were conducted using Stata version 16.1 (Copyright 1985-2019, StataCorp LLC, USA). Mixed effects multilevel regression analyses were performed and used to model cast metrics between groups. Mixed effects was used to account for clustering of multiple measurements per placenta (random effects). Cubic, quadratic or linear interaction (polynomial) terms were used in the models to find best fit for each data set and a p value of <0.05 was considered to be statistically significant. Data from this

analyses were presented as log of geometric means +/- standard deviation. In addition, other statistical analyses were conducted using GraphPad Prism® 7 (version 7.01 GraphPad Software, Inc., USA). Data from these analyses were represented as median and interquartile range (IQR) and compared by Mann Whitney test and a p value of <0.05 was considered to be statistically significant. In all results presented, forty-nine samples were analysed [16 normal (9 arterial, 7 venous) and 33 from pregestational diabetes pregnancies (16 arterial, 17 venous)]. Differences in the human placental macrovasculature and microvasculature are reportedly detectable at similar sample size from previous investigations in the literature [58, 83].

3.5 Placental casts data processing

3.5.1 Vascular Casts vessel biometry outputs

Reconstruction of scan slices derived from micro-CT of vessel casts as shown in **Figure 3.1** demonstrated 3D visualisation of the whole placental vascular tree and produced a digital replica for analysis. Maximum vessel resolution quality was achieved at 58µm (diameter) and differed from each whole placental cast. After segmentation and skeletonisation of reconstructed images using Avizo software, as described and illustrated in **Appendix 2**, the number of vessel segments, length, diameter and volume of each were generated as defined in **Table 3.2**. Avizo identifies bifurcations defined as nodes placed along the path of each vessel using the spatial graph view, these nodes represent a site of branching and/or any deviation of the vessel from a straight path and also separates the vessels into various segments. Segmented image volumes were visualised in 3D and interconnected features were skeletonised and shown in 3D for easier analysis as shown in **Figure 3.1E**. Visualising of skeleton thickness: segmented skeletonised vessels were volume rendered using spatial graph labels to leave them in different colours based on their diameter **Figure 3.1F**.

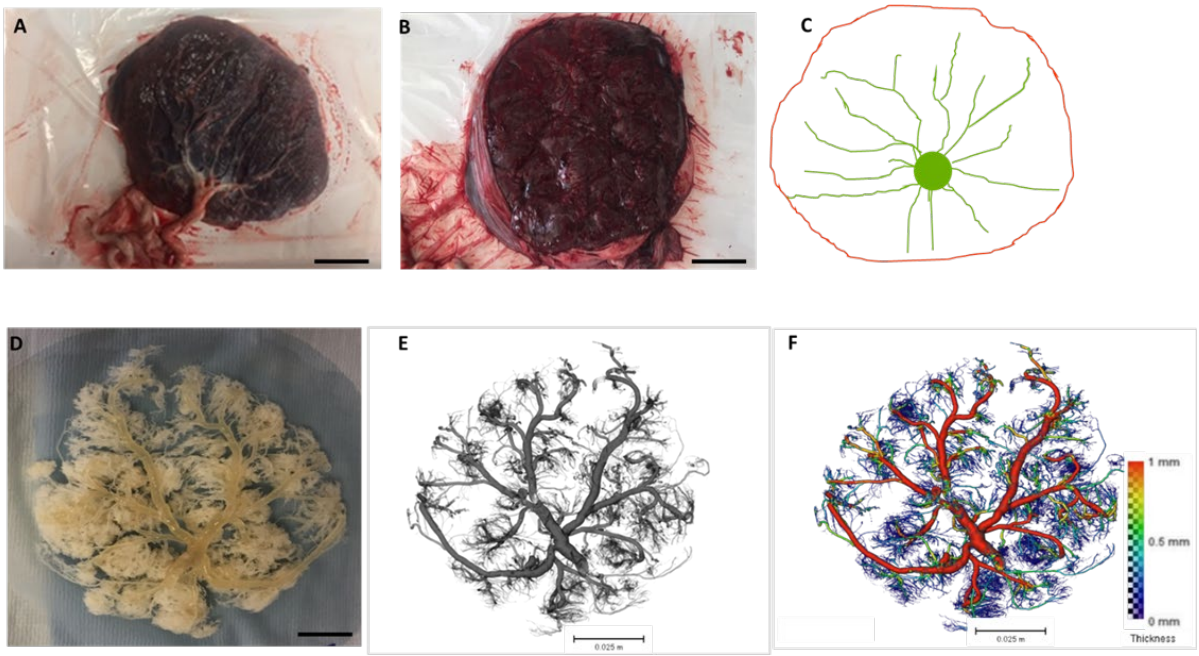

Figure 3.1 Imaged and Analysed placental vascular corrosion cast
Example Images show placenta from pregnancy complicated by pregestational diabetes (**A)** fetal surface shows chorionic plate with branches of the umbilical arteries and vein vessels to be cannulated for casting. (**B**) maternal surface of the placenta with visible lobules. (**C**) Image pro reconstruction of wet placenta surface in (**A**). A venous cast (**D**) following corrosion casting of placenta. (**E**) reconstructed skeletonised image of cast in Avizo software following micro-CT scanning and a 3D reconstructed image of the venous cast coloured based on thickness of diameter(**F**). Scale 0.025m (25mm)

3.5.2 Examination of extent of resin penetration into vessel walls

The casting material filled the vessels up to the level of capillaries measuring ~10-12µm (**Figure 3.2**). Upon further visual microscopic examinations of cast vessels, artefacts were observed on vessel walls. During injection of the polymer mixture, leaking vessels or excess pressure from the syringe may impair ability of resin fill up vessels accurately. This results in resin escaping on to the side of vessel walls and surrounding membrane tissue as shown in **Figure 3.2**, **Figure 3.3** and **Figure 3.4**. This causes artefacts on dried casts that are visualised under microscope and may contribute to their segmented volume computed measurements. Placental casts (4 casts) with this phenomenon of artefact build up were discarded from analysis. It was not established whether the cause of leaky vessels was due to a phenomenon from the diabetic milieu or surgical handling during delivery.

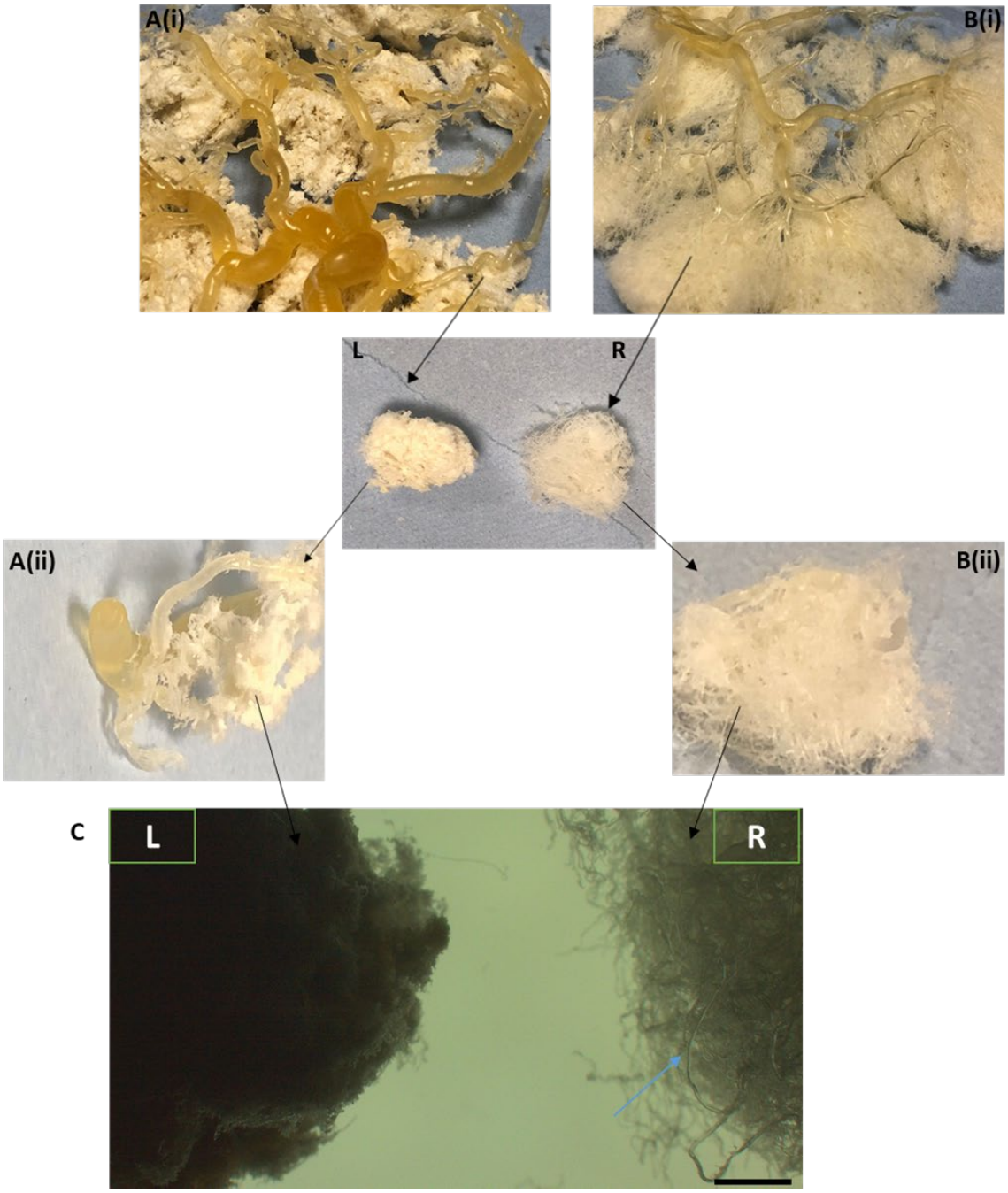

Figure 3.2 Example of cast with and without artefacts on vessel walls

Diagram illustrating extent of methacrylate penetration in vessel and artefact build up from resin on vessel segments in casts. A (Left) - Resin build up showing coarse periphery (edge)cast sample (Aii) from venous placenta (Ai). B (Right) periphery (edge) cast sample (Bii) showing clear methacrylate permeation in vessels from (Bi)venous placenta cast. Blue arrows show smallest vessels filled in with methacrylate resin in (C). A and B images taken with a digital camera; C taken with a Zeiss Axiocam ERc camera attached to a Zeiss Discovery V20 stereomicroscope. Magnification is 7.6x in C. Scale bars represent 1000µm.

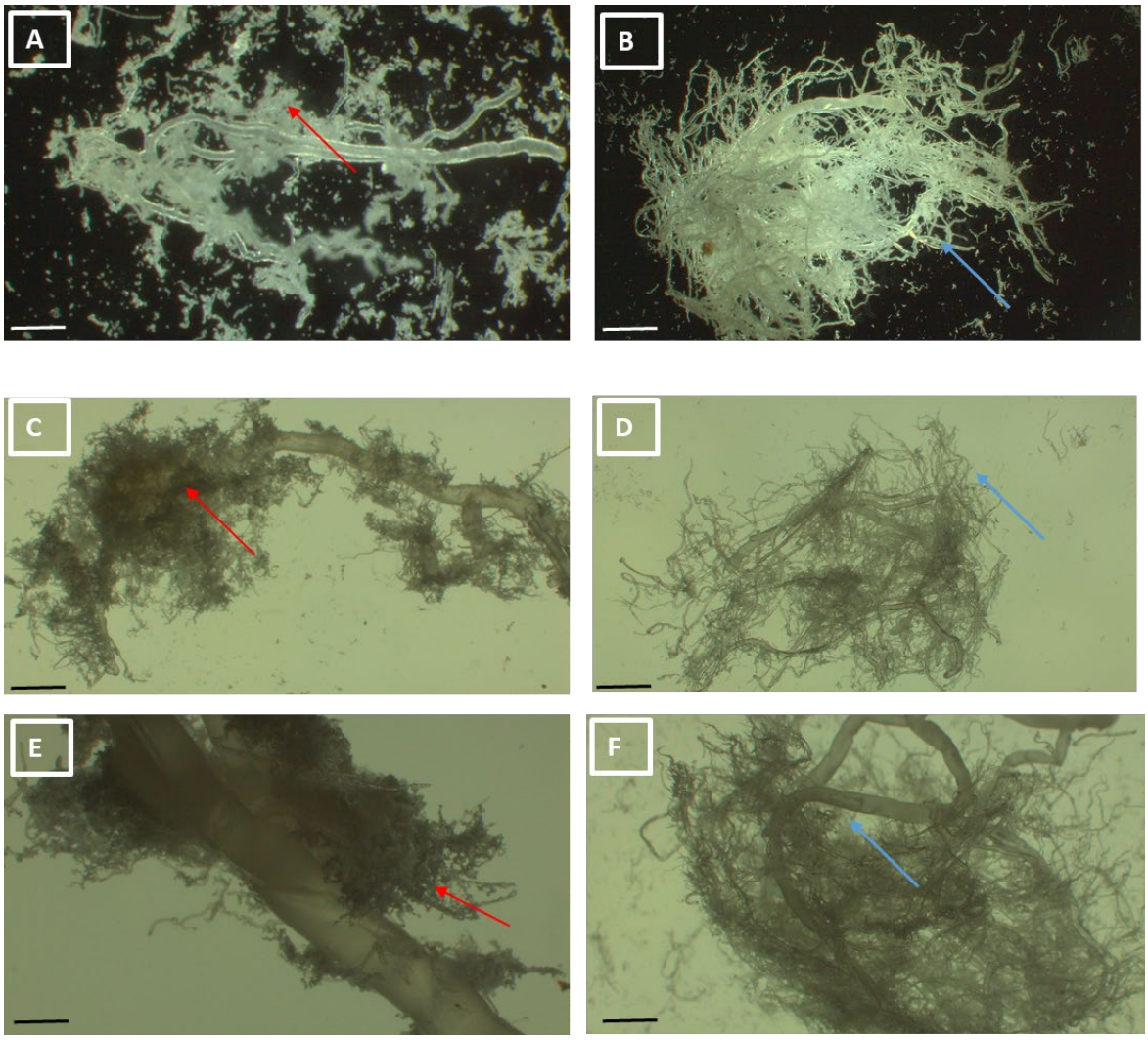

Figure 3.3 The level of methacrylate resin outside vessels in arterial casts with artefacts and without artefacts.

Dark field images of smaller vessels on the casts in (A) with artefacts and (B) without artefacts. Bright field images of smaller vessels on the casts in (C)(E) with artefacts and (D) (F) without artefacts. Red arrows show excess methacrylate resin attached in clumps to vessels. Blue arrows show smallest vessels filled in with methacrylate resin. Images taken with a Zeiss Axiocam ERc camera attached to a Zeiss Discovery V20 stereomicroscope Magnification for (A)(B) is 9.4x, (C)(D) is 7.6x and (E)(F) is 8.8x. Scale bars (1000µm).

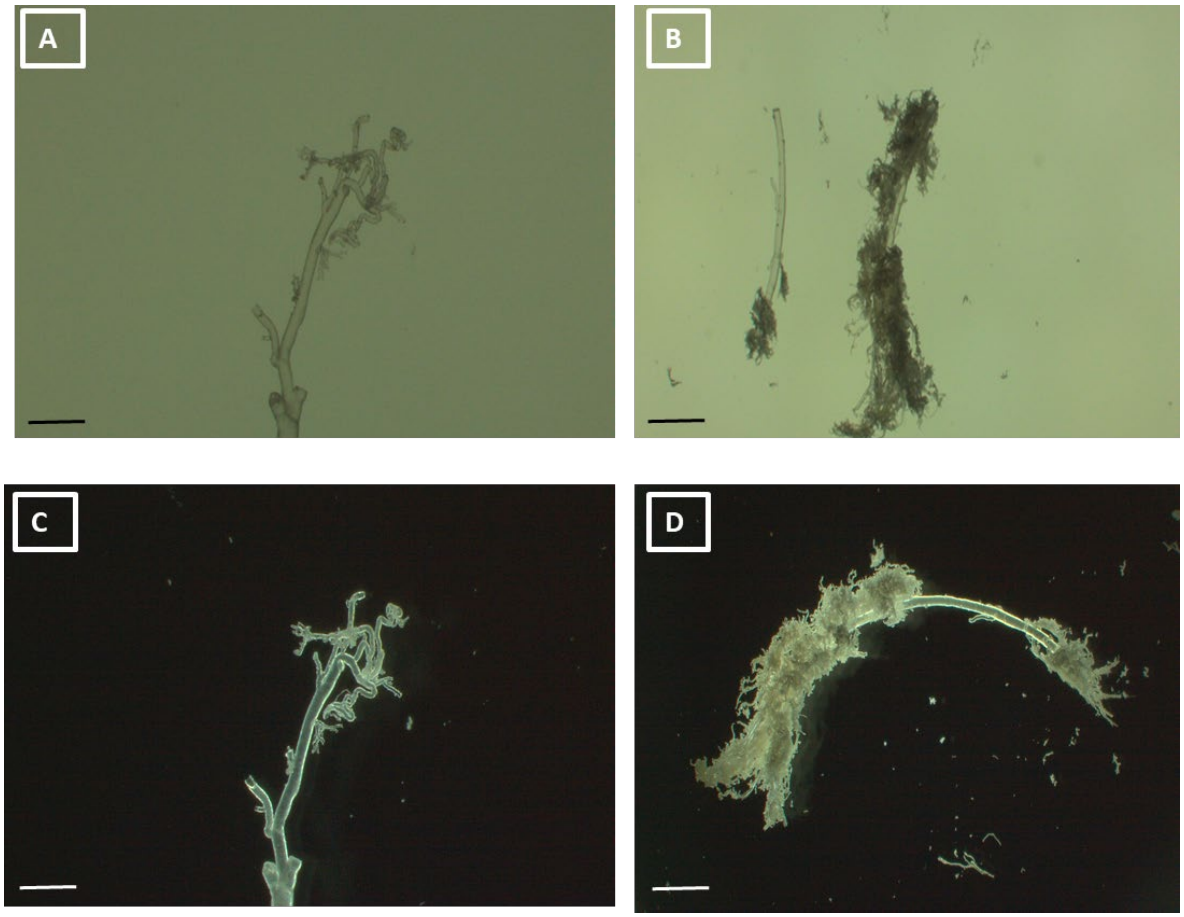

Figure 3.4 The level of methacrylate resin outside smaller vessels in venous cast.
Bright field and dark field images of smaller vessels on the casts in (A) and (C) compared to (B) (D) images showing vessels covered in artefacts of excess resin. Images taken with a Zeiss Axiocam ERc camera attached to a Zeiss Discovery V20 stereomicroscope. Magnification is (A)(B) IS 7.6x and (C)(D) is 21x respectively. Scale bars (1000µm).

3.5.3 Synthesis of Data Output

To ensure accurate measurement of relevant vessel vascularity area of chorionic plate vessels as described in **Figure 3.5**, further synthesis of the data was performed to refine data by exempting measured vessels variables associated to umbilical cord solidified polymer(umbilical artery or umbilical vein) (**Figure 3.6**) and excess resin on smaller vessels as shown in **Figure 3.4**. To ensure uniformity, only vessels ≥ 300µm in diameter were included in the analyses as described in **Table 3.1**.

An algorithm code in R (RStudio Version 1.4.1564.) was used to automatically tune data leaving the desired area/physiological relevant threshold of vessels for analysis see **Appendix 2(II)** for code protocol.

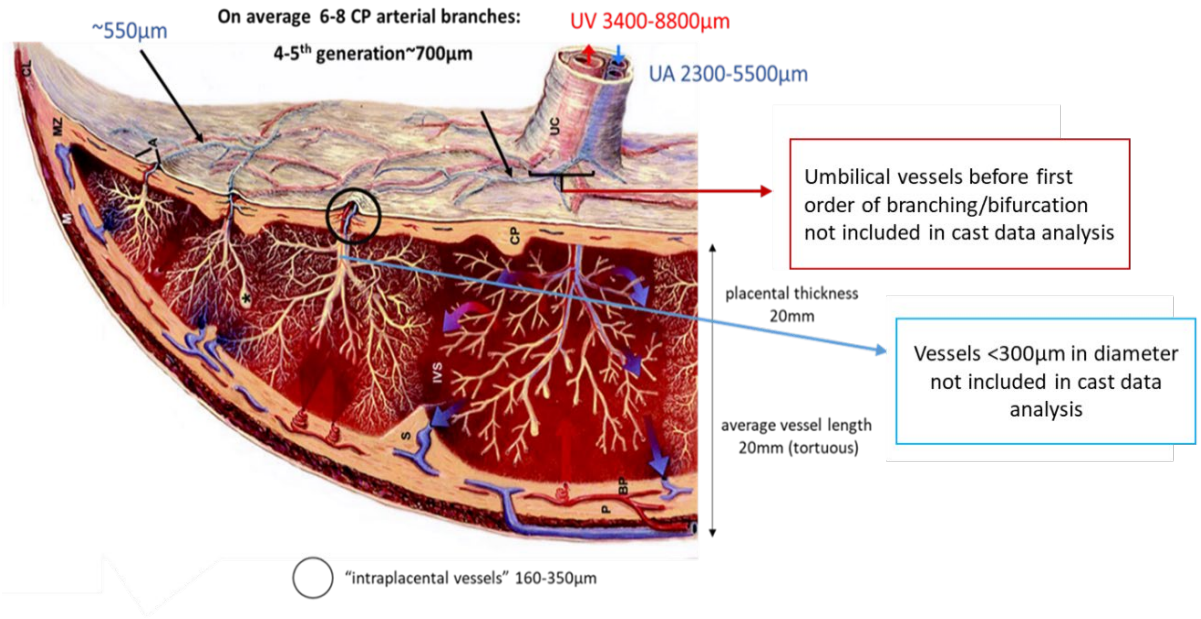

Figure 3.5: Illustration of anatomy of fetoplacental vasculature
Image showing information of diameter of vessels on vascular beds. UA (umbilical artery) and UV (umbilical vein). CP (chorionic plate). Image Adapted from Gordon et al. (2007) and Benirschke et al.(2012) [37, 51]

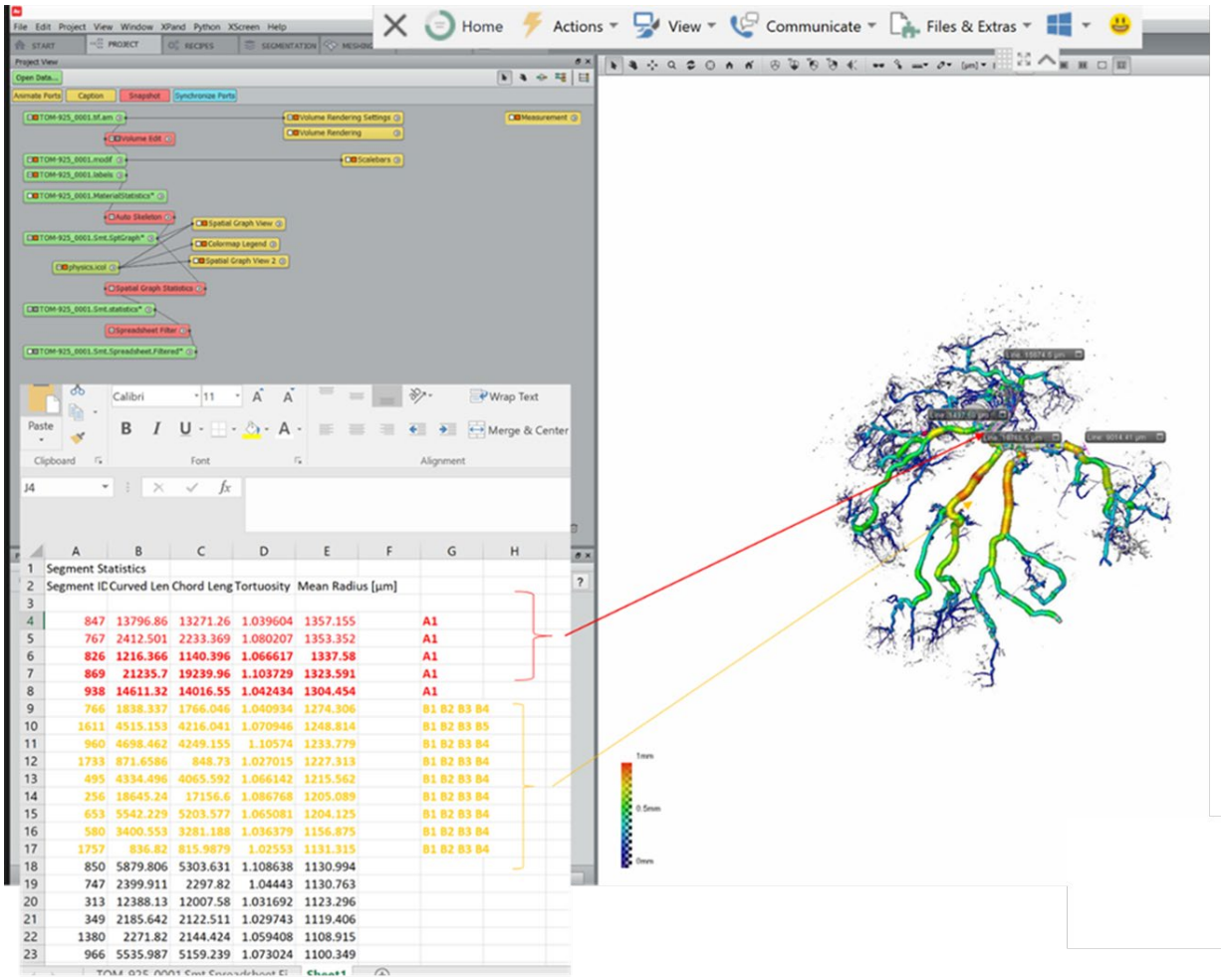

Figure 3.6 Snapshot of data synthesis protocol

Measurements corresponding to umbilical cord resin (red arrows) were uniformly identified and excluded using R code. Measurements corresponding to first level of branching (yellow arrow) were included in analyses and any vessel with diameter <300µm (150µm in radius) was excluded from output data using R code.

Table 3.1 Vascular corrosion cast measured vessel radius and diameter output with corresponding physiological level dimensions

Radius bin	Min radius bin (μm)	Max radius bin (μm)	Min diameter bin (μm)	Max diameter bin (μm)	Artery/Vein
1	0	50	50	100	Peripheral stem villus
2	50	100	100	200	
3	100	150	150	300	Intraplacental vessels
4	150	200	200	400	
5	250	300	300	600	7th order CP artery
6	300	350	350	700	6th order CP artery
7	350	400	400	800	5th order CP artery
8	400	450	450	900	
9	450	500	500	1000	4th order CP artery
10	500	600	600	1200	
11	600	700	700	1400	
12	700	800	800	1600	3rd order CP artery
13	800	900	900	1800	
14	900	1000	1000	2000	2nd order CP artery
15	1000	1200	1200	2400	Umbilical artery (min)
16	1200	1400	1400	2800	
17	1400	1600	1600	3200	1st order CP artery
18	1600	1800	1800	3600	Umbilical vein (min)
19	1800	2000	2000	4000	
20	2000	2500	2500	5000	
21	2500	3000	3000	6000	Umbilical artery (max)
22	3000	3500	3500	7000	
23	3500	4000	4000	8000	
24	4000	4500	4500	9000	Umbilical vein (max)
25	4500	5000	5000	10000	

CP = Chorionic plate, min=minimum, max=maximum. Radius bins = vessel segments grouped into bins according to measured radii. Information deduced from Gordon et al. 2007 [51].

Table 3.2 Avizo software measured variables and presented metrics

Variable	Definition	Measured metrics
Vessel Segment	**Node:** Avizo places nodes at along the course of each vessel representing a site of branching and/or any deviation of the vessel from a straight path., elements delimited by two junctions **Segment**: Each branch and bend along the course of a vessel separates the vessels into various segments.	*From each segment measurements of morphological parameters such as vessel length, diameter, volume and tortuosity were derived.* **No. of segments**: number of vessel segments in the analysed (cast) area or within a given diameter bin range. **Total segments length**: sum of length of all vessel segments in the analysed (cast)area.
Length	detects the measured distance or dimension from a node to another node in the path of a vessel.	**Mean Chord Length**: distance between start node and end node point of the segment. **Total Length**: cumulated sum length of all vessel segments in the analysed (cast) area or within a given diameter bin range.
Diameter	The diameter distribution is defined as the full distance between vessel walls along each vessel segment. This computed as twice the measured radius of the vessel segment.	**Radius:** distance measured from the centre of the vessel to one endpoint of the vessel wall in the 3D analysed cast. **Minimum radius**: the minimum measured radius along a vessel segment. **Maximum radius**: the maximum measured radius along a vessel segment. **Mean Radius**: the average measured radius along a vessel segment.
Volume	defined as the amount of 3-dimensional space occupied by lumen	**Mean Volume:** mean computed values for volume fraction of each vessel segment **Total Volume:** sum volume of all vessel segments within a given diameter bin range **Maximum Volume:** maximum vascular volume fraction of analysed cast area
Tortuosity	defined as equal to Chord-Length/Curved-Length of the vessel segment.	**Not presented**

-Avizo Software (FEI 9.40) measured metrics and definition

3.5.4 Mode of Data Presentation

The data derived from Avizo software refined in RStudio were then formatted into 2 different ways; one format showed data presented as groups of increasing radius size bins order in fixed increments of 50µm (**Figure 3.7(I and II)**). The other format was derived using RStudio to categorise the data in fixed group of 20 bins calculated as placental vascular vessel segment radius equally divided into 20 bins i.e. (maximum radius – minimum radius /20) per each cast, as shown in **Figure 3.7 (III and IV)** to attempt to ensure physiologically relevant areas of the placenta in bins were being compared across all placentas.

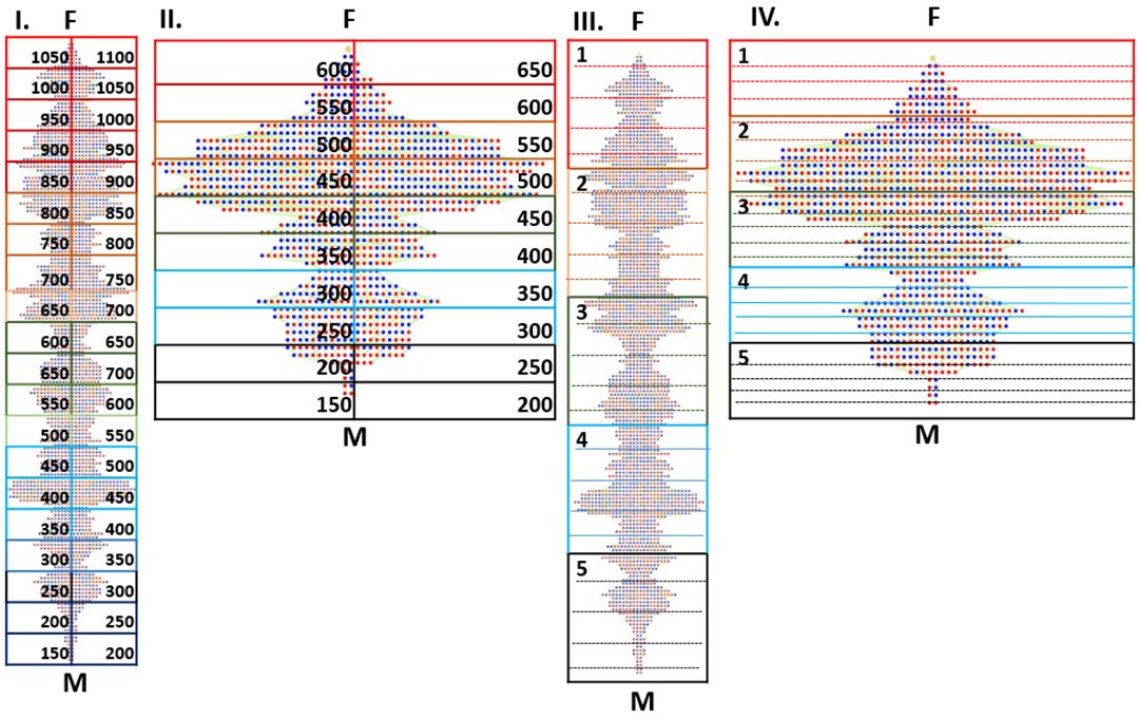

Figure 3.7 Diagrams illustrating modes of data presentation
Examples of distribution in measured vessel outputs of arterial and venous cast tree maps grouped in different ways of presentation. The yellow dot at the top of tree map represents the root of all the vessels (umbilical cord insertion point) (**F**= fetal side) and (**M**=maternal side). True branch points and terminal branch points are marked in blue and red dots respectively. Each point is labelled with alphabets designating the branch generation/level and numbers designating the number of branches at each level. Data presented as a distribution of fixed increasing radius size bins order **(I)(II)** per placenta compared to equally binned radius size numbers distributed as $1/20^{th}$ of each placenta **(III)(IV)**. Data presented as increasing radius size bin order **(I)**venous cast ***(II)*** arterial cast are grouped in fixed increments of 50µm. Data presented in binned size numbers; **(III)**venous cast **(IV**) arterial cast respectively are grouped in equally distributed 20 bins calculated as (maximum radius – minimum radius /20) per each placenta cast.

For the purpose of this study, data graphs in radius size bins format are presented in the main chapter and data graphs in binned size are attached in **Appendix 3**.

Table 3.3 Exemplary outline of measure radius bins in different output modes of presentation

A.

Radius bin Size Order	Min radius bin (µm)	Max radius bin (µm)
1	150	200
2	200	250
3	250	300
4	300	350
5	350	400
6	400	450
7	450	500
8	500	550
9	550	600
10	650	700
11	700	750
12	750	800
13	850	900
14	950	1000
15	1050	1100
16	1100	1150
17	1150	1200
18	1200	1250
19	1250	1300
20	1300	1350
21	1350	1400
22	1400	1450
23	1450	1500
24	1500	1550
25	1550	1600
26	1600	1650
27	1650	1700
28	1700	1750
29	1750	1800
30	1800	1850
31	1850	1900
32	1900	1950
33	1950	2000
34	2000	2050
35	2050	2100

B.

Radius binned size number	Min radius bin (µm)	Max radius bin (µm)
1	150	242.5
2	242.5	335
3	335	427.5
4	427.5	520
5	520	612.5
6	612.5	705
7	705	797.5
8	797.5	890
9	890	982.5
10	982.5	1075
11	1075	1167.5
12	1167.5	1260
13	1260	1352.5
14	1352.5	1445
15	1445	1537.5
16	1537.5	1630
17	1630	1722.5
18	1722.5	1815
19	1815	1907.5
20	1907.5	2000

A= Radius bin size order 1- 35 (150 -2100 µm) in increments of (50µm), **B**= binned size number 1-20 (max radius – minimum radius /20) i.e. min=150 µm, max =2000 µm.

3.5.5 Maternal demographics and placental features of samples studied

Following data synthesis and developing analysis tools to examine 3D reconstructed casts of placental vasculatures, vessel morphology in the selected placentas from normal and pregestational diabetes pregnancies were compared. The demographic and clinical details of the women and babies whose placentas were used are shown in **Table 3.4**. At delivery, the median gestational age, placental weight, fetal: placental weight ratio and mode of delivery were significantly different between the normal and pregestational diabetes-complicated clinical groups. Median placental weight was 496.0g (IQR 375.0 – 698.0g) and 604.0g (IQR 400.0 – 874.0g); p = 0.02 for the normal and pregestational diabetes groups respectively. Median gestational age was 273(261-295) days and 263 (217-280) days p< 0.00001 for the normal and pregestational diabetes pregnancy groups respectively. Median fetal: placental weight ratio was 6.36(4.96-8.78) and 5.34 (3.45-7.76); p=0.0002 for the normal and pregestational diabetes groups respectively. In mode of delivery (p=0.0474), 2 out of 16 women within the control group having normal pregnancy had vaginal births (12.5%) and 14 out of 16 delivered via caesarean-section (87.5%). On the other hand, 14 out of 33 women with pregnancies complicated by pregestational diabetes had vaginal births (42.4%) and 19 out of 33 delivered via caesarean-section (57.6%).

Table 3.4 Demographic, clinical and placental examination details of study

Demographic data	Normal Pregnancies (n=16)	Pregestational diabetes (n=33)		p value
Casts	Arterial **(9)** Venous **(7)**	Arterial **(16)** Type 1 (10) Type 2 (6) Diabetes-good control **(10)** Diabetes-poor control **(6)**	Venous **(17)** Type 1 (14) Type 2 (3) Diabetes-good control **(12)** Diabetes-poor control **(5)**	
Ethnicity **-White** **-Black** **-Asian** **-Mixed** **-Other**	 11(68.75%) 0(0.0%) 3(18.75%) 0(0.0%) 2(12.5%)	 21(63.3%) 4(10.0%) 7(16.7%) 0(0%) 1(10.0%)		
Maternal age, years	33 (29-41)	34 (19-44)		0.72786
Maternal BMI, Kg/m2	25.1 (19.6-33.2)	27.1 (20.3-44.5)		0.17702
Gestational age at delivery, (days)	273 (261-295)	263 (217-280)		**< 0.00001**
Deliveries under < 37 weeks	0	9		0.1556
Birth weight, g	3313 (2440-4400)	3270 (2107-4640)		0.13567
Placental weight, g	496 (375-698)	604 (400-874)		**0.01552**
Fetoplacental weight ratio, F:P	6.36 (4.96-8.78)	5.34 (3.45-7.76)		**0.0002**
Placental surface area (IP) m^2	328 (227-483)	340 (205-531)		0.58232
IBR, centile	37 (6-100)	72 (2-100)		0.0601
Smoking, number (%)	4/16 (25%)	5/33 (15.2%)		0.5892
Parity	4(0) 4(1) 6(2) 2(3)	6(0) 8(1) 6(2) 2(3) 1(5)		0.16452
Mode of delivery, number (%)				
Vaginal	2/16 (12.5%)	14/33 (42.4%)		**0.04746**
Caesarean section	14/16 (87.5%)	19/33 (57.6%)		
Fetal Sex: **Male** **Female**	 9 (56.25%) 7 (43.75%)	 15 (45.5%) 18 (54.5%)		0.15866
Cord Insertion number, (%)				
Central	4/16 (25%)	14/33 (42.4%)		0.16602
Non central	12/16 (75%)	19/33 (57.6%)		

Demographic data shown represent median and interquartile range (IQR) in parenthesis or number with percentage in parenthesis. p-value obtained from Mann Whitney U test, p <0.05 = significant. BMI, IBR represent body mass index and individualised birth weight ratio respectively. Arterial and venous refer to the vascular compartments casted for the respective placentas. Good control and poor control refer to maternal glycaemic status while Type 1 and Type 2 refer to clinical classifications of diabetes.

3.6 Results: Measurements of vascular morphology

3.6.1 Vessel segments in normal and pregestational diabetes casts presented in both outputs

Vessel segment in the Avizo software computation is defined as a path between two nodes. In both normal and pregestational diabetes casts, the number of vessel segments declined progressively from the smallest to the largest radii/diameter ranges. **Figure 3.8** shows the spread of vessel segments across increasing vessel diameter(A & B arteries ; C & D veins) measured in 50µm radii bins in placenta casts from normal and pregestational diabetes pregnancies. Data is grouped by vessel radius size.

Regression analysis examined the association between the measured variables (i.e. length or volume) and increasing radius size. Polynomial fit (cubic, quadratic or linear interaction terms) indicated whether the relationship between measured variables (i.e. length or volume) and radius size was linear or not. The group comparisons indicated whether there were overall differences in measured variables (i.e. length or volume) between clinical groups and significance in the interaction terms was indicative of differences in the relationship between measured variables (i.e. length or volume) and radius size present between the clinical groups.

In **Figure 3.9**, both modes of data presentation (radius size bins and binned size data) show that the mean number of vessel segments are significantly different within the microcirculation between control and pregestational groups, and not in the larger vessels of the chorionic plate. In arterial casts (**Figure 3.9**(A)(C)), the mean number of vessel segments was significantly higher in pregestational diabetes casts across radius bins ($p<0.0001$). There was also significantly fewer mean number of vessel segments in venous pregestational diabetes casts (**Figure 3.9**(B)(D)) across radius bins ($p <0.0001$).

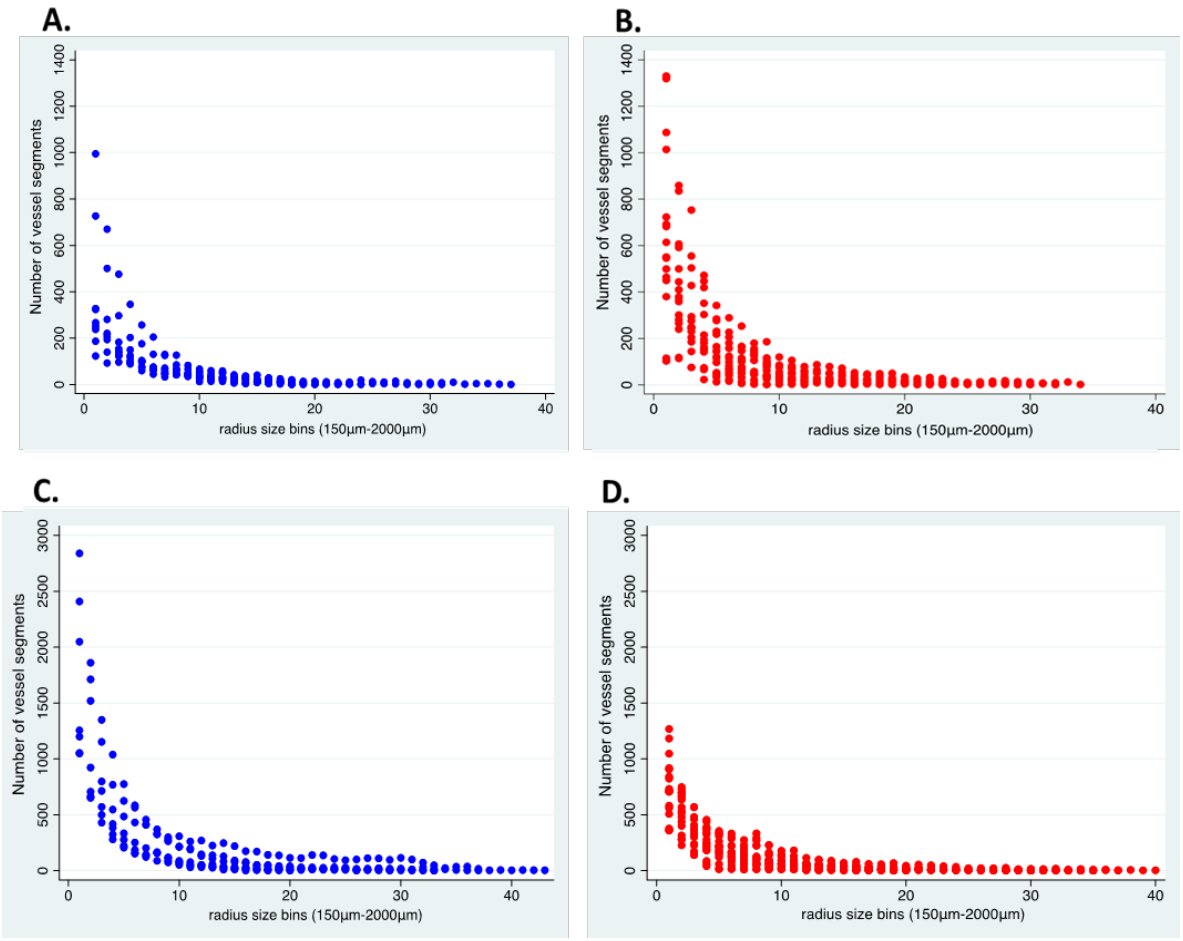

Figure 3.8 Number of Vessel segments in radius bins in normal and pregestational diabetes casts.

The number of vessel segments in arterial and venous placental casts from normal and pregestational diabetes pregnancies. **A**. (arterial, **control no diabetes**) and **B**. (arterial, **pregestational diabetes**) represent data presented in increasing radius size bins order format. **C**. (venous, **control no diabetes**) and **D**. (venous, **pregestational diabetes**) represent data in increasing radius size bins order. Data presented as scatter plot of number of vessel segments within a given radius size range, Control (no diabetes) = 16 (9 arterial, 7 venous) and pregestational diabetes = 33 (16 arterial, 17 venous).

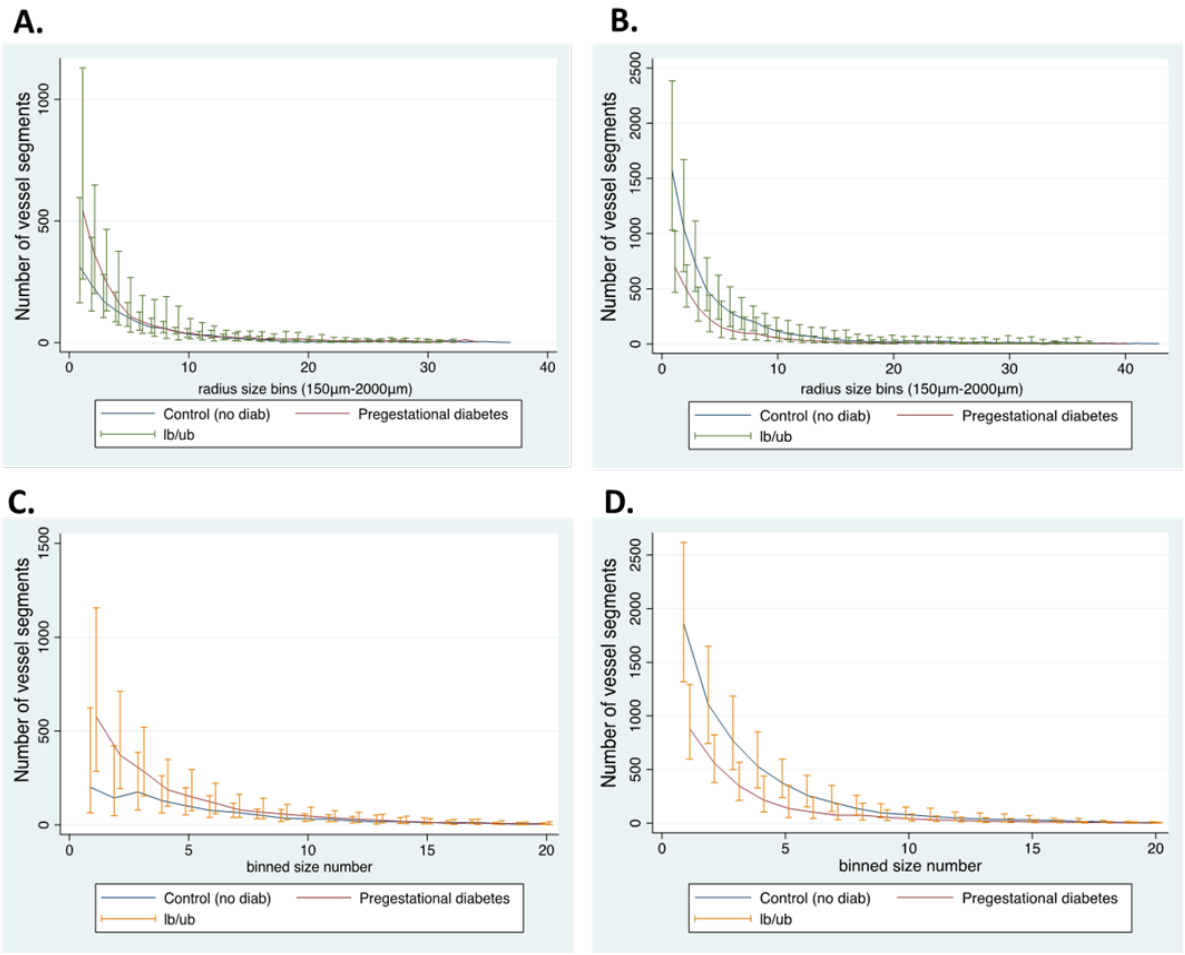

Figure 3.9 Mean number of vessel segments in arterial and venous casts from clinical groups demonstrated in different modes of data presentation (radius size bins and binned size numbers)

The mean number of vessel segments in arterial and venous placental casts from normal and pregestational diabetes casts. **A (arterial) and B (venous)** represent data presented in increasing radius size bins order format, ($p<0.0001$ control vs diabetes) while **C (arterial) and D (venous)** represent data in binned size number format, ($p<0.0001$ control vs diabetes). Data presented as line graphs of mean number of vessel segments within a given radius size range, Control (no diabetes) = 16(9 arterial, 7 venous) and Pregestational diabetes = 33 (16 arterial,17 venous).lb/ub=lower bound of confidence interval/upper bound of confidence interval 95%. Mixed effects – ML Regression analysis, $p < 0.05$ was taken as significant.

To correct for the effect of placental size on its vessel anatomy, vascular parameters measured for each placenta were adjusted for the individual pregnancy gestation at delivery (days) and divided by placental weight (PW). In addition, the relationship between maximum measured vascular volume of the placenta casts and birthweight and with gestation (**Figure 3.10**) was examined. There was not much change between the observed ratio which is an approximation of vascular density with gestation or with birthweight. However, as birth weight tends to vary across populations, it has been widely acknowledged that the appraisal of birth weight should rely on its position relative to the birth weight distribution of the background population[288]. This is commonly done by standardising birth weight through its deviation from the population mean in the given gestational age stratum. In this study, birthweight z-score was calculated using the WHO fetal growth centiles (i.e. zscore who mean) [289]. Data were also presented as z-score in **Figure 3.11**.

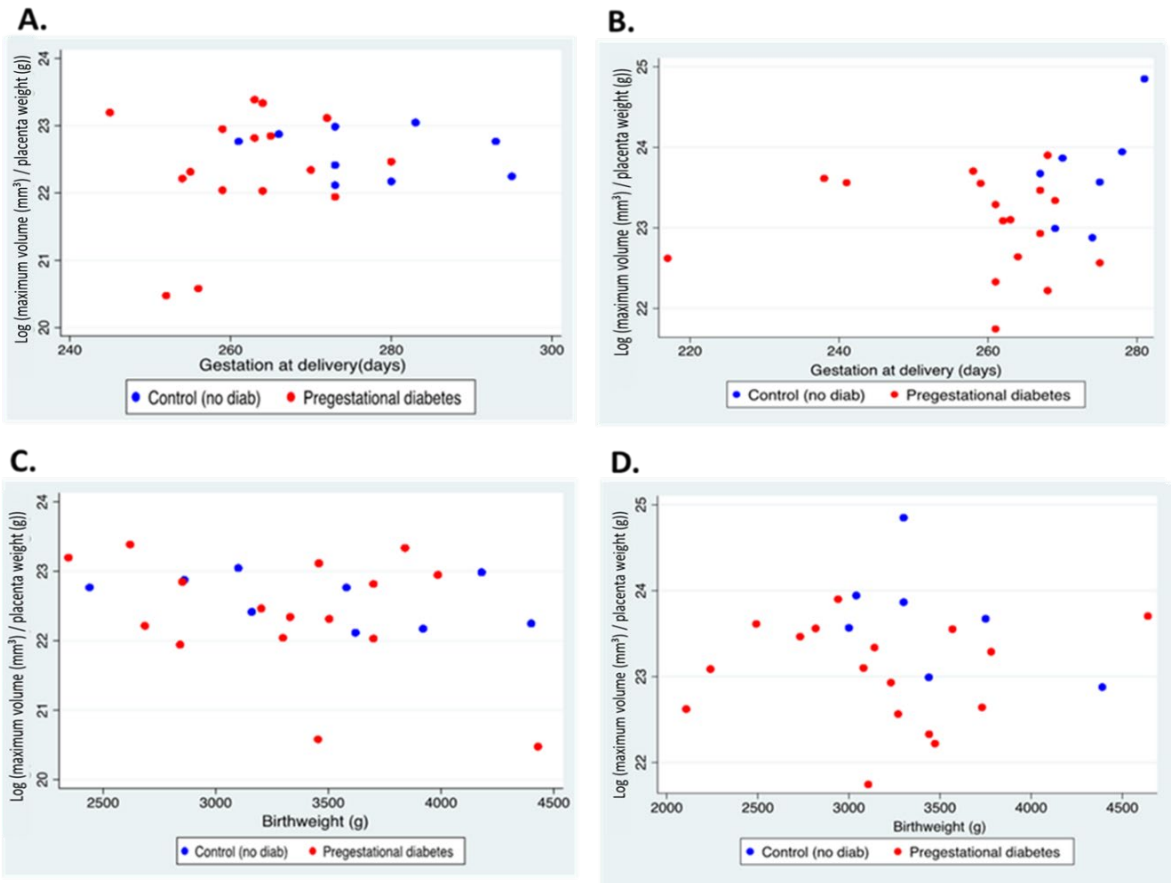

Figure 3.10 Relationship between vascular placenta volume, gestation and birthweight
The distribution of maximum measured vascular volume normalised to placenta weight in arterial and venous placental casts from normal and pregestational diabetes pregnancies. **A and B** represent relationship between logged maximum vascular volume normalised to placenta weight in arteries (A) and veins(B) and gestation at delivery. **C and D** represent relationship between logged maximum vascular volume placenta weight ratio in arteries (C) and veins(D) and birthweight. Data represented as scatter plots for each placenta. Control (no diabetes) = 16(9 arterial, 7 venous) and Pregestational diabetes = 33 (16 arterial ,17 venous).

The graphs presented in **Figure 3.11**(**A,B)** show a positive correlation between placental weight and z-score but not with vascular volume or vascular density (**C, D**). The maximum measured vascular volume was the adjusted for placenta weight in (**E, F**) and there was no relationship between maximum vascular volume and birthweight z-score either in pregestational diabetes or normal pregnancies**.** Maximum vascular volume estimates appeared to become more unpredictable (z-score) as the placental weight increases in arteries and veins for both normal and pregestational diabetes groups.

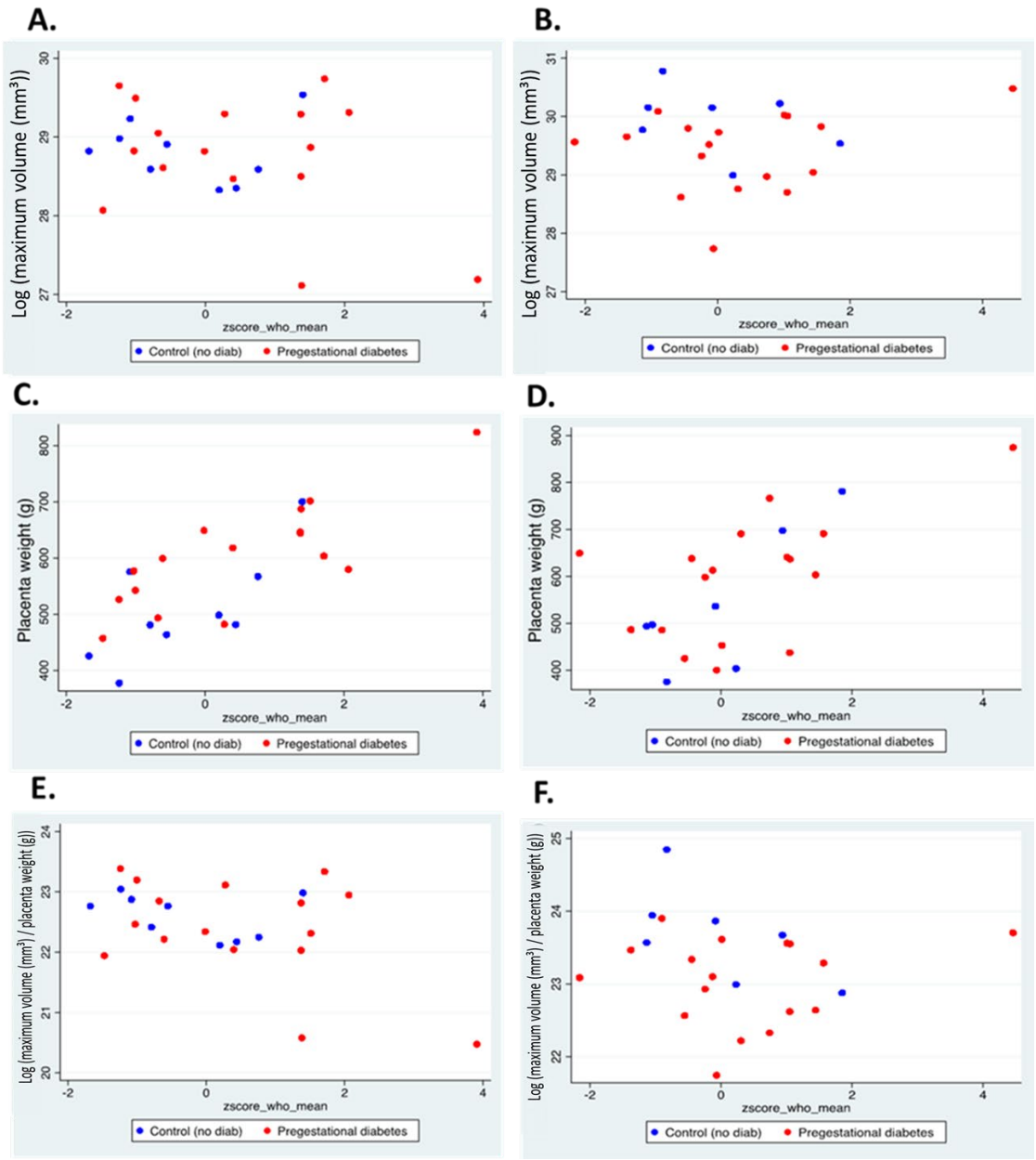

Figure 3.11 Relationship between maximum measured vascular volume and birthweight z-score

The distribution of maximum measured vascular volume normalised to placenta weight of arterial and venous placental casts from normal and pregestational diabetes pregnancies. **A** and **B** represent relationship between logged maximum vascular volume in arteries (A) and veins(B) and birthweight z-score (z-score who mean). **C** and **D** represent relationship between trimmed placental weight in arteries (C) and veins(D) and birthweight zscore (zscore who mean). **E** and **F** represent relationship between logged maximum vascular volume placenta weight ratio in arteries (E) and veins(F) and z-score who mean. Data represented as scatter plots for each placenta n = 16 normal (9 arterial,7 venous) and 33 Pregestational diabetes (16 arterial, 17 venous)

3.6.2 Vessel length alterations observed in pregestational diabetes

There was a non-linear relationship between measured chord length and radius size (**Figure 3.12**C) in arterial casts. In comparing vessel length in arterial placenta casts, there was an overall significant difference between clinical groups. The log mean chord length normalised to PW was longer in the control no diabetes group compared to the pregestational diabetes group, p≤0.0001 (**Figure 3.12**A). These findings were also observed in binned data format with p ≤0.0001 (**Figure A3.0.1**A, Appendix 3).

Similarly, there was an overall significant difference between clinical groups in venous placenta casts. The log mean chord length normalised to PW was longer in the control no diabetes group compared to the pregestational diabetes group, p = 0.036 (**Figure 3.12**B) as well as in binned size number data format with p=0.026 (**Figure A3.0.1**B**,** Appendix 3). There was a linear relationship between measured chord length and radius size in venous placenta casts.

There was no significant difference in the relationship between measured chord length and increasing radius size between the clinical groups in both types of casts and in both modes of data presentation.

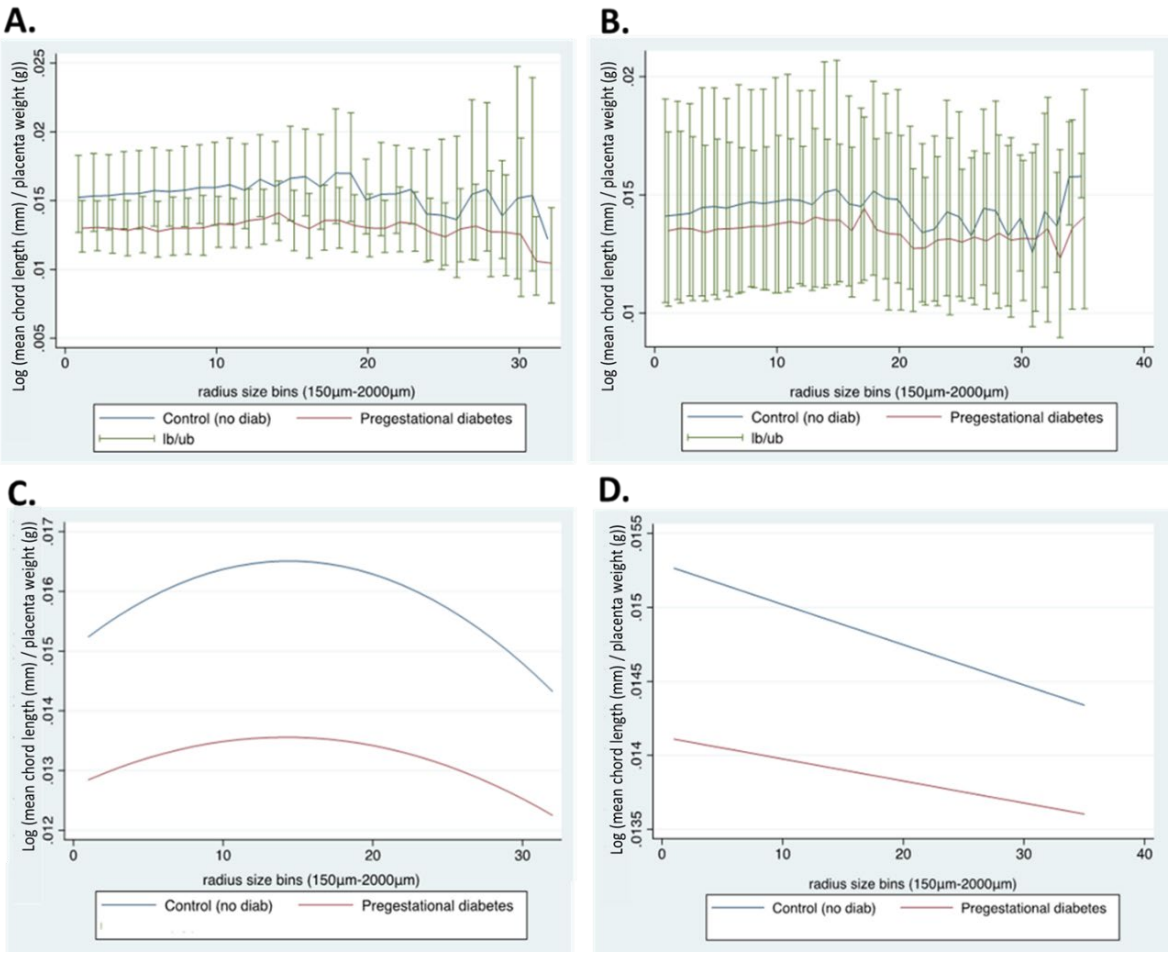

Figure 3.12 The length of arteries and veins in normal and pregestational diabetes casts
The mean chord length of vessels in arterial and venous casts of normal and pregestational diabetes. All data are normalised to placenta weight. **A (arterial,** p ≤0.0001 control vs diabetes**) and B (venous,** p=0.036 control vs diabetes**)** represent line graphs of mean chord length placenta weight ratio in increasing radius size bins format (150 µm-2000 µm) while **C(arterial) and D(venous)** represent linear prediction smooth graphs of **(A) and (B**) respectively. Data presented as (log) geometric mean ± SD. Control (no diabetes) = 16(9 arterial,7 venous) and Pregestational diabetes = 33 (16 arterial, 17 venous). Mixed effects – ML Regression analysis, $p < 0.05$ was taken as significant.

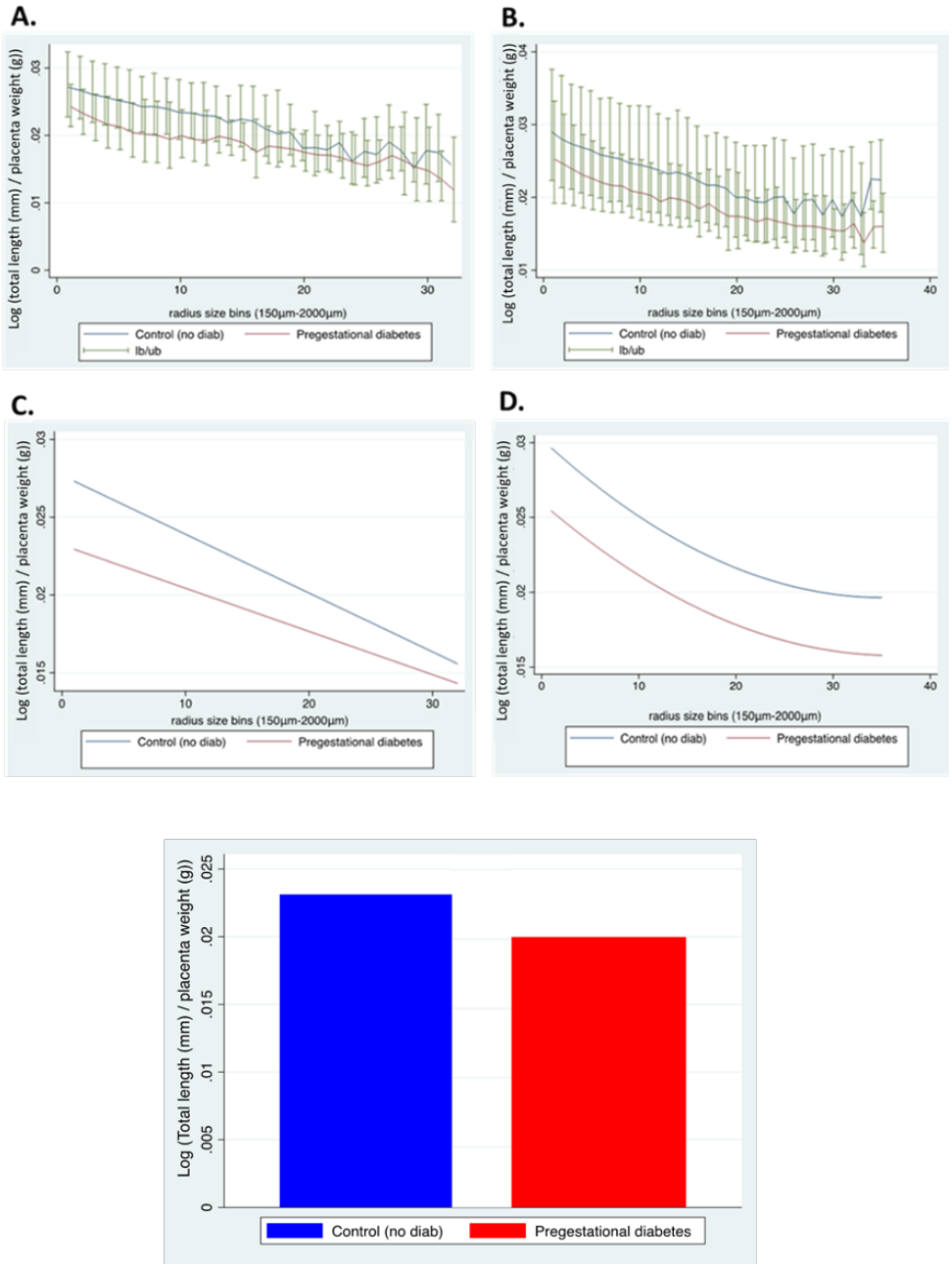

Figure 3.13 The total length of arteries and veins in normal and pregestational diabetes casts.

The total length of vessels in arterial and venous placenta casts from normal and pregestational diabetes pregnancies. All data are normalised to placental weight. **A (arterial,** p≤0.0001 control vs diabetes**) and B (venous** p = 0.001 control vs diabetes**)** represent line graphs of the total length placenta weight ratio in increasing radius size bins format (150 µm-2000 µm) while **C (arterial) and D (venous)** represent linear prediction smooth graphs of **(A) and (B**) respectively. **E** (total length of all vessels of all sizes, i.e. all binned cast data in **control no diabetes** and **pregestational diabetes**). Data presented as (log) geometric mean ± SD. Control (no diabetes) = 16(9 arterial, 7 venous) and Pregestational diabetes = 33 (16 arterial,17 venous). Mixed effects – ML Regression analysis, $p < 0.05$ was taken as significant.

In arterial placenta casts, there was a linear relationship between total length of vessels and radius size (**Figure 3.13**C). There was also an overall significant difference in total length of vessels between clinical groups. The log total length normalised to PW was longer in the control no diabetes group compared to the pregestational diabetes group p ≤0.0001 (**Figure 3.13**A). These findings were also observed in binned size number data format with p≤0.0001 (**Figure A3.0.2**A in *Appendix 3*). There was also a significant difference in the relationship between total length of vessels and radius size between the clinical groups p=0.02 (**Figure 3.13**A).

There was a non-linear relationship between total length of vessels and radius size in venous casts (**Figure 3.13**D). In common with arteries, in venous placenta casts there was an overall significant difference in total length of vessels between clinical groups. The log total length normalised to PW was longer in the control no diabetes group compared to the pregestational diabetes group p = 0.001 (**Figure 3.13**B). These findings were also observed in binned size number data format with p≤0.0001 (**Figure A3.0.2**B in Appendix 3).

3.6.3 Decreased vascular volume in casts from pregestational diabetes pregnancies

There was a non-linear relationship between measured mean vascular volume and radius size in arterial casts. The log mean volume normalised to PW in arterial placenta casts was greater in the control no diabetes group compared to the pregestational diabetes group but difference was not significant between the clinical groups (**Figure 3.14**A). Similar findings were observed in binned size number data format; however the overall difference in measured mean volume of vessels was significant between clinical groups p=0.004 (**Figure A3.0.3**A in Appendix 3).

Conversely in venous placenta casts, the log mean volume normalised to PW was greater in the pregestational diabetes group compared to the control no diabetes group but this difference was not significant; this was also observed in binned size number data format (**Figure A3.0.3**B in Appendix 3).). There was also a non-linear relationship between measured mean volume of vessels and radius size in venous casts. The relationship between mean volume of vessels and radius size between clinical groups was not significant in venous casts in bin order format (**Figure 3.14**B) but there was a significant difference observed in binned data format p=0.001 (**Figure A3.0.3**D in Appendix 3).

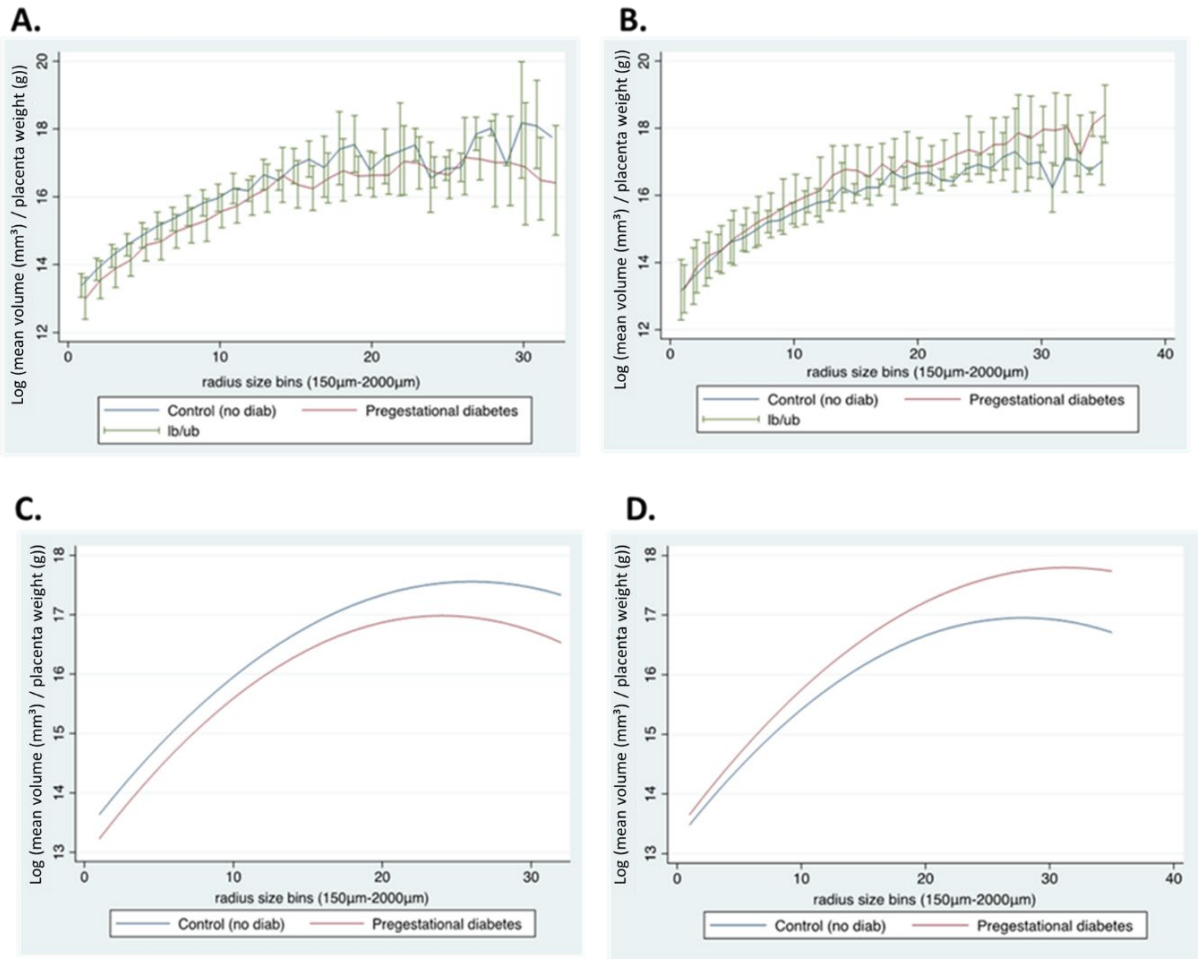

Figure 3.14 The mean volume of arteries and veins in normal and pregestational diabetes casts.

The mean volume of vessels in arterial and venous placental casts from normal and pregestational diabetes pregnancies. All data are normalised to placental weight. **A (arterial) and B (venous)** represent line graphs of the mean volume placenta weight ratio in increasing radius size bins format (150 µm-2000 µm) while **C (arterial) and D (venous)** represent linear prediction smooth graphs of **(A) and (B**) respectively. Data presented as (log) geometric mean ± SD. Control (no diabetes) = 16(9 arterial, 7 venous) and Pregestational diabetes = 33 (16 arterial, 17 venous). Mixed effects – ML Regression analysis, $p < 0.05$ was taken as significant.

The log total vascular volume normalised to PW in arterial placenta casts was significantly greater in the control no diabetes group compared to the pregestational diabetes group (**Figure 3.15**A), p=0.05. The relationship between measured total vascular volume and radius size was non –linear **Figure 3.15**C. There was also a significant difference in the relationship between total vascular volume and radius size between the clinical groups, p≤0.0001 (**Figure 3.15**A). Between radius size bin 15-28(1050µm-1700µm) the relationship switches to a significantly greater vascular volume in the pregestational diabetes group compared to the control group in that bin range, p≤0.0001. In binned size number data format, the difference in total vascular volume was not significant between clinical groups but the difference in the relationship between total vascular volume and radius size between clinical groups was significant with p=0.002 (**Figure A3.0.4**C in Appendix 3).

In venous placenta casts, the log total volume normalised to PW in arterial placenta casts was significantly greater in the control no diabetes group compared to the pregestational diabetes group (**Figure 3.15**B), p≤0.0001. There was also a linear relationship between total vascular volume and radius difference in venous casts. There was a significant difference in the relationship between total vascular volume and radius size between clinical groups, p=0.024 (**Figure 3.15**D). Likewise, in binned size number data format, significant differences were observed with greater total vascular volume in the control group compared to the pregestational diabetes, p≤0.0001 (**Figure A3.0.4**B in Appendix 3). There was also a significant difference in the relationship between total vascular volume and radius size between clinical groups, p≤0.0001 (**Figure A3.0.4**D in Appendix 3).

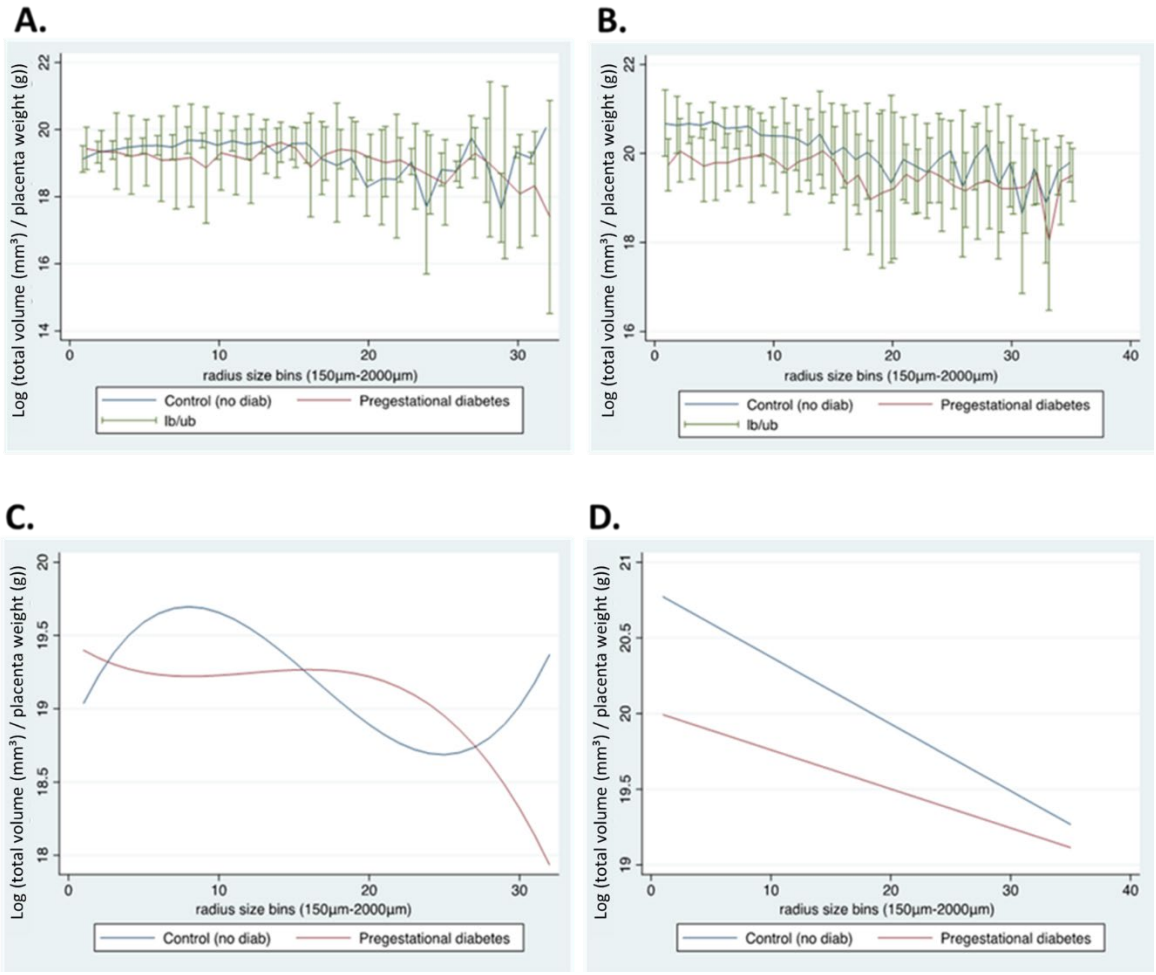

Figure 3.15 The total volume of arteries and veins in normal and pregestational diabetes casts in radius size bins.

The total vascular volume of vessels segments in arterial and venous placental casts from normal and pregestational diabetes pregnancies. All data are normalised to placental weight. **A (arterial,** p=0.05 control vs diabetes**) and B (venous,** p≤0.0001 control vs diabetes**)** represent line graphs of the total volume placenta weight ratio in increasing radius size bins format (150 µm-2000 µm) while **C(arterial) and D(venous)** represent linear prediction smooth graphs of **(A) and (B**) respectively. Data presented as (log) geometric mean ± SD. Control (no diabetes) = 16(9 arterial, 7 venous) and Pregestational diabetes = 33 (16 arterial,17 venous). Mixed effects – ML Regression analysis, $p < 0.05$ was taken as significant.

3.6.4 Summary

In summary, the first part of the study demonstrated that the mean number of vessel segments are significantly different within the microcirculation between control and pregestational groups, and not in the larger vessels of the chorionic plate. The data also demonstrated shorter mean arterial and venous vessel length in pregestational diabetes as well as decreased total arterial vessel length in casts from pregestational diabetes across increasing radius bin size adjusted for placental weight and gestation at delivery. Overall shorter total venous vessel length was also demonstrated in placenta casts from pregestational diabetes pregnancies.

We also showed decreased mean arterial volume and increased mean venous volume of vessels in casts from pregestational diabetes pregnancies. Overall, decreased total arterial and venous vascular volume was demonstrated across increasing radius size bins of vessel segments.

3.7 Placental vascular development associations to maternal glycaemic control in pregnancies complicated by pre-gestational diabetes.

Studies of placental pathology have not always reported findings in microvasculature at term in diabetes in relation to maternal glycaemic control, earlier events in pregnancy or pregnancy outcome. Inconsistencies in published data highlight the potential advantages of using an unbiased quantitative approach to assess placental arterial and venous structure in diabetes in relation to maternal glucose status and fetal outcome.

Within pathological groups of pregnancies characterised by diabetes, comparisons were made between women with diabetes with differing levels of glycaemic control. The pattern of glycaemic control was classified using measurements of HbA1c in first trimester and last trimester of pregnancy. These were grouped under good diabetes control (maternal glycaemic control from poor to good through pregnancy; most measurements at HbA1c (<48 mmol/mol) and poor diabetes control (poor to worse glycaemic control throughout pregnancy; most measurements ≥48 mmol/mol). These observations were stratified to fetoplacental vascular measurement at term to assess the relationship between pregnancies complicated by maternal diabetes and the disparate adverse outcomes.

3.7.1 Demographic and clinical details of study participants

The demographic and clinical details of the women and babies whose placentas were used are shown in **Table 3.5**. At delivery, the median gestational age, birthweight, placental weight, IBR centile, fetal: placental weight ratio and parity were significantly different between the good control pregestational diabetes group and poor control pregestational diabetes groups. Median placental weight was 578.0g (IQR 400.0 – 766.0g) and 649.0g (IQR 437.0 – 874.0g); $p<0.0001$ for the good control pregestational diabetes group and poor control pregestational diabetes groups respectively.

Similarly, median gestational age was 264(240-280) days and 255 (217-280) days $p< 0.00001$ for the good control pregestational diabetes group and poor control pregestational diabetes groups respectively. Birthweight was 3216g (2240-3986) and 3454g (2107-4640), $p= 0.0005$ for the good control pregestational diabetes group and poor control pregestational diabetes groups. In addition, Individualised birthweight ratio was 49(1.5-99) and 97 (55.3-100) $p< 0.0001$ for the good control pregestational diabetes group and poor control pregestational diabetes groups. There was also a significant difference in

the amount of deliveries under 37 weeks between both groups (good control vs poor control), p=0.00087. There was also a significant difference in fetal: placental weight ratio for both groups (good control; 5.61(3.45-7.76) vs poor control; 5.02 (4.21-6.36)), p=0.01786.

There was no significant difference in maternal age, maternal BMI, mode of delivery or fetal sex between good control pregestational diabetes group and poor control pregestational diabetes group.

Table 3.5 Demographic and clinical details of study participants

Demographic data	Normal Pregnancies (n=16)	Pregestational diabetes (n=22) Good control	Pregestational diabetes (n=11) Poor control	*p* value
Casts	Arterial (9) Venous (7)	Arterial (10) Venous (12)	Arterial (6) Venous (5)	
Ethnicity -White -Black -Asian -Mixed -Other	 11(68.75%) 0(0.0%) 3(18.75%) 0(0.0%) 2(12.5%)	 13(59.1%) 3(13.6%) 5(22.7%) 0(0%) 1(4.6%)	 8(72.7%) 1(9.1%) 2(18.2%) 0(0%) 0(0%)	
Maternal age, years	33(29-41)	33(19-36)	35 (25-44)	*0.27326*
Maternal BMI, Kg/m2	25.1 (19.6-33.2)	27.2(20.3-44.5)	27.6(21- 35)	*0.1165*
Gestational age at delivery, (days)	273(261-295)	264(240-280)	255(217-280)	***<0.0001***
Deliveries under < 37 weeks	0	1	8	***0.00087***
Birth weight, g	3313(2440-4400)	3216(2240-3986)	3454 (2107-4640)	***0.0005***
Placental weight, g	496(375-698)	578.2(400.3-766.5)	649 (437.4-874.7)	***<0.0001***
Fetoplacental weight ratio, F:P	6.36(4.96-8.78)	5.61(3.45-7.76)	5.02 (4.21-6.36)	***0.01786***
Placental surface area (IP)	328(227-483)	327.3(219.6-530.5)	350.2(205.1 - 495.2)	*0.1405*
IBR, centile	37(6-100)	49.5(1.5-99)	97.1(55.3-100)	***<0.0001***
Smoking, number (%)	4/16 (25%)	2/22(9.1%)	3/11(27.3%)	*0.21476*
Parity	4(0) 4(1) 6(2) 2(3)	2(0) 6(1) 3(2) 1(3)	3(0) 2(1) 3(2) 1(3) 1(5)	***0.0008***
Mode of delivery, number (%)				
Vaginal	2/16(12.5%)	11/22(50%)	4/11(42.4%)	*0.27093*
Caesarean section	14/16(87.5%)	11/22 (50%)	7/11(57.6%)	
Fetal Sex: Male Female	 9(56.25%) 7(43.75%)	 10/22(45.5%) 12/22(54.5%)	 5/11(45.5%) 6/11(54.5%)	*0.49202*
GPRI Centile				
AGA		14/22(63.6)	5/11(45.5%)	*0.31561*
LGA		5/22(22.7)	6/11(54.5%)	
SGA		3/22(13.6)		

Demographic data shown represent median and interquartile range (IQR) in parenthesis or in a number with percentage in parenthesis. p-value between pregestational diabetes **good control** and **poor control** obtained from Mann Whitney U test, p <0.05 = significant. BMI, IBR represent body mass index and individualised birth weight ratio respectively. Arterial

and venous refer to the vascular compartments casted for the respective placentas. Good control and poor control refer to maternal glycaemic status while Type 1 and Type 2 refer to clinical classifications of diabetes.

3.7.2 Shorter vessel length observed in poor diabetes control clinical group

In arterial placenta casts, the log mean chord length normalised to PW was longer in the no diabetes group compared to both pregestational diabetes groups. (**Figure 3.16**A). The difference in measured mean chord length was significant between the no diabetes group and the pregestational diabetes poor control group, p≤0.0001 but not between the no diabetes group and the pregestational diabetes good control group. There was a non-linear relationship between mean chord length and radius size in arterial casts and the interaction term indicated that the differences in the relationship between mean chord length and radius size between the clinical groups (no diabetes group and pregestational diabetes poor control) was not significant; however, the differences in the relationship between mean chord length and radius size between the controls and pregestational diabetes good control was significant, p=0.047 (**Figure 3.16**C). Likewise, in binned size number data format, longer log mean chord length normalised to PW was shown in the no diabetes group compared to both the pregestational diabetes groups, p≤0.0001 for both groups respectively (**Figure A3.0.5**A in Appendix 3). However, the relationship between mean chord length and radius size between the no diabetes group and the pregestational diabetes poor control was significantly different, p= 0.034.

In venous placenta, the log mean chord length normalised to PW was longer in the no diabetes group compared to both pregestational diabetes groups (**Figure 3.16**B). The difference was significant between the no diabetes group and the pregestational diabetes poor control group, p= 0.035 but not between the no diabetes group and the pregestational diabetes good control (**Figure 3.16**). In binned size number data format, the log mean chord length normalised to PW was longer in the no diabetes group compared to both pregestational diabetes groups. (**Figure A3.0.5**B). The difference was significant between the no diabetes group and the pregestational diabetes good control group, p=0.05 and between the control and pregestational diabetes poor control(p=0.040) (**Figure A3.0.5**D in Appendix 3). The was a linear relationship between mean chord length of vessels and radius size in venous casts groups in both modes of data presentation.

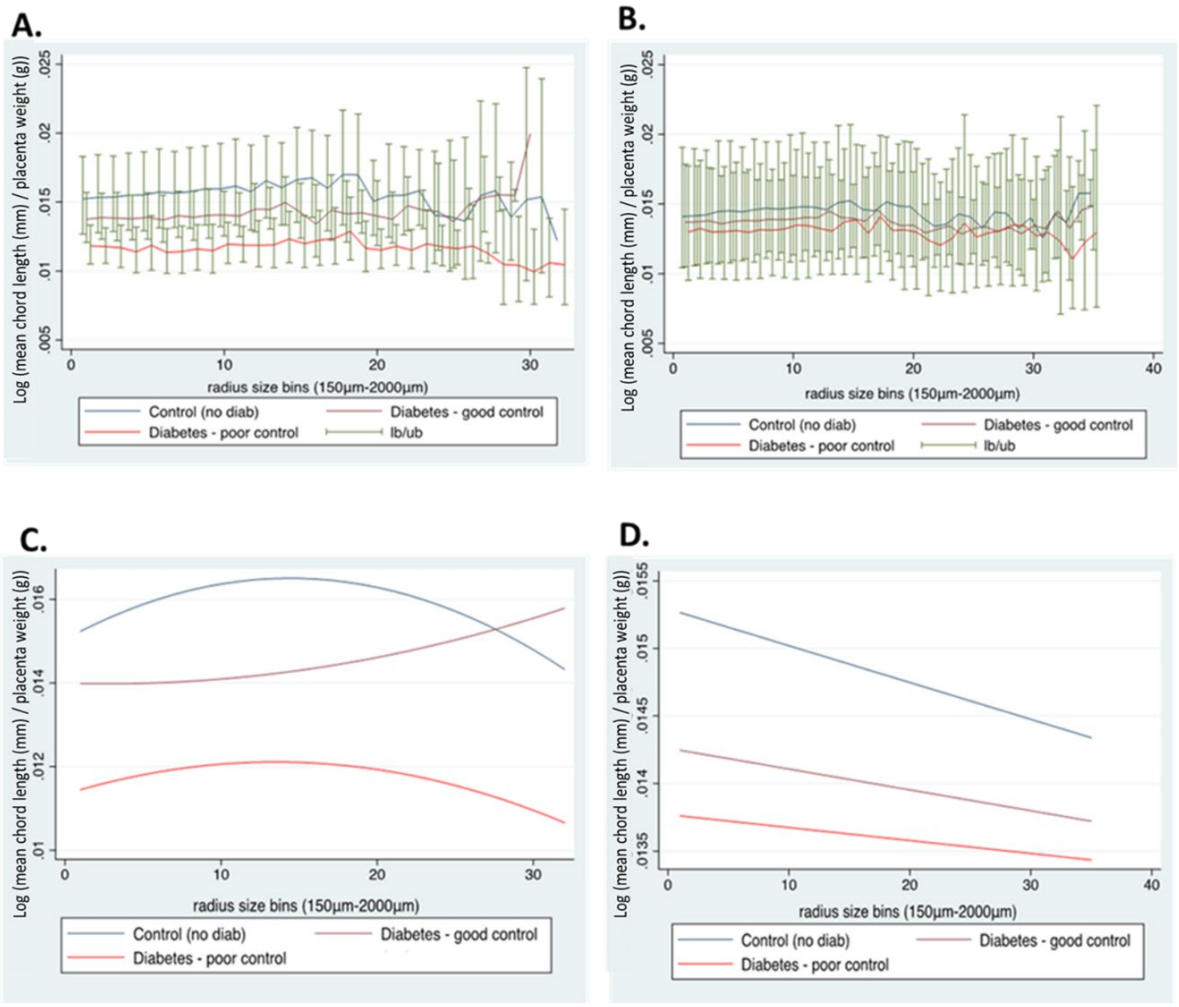

Figure 3.16 The chord length of arteries and veins in normal and maternal glycaemic status groups in pregestational diabetes casts.

The mean chord length of vessels in arterial and venous placental casts from normal and pregestational diabetes categories of glycaemic control over the course of pregnancy**.** All data are normalised to placental weight. **A (arterial:** control no diab vs Diabetes poor control, p≤0.0001) **and B (venous:** Control no diab vs Diabetes poor control, p=0.035) represent line graphs of mean chord length placenta weight ratio in increasing radius size bins format (150 µm-2000 µm) while **C (arterial) and D (venous)** represent linear prediction smooth graphs of **(A) and (B**) respectively. Data presented as (log) geometric mean ± SD. Control (no diabetes) = 16(9 arterials,7 venous and Pregestational diabetes = 33 (16 arterial cast =10 good control ,6 poor control) (17 venous casts= 12 good control, 5 poor control). Data presented. Mixed effects – ML Regression analysis, $p < 0.05$ was taken as significant.

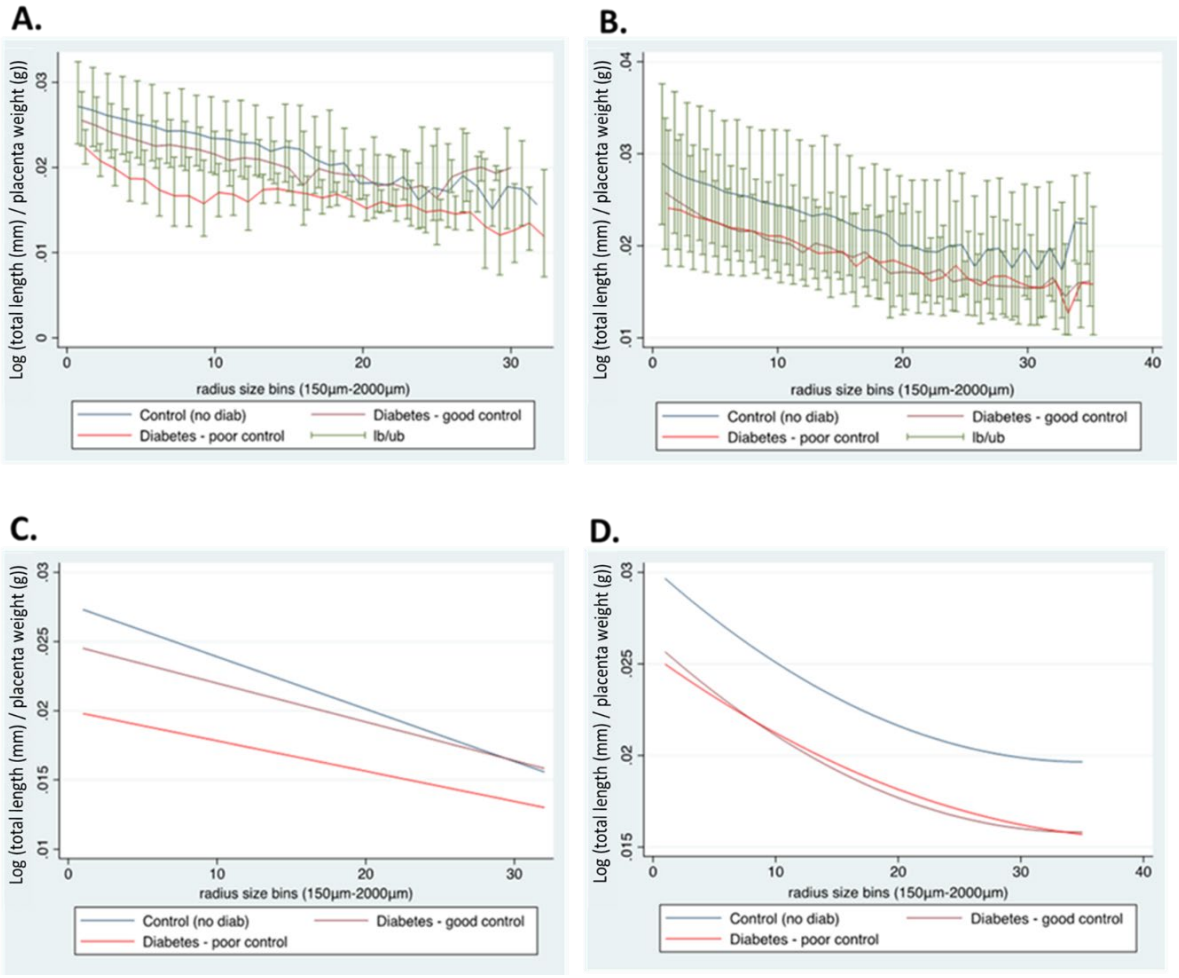

Figure 3.17 The total length of arteries and veins in normal and maternal glycaemic status groups in pregestational diabetes casts

The total length of vessels segments in arterial and venous placental casts from normal and pregestational diabetes categories of glycaemic control over the course of pregnancy. All data are normalised to placenta weight. **A (arterial**: control no diab vs Diabetes poor control and vs good control, p≤0.0001**) and B (venous:** control no diab vs Diabetes good control (p=0.003) and vs good control, p=0.004**)** represent line graphs of total length placenta weight ratio in increasing radius size bins format (150 µm-2000 µm) while **C (arterial) and D (venous)** represent linear prediction smooth graphs of **(A) and (B**) respectively. Data presented as (log) geometric mean ± SD. Control (no diabetes) = 16(9 arterial,7 venous and Pregestational diabetes = 33 (16 arterial cast =10 good control ,6 poor control) (17 venous casts= 12 good control, 5 poor control). Data presented. Mixed effects – ML Regression analysis, $p < 0.05$ was taken as significant.

In arterial placenta casts, the log total length normalised to PW was longer in the no diabetes group compared to both pregestational diabetes groups (**Figure 3.17**A). The difference in total length of vessels was significant between the no diabetes group to pregestational diabetes good control group, p≤ 0.0001 and pregestational diabetes poor control group, p≤0. 0001.There was a linear relationship between measured total length of vessels and radius size in arterial casts. There was also a significant difference in the relation between total length of vessels and radius size between clinical groups; no diabetes group vs pregestational diabetes good control, p=0.029 and between the no diabetes group vs pregestational diabetes poor control, p≤ 0.0001(**Figure 3.17**C). These findings were also observed in binned size number data format; the log total length per PW was longer in the no diabetes group compared to both pregestational diabetes groups. (**Figure A3.0.6**A in Appendix 3). The difference was significant between the no diabetes group and the pregestational diabetes good control group, p = 0.035 and between the no diabetes group and the pregestational diabetes poor control group, p≤0.00001. There was also significant difference in the relationship between measured total length of vessels and radius size between the no diabetes group and the pregestational diabetes poor control group, p=0.041 (**Figure A3.0.6**C in Appendix 3).

Similarly, in venous placenta casts, the log total length normalised to PW was longer in the no diabetes group compared to both pregestational diabetes groups. (**Figure 3.17**B). The difference was significant between the no diabetes group and the pregestational diabetes good control group, p=0.003 and the control no diabetes group compared to pregestational diabetes poor control group, p=0.004 (**Figure 3.17**B). There was a non-linear relationship between measured total length of vessels and radius size in venous casts (**Figure 3.17**D).
In binned size number data format, the log total length normalised to PW was longer in the no diabetes group compared to both pregestational diabetes groups (**Figure A3.0.6**B in Appendix 3). The difference was significant between the no diabetes group and the pregestational diabetes good control group, p≤0.0001 and between the control no diabetes group and the pregestational diabetes poor control group, p=0.001. There was also a significant difference in the relationship between total length of vessels and radius size between clinical groups; the no diabetes group and the pregestational diabetes good control group, p=0.046 (**Figure A3.0.6**D in Appendix 3).

3.7.3 Vascular volume alterations in both pathological clinical groups of maternal glycaemic control

The log mean volume normalised to PW in arterial placenta casts was greater in the no diabetes group compared to both pregestational diabetes groups (**Figure 3.18**A). The difference in mean volume of vessels was significant between the no diabetes group and the pregestational diabetes poor control group, p = 0.006 but not between the no diabetes group and the pregestational diabetes good control group. There was a non-linear relationship between measured mean volume of vessels and radius size in arterial casts. Findings in binned size number data format showed greater log mean volume normalised to PW in the no diabetes group compared to both pregestational diabetes groups. (**Figure A3.0.7**A in Appendix 3). The difference in mean volume of vessels was significant between the no diabetes group and the pregestational diabetes good control group, p = 0.049 and the pregestational diabetes poor control group, p≤0.0001(**Figure A3.0.7**A in Appendix 3).

Conversely in venous placenta casts, the log mean volume normalised to PW was less in the no diabetes group compared to the pregestational diabetes good control group and poor control group. This difference was not significant between the clinical groups (no diabetes vs good/poor diabetes control). There was a non-linear relationship between measured mean volume of vessels and radius size in venous casts however there was a significant difference in the relationship between mean vessel volume and radius size between the clinical groups ; the no diabetes group and the pregestational diabetes good control, p=0.003 (**Figure 3.18**D) and between the poor control and good control pregestational diabetes, p≤0.0001 (**Figure 3.18**D). Similar findings were shown in binned size number data format; the log mean volume normalised to PW in venous placenta cast was less in the no diabetes group compared to the pregestational diabetes good control group and poor control group. There was also a non-linear relationship (quadratic fit) between measured mean volume of vessels and radius size in venous casts as well as a significant difference in the relationship between measured mean volume of vessels and radius size between clinical groups; no diabetes group and pregestational diabetes good control group, p≤0.0001(**Figure A3.0.7**D in Appendix 3).

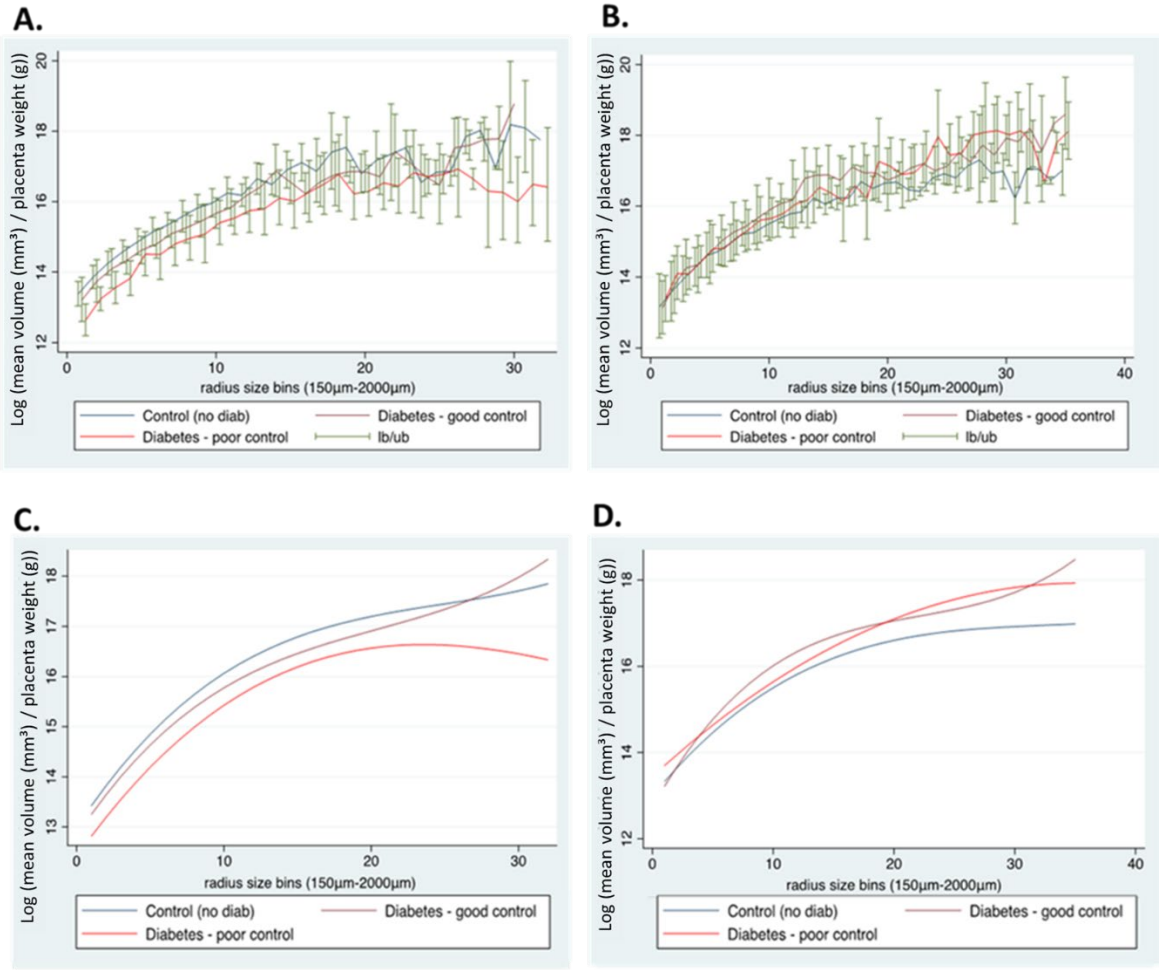

Figure 3.18 The mean volume of arteries and veins in normal and maternal glycaemic status groups in pregestational diabetes casts.

The mean volume of vessels in arterial and venous placental casts from normal and pregestational diabetes categories of glycaemic control over the course of pregnancy. All data are normalised to placental weight. **A (arterial:** control no diab vs Diabetes poor control p=0.006) **and B(venous)** represent line graphs of mean volume placenta weight ratio in increasing radius size bins format (150 µm-2000 µm) while **C (arterial) and D (venous)** represent linear prediction smooth graphs of **(A) and (B**) respectively. Data presented as (log) geometric mean ± SD. Control (no diabetes) = 16(9 arterial, 7 venous and Pregestational diabetes = 33 (16 arterial cast =10 good control ,6 poor control) (17 venous casts= 12 good control, 5 poor control). Data presented. Mixed effects – ML Regression analysis, $p < 0.05$ was taken as significant.

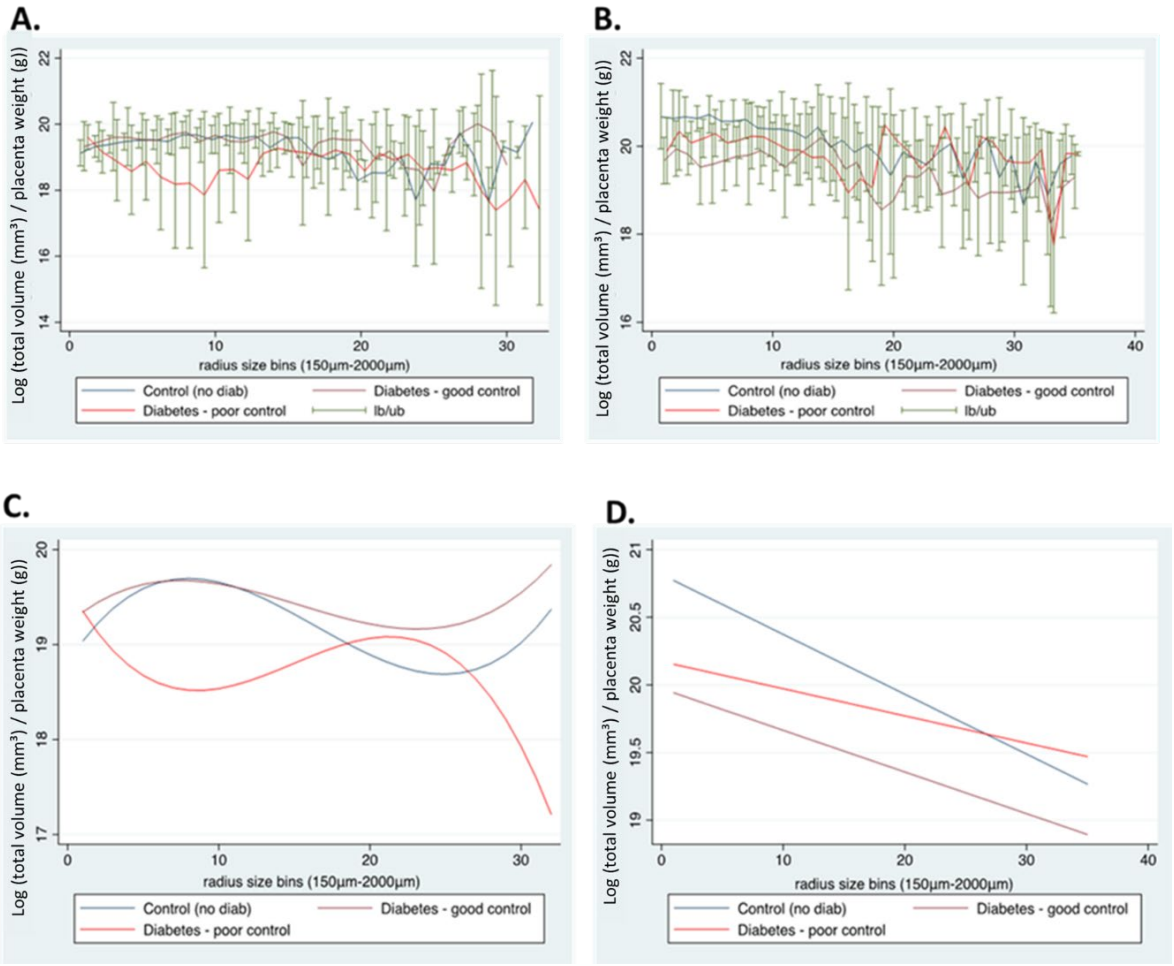

Figure 3.19 The total volume of arteries and veins in normal and maternal glycaemic status groups in pregestational diabetes casts.

The total vascular volume of vessel segments in arterial and venous placental casts from normal and pregestational diabetes categories of glycaemic control over the course of pregnancy**.** All data are normalised to placental weight. **A (arterial:** control no diab vs Diabetes poor control p=0.043**) and B (venous:** control no diab vs Diabetes good control (p≤0.0001) and vs good control, p=0.001**)** represent line graphs of total volume placenta weight ratio in increasing radius size bins format (150 µm-2000 µm) while **C (arterial) and D (venous)** represent linear prediction smooth graphs of **(A) and (B**) respectively. Data presented as (log) geometric mean ± SD. Control (no diabetes) = 16(9 arterial, 7 venous and Pregestational diabetes = 33 (16 arterial cast =10 good control ,6 poor control) (17 venous casts= 12 good control, 5 poor control). Data presented. Mixed effects – ML Regression analysis, $p < 0.05$ was taken as significant.

The log total volume normalised to PW in arterial placenta casts was less in the no diabetes group compared to the pregestational diabetes good control group but greater than the poor control group. (**Figure 3.19**A). The difference in total vascular volume was significant between the no diabetes group and the pregestational diabetes poor control group p=0.043 but not between the no diabetes group and the pregestational diabetes good control group. There was a non-linear relationship between measured total vascular volume and radius size in arterial casts and there was also a significant difference in the relationship between measured total vascular volume and radius size between clinical groups; no diabetes group and pregestational diabetes poor control group, p≤0.0001 (**Figure 3.19**C). There were also changes in vascular volumes between the no diabetes and poor control pregestational diabetes across bin ranges in 19 -28 (1250µm-1700µm) and this was significantly different p≤0.0001. Similar findings were observed in binned size number data format; the log total volume normalised to PW in arterial placenta casts was less in the no diabetes group compared to the pregestational diabetes good control group but greater than the poor control group (**Figure A3.0.8**A in Appendix 3). The overall difference in total vascular volume between clinical groups was not significant in binned size number data format. However, there was a significant difference in the relationship between measured total vascular volume and radius size between clinical groups; no diabetes group and pregestational diabetes poor control group, p≤0.0001 (**Figure A3.0.8**C in Appendix 3).

In venous placenta casts , the log total volume normalised to PW was greater in the no diabetes group compared to pregestational diabetes good control group (p=0.0001) and poor control group (p=0.001)(**Figure 3.19**B). There was a linear relationship between measured total vascular volume and radius size in venous casts as well as a significant difference in the relationship between measured total vascular volume and radius size between clinical groups; no diabetes group and pregestational diabetes poor control group, p=0.020 (**Figure 3.19**D) Likewise in binned size number data format, the log total volume normalised to PW in venous placenta casts was greater in the no diabetes group compared to the pregestational diabetes good control group, (p≤0.0001) and poor control group, (p=0.05)(**Figure A3.0.8**B in Appendix 3). There was also a linear relationship between measured total vascular volume and radius size in venous casts as well as a significant difference in the relationship between measured total vascular volume and radius size

between clinical groups; no diabetes group and pregestational diabetes good control group, p≤0.0001 (**Figure A3.0.8**D in Appendix 3).

3.7.4 Summary

In summary, this investigation demonstrated shorter mean arterial and venous vessel length in poor control pregestational diabetes compared to the no diabetes group. Overall shorter total arterial vessel length was also demonstrated in placenta casts from good control and poor control pregestational diabetes pregnancies across increasing radius bin size compared to the no diabetes group. Furthermore, shorter venous total vessel length was demonstrated in good and poor control clinical groups when compared to the no diabetes group.

We also showed decreased mean arterial volume of vessels and in casts from poor control pregestational diabetes pregnancies, but increased mean venous volume of vessels in good control pregestational diabetes group when compared to the no diabetes group. Overall, decreased total arterial vascular volume in poor control diabetes group and decreased venous vascular volume was demonstrated across increasing radius size bin of vessel segments in both pregestational diabetes glycaemic control groups in comparison to the no diabetes group.

3.8 Placental vascular development associations to maternal (PIGF) levels in pregnancies complicated by pregestational diabetes.

Placental expressions of many growth factors outlined in section **1.4.1.2** contribute to increased efficiency in coordinating development of the vascular system [27, 93]. PlGF is an angiogenic factor of the VEGF family, expressed in trophoblast, and functions to control trophoblast growth and differentiation. The secretion of PlGF by trophoblast giant cells usually in rodents, has been reported to be the signal that initiates and coordinates vascularisation in the decidual and placenta during early embryogenesis[104, 118]. PlGF concentrations in maternal serum rise during pregnancy, peaking at the end of the mid trimester of pregnancy. Low PlGF concentrations during pregnancy are associated with pregnancy complications including recognized later-life maternal cardiovascular risk [121].

Observations and measurements of the fetoplacental vasculature made at term are likely to reflect earlier events in vessel development. In this investigation, measured vascular biometry output of placental casts were related to clinically categorised PIGF profile groups of women during pregnancy. Maternal plasma PIGF measurements was taken (section **3.3**) across three trimesters (**Figure 3.20**) and classified into women with a normal PIGF (≥100pg/l) in the third trimester and women with a third trimester PlGF < 100 pg/L [290] (**Figure 3.20**). Normal and low PlGF profiles of women were related to data obtained from their vascular placental casts.

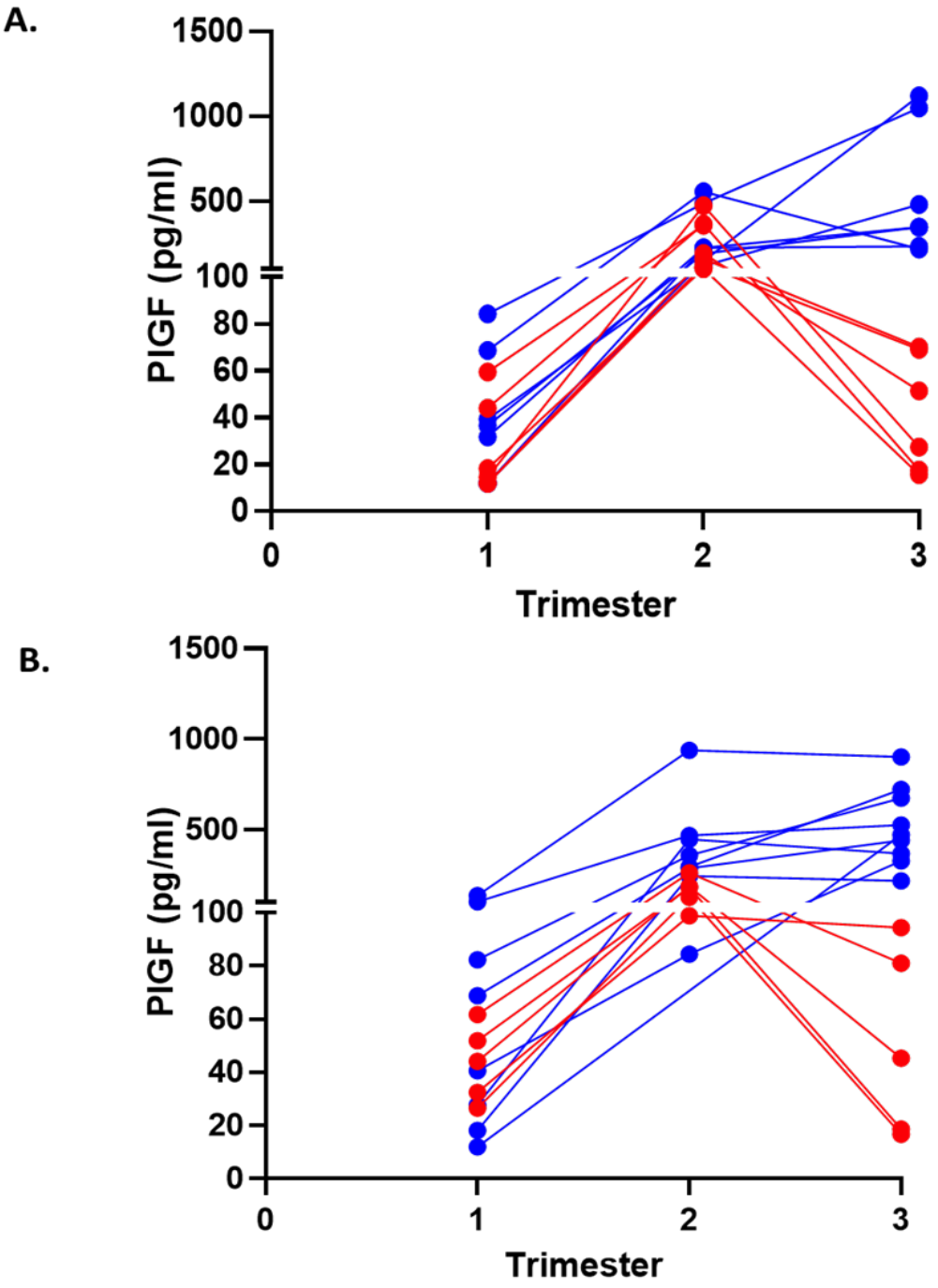

Figure 3.20 The PIGF profiles women with pregestational diabetes over the course of pregnancy in categories of trimester

PIGF profiles of women from the Velocity study**;** **blue points (16)** represent those women with a normal PIGF profile during pregnancy; **red points (12)** represent those with a lower PIGF profile during pregnancy. (1,2,3 represent early, mid and late trimester respectively). Data presented as scatter plots of normal and low PlGF profiles of women related to data on **A**- arteries and **B** - veins from 28 placental vascular casts.7 arterial casts were related to normal maternal plasma PlGF concentration and 7 arterial casts were related to lower maternal plasma PlGF concentration. 9 venous casts were related to normal maternal plasma PlGF concentration and 5 venous casts were related to lower maternal plasma PlGF concentration.

3.8.1 Demographic and clinical details of study participants

The demographic and clinical details of the women classified with either normal or lower PIGF in the third trimester group whose placentas were used are shown in **Table 3.6**. There were no significant differences demographic and clinical data between the normal and lower PIGF groups in pregestational diabetes with arterial and venous casts data pooled together.

Table 3.6 Demographic and clinical details of study participants

	Normal PIGF group (n=16) Arterial=7 Venous=9	Lower PIGF group (n =12) Arterial=7 Venous=5	*p* value
Diabetes-Classification	Type 1 **(10)** Type 2 **(2)**	Type 1**(11)** Type 2**(5)**	
Diabetes- good control	12/16 **(75%)**	7/12 **(58.3%)**	
Diabetes- poor control	4/16 **(25%)**	5/12 **(41.7%)**	
Maternal BMI	20.3-44.5 **(27.1)**	21-34.6 **(26.8)**	*0.429*
Placenta weight(g)	400-766.51**(641.1)**	453.5-823.8 **(589.5)**	*0.101*
Birthweight(g)	2346-3780 **(3385)**	2240-4430 **(2847)**	*0.184*
Gestation(days)	245-275 **(264)**	238-273 **(261)**	*0.176*
IBR, centile	36-99 **(77.5)**	2-100 **(64)**	*0.445*
Hba1c first (mmol/L)	37-75 **(46)**	35-73 **(45.5)**	*0.348*
Hba1c last (mmol/L)	31-63 **(39)**	31-56 **(42.5)**	*0.093*

Data shown are median and interquartile range (IQR) or number with percentage in parenthesis as appropriate. Comparisons by Mann Whitney U test; p ≤0.05 is significant. BMI, IBR, represent body mass index, individualised birth weight ratio respectively. Arterial and venous refer to the vascular compartments casted for the respective placentas. Good control and poor control refer to maternal glycaemic status while Type 1 and Type 2 refer to clinical classifications of diabetes.

3.8.2 Vessel length discrepancies in lower PIGF profile group in pregestational diabetes

Comparing arterial placental casts of categorized groups of women with normal PIGF levels and lower PIGF levels in the third trimester within pregestational diabetes group, the log mean chord length normalised to PW was longer in the lower PIGF group compared to the normal PIGF group in pregestational diabetes, p= 0.015 (**Figure 3.21**A). There was a linear relationship between the mean chord length and radius size in arterial casts as well as significant differences in the relationship between mean chord length and radius size between the clinical groups (normal PlGF group and lower PlGF group), p=0.003(**Figure 3.21**C). These findings were also observed in binned size number data format where the log mean chord length normalised to PW was longer in the lower PIGF group compared to the normal PIGF group in pregestational diabetes, p = 0.026 (**Figure A3.0.9**A in Appendix 3).

On the other hand, in venous placenta casts, the log mean chord length normalised to PW was shorter in the lower PIGF group compared to the normal PIGF group in pregestational diabetes, p = 0.025 (**Figure 3.21**B). There was also a linear relationship between the mean chord length and radius size in venous casts as well as significant differences in the relationship between mean chord length and radius size between the clinical groups(normal PlGF group and lower PlGF group), p=0.006 (**Figure 3.21**D). Likewise, in binned size number data format, the log mean chord length normalised to PW was shorter in the lower PIGF group compared to the normal PIGF group in pregestational diabetes but the difference was not significant (**Figure A3.0.9**B in Appendix 3).

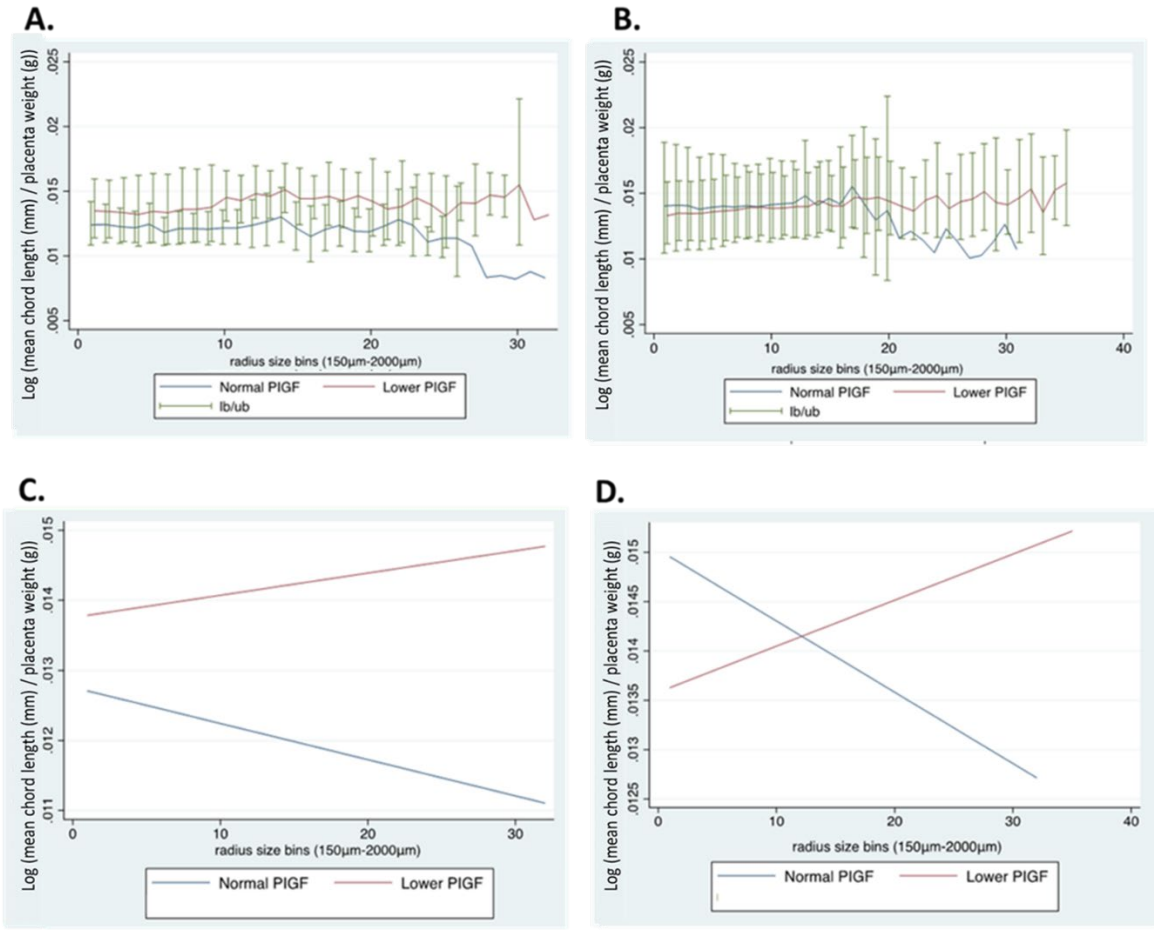

Figure 3.21 The length of arteries and veins in maternal PIGF profile groups in pregestational diabetes casts.

The mean chord length of vessels in arterial and venous casts of normal and lower PIGF groups in pregestational diabetes**.** All data are normalised to placental weight. **A (arterial:** Normal PlGF vs Lower PlGF p=0.015**) and B (venous**: Normal PlGF vs Lower PlGF p=0.025**)** represent line graphs of mean chord length placenta weight ratio in increasing radius size bins format (150 µm-2000 µm) while **C (arterial) and D (venous)** represent linear prediction smooth graphs of **(A) and (B**) respectively. Data represented as (log) geometric mean ± SD, Normal PIGF group = (7 arterial, 9 venous) casts and Lower PIGF group (7 arterial,5 venous) casts. Mixed effects – ML Regression analysis, $p < 0.05$ was taken as significant.

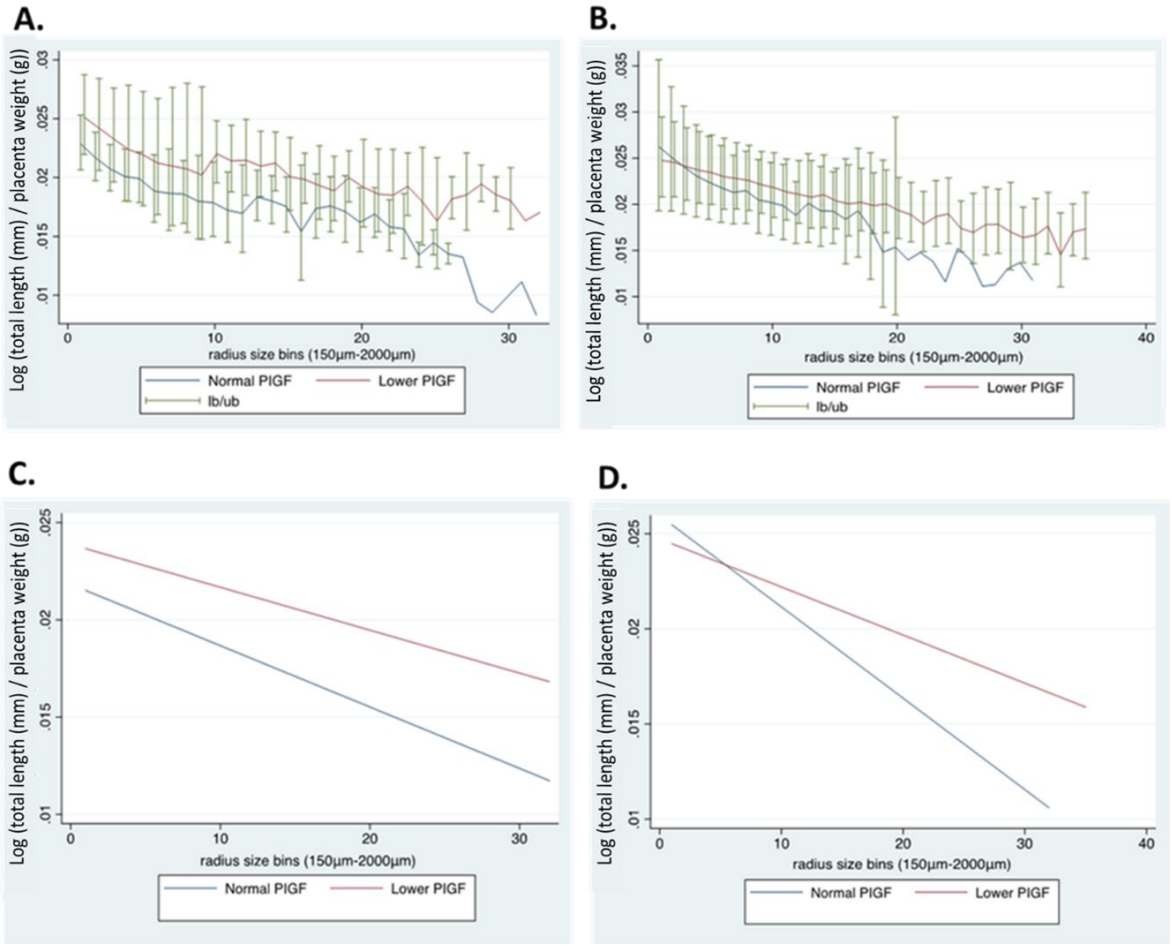

Figure 3.22 The total length of arteries and veins in maternal PIGF profile groups in pregestational diabetes casts.

The total length of vessels in arterial and venous casts of normal and lower PIGF groups in pregestational diabetes**.** All data are normalised to placental weight and adjusted for HbA1C. **A (arterial:** Normal PlGF vs Lower PlGF p=0.002**) and B(venous)** represent line graphs of total length placenta weight ratio in increasing radius size bins format (150 µm-2000 µm) while **C(arterial) and D(venous)** represent linear prediction smooth graphs of **(A) and (B**) respectively. Data represented as (log) geometric mean ± SD, Normal PIGF group = (7 arterials, 9 venous) casts and Lower PIGF group (7 arterial,5 venous) casts. Mixed effects – ML Regression analysis, $p < 0.05$ was taken as significant.

In arterial placenta casts, the log total length normalised to PW was longer in the lower PIGF group compared to the normal PIGF group in pregestational diabetes, p= 0.002 (**Figure 3.22**A). There was a linear relationship between total length of vessels and radius size in arterial casts. There was also a significant difference in the relationship between total length of vessels and radius size between the normal PIGF group and the lower PIGF group in pregestational diabetes, p=0.032(**Figure 3.22**C). These findings were also observed in binned size number data format where the log total length normalised to PW was longer in the lower PIGF group compared to the normal PIGF group in pregestational diabetes, p=0.004(**Figure A3.0.10**A in Appendix 3).

There was also a significant difference in the relationship between total length of vessels and radius size between the normal PIGF group and the lower PIGF group in pregestational diabetes when adjusted for maternal glycaemic status (HbA1C measurement) in the interaction term for first trimester measurements, (p=0.003) and last trimester measurements (p=0.003).

There was a linear relationship between total length of vessels and radius size in venous casts. Similarly, in venous placenta casts, the log total length normalised to PW was longer in lower PIGF group compared to normal PIGF group in pregestational diabetes but this difference was not significant between groups. However, the difference in the relationship between total length of vessels and radius size between the normal PIGF group and the lower PIGF group in pregestational diabetes was significant, p≤0.0001(**Figure 3.22**D). In binned size number data format, there was no significant differences in total length of vessels between the normal PlGF group and the lower PlGF group in pregestational diabetes.

There was also a significant difference in the relationship between total length of vessels and radius size between the normal PIGF group and the lower PIGF group in pregestational diabetes when adjusted for maternal glycaemic status (HbA1C measurement) in the interaction term for first trimester measurements, (p=0.027) but not with last trimester measurement.

3.8.3 Vascular volume alterations in PIGF profile groups in pregestational diabetes

There was a non-linear relationship between measured mean vascular volume and radius size in arterial casts. The log mean vascular volume normalised to PW in arterial placenta casts was greater in the lower PIGF group compared to the normal PIGF group in pregestational diabetes; this difference was not significant (**Figure 3.23**A). However, the relationship between mean vascular volume and radius size between the normal PIGF group and lower PIGF group in pregestational diabetes was significantly different, p=0.008(**Figure 3.23**C). Similar findings were observed in binned size number data format but differences were not significant between groups (**Figure A3.0.11(**A)(C) in Appendix 3).

Similarly, in venous placenta casts, there was a non-linear relationship between measured mean vascular volume and radius size. The log mean volume normalised to PW in venous placenta casts, was lower in the lower PIGF group compared to normal PIGF group in pregestational diabetes between bin (1-25) but higher in larger radius bins >25. This difference was not significant but there was a significant difference in the relationship between measured mean vascular volume and radius size between the different pregestational diabetes groups; normal PlGF and lower PlGF group, p≤0.0001(**Figure 3.23**D). However, in binned size number data format, the log mean volume normalised to PW was significantly greater in lower PIGF group compared to normal PIGF group in pregestational diabetes, p=0.024 (**Figure A3.0.11**B in Appendix 3).

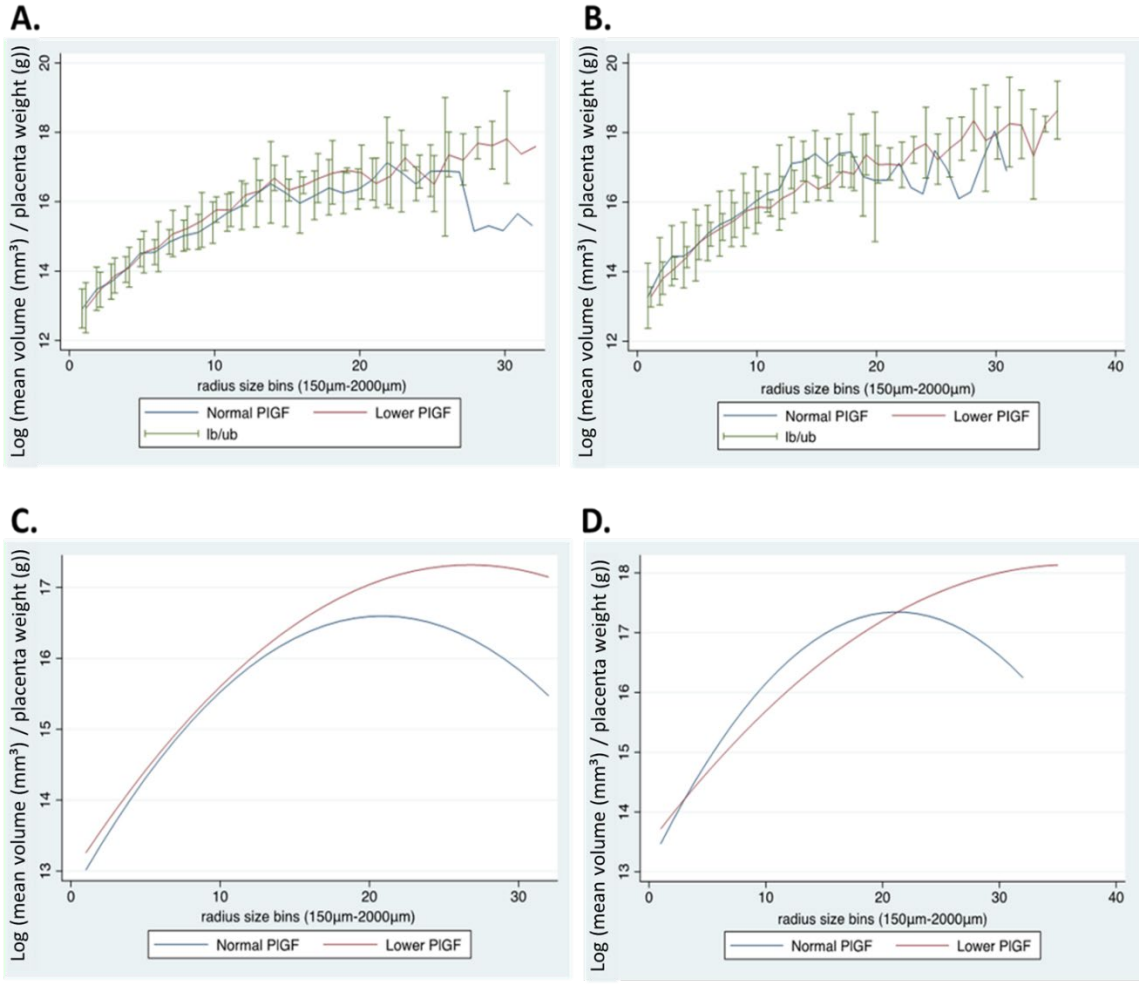

Figure 3.23 The mean volume of arteries and veins in maternal PIGF profile groups in pregestational diabetes casts.

The mean volume of vessels in arterial and venous casts of normal and lower PIGF groups in pregestational diabetes**.** All data are normalised to placental weight. A**(arterial) and B(venous)** represent line graphs of mean volume placenta weight ratio in increasing radius size bins format (150 µm-2000 µm) while **C(arterial) and D(venous)** represent linear prediction smooth graphs of **(A) and (B**) respectively. Data represented as (log) geometric mean ± SD, Normal PIGF group = (7 arterial, 9 venous) casts and Lower PIGF group (7 arterial,5 venous) casts. Mixed effects – ML Regression analysis, $p < 0.05$ was taken as significant.

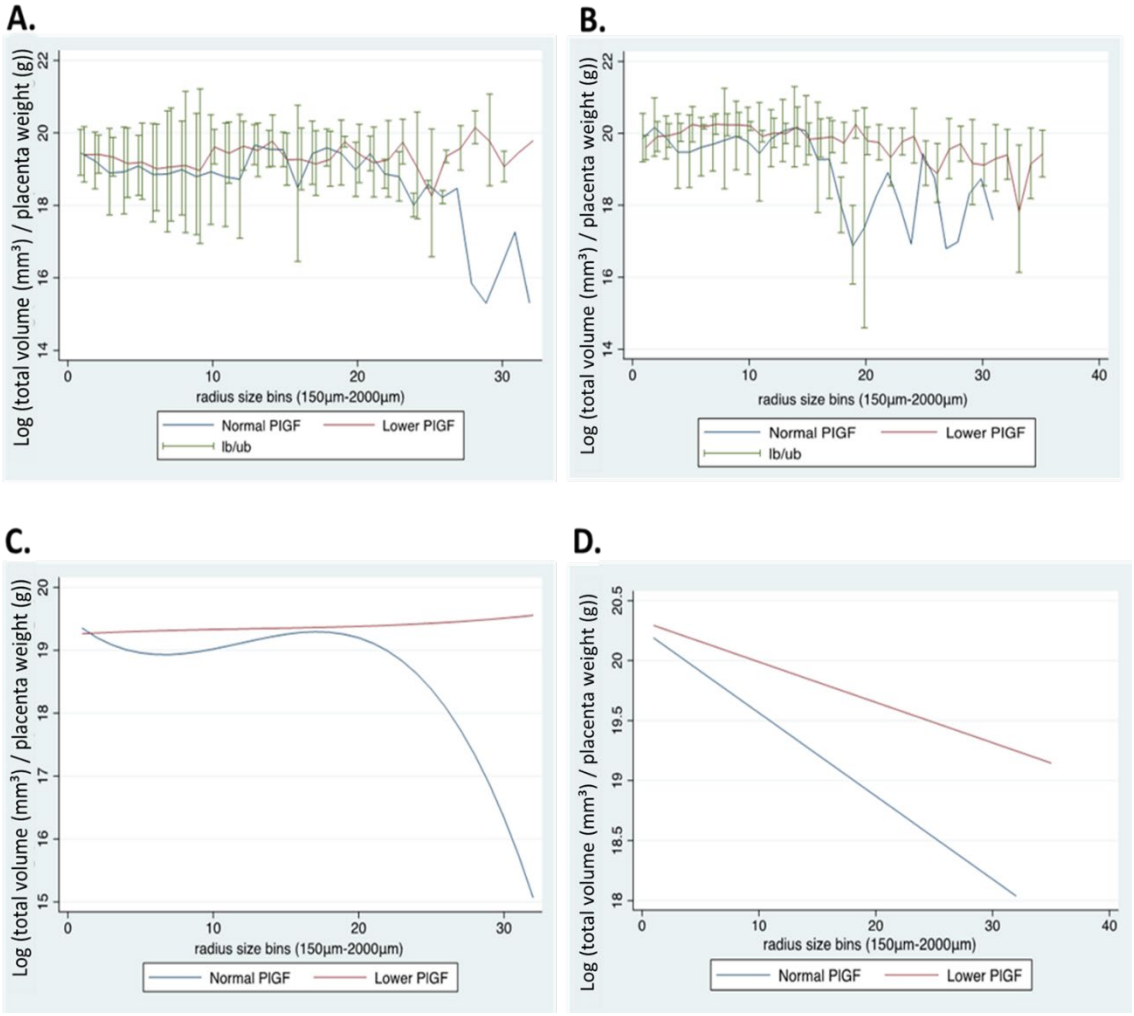

Figure 3.24 The total volume of arteries and veins in maternal PIGF profile groups in pregestational diabetes casts.

The total volume of vessel segments in arterial and venous casts of normal and lower PlGF groups in pregestational diabetes**.** All data are normalised to placental weight. **A(arterial) and B(venous)** represent line graphs of total volume placenta weight ratio in increasing radius size bins format (150 µm-2000 µm) while **C(arterial) and D(venous)** represent linear prediction smooth graphs of **(A) and (B**) respectively. Data represented as (log) geometric mean ± SD, Normal PIGF group = (7 arterial, 9 venous) casts and Lower PIGF group (7 arterial,5 venous) casts. Mixed effects – ML Regression analysis, $p < 0.05$ was taken as significant.

There was a non-linear relationship between measured total vascular volume and radius size in arterial casts. The log total vascular volume normalised to PW in arterial placenta casts was greater in the lower PIGF group compared to the normal PIGF group in pregestational diabetes; this difference was not significant (**Figure 3.24**A). However, there was a significant difference in the relationship between total vascular volume and radius size between the normal PIGF group and the lower PIGF in pregestational diabetes, p=0.027 (**Figure 3.24**). Similar findings were observed in binned size number data format but the difference was not significant. (**Figure A3.0.12**(A)(C) in Appendix 3).

There was also a significant difference in the relationship between total vascular volume and radius size between the normal PIGF group and the lower PIGF group in pregestational diabetes when adjusted for maternal glycaemic status (HbA1C measurement) in the interaction term for first trimester measurements, (p=0.028) and last trimester measurements (p=0.011).

There was a linear relationship between measured total vascular volume and radius size in venous placenta casts. The log total volume normalised to PW was greater in the lower PIGF group compared to the normal PIGF group in pregestational diabetes. This difference was not significant (**Figure 3.24**B). However, there was a significant difference in the relationship between total vascular volume and radius size between the normal PIGF group and the lower PIGF group in pregestational diabetes, p=0.005(**Figure 3.24**D). There was also a significant difference in the relationship between total vascular volume and radius size between the normal PIGF group and the lower PIGF in pregestational diabetes when adjusted for maternal glycaemic status (HbA1C measurement) in the interaction term for first trimester measurements, (p=0.036) and last trimester measurements (p=0.036).

In binned size number data format, there was a greater log total volume normalised to PW in the lower PIGF group compared to the normal PIGF group in pregestational diabetes. This difference was not significant (**Figure A3.0.12**B). However, there was a significant difference in the relationship between total vascular volume and radius size between the normal PIGF group and the lower PIGF group in pregestational diabetes=0.012(**Figure A3.0.12**D in Appendix 3). There was also a significant difference in the relationship between total vascular volume and radius size between the normal PIGF group and the lower PIGF in pregestational diabetes across increasing radius size bins (bin 15 p=0.004 and bin 16 p=0.003) (**Figure A3.0.12**(B)(D) in Appendix 3).

3.8.4 Summary

In summary, this examination demonstrated longer mean arterial vessel length and shorter venous vessel length across increasing radius size bins in lower PIGF group in pregestational diabetes. This finding was also reflected in the overall total length of vessel segments with longer total arterial vessel length and shorter venous vessel total length across increasing radius size bins in the lower PIGF group, with maternal glycaemic status adjusted for in both groups using the using their first and last HbA1c measurements during pregnancy.

A trend was seen towards greater mean arterial vascular volumes and mean venous vascular volume in lower PIGF group but these differences were not significant. Similarly, greater total arterial vascular volumes and total venous vascular volume observed in the lower PIGF group did not reach significance. However, interaction terms demonstrated significant differences in the relationship between total vascular volume and radius size between the normal PIGF group and the lower PIGF group in pregestational diabetes. Significant differences in the relationship between total vascular volume and radius size between the normal PIGF group and the lower PIGF group in pregestational diabetes were also demonstrated with factored in adjustments for maternal glycaemic status of women using their first and last HbA1c measurements during pregnancy.

3.9 Discussion

Studies assessing fetoplacental vascular development in pregnancies complicated by diabetes have differed and also shown inconsistencies in findings which could potentially reflect differences in the type of diabetes, the glycaemic control of study participants, or the study methodology/approaches to assess fetoplacental vascular development. Even fewer studies have quantified the human fetoplacental vasculature at a whole organ level in pregnancies complicated by pregestational diabetes. This has probably been due to unavailability of suitable techniques that offer a better and more accurate assessment of the fetoplacental vasculature at term.

High resolution micro-CT imaging of corrosion cast vessel models have proven to successfully reproduce defined vessel anatomy that can be used to address the issue of examining the human fetoplacental vasculature as previously reported[58, 83, 291]. This study has successfully utilised 3D digital replicas of the vascular tree for the first time to illustrate significant differences in vessel length, diameter, and vascular volume of placentas from pregnancies complicated by maternal diabetes to those from normal pregnancies.

Previously reported techniques used in the literature to assess vascular structure have largely been based on popular and easily accessible methodologies that involve direct visualisation and examination of the placenta with observations of gross feature of the placenta such as weight, thickness, shape, cord insertion, chorionic plate vessels, as well as 2D examinations of placenta vascular bed structures via histology, stereology and computer simulated 3D reconstruction of vascular beds[46, 76, 77, 91, 292].

However as discussed earlier, these approaches do not provide parameters independent of 3D structural(topological) properties i.e., differences found in volumes of tissue using stereology or histology does not provide information on 3D structural changes and is reliant on sampling of representative areas from usually heterogeneous vascular beds. In addition, these approaches i.e., histology can prove to be burdensome and unreliable due to observer dependent classification of placental lesions as well as laborious examinations of photographic images of placentas that can obscure many vessels, especially deep-seated ones.

Over the last few decades, vascular corrosion casting has been used to produce replicas of normal and abnormal vasculature and microvasculature of various tissues and organs that

could be viewed at the ultrastructural level. This has been utilised in combination with the likes of scanning electron microscopy (SEM) and Micro-CT in describing the morphology and anatomical distribution of blood vessels in these tissues [291, 293, 294]. Earlier protocols of vascular corrosion casting involved infusing highly viscous polymer i.e. diluted resin into the vasculature which presented limitations to how much could fill vessel walls and surrounding tissues were removed with KOH, hot water, and formic acid, and the resulting dried casts were observed with routine SEM. Furthermore, commercially available perfusate did not have the duality of corrosion casting and a contrast agent. For instance, radio-opaque media such as microfil, barium sulphate and iodine solutions are low viscosity agents with excellent contrast properties but they do not polymerize, making them unsuitable for corrosion experiments.

In recent years, the technique has been modified and improved to accommodate limitations with the use of polymethylmethacrylate (PMMA) mixtures available for anatomical corrosion casting, such as Batson's no.17. Batson's no.17 kit is a low viscosity perfusate with proven success in creating durable casts [83, 291]. Corrosion casting requires material to be biocompatible i.e. easily perfuse into vascular vessels and polymerise to generate replica of the vascular tree. This technique is now routinely used in 3D examinations of anatomical vascular structures including blood vessels of various organs[294] [295] [291] particularly in diabetes; in the liver [296], the retinal and choroidal vasculature of the eyes[297, 298] and the cutaneous microvascular architecture of human diabetic toe [299].

In the human placenta, vascular corrosion casting enables visualisation of fetoplacental vessels up to the small terminal branches at term. A previous investigation in the literature using vascular corrosion casting in the placenta has shown that resin can fill the smallest vessels of 6-10μm diameter [58]. The use of computer-aided analysis software with micro-CT imaging provides an effective tool for quantification of the fetoplacental vasculature. Previous investigations in vascular corrosion casting of the placenta have been performed in pregnancies complicated with pre-eclampsia [300] demonstrating a decreased volume of the vascular bed, smaller diameters of grade 1-3 veins(as characterised by level of branching) and grade 2-3 arteries, and an increased peripheral artery-to-vein ratio, which may be a cause of the placental dysfunction during severe pre-eclampsia(n=40 normal placenta and 40 pre-eclamptic placentas). Similarly, investigations have been carried out in placentas from pregnancies complicated by fetal growth restriction that have reported

significant discrepancies in vessel length density in FGR placentas (median vessel length density was significantly shorter in arterial but longer in venous FGR networks compared to normal) [58].

To our knowledge, this is the first-time investigations of vascular corrosion placenta casts have been performed and reported in pregnancies complicated by pregestational diabetes.

3.9.1 Unreported differences were observed in the vasculature of placentas from normal and pregestational diabetes complicated pregnancies.

Our study demonstrated for the first time using Micro-CT of vascular corrosion casts shorter arterial and venous paths in pregestational diabetes placentas with significant differences in shorter paths observed as vessel diameter increased. The mean number of vessel segments were also significantly different within the microcirculation between normal and pregestational group placentas, and not in the larger vessels of the chorionic plate (fewer venule segments and higher arterial segments in placentas from pregestational diabetes compared to placentas from normal pregnancies). We also demonstrated decreased arterial volume in pregestational diabetes placentas as observed across increasing order of vessel diameter. The mean venous volume in pregestational diabetes was increased compared to normal placentas; however, we observed an overall decreased total venous volume in pregestational diabetes group across increasing order of vessel diameter. No differences were observed in tortuosity/loopiness of vessels in the networks. This finding, together with our finding of similar total number of vessel branches in the normal and pregestational diabetes vessel casts, suggests that the discrepancies observed in vessel length was not due to variations in number of branches or tortuosity of the vessels in the placentas.

3.9.2 Alterations were observed in the vasculature of placentas from normal and maternal glycaemic control groups in pregestational diabetes complicated pregnancies.

In relating vascular morphological measurements to classified groups of maternal glycaemic control, we demonstrated shorter arterial vessel length in placentas from both good control and poor control diabetes group across increasing vessel diameter. Shorter venous vessel length was also demonstrated in pregnancies associated with good glycaemic

control and poor control. We also showed decreased arterial vascular volume in placentas from the poor control group as well as decreased venous volume in good and poor glycaemic control groups across increasing vessel diameter. It still remains unclear whether arterial branching influences venous tree development or vice versa.

These findings are similar to observations made in vascular corrosion cast examination of pre-eclamptic placentas that reported significantly lower vascular volume in severe pre-eclampsia (PE) compared to normal placentas [300, 301]. A water displacement method has been used to determine the volume of the placental vascular bed[300]while manual calculations of artery-to-vein ratio per cm^2 was used to examine the peripheral vascular network; 10 spots were selected along the edge of the placentas, and a further 10 spots were selected in between the umbilical cord and the edge of the placenta. The levels of branching and the diameters of placental veins and arteries were also recorded. The results from this study indicated that the venous system of normal placentas was divided into 5-7 grades of branches and the volume of the vascular bed was 155.5±45.3ml while in severe pre-eclamptic placentas, the volume was 106.4±36.1ml, which was significantly lower compared with normal placentas ($P<0.01$). The venous system of pre-eclamptic placentas was divided into 4-5 grades of branches, which was much sparser compared with normal placentas. In additions, the diameters of grade 1-3 veins and grade 2-3 arteries were significantly smaller in severe pre-eclampsia ($P<0.05$) [300]. Whereas a study by Peker et al.,2002 focused on examining cross-sections taken from umbilical artery branches at different levels within the placenta using both light and scanning electron microscopy (SEM)[301]. It was suggested that the decreased vascular volume and vessel diameters were a result of hypertension and the deposition of immunocomplexes in the vessel walls of uteroplacental vasculature leading to narrowing of blood vessels and poor blood flow [302].

Pregestational diabetes is a risk factor for preeclampsia and women with pregestational and gestational diabetes mellitus (GDM) have been reported to have both increased risk of preeclampsia (10–50 and 10–30%, respectively) and insulin resistance when compared with women with normal glucose tolerance whose rate of preeclampsia is 5–7% (1–6). Several studies have reported an association between preeclampsia and insulin resistance as characterized by higher glucose and/or insulin levels when compared with normotensive women [303-308]. Furthermore, hallmarks of the maternal diabetic milieu such as

hyperglycaemia, oxidative stress, inflammation and vascular dysfunction have all been implicated in the aetiology of preeclampsia [309]. However as discussed earlier, glycaemic status of women in these studies are rarely related to placenta vascular morphological findings but findings from the Yin et al. (2017) study were related to types of PE (mild or severe).They reported that placental vascular volume in severe pre-eclampsia was significantly lower compared with normal placentas; however, the vascular volumes in normal placentas compared with mild pre-eclampsia placentas did not differ significantly. In addition, the results indicated that the branching patterns of the umbilical vein and arteries differed between normal and pre-eclamptic placentas [300].

The consequences of these previously unreported altered vessel lengths as defined in **Table 3.2** from our study on blood flow to the fetus are unknown, but research studies have proposed theoretical models to analyse fetal blood flow based on simulated vascular structures [310]. Given that placental veins convey oxygenated blood and nutrients to the fetus, it may be that a shorter venous return path in pregestational pregnancies increases efficiency of materno-fetal nutrient and gas transfer, such that fetus is at risk of macrosomia or LGA (increased fetal growth velocity). The placenta may also respond to enhanced fetal oxygen demand by enlarging the surface area of exchange as seen in increased placenta weight and surface area in pregestational diabetes especially in poor control pregestational diabetes (**Table 3.5**). Birthweight and placenta weight were increased in poorly control pregestational diabetes group vs good control but F: P ratio was reduced, suggesting that bigger placentas are less efficient in poorly controlled diabetes. The proposed capacity-load model of placenta adaptation suggests that during pregnancy, the placenta has a homeostatic capacity to help maintain fetoplacental homeostasis and protects the fetus from adverse consequences of a disturbed intrauterine environment [311].

At a certain level of maternal metabolic load, the placenta can respond to signals such as insulin and coordinate adaptive homeostatic responses that preserve an optimal metabolic milieu for fetal development. A recent study hypothesises that this capacity is negligible during the early weeks in pregnancy and fully developed at the end. However, above the limiting threshold, placenta capacity is exhausted or overwhelmed by an excessive maternal metabolic load associated with diabetes, obesity or both, leading to adverse fetal outcomes [311].

3.9.3 Discrepancies in vasculature of placentas associated with lower PlGF levels in pregnancies complicated by pregestational diabetes.

For the first time, our study demonstrated increased arterial length and venous length in the lower PlGF group within pregestational diabetes cohort observed across increasing vessel diameter. Greater arterial and venous volume were also associated with lower PlGF group compared to normal PlGF in pregestational diabetes however these differences were not statistically significant. There were significant differences demonstrated in the relationship between measured vascular volume and increasing radius size bin of vessel segments between groups of PlGF levels in pregestational diabetes with glycaemic status of women adjusted for in the regression analysis.

Little is known about the effects of PlGF in the fetoplacental vasculature in pregestational diabetes and even less on the larger calibre vessels of the vasculature as measured in our study. Previous studies documented a link between PlGF and the occurrence of pregnancy disorders such as PE, early-onset IUGR and FGR and recently in GDM [123, 125, 312]. Studies showed that, decreased maternal PlGF was associated with late-onset SGA fetuses with histological lesions of placenta under perfusion, suggesting an association between PlGF and placental dysfunction in these pregnancies as indicated by the presence of significant placental pathology(fetal villous stromal maldevelopment, villitis, perivillous fibrin deposition, fetal thrombotic vasculopathy, abruption, intraplacental hematoma and chorioamnionitis) [125].

In addition, Benton et al. (2016) demonstrated that PlGF outperformed other readily-available clinical parameters (GA, AC percentile, umbilical artery RI percentile) in predicting placental FGR. A recent study in GDM, compared placental and maternal blood anti-angiogenic soluble fms-like tyrosine kinase-1 (sFlt1) and pro-angiogenic Placental Growth Factor (PlGF) expressions in GDM and GDM-PE pregnancies compared to controls (CTRL) and PE cases. It was reported that placental PlGF gene expression was significantly decreased in GDM, PE and GDM-PE relative to control group. However, PlGF protein levels were significantly increased in GDM and GDM-PE relative to control group and PE placentae [312].

The implication of our findings in light of presented literature is that there is an association between maternal PIGF levels and placental dysfunction in pregestational diabetes and perhaps measured maternal plasma PlGF levels may not reflect local placental concentrations. However, the impact vessel structure(length/volume) still remains unclear and will require further investigation.

3.9.4 Strengths and limitations of study

The major strengths of this study are the ability to demonstrate vascular differences in chorionic plate vessels >300µm diameter in placentas from pregnancies complicated with pregestational diabetes. The study also demonstrated differences within populations of good and poor control pregestational diabetes and vascular structure associations with maternal levels of PIGF in diabetes. The use of a vascular corrosion casting technique in combination with Micro-CT imaging allowed for a holistic visualisation of a three-dimensional digital replica of each vascular tree. In addition, investigations in this study enabled analyses of each vascular level in continuity with subsequent vascular levels in the tree i.e., increasing radius vessel diameter across vessel segments. Automated computation of measured vessel biometry output also allowed for objectivity in the morphometric analyses of the vessels.

Limitations encountered in this investigation were that in using this casting technique, arterial and venous networks could not be examined simultaneously in the same placenta. Commercially available coloured pigments added to casting material addresses the issue of creating casts with both arterial and venous network in the same placenta. However, in addition to pigments being reproductive system carcinogens (refer to product sheet), the coloured pigments render incompatibility with micro-CT imaging and make it impossible to differentiate the vessel network after as the colours do not show on radiographs. Hence separate casts of the arteries and veins were made to address this limitation and to enable easier imaging analysis on casts.

In creating casts, technical problems were encountered when injecting polymer into vessels, with back flow pressure and leaky/damaged vessel structure, possibly from surgical delivery handling or other clinical variables. When digesting the tissue surrounding casts, problems occurred such as small fragments of vasculature breaking off in the dissolved tissue mix. These were usually smallest vessel fragments (~10-12µm diameter) in the

placental vasculature. Micro-CT imaging resolution was limited to vessels measuring about 58µm in diameter. This was dependent on size of cast that fit into the scanning and detector frame, taking into consideration the specimen rotation. Hence the resolution attainable was dependent on size of cast scanned. Therefore, the smaller the cast the greater resolution of its structure obtained.

To achieve greater resolution of all vessel structures in a cast, small regions of casts could be scanned at higher resolutions separately and then combined together but this opens room for overlapping errors and can also prove to be challenging. Other ways suggested by previous investigations from our laboratory [58] involve breaking casts into pieces, however this defeats the purpose of scanning the vascular tree in its entirety and limits continuity of analysis we hoped to achieve. Nanoscale scanning such as near-field scanning optical microscope (NSNOM) [313] although expensive could be beneficial in addressing this limitation in combination with advanced super-resolution imaging tools.

Finding placental–appropriate 3D analysis software still remains a major challenge. Previous studies have been able to utilise general vascular tree analysis software such as AnalyzeDirect (predominantly used for biomedical imaging), Neurolucida (designed for medical imaging of neuronal dendritic trees) and Avizo (used in material sciences, structural engineering and medical equipment) [58, 314]. Avizo software was adapted to accommodate morphometric analysis of placental vascular trees but did not completely suit placenta data sets. Intermediate and terminal branching nodes generated in Avizo as well as branch trees highlighted in Analyze could not be linked to spatial localisation of the corresponding vessel segments. Interpretation of some measured vascular biometry outputs from the software proved difficult as their physiological relevance to placenta vasculature could not be ascertained.

In comparisons of study populations of women whose placentas were used, longitudinal changes in maternal glycaemia via CGM could offer a more accurate reflection of maternal glycaemic control instead of first and last HbA1c measurements. In addition, PIGF measurements in control groups would enable comparisons with groups with normal PIGF in pregestational diabetes, and groups with low PIGF in pregestational diabetes. Although the population studied was relatively tightly defined and differences were observed, the numbers were too small when categorised into diabetes glycaemic control groups and when further attempts were made to group categories by diabetes type.

Overall, this study sufficiently addressed its aims of comparing placenta vascular structure

at term between clinical groups as well as allowing observations of the effects of events during pregnancy such as maternal glycaemic control and PIGF levels on fetoplacental vascular structure after delivery.

3.9.5 Chapter 3 Overall Summary

This present study demonstrates vascular structural differences in fetoplacental vessels of placenta from pregnancies complicated by maternal diabetes. These differences were observed in shorter arterial and venous length of vessels in placentas from pregestational diabetes pregnancies compared to normal pregnancies. Decreased arterial vascular volume in placentas from pregestational diabetes. Overall decreased total venous vascular volume in placentas from pregestational diabetes. Shorter arterial and venous vessel length in placentas from poor glycaemic control pregestational diabetes. Decreased arterial vascular volume in placentas from poor glycaemic control pregestational diabetes. Decreased venous vascular volume in placentas from poor as well as good glycaemic control groups in pregestational diabetes compared to normal pregnancies. Reduced vascular volumes in placentas from pregestational diabetes pregnancies were not related to low maternal serum PlGF concentration in the third trimester. Further investigations can help provide understanding of the implication of these alterations on placenta function and subsequently pregnancy outcomes.

4 Chapter Four: *In vitro* Examination of the Effects of Hyperglycaemia, Insulin and Metformin on Placental Angiogenesis

4.1 Background

4.1.1 Diabetes and Angiogenesis

Pregnancies complicated by maternal diabetes face increased risks of adverse fetal outcomes as a result of hyperglycaemia, maternal insulin resistance and other components of the diabetic environment *in utero*. Fetoplacental vascular complications in diabetes mellitus have been associated with excesses or defects in angiogenic processes [36]. Angiogenesis, the generation of new blood vessels from pre-existing ones is essential in providing sufficient blood flow and oxygen for growing tissues. Endothelial cells are the main cells involved in the angiogenesis process with physiological angiogenesis contributing to events such as embryonic development in pregnancy, wound healing and menstruation [35, 36, 315]. During early pregnancy extensive angiogenesis occurs in fetal placenta tissues with further expansion in the placental vasculature in late gestation [94, 95].

Angiogenesis is a complex process driven by multiple molecular mechanisms directly involved in physiological and pathological conditions such as regulatory growth factors and cytokines of placental angiogenesis ; vascular endothelial growth factor (VEGF), fibroblast growth factor (FGF-2), angiopoietins, placental growth factor (PlGF), tumour necrosis factor (TNF-α), interleukin 8 (IL-8) and insulin- like growth factors 1 and 2 (IGF1, IGF2 [30, 32, 172]. However, disorders in physiologic angiogenesis can arise when regulatory factors are altered as a result of metabolic insults [149, 316]. Abnormalities in angiogenesis are prevalent and well documented in non-pregnant diabetic vascular complications, with both excessive and defective angiogenesis observed in various organs and tissues such as lungs, kidneys, skin, eyes, brain, heart, skin and adipose tissue as a result of reported altered expression/levels of angiogenic factors [36] .Complications are characterised under (organ dependent) altered angiogenesis (microvasculature) and formation of anastomoses or collaterals (macrovasculature) in retina, heart, kidneys or nerves . Reconciling how and why both excessive and defective abnormalities in angiogenesis have been reported in diabetes has been a major challenge with limited understanding of the effects of factors that underlie dysregulation of angiogenesis in the placenta. Studies in the literature have attempted to elucidate the underlying causes of abnormalities in fetal growth caused by maternal diabetes and their direct/indirect effects on altering angiogenic factors in placental vasculature development. The following subsections will outline effects of factors

such as hyperglycaemia, insulin and metformin on angiogenesis *in vivo* and *in vitro*.

4.1.1.1 Glucose and Angiogenesis

Hyperglycaemia, or fluctuating glucose levels have been reported to dysregulate angiogenesis. Angiogenesis modulates vascular development, any disruption in angiogenesis during vascular development may possibly affect placental vascular permeability and function. Hyperglycaemia is defined as an excessive amount of glucose circulating in the blood plasma (has been defined by the World Health Organisation as blood glucose levels greater than 7.0 mmol/L (126 mg/dl) when fasting and blood glucose levels greater than 11.0 mmol/L (200 mg/dl) 2 hours after meals) [5]. Hyperglycaemia has direct effects by acting as pro-constrictor, proangiogenic, pro-permeability and pro-inflammatory agent [205]. Hyperglycaemia affects regulation of angiogenesis by inducing expression of inhibitory genes to promote neovascularisation via increased production of reactive oxygen species (ROS) leading to increase in VEGF mRNA expression [243, 317]. Many studies of factors modulating angiogenesis are conducted using ECs, either from cell lines (e.g. HUVECs, HMECs,) or primary ECs from the organ of interest. Using *in vitro* models and cell lines , the effects of high glucose on dysregulation of angiogenesis with endothelial cell tube formation [318] as well investigations on fluctuating glucose levels have been established [319-321]. The proposed mechanisms through which hyperglycaemia alters angiogenesis are via increased production of ROS in response to other factors such as formation of advanced glycation end products (AGE's) and its role in altered expression of growth factors (VEGF) which may influence placenta development (angiogenesis) and function in diabetic mothers. In addition, recent evidence in the literature suggests that glucose variability, characterized by fluctuating glucose levels during gestation , give rise to a risk of diabetes-related complications [322] [323]. Evidence shows that fluctuating blood glucose levels prompt an increase in free radicals and endothelial dysfunction, which link hyperglycaemia with the activation of pathological pathways that lead to tissue damage with reported greater glucose variability in pregnant women with type 1 diabetes than in cases of GDM or healthy controls [322].

4.1.2 Insulin and Angiogenesis

Hyperinsulinaemia is also another factor that has been suggested as a contributing factor in altering placental angiogenic factors and thus altered placental vascular development and dysfunction in diabetes. Hyperinsulinaemia is defined as elevated circulating insulin in relationship to its usual level relative to blood glucose. Various growth factors have been implicated in the regulation and stimulation of angiogenesis in the human placenta with distinct actions throughout gestation (**Figure 1.11**). Notably the insulin/insulin-like growth factor (IGF) system, i.e. insulin, IGF1, IGF2 and the IGF-binding proteins IGFBP1 and IGFBP3, are involved in the regulation of fetal and placental growth and development [149].

Alterations of the insulin/IGF system in the placenta in maternal diabetes have been well documented [149, 324-327] . Various factors are reportedly altered in maternal and fetal circulation and in the placenta in maternal diabetes, particularly GDM and T1D reportedly increased levels of components of insulin/IGF system [149, 328].

In term placentas, the majority of placental IRs are located on the placental endothelium i.e. at sites of proliferation which suggests insulin involvement in vascular growth and is consistent with studies that report enhanced branching angiogenesis in maternal diabetes characterised by elevated fetal insulin levels as a result of maternal, and hence fetal, hyperglycaemia [91, 329]. Therefore, elevated fetal insulin levels may stimulate endothelial cell proliferation and vascular branching by binding to IR present on the sites of villus ramification.

Further studies have investigated the effects of insulin-induced angiogenesis in human umbilical venous endothelial cells (HUVEC) [330]and regulatory pathways involved.

The *in utero* environment of pregnancies complicated by diabetes have been demonstrated to alter insulin, IGF and IGFBP and thus likely to influence placental cells in a manner different from normal pregnancies [149]. Studies have suggested that fetal insulin is involved in the control of placental angiogenesis and permeability of the vasculature as evidence points to the enhancement of VEGF protein expression and secretion by insulin [149, 229]. Any dysregulation or altered levels of insulin and IGFs may have profound effects on angiogenic processes in placenta vasculature development. The combinations of these scenarios of hyperglycaemia and hyperinsulinaemia could underlie the disparate findings of altered fetoplacental vascular development in diabetic women. This is further complicated by treatment regiments such as metformin in diabetic mothers.

4.1.3 Metformin and Angiogenesis

As an anti-hyperglycaemic oral agent, metformin is increasingly used before and during pregnancy due to its relatively lower cost and ease of administration as compared to insulin. It has the distinct advantages of ease of administration, lack of hypoglycaemic risk and lower cost as compared to insulin, which can only be administered through injection [331]. Thus, the use of metformin before and during pregnancy is increasingly prevalent in cases whereby maternal hyperglycaemia and/or insulin resistance cannot be easily controlled by lifestyle changes. The typical clinical settings in which metformin has been prescribed during pregnancy include in pre-gestational type 2 diabetes (T2D), GDM and in women with Polycystic ovary syndrome (PCOS) [332, 333].

Metformin is a common first-line of treatment for T2D individuals and the continued use of metformin before and during early pregnancy is inevitable in many cases. However, the decision on whether to continue with metformin treatment or not once pregnancy is confirmed is still a matter of debate. Clinicians have raised concerns on the introduction of an alternative treatment regimen of insulin for diabetes early in the pregnancy without worsening glycaemic control [277].

Studies have shown that metformin modulates angiogenesis [273, 334-338]. Metformin may create both promoting and inhibiting effects on angiogenesis, and its role depends mainly on its action pathway, the type of cells being investigated, and the nature and conditions of the disease [339]. The specific mechanistic action of metformin still remains unclear however the overall consensus is that metformin exerts its effects via activation of the AMPK signalling pathway. The AMPK signalling pathway is a regulator of cellular energy homeostasis. It is known to be activated by falling cellular energy status i.e. increasing ratio of ADP/ATP and AMP/ATP – and thus has been hypothesised to be a possible glucose sensing mechanism .It has been reported that metformin activates the AMPK signalling pathway by increasing phosphorylation of the Thr172 site in AMPK alpha subunit in primary hepatocytes [340].

However, as suggested by a review, metformin can have varied working mechanisms depending on its bioavailable concentration and there is relatively little known about the extent and full implications of metformin exposure *in utero*; specifically how it can affect embryonic and fetal development [341]. Following on from this, there is a need to explore

the concentration dependency of dysfunctional angiogenesis on glucose, effects of fluctuation in glucose concentrations, interactions between glucose and insulin and how these could be influenced by metformin.

4.2 Hypothesis

This study tested the hypotheses that high glucose concentrations, + physiological/patho-physiologically relevant concentrations of insulin, alter the ability of HUVECs to form cellular networks *in vitro* and that metformin, at therapeutically relevant concentrations, can mitigate their effects.

a. Determine the relationship between glucose concentration, and fluctuating glucose concentrations, on the development of cellular networks by HUVECs
b. Determine whether glucose modulation of HUVEC cellular network development is modulated by insulin in the presence and absence of metformin

4.3 Materials and Methods

4.3.1 Maternal Plasma glucose concentrations in diabetes

Intrauterine exposure to maternal diabetes environment or impaired glucose tolerance measured in mid-pregnancy and late pregnancy is associated with increased risks of adverse maternal and fetal perinatal outcomes [205, 342].

In the current study 5mM glucose control was chosen to simulate normoglycaemic conditions in diabetic mothers and this concentration has been widely used in *in vitro* studies of effects of glucose concentrations on HUVECs [343]. Increasing levels of glucose concentrations (7-25mM) were also assessed to establish the effects of varying concentrations on cells. 18mM was considered as a raised/elevated level of glucose as compared to a concentration >20mM which is also widely considered as high glucose concentration in *in vitro* studies [319, 344, 345]. Classification of 18mM as a raised level of glucose is also derived from CGM data studies on glucose variability in pregnancies complicated by maternal diabetes [322, 323, 346, 347]. Insulin levels 100pmol/L, 10nmol/L and 1nmol/L were chosen to represent a range of physiological and pathophysiological

concentrations of fetal insulin in response to maternal hyperglycaemia [348]. Osmotic control experiments using mannose were also conducted in pilot experiments.

4.3.2 Effects of glucose, insulin and metformin on cellular network formation by HUVECs *in vitro*

The effects of glucose, insulin and metformin, alone and in combination, were assessed on the ability of HUVECs to form a cellular network, when maintained on Matrigel, as a model of fetoplacental angiogenesis. Cells were maintained as described in Methods, section (**2.4.1**). Initial pilot studies were performed to determine optimum cell plating density, time of culture and cellular network formation and effect of VEGF in experiments. Informed by these data (**Appendix 4(II)**), HUVECs were plated at 15000 cells per well for 18h and 4 studies were conducted.

4.3.3 Effect of glucose concentration on HUVEC cellular networks

HUVECs (n=6 passages) were maintained in media containing 5, 7, 12, 15 or 25mM glucose. 5mM (control) was used to reproduce maternal fasting plasma glucose concentration in normal pregnancy [342], and 25mM was used to represent a high glucose concentration. The culture medium contained 5mM glucose and extra glucose was prepared by adding D-glucose to the medium to achieve subsequent glucose concentrations (7, 12, 15mM) and a final concentration of 25mM. Cells were observed at 18h and 4 images per well were taken under a light microscope as illustrated in **Figure 2.5**. The cellular networks were then analysed using Image J software with an angiogenesis analyser extension for the network variables described in **Table 4.1**.

In some experiments (n=3) live bio imaging using a Incucyte ZOOM Plate Imager (described in section (**4.3.6**) (n=3, passage 5) was used to assess whether glucose concentration (5,7,12 or 15mM) altered the time course of cellular networks formed by HUVECs over 3, 6 and 9 h after plating (0h). Qualitative assessments were made on the influence of glucose concentration based on observations of the images.

4.3.4 Effect of fluctuating glucose concentration on HUVEC cellular networks

Maintaining a stable plasma glucose concentration over the course of gestation in diabetic women is challenging and plasma glucose concentration can often fluctuate during pregnancy [322, 347]. To assess whether fluctuation in glucose concentration alters the ability of HUVECs to form cellular networks, HUVECs (n=6 passages) were cultured in media containing 2 different glucose concentrations changed alternately at 4h intervals for a total of 16h. Cells were plated in 5mM glucose (control) at time zero and after 4hr the medium was changed to 18mM for 4h, then returned to 5mM for 4h, changed to 18mM for 4h and finally returned to 5mM. The control cells had medium changed every 4h but each time the medium contained 5mM glucose and in another control well, cells had medium changed very 4h but each time with 18mM glucose. In addition, the cells were also initially maintained in medium with 5mM glucose and the medium was changed to 25mM (high glucose concentration), then 5mM and 25mM at 4h intervals; the control cells had medium changed very 4h but each time with 25mM glucose. Live bio imaging section (**4.3.6**) was conducted on the cells to capture any effects of glucose concentration changes on the cellular networks. Images taken at the end of the experiment (16h) were assessed for cellular network formation using Image J software to determine variables described in **Table 4.1**.

4.3.5 Effect of glucose +/- insulin and metformin on HUVEC cellular networks

To determine whether metformin modulates the ability of HUVECs to form cellular networks in response to glucose +/- insulin, cells (n=6 passages), were maintained in culture medium with 5, 18 or 25 mM glucose, or in medium with each glucose concentration + insulin at 100 pmol/L, 1 nmol/L 10 nmol/L +/- metformin (100nmol/L); these insulin concentrations represented a range of physiological to pathophysiological levels of insulin. As serum contained insulin, medium was prepared by adding insulin to reach each final concentration. A therapeutically relevant concentration of metformin (100nmol/L) was added to the medium. 4 images were taken per well at 18h for analysis of cellular networks using Image J software.

4.3.6 Live Bio-imaging system

Cells were plated in respective concentrations outlined in section (**4.3.4**) to capture any effects of glucose concentration on changes in the cellular networks. Incucyte® Live-Cell Zoom Plate Imager automatically acquired images around the clock in wells at stipulated time increments (in this study images were set to be captured every 30 minutes), providing information on changes to network structures in the different wells. Incucyte Imager enabled visualisation and quantification of cell behaviour over time within a standard laboratory incubator environment (5% CO_2 at 37 °C and 95% humidity). The images at different time points 4h, 8h, 12h, 16h were selected for analysis of cellular networks using Image J software.

4.4 Analysis of HUVEC cellular networks

Quantification of the cellular network formation was analysed from images taken from microscopes (light microscope (Olympus BX41) at 4× objective or Incucyte Zoom Plate Imager). The images were then analysed using Image J software with an angiogenesis analyser extension described in the protocol in **Appendix 4(I)**. The use of an angiogenic analyser plugin on Image J software enabled quantitative analysis of cellular networks to determine measurements such as total length of mesh networks, number of branches, number of segments, total number of nodes, extremities, junctions and meshes formed. The detail outline of all measurements from the Angiogenesis Analyzer are shown in **Table 4.1**. This enabled extracting characteristic information of the network as shown in **Figure 4.2**. The variables analysed (Analysed area = area of the image or the user selection concerned by the analysis) in the study were defined in the table below (**Table 4.1**).

Table 4.1 Angiogenesis Analyzer measured data variables and their definitions

Variable	Definition	Measured metrics
Extremities	detects the extremities in a binary tree. It returns results as overlays and binary map	**No. of extremities**: number of extremities in the analysed area.
Nodes	detects nodes (pixels with 3 neighbours) as a circular dot	**No. of nodes**: number of nodes in the analysed area.
Junctions	Junctions correspond to nodes or group of fusing nodes.	**No. of Junctions:** number of junctions in the analysed area.
Segment	elements delimited by two junctions	**No. of segments**: number of segments in the analysed area **Total segments length**: sum of length of the segments in the analysed area.
Branches	elements delimited by a junction and one extremity	**No. of branches**: number of branches in the analysed area. **Total branches length**: sum of length of the branches in the analysed area. **Branching interval:** mean distance separating two branches in the trees in the analysed area. (Tot. segments length / No.of branches).
Twigs	a twig is a branch whose size is lower than a user defined threshold value.	
Isolated elements(isol.)	are binary lines which are not branched	**No. of isol. segment**: number of isolated elements in the analysed area. **Total isol. branches length**: sum of length of the isolated elements in the analysed area.
Master segments	consist in pieces of tree delimited by two junctions none exclusively implicated with one branch, called master junctions.	**No. of master segments**: number of master segments in the analysed area. **Total master segments length**: sum of the length of the detected master segments in the analysed area
Master junctions	are junctions linking at least three master segments. Optionally, two close master junctions can be fused into unique master junction.	**No. of master junction**: number of master junctions in the analysed area
Meshes	are areas enclosed by segments or master segments.	**No. of meshes**: number of meshes in the analysed area. **Total meshes area**: sum of mesh areas detected in the analysed area. **Mesh index**: mean distance separating two master junctions in the trees in the analysed area. (Tot. master segments length / No. of master segments). **Mean Mesh Size**: mean mesh size in the analysed area.

Data analysis variable and their definitions; Analysed area is the area of the image or the user selection concerned by the analysis and unit of area and length is pixel. Theses variables are also illustrated in **Figure 4.1**.

The variables number of nodes, segments, master junctions, master segments, all segments+ branches and meshes were chosen to be presented in subsequent experiments as they provided information that represented the gradual formation of the cellular network from nodes to complete meshes.

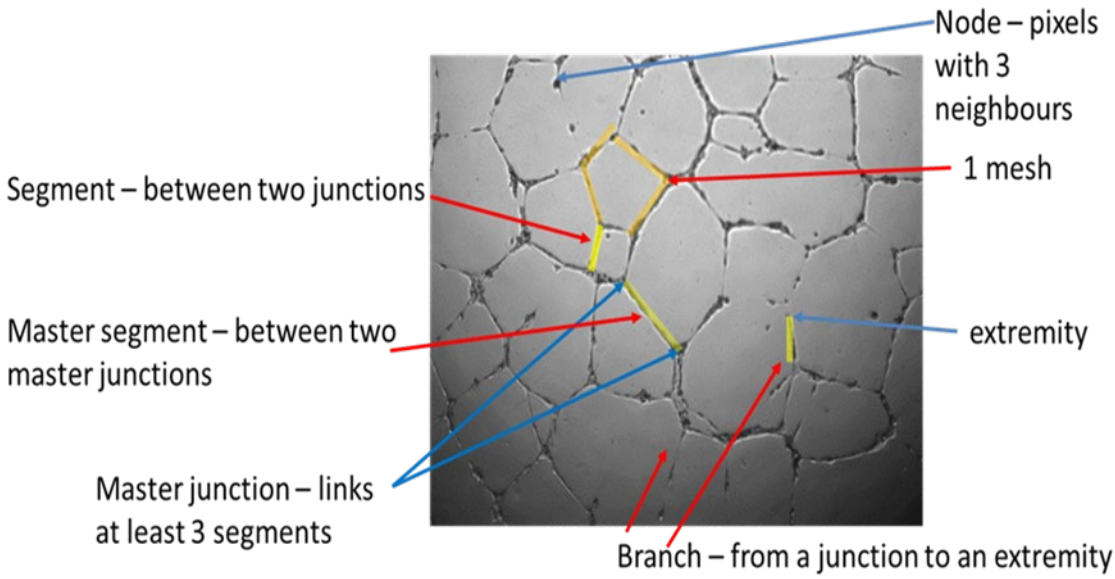

Figure 4.1 Diagram to show variables measured to assess cellular networks formed by human umbilical endothelial cells *in vitro*
Definitions of variables displayed on diagram as defined in **Table 4.1**

4.4.1 Cellular network formation Analysis

Quantification of the cellular mesh network formation was then analysed using the ImageJ software with an angiogenesis analyser extension. The use of an angiogenic analyser plugin on ImageJ Software enabled quantitative analysis of cellular network formation to determine measurements such as total length of mesh networks, number of branches, number of segments, total number of nodes, extremities, junctions and meshes formed as shown in **Figure 4.1** and **Figure 4.2**.

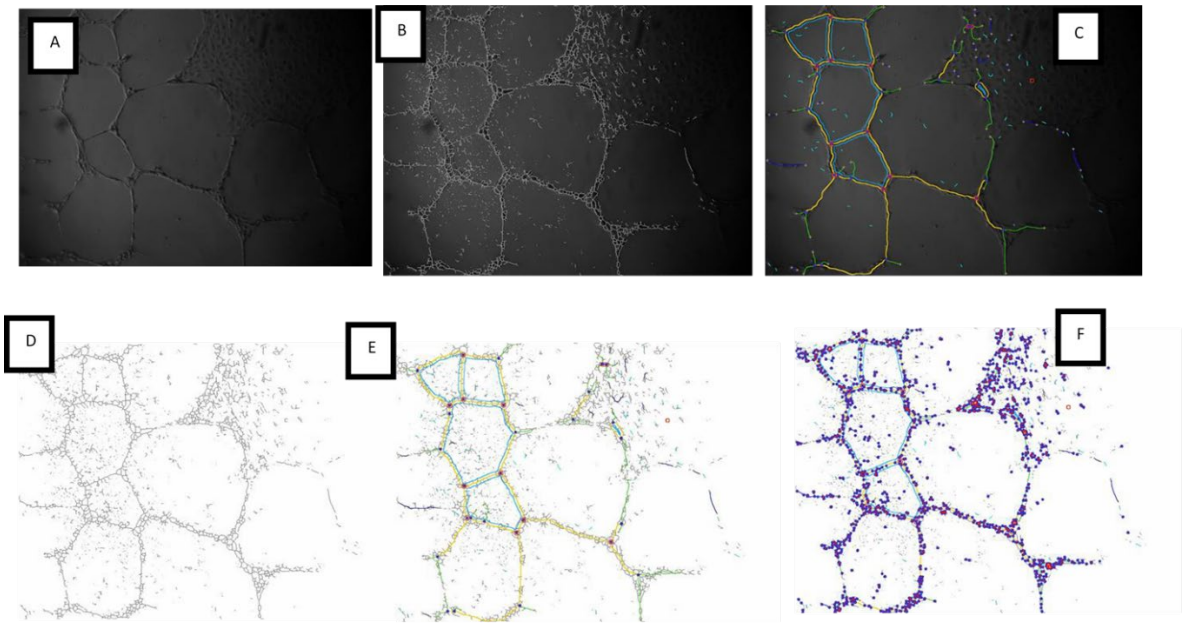

Figure 4.2 Example Image J Plugin Analysis
(A) Image of Human umbilical vein endothelial cell (HUVEC) cellular mesh network formation on a basement membrane substrate after 18hrs in no VEGF at 15,000 cells/well. (B) Image with calculated mesh layover showing branch pattern. (C) Image of analysis tree in colour (D) Image showing mesh network with branch pattern(E) Images showing mesh network in colour with extremities(F) Image showing total number of segments and nodes.

4.4.2 Statistical Analysis

Statistical analyses were conducted using GraphPad Prism® 7 (version 7.04 GraphPad Software, Inc., USA). ANOVA or MANOVA was conducted unless otherwise stated to compare all concentrations to control concentration data depending on amount of independent variables analysed. A Dunnett's test was used for post hoc analysis of the significant ANOVA. A difference in mean values between groups was considered to be significant when $p \leq 0.05$. In addition, as there were different glucose concentrations, tests were made to compare differences of each concentration to the rest e.g. 5mM vs all concentrations (7mM, 12mM, 15mM, 25mM), 7mM vs all concentrations, 12mM vs all concentrations, 15mM vs all concentrations and 25mM vs all concentrations. Data were represented as mean ± standard error of mean (SEM).

4.5 Results

4.5.1 The effect of glucose concentration on HUVEC cellular networks

Pilot data indicated that HUVECs formed extensive cellular networks by 18h of culture in 5mM glucose **(Appendix 4(II)).** Accordingly, the effect of increasing medium glucose concentration (5, 7, 12, 15 and 25mM) on the ability of HUVECs to form networks was assessed at 18h of culture and representative images are shown in **Figure 4.3**. In comparison to 5mM glucose, networks appear sparser when cells were exposed to 15 and 25mM glucose. Cellular networks were analysed using Image J software and these data are shown in **Figure 4.4** and **Figure 4.5**.

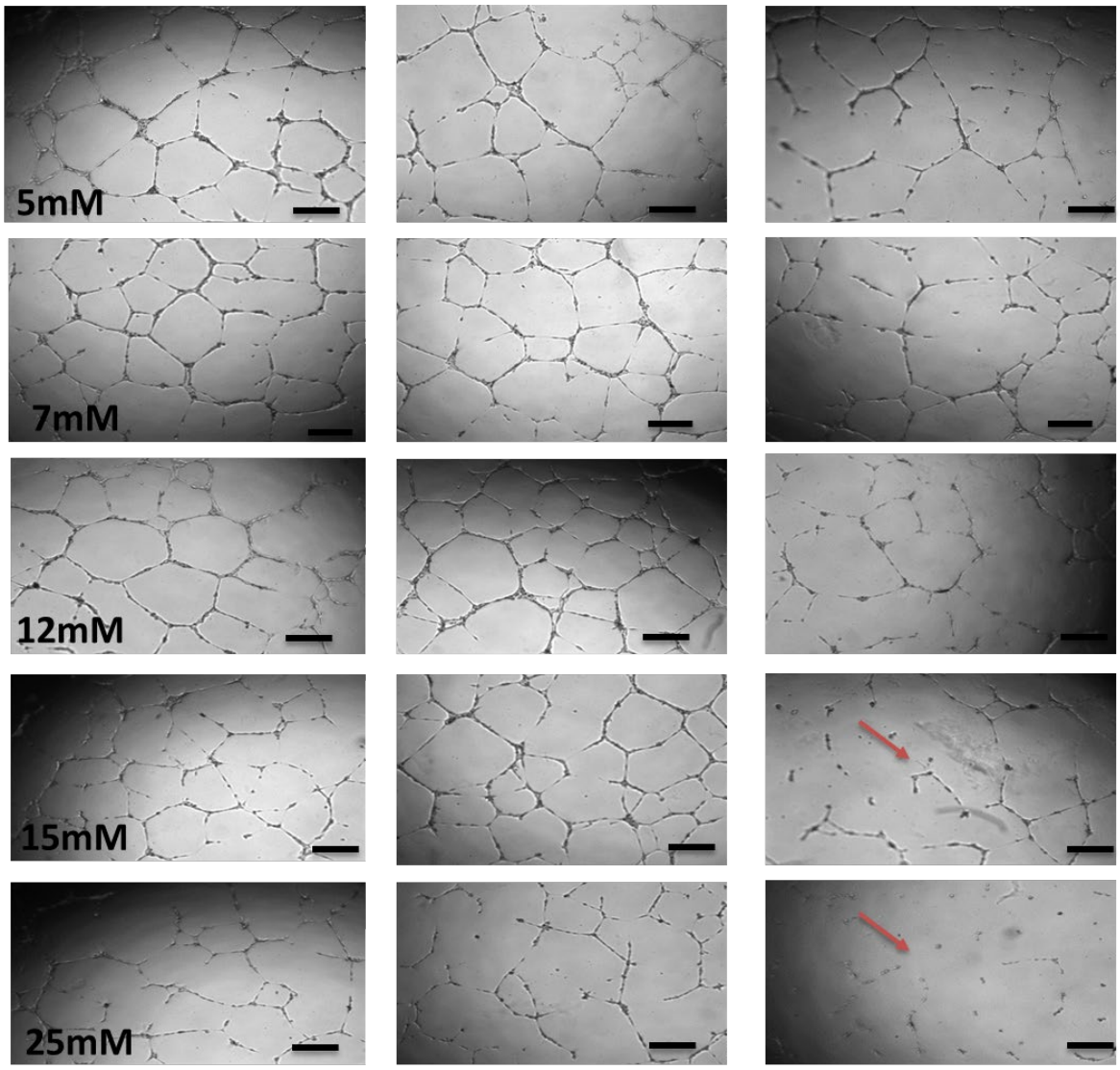

Figure 4.3 Representative images to show the effect of medium glucose concentration on HUVEC cellular networks after 18h of culture.

Representative images of human umbilical vein endothelial cell (HUVEC) cellular network formation on a basement membrane substrate after 18h (from n=6 passages). Cells were seeded at 15,000 cells/well in medium containing 5, 7,12,15 or 25mM glucose and images taken under a light microscope (Olympus BX41) at 4× objective. Each column shows representative images from different passages. Red arrows show sparse networks in wells. Each scale bar represents 1000µm.

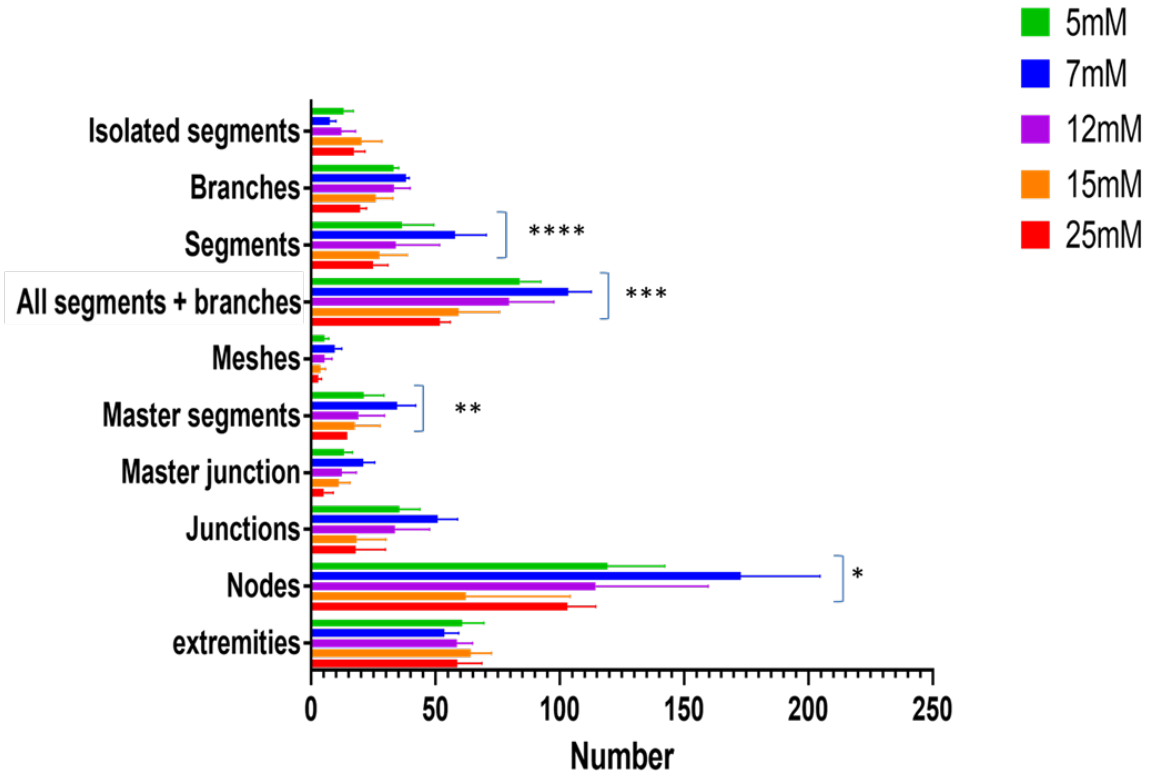

Figure 4.4 Effect of medium glucose concentration on variables of cellular networks formed by HUVECs

The effects of glucose concentration on human umbilical vein endothelial cell (HUVEC) cellular network variables after 18h of culture (n=6 passages; mean + SEM). -*: Here indicate variable groups rather than degree of significance

ANOVA and Dunnett's multiple comparison test:

Nodes - *p ≤ 0.001; 7mM vs all concentrations,

Master segments - **p ≤ 0.05; 5mM vs 7mM and 7mM vs 25mM, **p<0.05 for 7mM vs 15mM

All branches and segments - ***p<0.001; 7mM vs all concentrations

Segments - ****p<0.01; 7mM vs 15mM

ANOVA was conducted to check for significance in interaction, row factor and column factor (all significant, $p<0.0001$) and then post hoc Dunnett's multiple comparison test conducted to compare all concentrations to control concentration data. In addition, as they were different multiple glucose concentrations, tests were made to also compare differences of each concentration to the other concentrations. Significant effects of glucose were observed on the no of segments, master segments, all segments and branches, and the number of nodes (**Figure 4.4**). For these variables, the numbers were highest in 7mM glucose, and lowest in 25mM (significant for nodes, master segments and all branches and segments). The mean number of segments formed in 7mM glucose was 65 ±11 compared to 20 ±5 in 15mM, ($p=0.001$). 7mM glucose significantly elevated the mean number of segments and branches compared to all the other glucose concentrations ($p=0.001$). The mean number of master segments in 5mM glucose (control) was 20±10 compared to 35±10 in 7mM ($p=0.001$),7mM vs 18±7 in 15mM ($p=0.028$) and 7mM vs 15±2 in 25mM glucose($p=0.0049$). The mean number of nodes in 7mM glucose was 175±30 compared to 120±20 in 5mM, 115±45 in 12mM, 63±42 in 15mM and 105±10 in 25mM (all $p=0.001$).

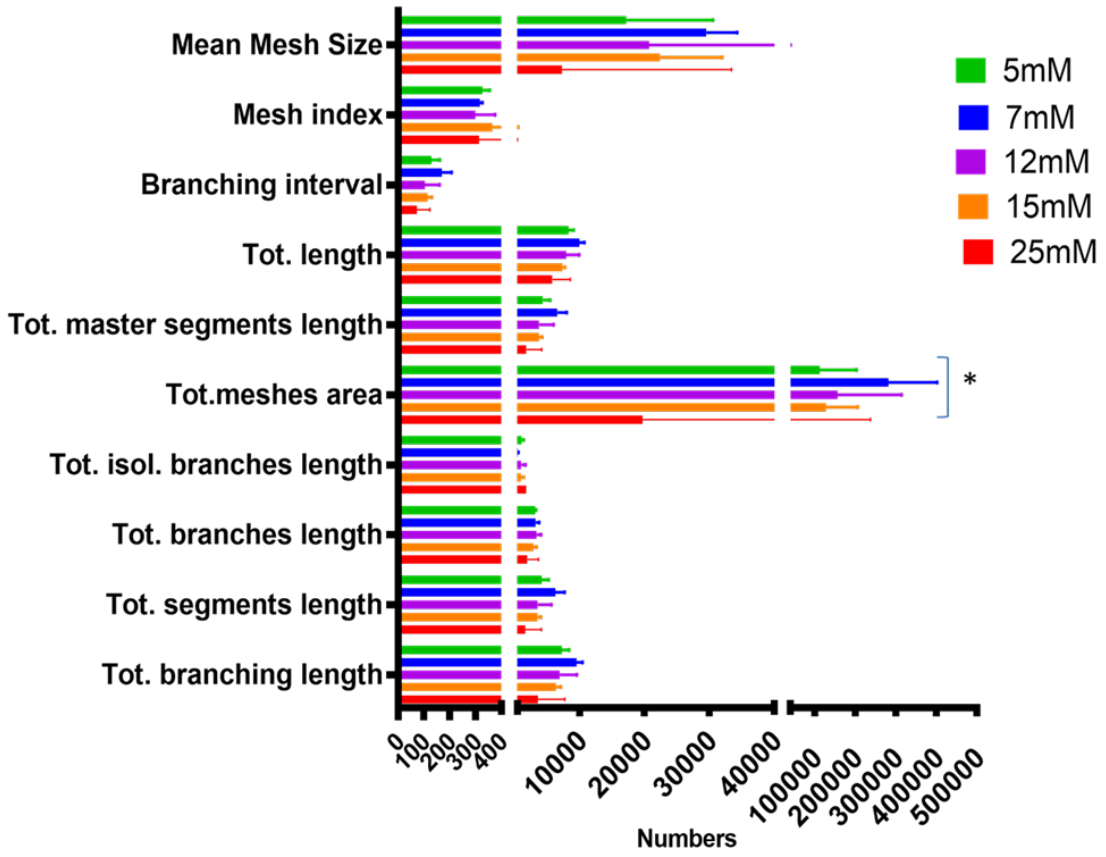

Figure 4.5 Effect of medium glucose concentration on the sum of variables of cellular networks formed by HUVECs

The effects of glucose concentration on the sum of human umbilical vein endothelial cell (HUVEC) cellular network variables (Tot = total). (n=6 passages; mean + SEM).
ANOVA and Dunnett's multiple comparison test: *p ≤ 0.01; 7mM vs all concentrations).

There was no effect of glucose on the sum of HUVEC network variables (**Figure 4.5**) with the exception of the total mesh area which was significantly greater in medium containing 7mM glucose compared to all other glucose concentrations.

To assess whether glucose concentration altered the time course of cellular network formation by HUVECS, cells were cultured in medium containing 5,7,12 and 15mM glucose and observed by live bio imaging (n=3) (**Figure 4.6**). HUVECs were observed to attach to the underlying matrigel within 3h. Cells formed cellular network structures that were visible (complete meshes) by 3h in 15mM glucose and by 6h in 5mM, 7mM and 12mM glucose (**Figure 4.6**).

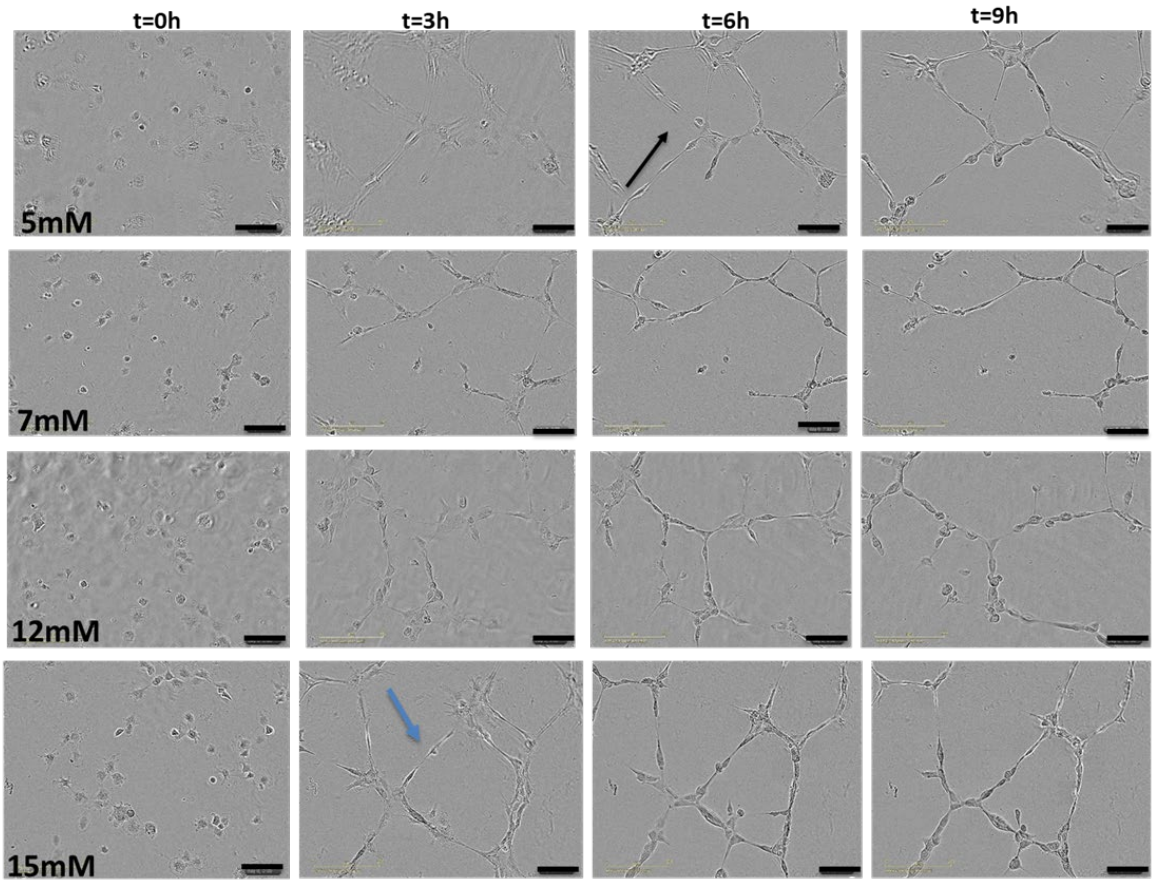

Figure 4.6 Representative live images to illustrate the effect of medium glucose concentration on the time course of development of HUVEC cellular networks.
Representative live bio images (Incucyte ZOOM Plate Imager) of the time course (0h-9h) of human umbilical vein endothelial cell (HUVEC) cellular network formation by cells maintained in medium containing 5,7,12 or 15mM glucose. Black arrow shows cells lining into networks at 6h in 5mM. Blue arrow shows cells lining into networks as early as 3h in 15mM. Scale bar represents 200µm.

4.5.2 Effect of fluctuating glucose concentrations on HUVEC cellular networks

The effect of fluctuating glucose concentrations on HUVEC cellular network formation was investigated by changing glucose in the culture medium at 4 hourly intervals for 16hr (4 media changes) as described in section **4.3.4**. Representative live bio images of cellular networks in cells maintained in medium containing 5mM glucose at time zero, and thereafter at 4 hourly intervals following alternate changes in glucose concentration to 18mM, 5mM, 18mM and back to 5mM, are shown in **Figure 4.9**; the cellular networks formed in the corresponding control (cells maintained in medium containing 5mM glucose throughout and 18mM throughout) are shown in **Figure 4.7** and **Figure 4.8** respectively.

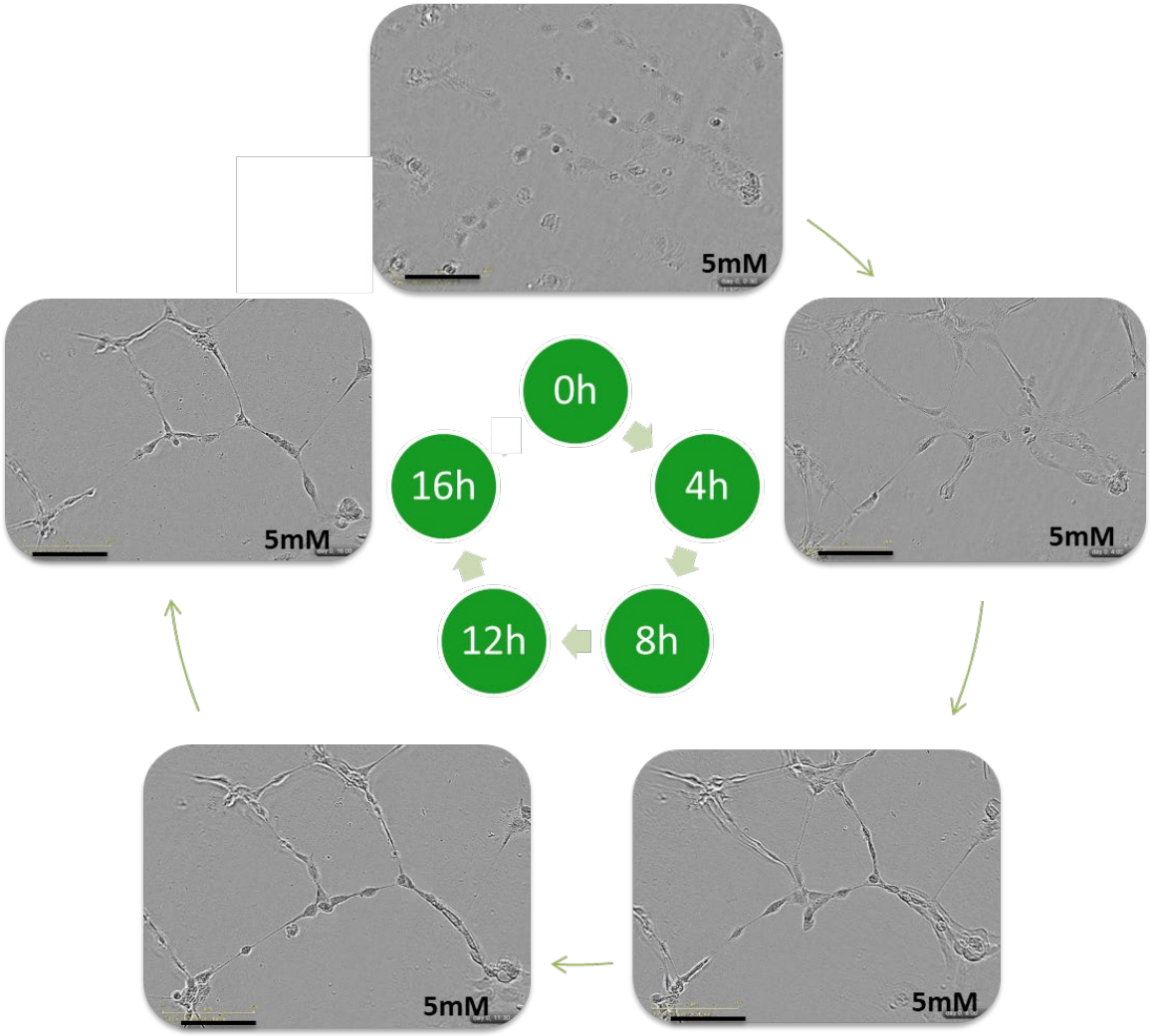

Figure 4.7 Representative live bio images of HUVEC cellular networks formed in response to changing medium glucose concentration every 4h: control experiment with 5mM glucose

Representative bio images, from n=6 passages, (Incucyte ZOOM Plate Imager) of human umbilical vein endothelial cell (HUVEC) cellular network formation at 4 hourly intervals following changes in culture medium. Control experiment: medium replaced with 5mM glucose. Scale bar represents 200µm.

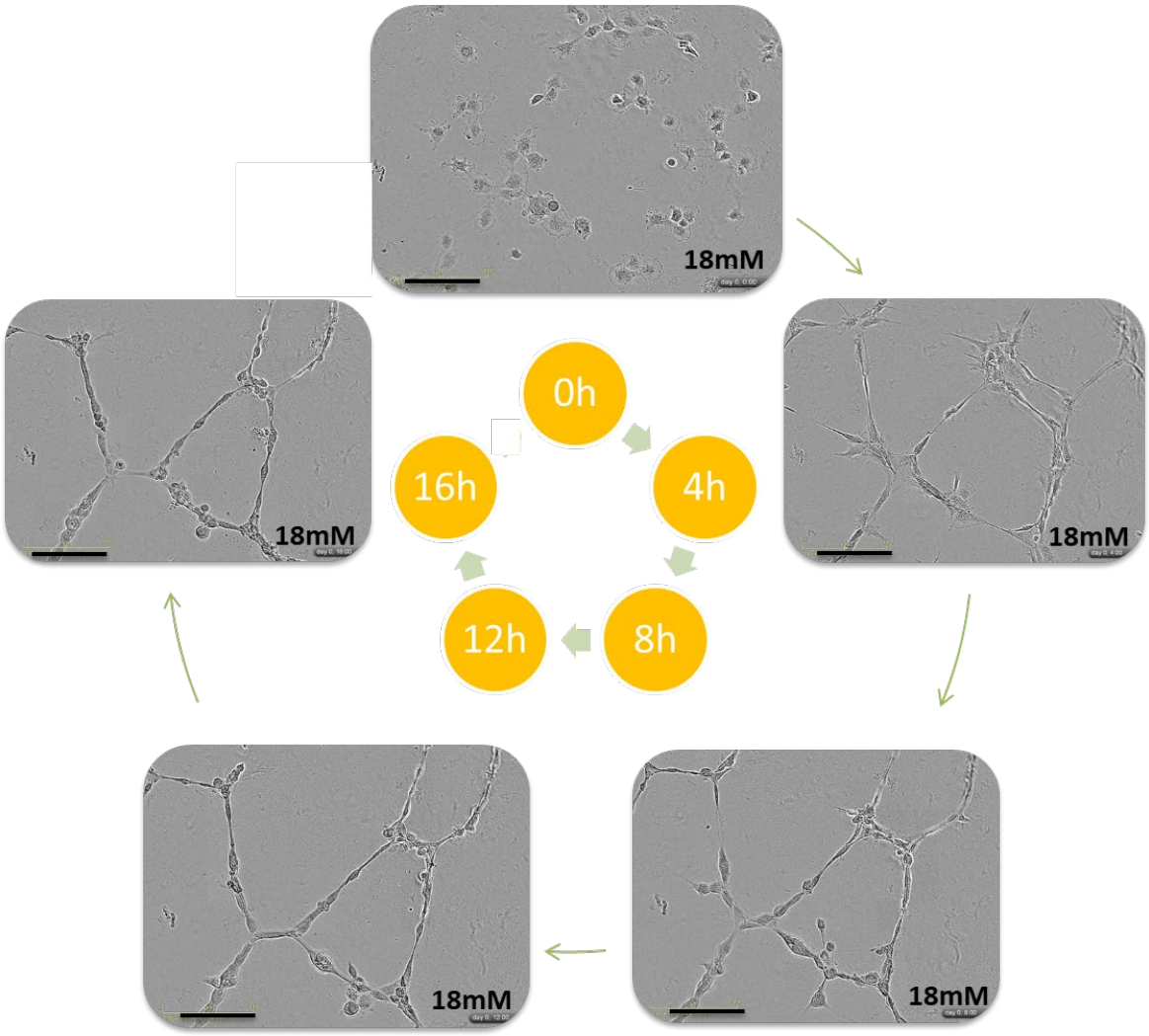

Figure 4.8 Representative live bio images of HUVEC cellular networks formed in response to changing glucose concentration every 4 h: control experiment with 18mM glucose
Representative bio images, from n=6 passages, (Incucyte ZOOM Plate Imager) of human umbilical vein endothelial cell (HUVEC) cellular network formation at 4 hourly intervals following changes in culture medium. Control experiment: medium replaced with 18mM glucose. Scale bar represents 200µm.

HUVEC cellular networks were evident at each 4h time interval in 5mM glucose controls (**Figure 4.7**) and at 18mM glucose control but started diminishing after 12h in the 18mM control (**Figure 4.8)**. In fluctuating experiments, networks were diminished in 18mM glucose and did not recover following return to medium with 5mM glucose (**Figure 4.9**).

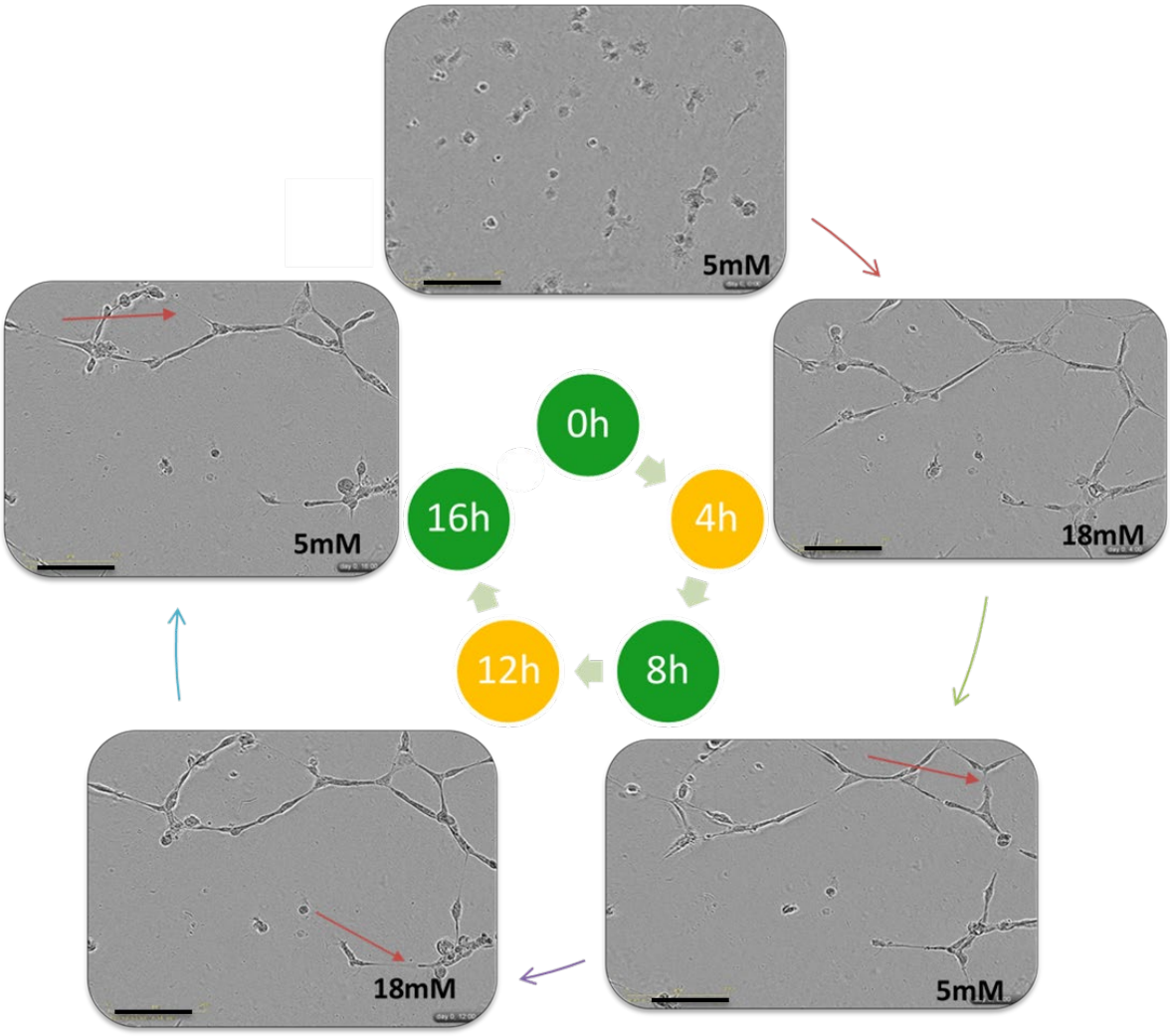

Figure 4.9 Representative live bio images of HUVEC cellular networks formed in response to changing glucose concentration every 4 h: experiment with 5mM glucose to 18mM fluctuating glucose concentrations

Representative bio images, from n=6 passages (Incucyte ZOOM Plate Imager) of human umbilical vein endothelial cell (HUVEC) cellular network formation at 4 hourly intervals following changes in culture medium. Experiment with 5mM glucose – 18mM fluctuating glucose concentrations on HUVEC cellular networks. Red arrows show regression of segment branches. Scale bar represents 200µm.

Images obtained at 4 hourly intervals were analysed for network variables using Image J and the data are presented in **Figure 4.10**. Angiogenesis Analyzer measured network variables: Meshes ,Master Segments, Master junctions and All Segments + Branches were chosen to be presented as they demonstrated differences between glucose concentrations amongst all network variables measured in preliminary experiments see (**Figure 4.4** and **Figure 4.5**). These network variables also served as indicators for well-formed cellular network structures.

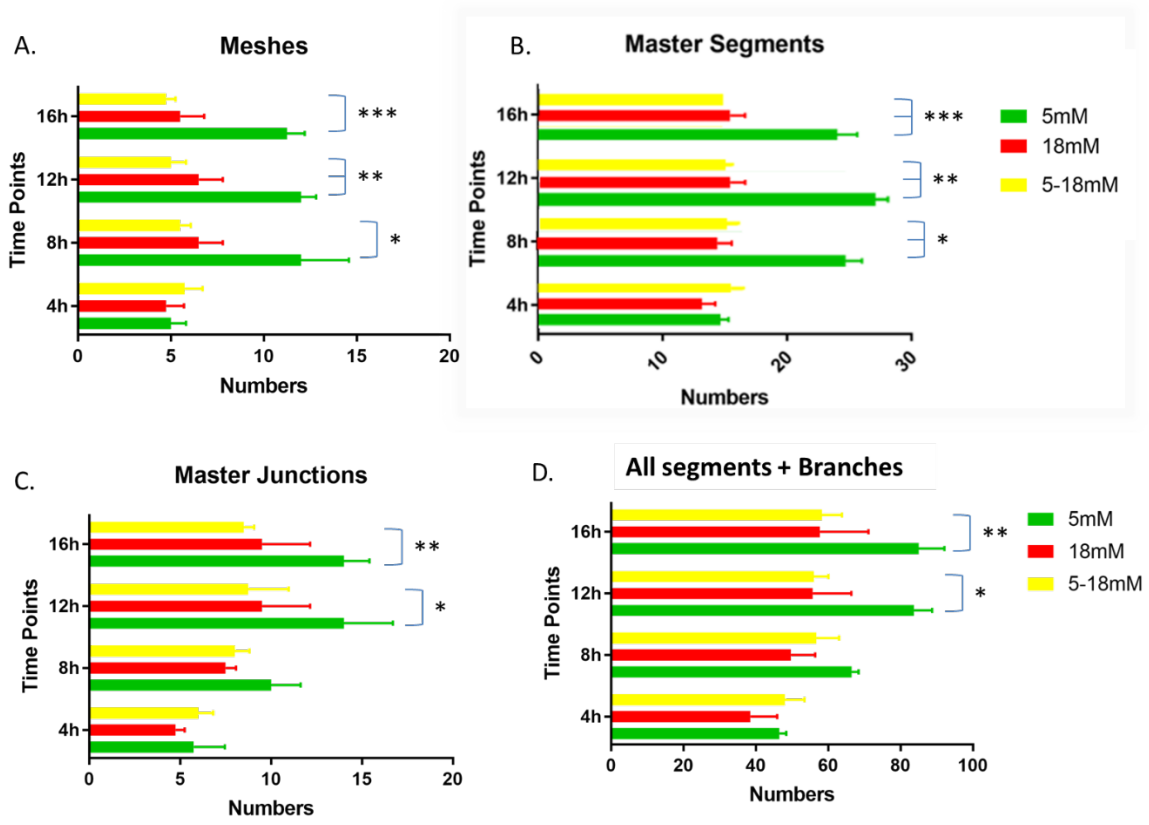

Figure 4.10 The effects of fluctuating glucose concentration(5mM-18mM) on HUVEC cellular network

The effects of alternating glucose concentration (5mM -18mM) in 4h intervals on HUVEC cellular network variables analysed by Image J. (n=6 passages; mean and SEM) ANOVA and Dunnett's multiple comparison test between concentrations at each time point.

(A) Meshes: [(At t=8h *p < 0.01 for 5mM vs 18mM and 5mM vs 5mM -18mM), (At t=12h ** p < 0.05 for 5mM vs 18mM and **p<0.01 for 5mM vs 5mM-18mM)], [(At t=16h ***p < 0.01 for 5mM vs 18mM and 5mM vs 5mM -18mM)]

(B) Master segments: [At (t=8h*, t=12h**and t=16h***p < 0.01 for 5mM vs 18mM and 5mM vs 5mM -18mM)]

(C) Master Junctions: [(At t=12h * and t=16h** p ≤0.05 for 5mM vs 5mM -18mM)].

(D) All segments+ branches: [(At t=12h * and t=16h**p ≤0.05 for 5mM vs 18mM and 5mM vs 5mM –18mM)]

At all-time points, measured variables increased in 5mM glucose concentrations. After 16h 5mM had the highest number of meshes of cellular network formed. There was no effect on master segments in 18mM over the time course and slight changes to other variables meshes, master junctions and all segments and branches in 18mM. In 5 to 18mM switch experiments there were effects demonstrated in the increase in master junctions but no effects on the other variables.

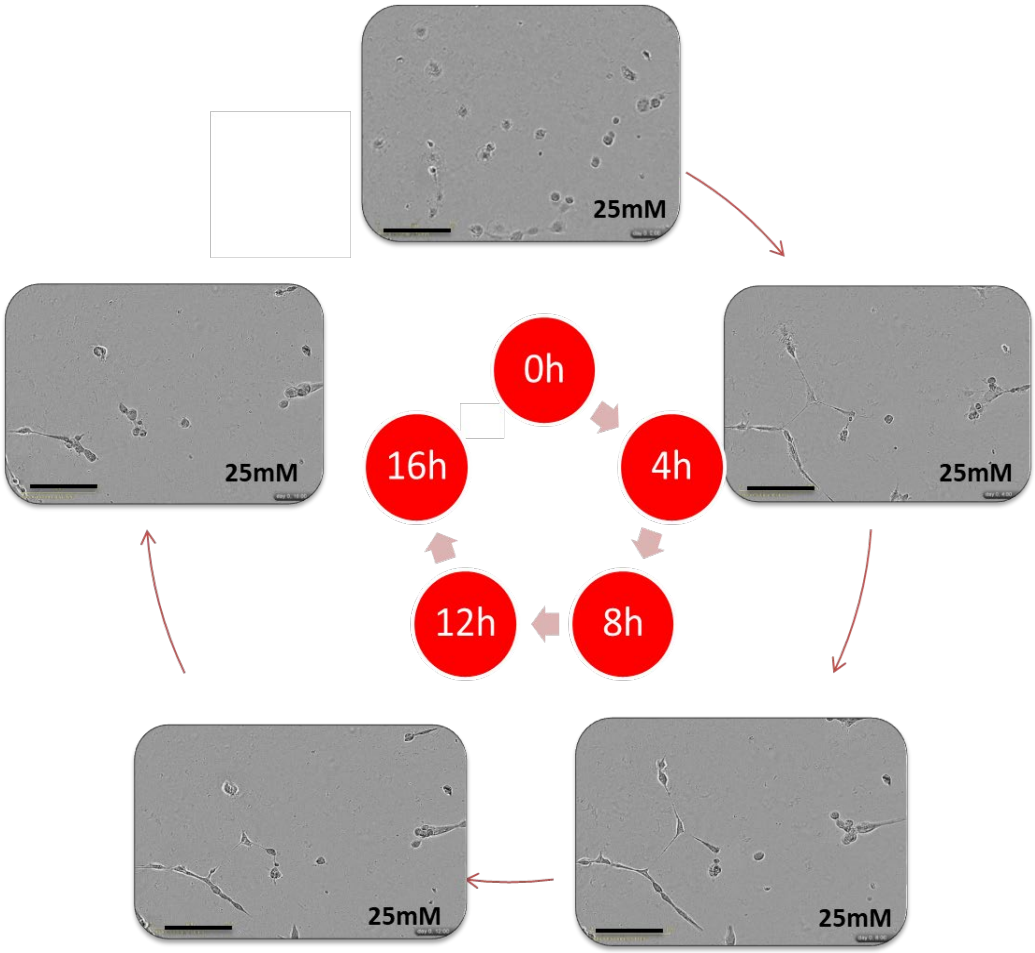

Figure 4.11 Representative live bio images of HUVEC cellular networks formed in response to changing medium glucose concentration every 4 h: control experiment with 25mM glucose

Representative bio images, from n=6 passages, (Incucyte ZOOM Plate Imager) of human umbilical vein endothelial cell (HUVEC) cellular network formation at 4 hourly intervals following changes in culture medium. Control experiment: medium replaced with 25mM glucose. Scale bar represents 200µm.

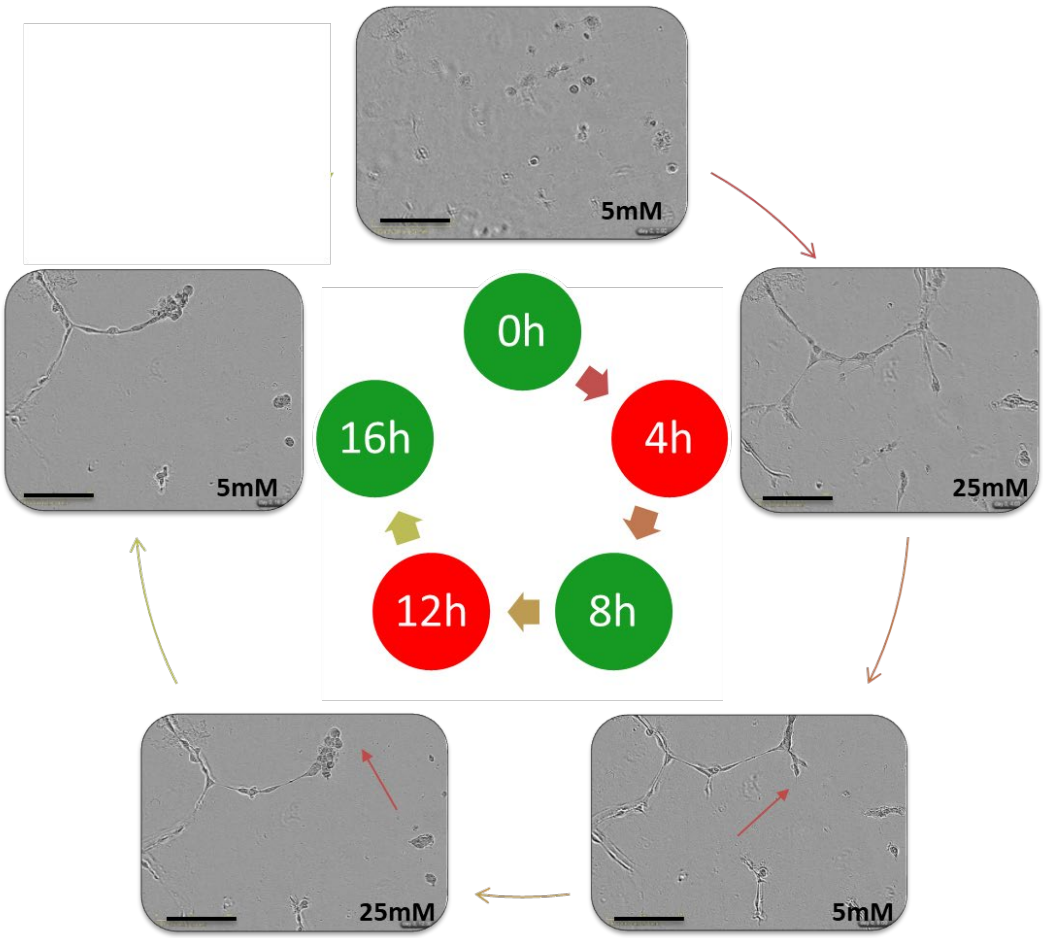

Figure 4.12 Representative live bio images of HUVEC cellular networks formed in response to changing glucose concentration every 4 h: experiment with 5mM glucose to 25mM fluctuating glucose concentrations

Representative bio images, from n=6 passages, (Incucyte ZOOM Plate Imager) of human umbilical vein endothelial cell (HUVEC) cellular network formation at 4 hourly intervals following changes in culture medium. Experiment with 5mM glucose – 25mM fluctuating glucose concentrations on HUVEC cellular networks. Red arrows show regression of segment branches. Scale bar represents 200µm.

The ability of endothelial cells to continue forming HUVEC cellular networks was evident at each 4h time interval in 25mM glucose control and sparsely formed networks started diminishing after 8h in the 25mM control as seen in **Figure 4.11**. In fluctuating experiments, cellular network formation was visibly inhibited in wells that switched from 5mM to 25mM and stayed in similar structure even after being switched back to 5mM with segment branches regressing as seen in **Figure 4.12** and in the summarised live bio images of HUVEC cellular networks from all experiments. The measurement of cellular network formation via mean number of master segments, meshes, segment +branches and master junctions are represented in **Figure 4.13**.

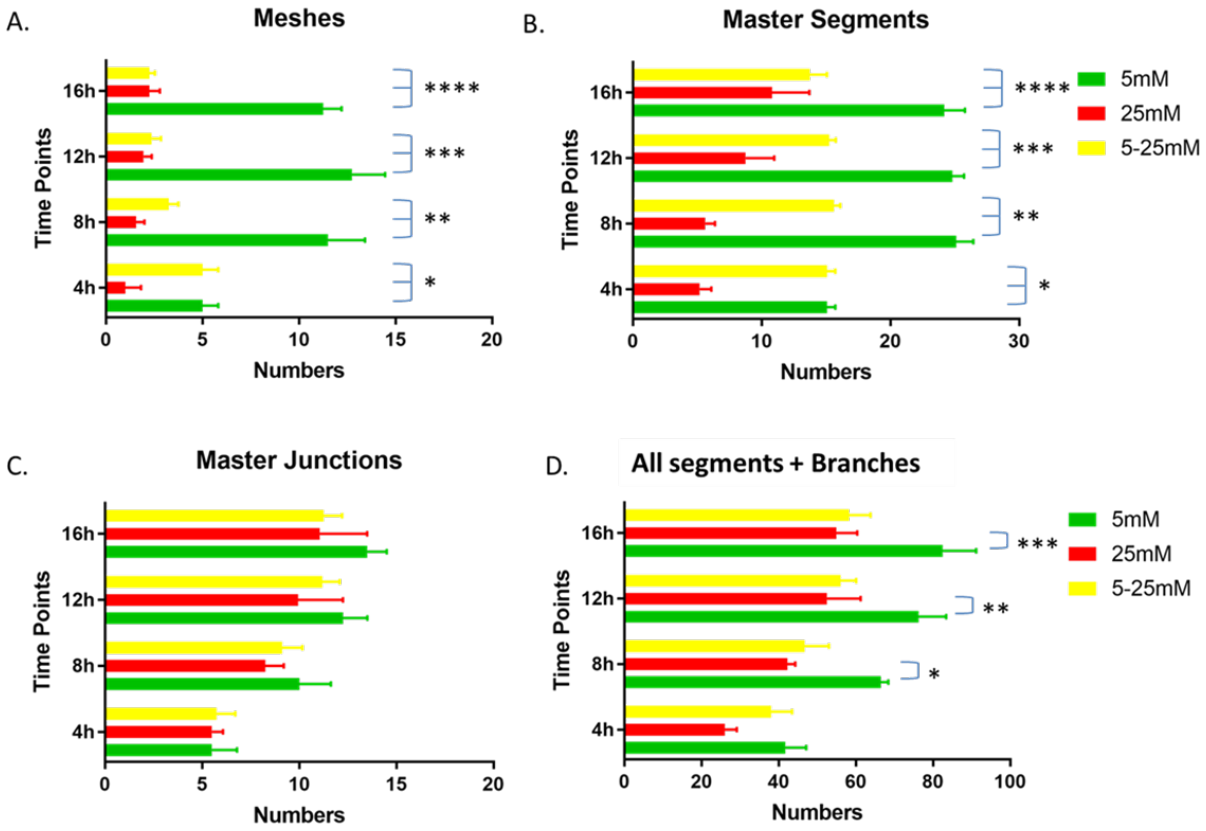

Figure 4.13 The effects of fluctuating glucose concentration(5mM-25mM) on HUVEC cellular network

The effects of alternating glucose concentration (5mM -25mM) in 4h intervals on HUVEC cellular network variables analysed by Image J. (n=6 passages; mean and SEM) ANOVA and Dunnett's multiple comparison test between concentrations groups at each time point.

(A)Meshes: [(At t=4h *p < 0.01 for 5mM vs 25mM and 25mM vs 5mM-25mM), (At t=8h **, t=12h*** and t=16h***p < 0.01 for 5mM vs 25mM and 5mM vs 5mM-25mM)].

(B)Master segments: [(At t=4h *p < 0.05 for 5mM vs 25mM and 5mM-25mM vs 25mM), (At t=8h**p < 0.01 for 5mM vs 25mM, p<0.05 for 5mM vs 5mM-25mM and p<0.05 for 5mM-25mM vs 25mM)), (At t=12h***p < 0.01 for 5mM vs 25mM, p<0.05 for 5mM vs 5mM-25mM)), (At t=16h****p < 0.01 for 5mM vs 25mM, p<0.05 for 5mM vs 5mM-25mM)].

(C)Master Junctions: No significant difference in number of master junctions between concentrations at each time point.

(D)All segments+ branches: [(At t=8h *p < 0.05 for 5mM vs 25mM and 5mM-25mM vs 25mM), (At t=12h**p < 0.05 for 5mM vs 25mM, p<0.05 for 5mM vs 5mM-25mM and p<0.05 for 5mM-25mM vs 25mM)), (At t=16h***p < 0.05 for 5mM vs 25mM and 5mM vs 5mM-25mM)].

In fluctuating experiments, at 25mM concentration only, there was no noticeable increase in the mean number of meshes over time but there was a noticeable increase in other measured variables; master segments, master junctions and all segments +branches. 5 to 25 mM switch experiments showed no effect on master junctions in contrast to the 5 to 18mM switch experiments. The graphs also demonstrate that there was a partial recovery in the number of master segments in 5 to 25 mM switch experiments which is not evident in the 5 to 18mM switch experiments. Representative mages from all experiments are summarised in **Figure 4.14**.

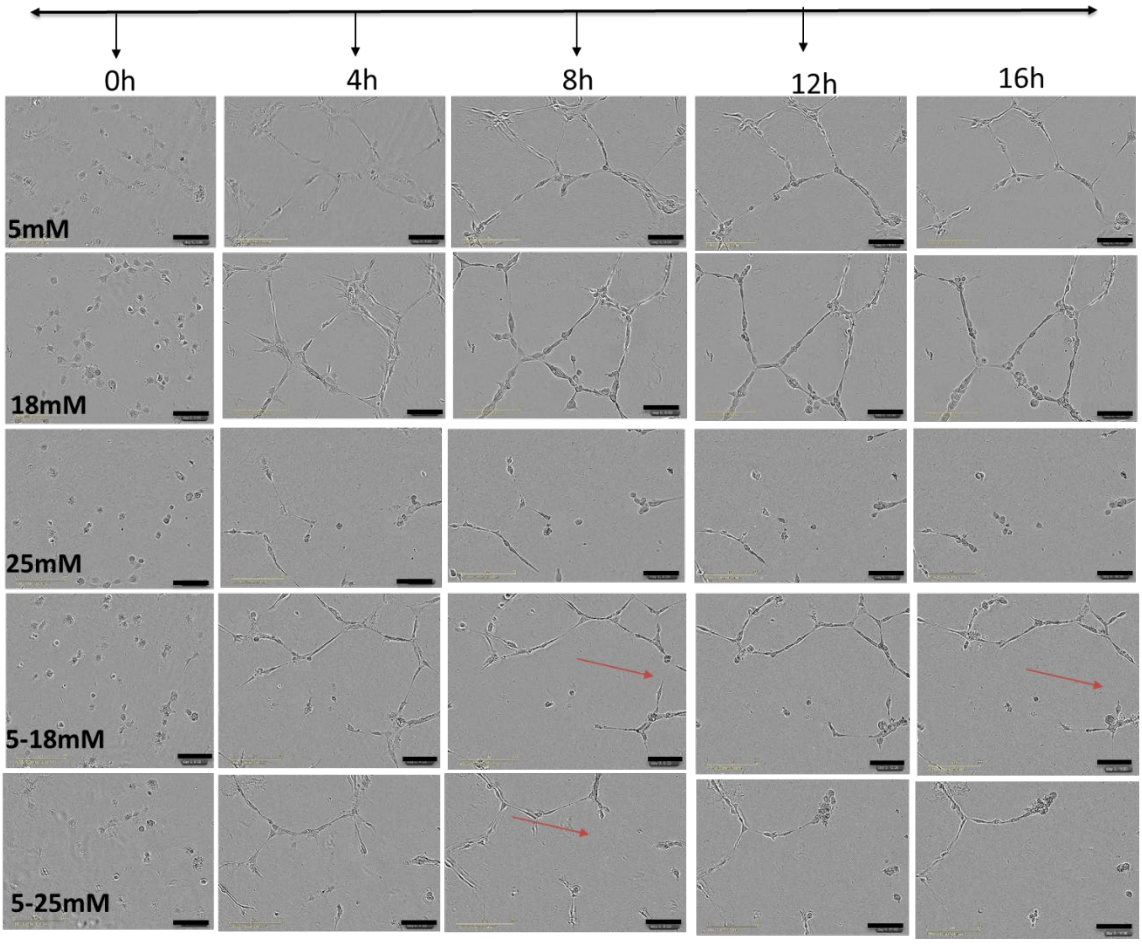

Figure 4.14 Summarised representative live bio images of HUVEC cellular networks formed in response to medium, high and changing glucose concentrations
Representative bio images, from n=6 passages, (Incucyte ZOOM Plate Imager) of human umbilical vein endothelial cell (HUVEC) cellular network formation at 4 hourly intervals following changes in culture medium. In 5mM, 18mM, 25mM, 5-18mM and 5 to 25 mM Red arrows show regression of segment branches. Scale bar represents 200µm.

4.5.3 Effect of glucose +/- insulin and metformin on HUVEC cellular networks

Representative images, at 18h of culture, of HUVEC cellular networks formed by cells grown in medium containing 5mM, 18mM or 25mM glucose +/- insulin (100 pmol/L, 1 nmol/L and 10 nmol/L) and +/- metformin (100nmol) are shown in **Figure 4.15**,**Figure 4.16** and **Figure 4.17** respectively. Qualitative assessment of the images indicates that the ability of HUVECs to form networks was inhibited in 25mM glucose (**Figure 4.17**) compared to control (5mM; **Figure 4.15**), in accord with previous data (**Figure 4.3**,**Figure 4.4**). Insulin at 100pmol/L appeared to improve network formation in 25mM (high) glucose (**Figure 4.17**). Metformin appeared to enhance networks formed by HUVECs maintained in medium containing 25mM glucose with insulin at all three concentrations (**Figure 4.17**).

Quantification of HUVEC network variables, analysed using Image J software, is presented in **Figure 4.17**, **Figure 4.18** and **Figure 4.19**. There was a significant inhibitory effect of raised glucose concentration (18 and 25mM) vs 5mM glucose (control) on each network variable. The mean number of meshes was 12 ±0.5 in 5mM compared to 25mM (2 ±0.5) and to 18mM (5 ±1), $p \leq 0.01$. The mean number of all segments +branches was 80 ±5 in 5mM compared to 25mM (50 ±10) and to 18mM (58 ±9), $p= 0.02$. The mean number of master segments was 24 ±2 in 5mM compared to 25mM (16 ±0.5) and to 18mM (17 ±1), $p \leq 0.01$ The mean number of master junctions was 14 ±2 in 5mM compared to 25mM (6 ±1) and to 18mM (8 ±2), $p \leq 0.01$.

The addition of insulin in raised glucose concentration (18 and 25mM) vs 5mM glucose (control) on each network variable had 5mM concentration with the highest numbers. However, insulin at 100pmol/L appeared to improve network formation in 25mM. After 18h cells in high glucose concentration control the mean number of meshes formed in 25mM was 2 ±0.5 compared to 25mM+ insulin 100pmol/L 6 ±2, 25mM+ insulin 1nmol/L (7 ±2) 25mM+ insulin 10nmol/L (7 ±1) $p \leq 0.0001$. Network variables at 18mM concentration were not significantly affected by the addition of insulin.

The effects of metformin on the network variables at each insulin/glucose concentration +insulin was noticeable in the mean number of meshes and master junctions with 25mM.The mean number of meshes formed in 25mM was 2 ±0.5 compared to 25mM+ insulin 10nmol/L +metformin 10 ±2, $p=0.001$ and significant against other concentrations of high glucose +insulin and metformin(vs 25mM+ insulin 100pmol/L +metformin 8±1,

p=0.01 and vs 25mM+ insulin 1nmol/L +metformin 9±1, p=0.01 .Similarly the mean number of meshes formed in 18mM was 5 ±1 compared to 18mM+ insulin 10nmol/L +metformin 12 ±1, p=0.05. The mean number of master junctions in 25mM was 6±1 compared to 11±1 in 25mM +insulin1 nmol/L+metformin (100nmol) and 12±1 in 25mM +insulin 10 nmol/L+ metformin(100nmol) p=0.043.

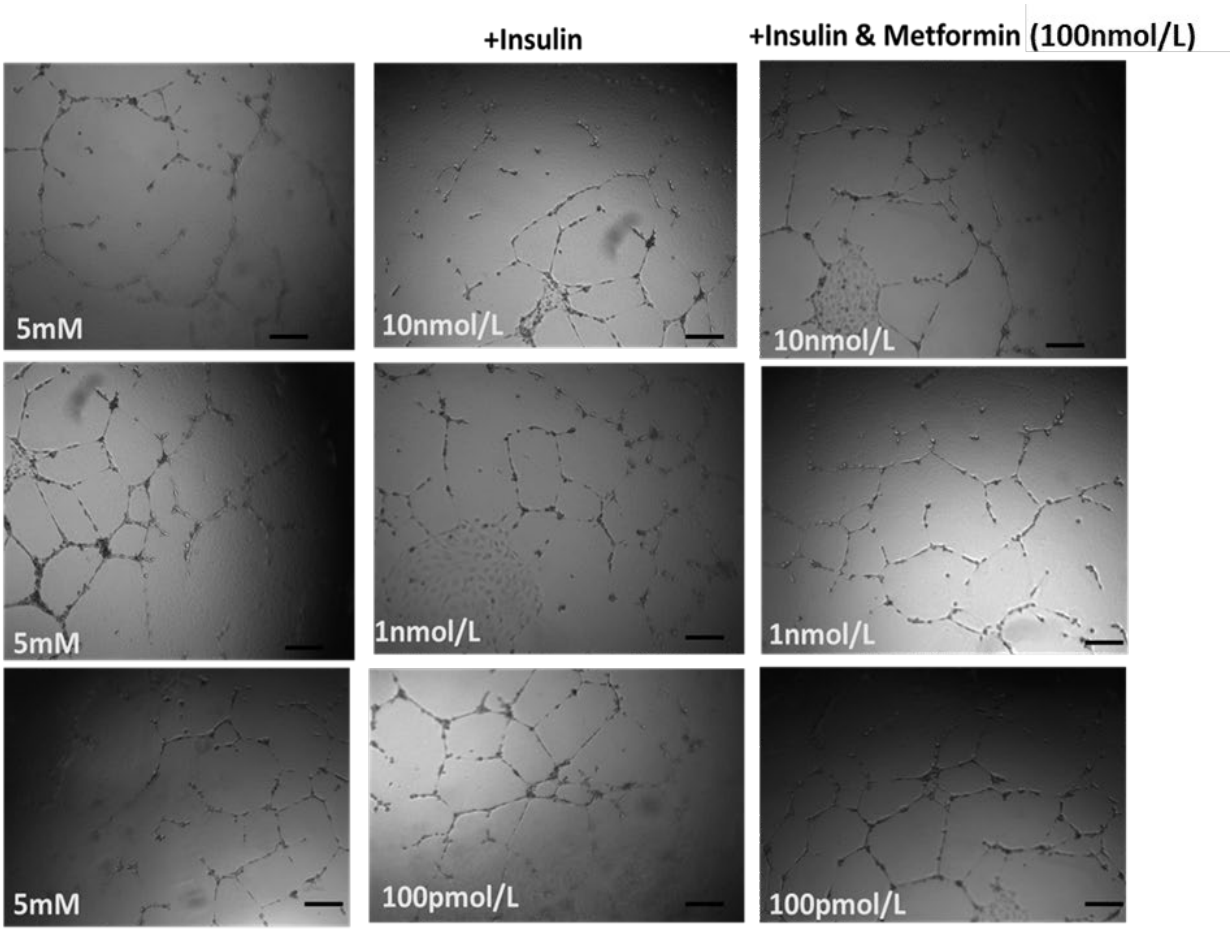

Figure 4.15 Effects of insulin +/- metformin on cellular networks formed by HUVEC cells maintained in 5mM glucose

Representative images of human umbilical vein endothelial cell (HUVEC) network formation at 18h (n=6 passages) by cells maintained in medium with 5mM glucose +/- insulin (100 pmol/L, 1 nmol/L or 10 nmol/L) and insulin + metformin (100nmol/L). Images taken under a light microscope (Olympus BX41) at 4× objective. Each scale bar represents 1000μm.

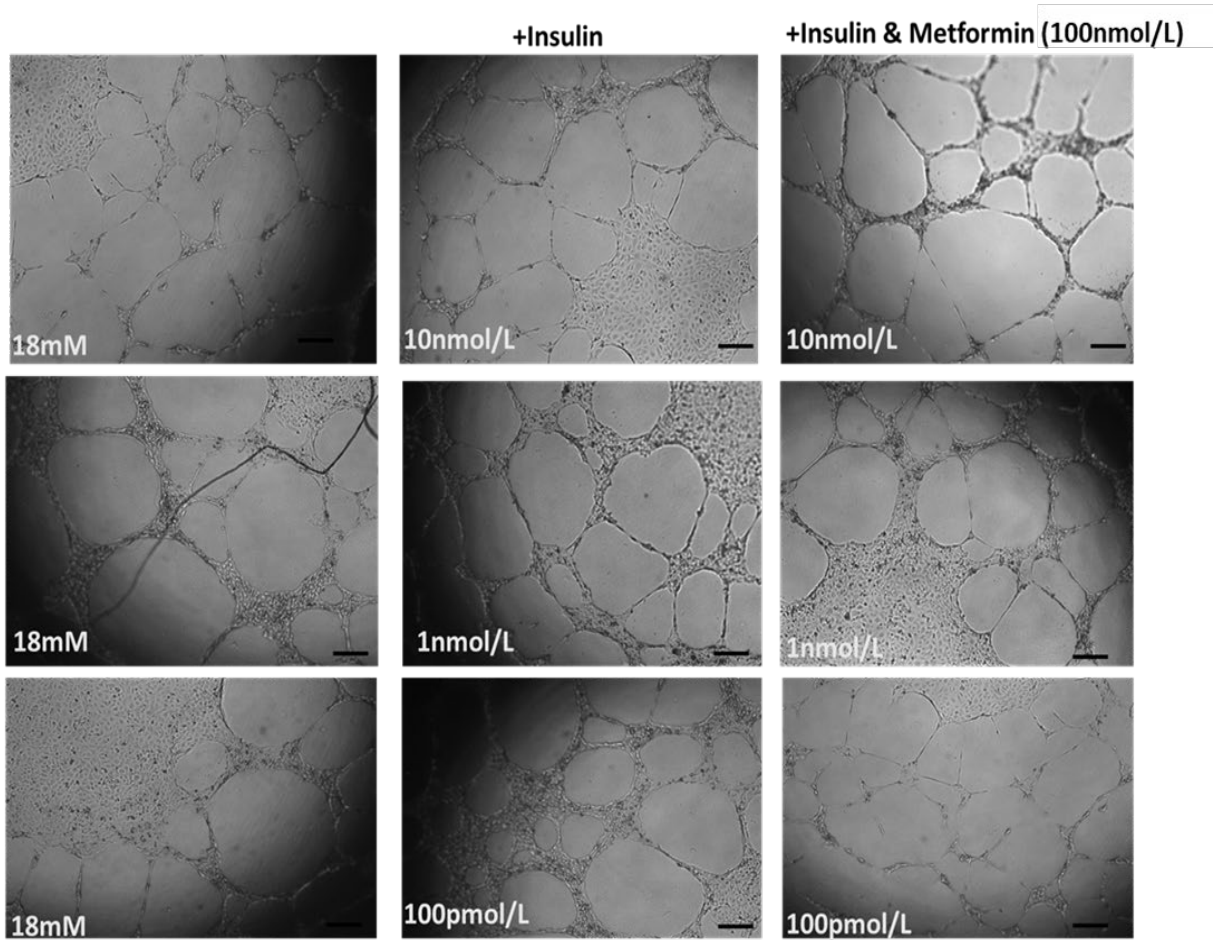

Figure 4.16 Effects of insulin +/- metformin on cellular networks formed by HUVEC cells maintained in 18mM glucose

Representative images of human umbilical vein endothelial cell (HUVEC) network formation at 18h (n=6 passages) by cells maintained in medium with 18mM glucose +/- insulin (100 pmol/L, 1 nmol/L or 10 nmol/L) and insulin + metformin (100nmol/L). Images taken under a light microscope (Olympus BX41) at 4× objective. Each scale bar represents 1000µm.

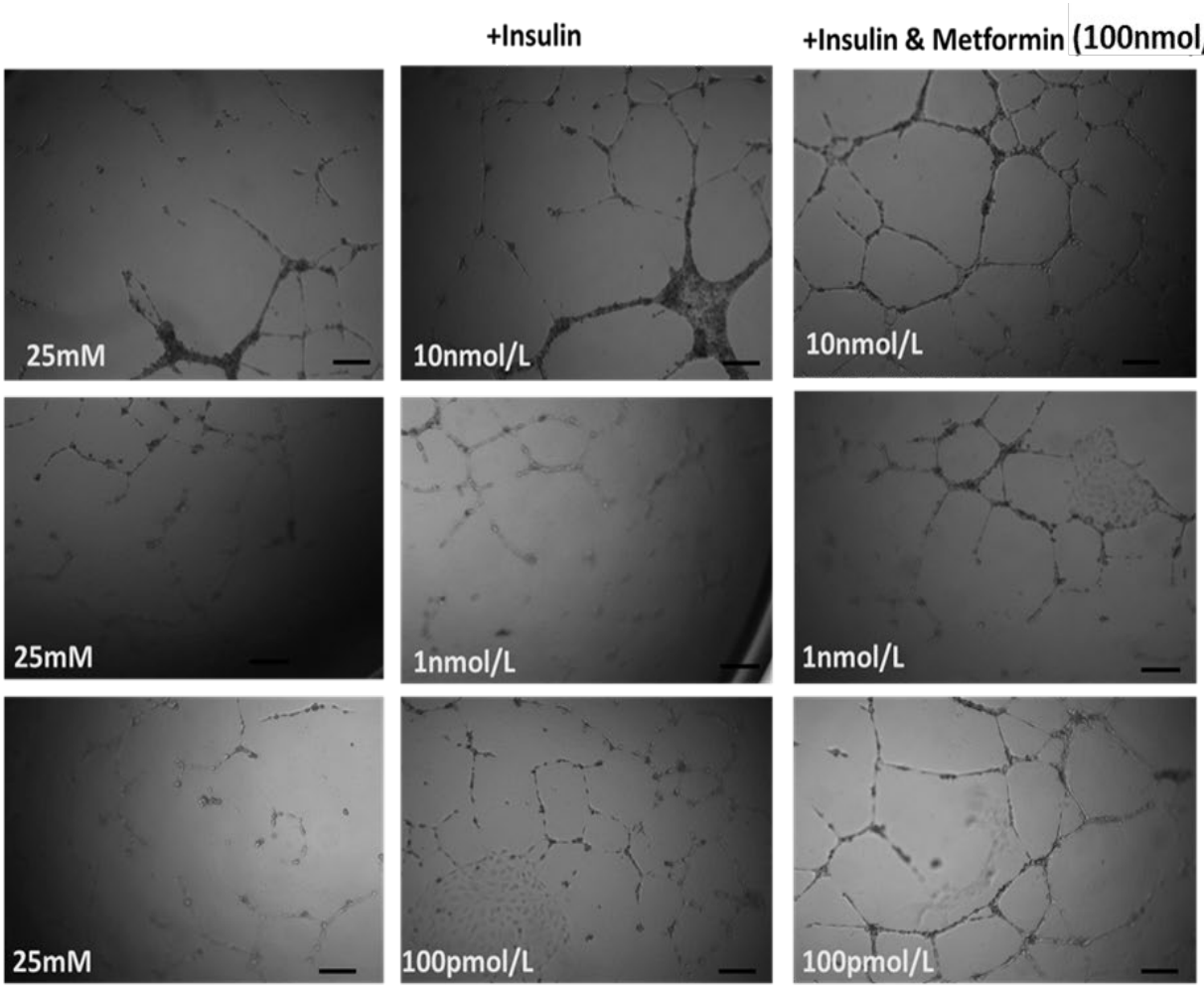

Figure 4.17 Effects of insulin +/- metformin on cellular networks formed by HUVEC cells maintained in 25mM glucose

Representative images of human umbilical vein endothelial cell (HUVEC) network formation at 18h (n=6 passages) by cells maintained in medium with 25mM glucose +/- insulin (100 pmol/L, 1 nmol/L or 10 nmol/L) and insulin + metformin (100nmol/L). Images taken under a light microscope (Olympus BX41) at 4× objective. Each scale bar represents 1000µm.

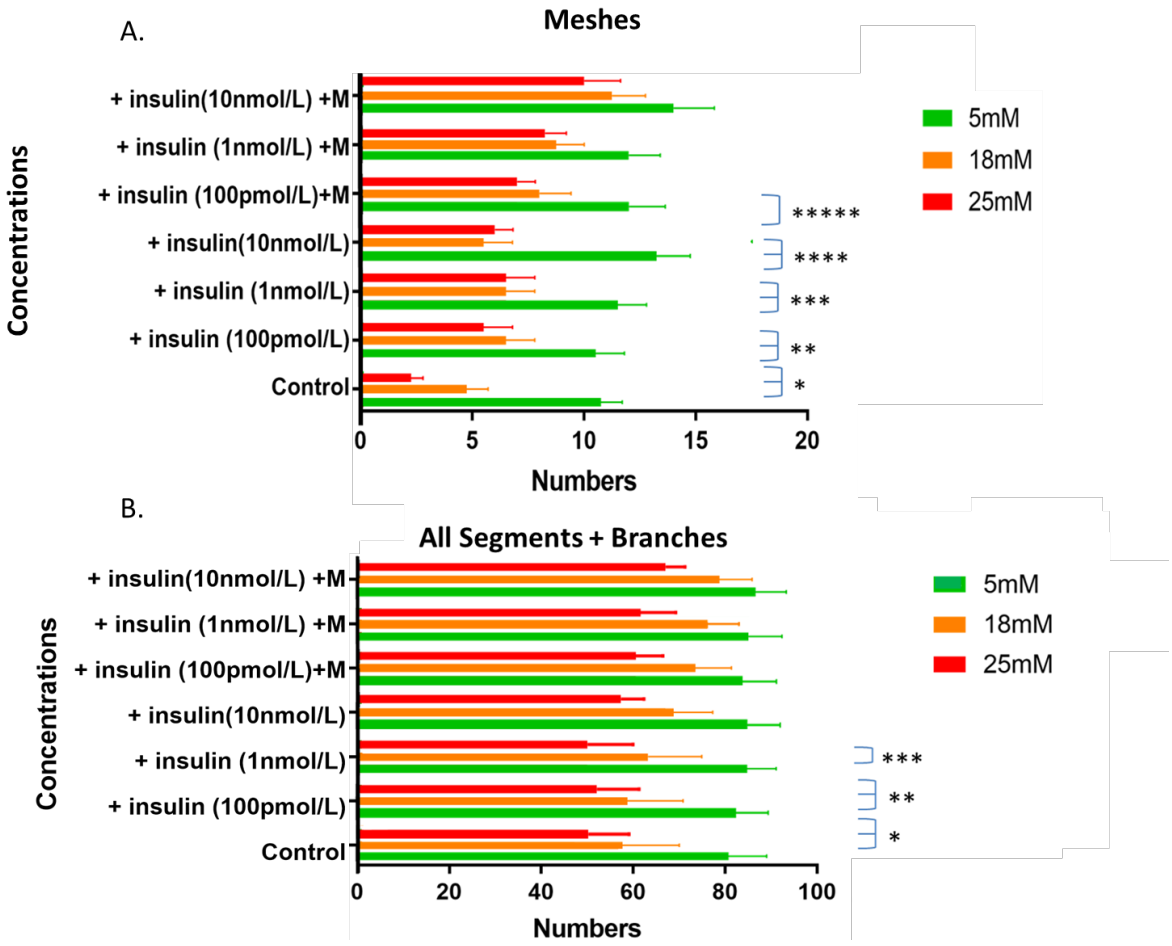

Figure 4.18 Effects of insulin +/- metformin on cellular network meshes, segments and branches, formed by HUVECs maintained in 5mM, 18mM or 25mM glucose

The effects of insulin (100 pmol/L, 1 nmol/L or 10 nmol/L), +/-metformin (+M; 100nmol/L) on network variables formed by human umbilical vein endothelial cells (HUVECs) maintained in medium with 5mM, 18mM or 25mM glucose (n-6 passages; mean and SEM). Data analysed by MANOVA and post hoc Dunnett's multiple comparison test

(A) Meshes: [(*p ≤ 0.01 for 5mM vs 18mM,25mM)], [(**p ≤ 0.05 for 5mM+ insulin 100 pmol/L, vs 18mM,25mM +insulin100 pmol/L)], [(***p ≤ 0.05 for 5mM+ insulin 1 nmol/L, vs 18mM,25mM +insulin 1nmol/L)],[(****p <0.01 for 5mM+ insulin 10nmol/L, vs 18mM,25mM +insulin 10nmol/L)], [(*****p ≤0.05 for 5mM+ insulin 100pmol + metformin(100nmol) vs 18mM,25mM +insulin100 pmol/L + metformin(100nmol). {p≤0.01 for 25mM concentration vs 25mM +insulin 100 pmol/L,1 nmol/L and 10 nmol/L + metformin(100nmol)]. [(p<0.05 for 18mM vs 18mM+ 10 nmol/L+ metformin(100nmol/L). No significant difference between 18mM concentration vs 18mM +insulin100 pmol/L and 1 nmol/L as well as vs 18mM+insulin100 pmol/L and 1 nmol/L + metformin(100nmol)].

(B) All segment branches*:* [(*p < 0.05 for 5mM vs 18mM,25mM)], [(**p ≤ 0.05 for 5mM+ insulin 100 pmol/L, vs 18mM,25mM +insulin100 pmol/L)], [(***p ≤ 0.05 for 5mM+ insulin 1 nmol/L, vs 18mM,25mM +insulin 1nmol/L)]. No significant differences between glucose concentrations +insulin vs glucose concentrations +insulin +metformin

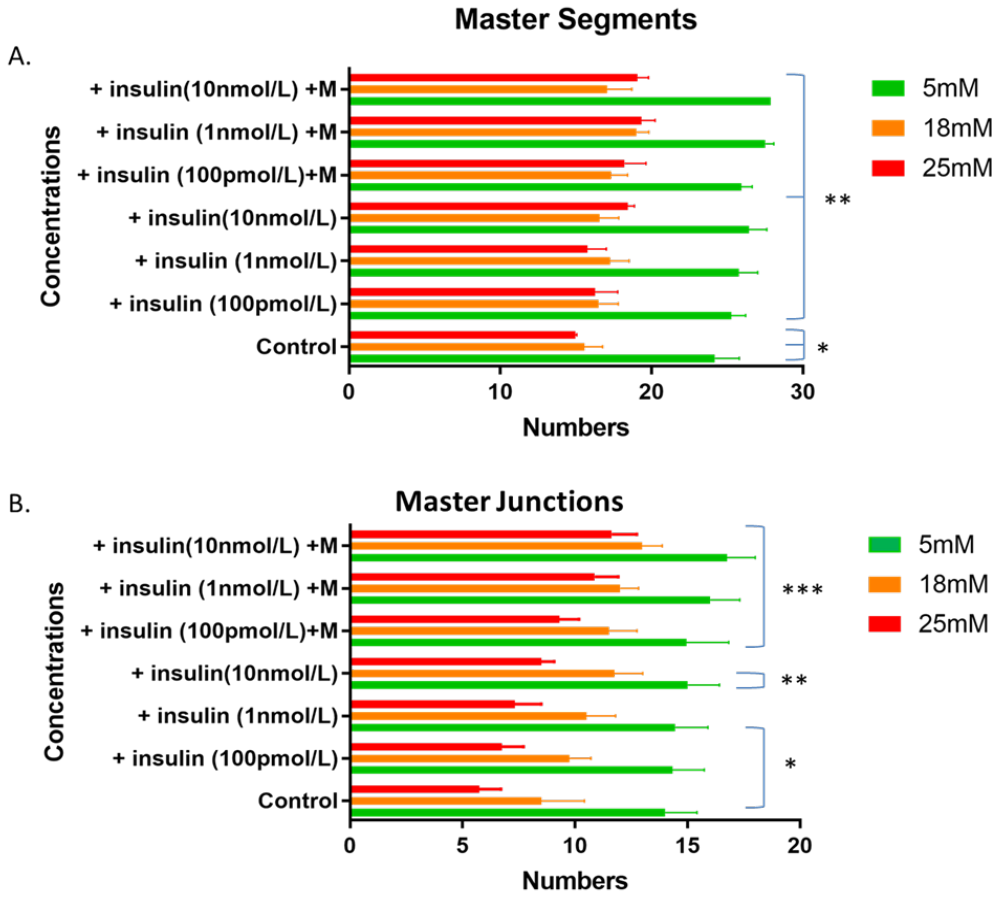

Figure 4.19 Effects of insulin +/- metformin on cellular network master segments, and master junctions, formed by HUVECs maintained in 5mM, 18mM or 25mM glucose

The effects of insulin (100 pmol/L, 1 nmol/L or 10 nmol/L), +/-metformin (+M; 100nmol/L) on network variables formed by human umbilical vein endothelial cells (HUVECs) maintained in medium with 5mM, 18mM or 25mM glucose (n-6 passages; mean and SEM). Data analysed by MANOVA and post hoc Dunnett's multiple comparison test.

(A) Master segments: [(*p ≤ 0.01 for 5mM vs 18mM,25mM)], [(**p ≤ 0.05 for 5mM+ insulin 100 pmol/L, 1 nmol/L and 10 nmol/L) vs 18mM,25mM +insulin100 pmol/L, 1 nmol/L and 10 nmol/L),(** p ≤ 0.05 for 5mM+ insulin 100 pmol/L, 1 nmol/L and 10 nmol/L+ metformin(100nmol/L) vs 18mM,25mM +insulin100 pmol/L, 1 nmol/L and 10 nmol/L+ metformin(100nmol/L)]. No significant difference between 18mM +insulin 100pmol/L, 1nmol/L and 10 nmol/L vs 18mM +insulin 100pmol/L, 1nmol/L and 10nmol/L+ metformin(100nmol/L). No significant difference between 25mM +insulin 100pmol/L, 1nmol/L and 10 nmol/L vs 25mM +insulin 100pmol/L, 1nmol/L and 10 nmol/L+ metformin(100nmol/L)].

(B) Master Junctions: [(*p ≤ 0.01 for 5mM vs 18mM,25mM)(,*p ≤ 0.05 for 5mM+ insulin 100 pmol/L, 1 nmol/L vs 18mM,25mM +insulin100 pmol/L, 1 nmol/L)] ,[(** p < 0.01 for 5mM+ insulin 10 nmol/L vs 25mM insulin 10 nmol/L)] , [(*** p <0.05 for 5mM+ insulin 100 pmol/L, 1 nmol/L and 10 nmol/L + metformin(100nmol/L) vs 18mM,25mM +insulin100 pmol/L, 1 nmol/L and 10 nmol/L + metformin),(***p<0.05 for 25mM concentration vs 25mM +insulin1 nmol/L and 10 nmol/L+ metformin(100nmol/L)].

4.6 Discussion

The HUVEC tube-formation assay is a well-established *in vitro* angiogenesis assay based on the ability of endothelial cells to form a network of three-dimensional capillary-like cellular structures when cultured on a gel of growth factor-reduced basement membrane extract [349, 350].

Utilising HUVECs, the data presented in this study show: Analysis of cellular networks formed by HUVECs over 18hr showed that several variables were significantly affected by glucose concentration. In comparison to 5mM glucose (normoglycaemia), 7mM significantly increased the number of segments + branches, master segments and nodes, and increased the total mesh area, consistent with a promotion of cellular networks.

In contrast, HUVEC network formation was diminished in higher glucose concentrations and the number of master segments, master junctions, segments + branches and meshes was significantly lower in 18mM and 25mM glucose compared to normoglycaemia (5mM) (**Figure 4.3**, **Figure 4.4**).

Experiments to explore effects of fluctuating glucose concentrations, by alternating (2x) between 5mM/18mM or 5mM/25mM, to simulate unstable maternal plasma glucose in diabetes, showed that HUVEC cellular network variables (meshes, master segments, segments + branches) were signigficantly inhibited by the higher glucose concentrations and did not fully recover when normogylcemia was restored.

The addition of insulin (100pmol/L, 1nmol/L and 10nmol/L) +/- metformin at a therapeutically relevant concentration (100nmol/L), did not alter cellular network variables formed by HUVECs maintained in 5mM glucose. The addition of insulin in raised glucose concentration (18 and 25mM) vs 5mM glucose (control) on each network variable had 5mM concentration with the highest numbers. However insulin at 100pmol/L appeared to improve network formation in raised glucose concentrations particularly at 25mM (**Figure 4.17**). Network variables at 18mM glucose were not significantly affected by the addition of insulin only but network formation (i.e meshes) improved with the addition of metformin. Metformin also appeared to enhance networks formed by HUVECs maintained in medium containing 25mM glucose with insulin at all three concentrations.

The signigificance of these effects of glucose concentration, insulin and metformin on the HUVEC model of angiogensis are discussed below in relation to the underlying causes of abberant fetoplacental microvasclular morphology that is evident in diabetic women.

4.6.1 Angiogenesis cellular network formation Assays

During angiogenesis, endothelial cells (ECs) undergo activation after binding of angiogenic factors to their receptors, release of proteases to dissolve the basement membrane, migration towards an angiogenic signal, proliferation, and an increase in cell number for new blood vessel formation [315, 351, 352]. Assays that quantify 'angiogenesis' have increasingly been used in development of agents to combat angiogenic diseases like vascular complications and cancers.These assays are based on the principle that new vessels will grow in an area that was previously devoid of blood vessels [353]. HUVEC tube-formation assay is one of the simple, but well-established *in vitro* angiogenesis assays based on the ability of ECs to form three- dimensional capillary-like tubular structures, when cultured on a gel of growth factor- reduced basement membrane extracts [354] [355]. During the assay, ECs differentiate, directionally migrate to align, branch, and form the tubular polygonal networks. The formation of cellular network is rapid and quantifiable. The formation of endothelial tubules on basement membrane has been used in investigations not only to study factors that regulate the process of angiogenesis, but also to define genes and signalling events in early angiogenesis [351].

In the current study, HUVECS were used to assess effects of glucose, insulin and metformin on cellular network formation *in vitro* with a view of assessing effects on Human placental arterial endothelial cells (HPAECs) derived from placenta chorionic plate arteries in the future. Initial pilot studies determined an optimal seeding density of 15,000 cells/96 well, in agreement with previous studies (reviewed by [35] [351]). The pilot experiments also assessed effects of different doses of the angiogenic factor VEGF as a positive control (**Appendix 4(II)).** Cells treated with VEGF (6.67ng/ml) showed the appearance of colonies, maybe as a result of increased proliferation of the HUVECs. However, cellular network formation was evident in both VEGF- free controls and in low levels of VEGF. This could be sustained by the growth factors, albeit reduced, in the Matrigel such IGF-1,TGF-bFGF-2, EGF, PDGF,NGF and VEGF which are essential for network formation. Based on these data

in pilot experiments (**Appendix 4 (II)**), additional VEGF was not added to the culture medium for the studies exploring the effects of glucose, insulin and metformin on angiogenesis.

4.6.6.1 Significance of HUVEC cellular network variables quantified by Image J

The "Angiogenesis Analyzer" image analysis software program was developed to extract characteristic points and elements of endothelial cells network formation and has successfully been used to characterize endothelial *in vitro* cell differentiation in phase contrast, fluorescence microscopy, and *in vivo* studies [356, 357]. Most *in vitro* angiogenesis models were designed based on the so-called "sprouting angiogenesis" differentiation process, whereby pseudo-capillary formation mimics several steps of the *de novo* angiogenesis. 3D microscopy was not performed to ascertain whether the HUVEC experiments in this study formed tubes in the networks observed (testing for lumen formation); however other studies in the literature have shown and confirmed lumen formation as well as visualisation of angiogenic sprouting using 3D microvasculature models [354, 355].The network formation in this study was characterised by variables that define tree structure analysis such as nodes, a pixel corresponded to a node when it had at least 3 neighbours, junctions were formed by the group of dots associated to a bifurcation, branch and segmement content;branches were lines, which are linked to one Junction and one extremity and segments were lines connected to the main tree by two junctions. HUVECs in matrigel grow according to a meshed network which quantified the level of cellular organisation corresponding to closed areas delimited by segments and associated junctions.This was represented by a vectorial object parameter measured as - "Meshes" (**Figure 4.2**). The final representation summarizes all the detected structures from the initial image all defined in **Table 4.1**. The variables number of master segments, segments + branches, master junctions and meshes were chosen to be presented as they provided information that represented gradual formation of the cellular network from nodes to complete meshes and mirrored proposed mechanisms of sequential regulation of sprouting/ branching angiogenesis [27, 358]. The nodes on the angiogenesis Analyzer represent the points of the endothelial cells lysis of the basement membrane and extracellular matrix in the angiogenesis process whereas the meshes (**Figure 4.2**) represent

a complete(joined) area of branching as a result of EC migration on the matrigel. Regression of celluar networks were also observed in high glucose concentrations as well as colonies of cells forming in the middle of wells. Endothelial cells have been reported to proliferate, differentiate and form tube-like structures when cultured on a matrix of basement membrane extract (BME) [359].This could explain the observed formation of colonies in certain wells; however, no proliferation assays were conducted to confirm this. The mechanism of vessel regression in angiogenesis is still largely unknown or undefined with deliberations on whether regression is induced by active signalling pathways or merely results from the withdrawal of survival factors (or a combination of both) [360].

4.6.2 Exposure to high glucose concentrations impair cellular network formation *in vitro* model of angiogenesis.

When cells were cultured in medium supplemented with various increasing concentrations of glucose, the exposure to the increasing levels of glucose accelerated the appearance and ability to form well-structured cellular networks(as indicated by networks forming to cover total mesh areas) of cells in wells .

The quantitative analysis of cellular network formation via measurement of number of master segments ,branches , master junctions and meshes demonstrated that in high glucose concentrations cellular network formation was hindered. The networks seem to form faster at the higher glucose concentration up to 9h. But at 18h, several network variables (nodes, segments, master segments, all segments + branches and total mesh area) are higher at 7mM vs 5mM and 15mM implying that the network formation/stability is promoted later at these concentration . Whereas in raised glucose concentrations such as 18Mm, networks might have formed quicker and regressed. In 25mM glucose, they might not have formed at all as shown in live bio imaging.

The ability of HUVECs to form cellular structures appeared to be inhibited under high glucose environment (25mM) as indicated by the significant decrease in total mesh area at 25 mM compared to 5mM, in agreement with previous studies [318, 321]. The data with the higher glucose concentration could be interpreted as an indication of apoptosis induced by 25mM. Decades ago, studies first demonstrated for the first time that high glucose levels of 20 and 40 mM hindered proliferation, disrupted the cell cycle and induced apoptosis of HUVECs cultured *in vitro* [361] and glucose concentrations of 30 mM induced

DNA damage in cultured HUVECs [362]. Studies have continued to explore the effects of raised glucose levels ranging from 11 -33mM on HUVECs. A study reported that exposure of HUVECs to high glucose(30 mmol/L) and AGEs resulted in a significant increase in Ang-2 expression; this was accompanied by a dramatic decrease in VEGF expression as compared to low glucose conditions (LG; 5 mmol/L) [318]. Song et al. (2005) demonstrated that, HUVECs structures in normal and mannitol medium form capillary-like structures on matrigel whereas cells treated with high glucose showed extended cytoplasm on matrigel and contacted each other. Between these cells, a lumen-like structure was observed. In addition, high glucose and AGEs inhibited the ability of HUVECs to form vascular like structure as evidenced by significantly reduced cellular network length and total number of branch points compared to control and mannitol condition. This inhibition was associated to relatively higher than normal expression of Ang-2 and VEGF- Tie 2 receptor differential expression in endothelial cells treated with high glucose concentrations(30 mmol/L) [318].

Yang et al. (2008) also reported that decrease in VEGF plays a critical role in apoptosis of endothelial cells induced by glucose levels of 25 mM[317].

Similarly, Peng et al. (2018) reported that high level of glucose of 25 mM increased the expression of inflammatory cytokine interleukin IL-6, and decreased the production of IL-8, vascular endothelial growth factor (VEGF) and angiogenesis of HUVECs in vitro [363]. Others have shown that apoptosis of HUVECs is mediated by ROS [364], by sequential activations of c-Jun NH(2)-terminal kinase and caspase-3 [365]. Furthermore, Ido et al. demonstrated that hyperglycaemia of 30 mM induces apoptosis in HUVECs by decreasing mitochondrial membrane potential and cellular ATP content and by inhibition of fatty acid oxidation [366]. High glucose levels of 30 and 33 mM were shown to induce apoptosis in human vascular endothelial cells through NF-kappaB and c-Jun NH2-terminal kinase [367] and also through a phosphoinositide 3-kinase-regulated cyclooxygenase-2 pathways [368]. Zhao et al. (2015) also reported that high-glucose concentration of 25mM in the culture medium upregulated myosin light chain phosphorylation and increased HUVECs permeability by activating the transforming protein RhoA – Rho-associated protein kinase signaling pathway [369]. Similarly, other studies report HUVECs exposed to high concentrations (16.5 and 33mM) of glucose demonstrated a significantly decreased cell viability, increased cell apoptosis and cleaved caspase-3 levels, compared with HUVECs exposed to a low glucose (5.5.mM). Zhang J et al. (2019) showed that high glucose levels of

16.5 and 33 mM induced apoptosis of HUVECs in a mitochondria-dependent manner by suppressing hexokinase 2 expression [370]. Furthermore, a study by Alvarado-Vásquez N et al. (2007) showed that HUVECs obtained from healthy newborns with a family history of type 2 diabetes, cultured in medium with glucose level of 30 mM showed 50% decrease in cell proliferation and 90% reduction in mitochondrial activity compared to the control group of HUVECs obtained from healthy newborns without a family history of type 2 diabetes [343, 371]. These and many reports have published on the effects of hyperglycaemia-induced apoptosis of vascular endothelial cells and its a role in the pathogenesis of both macrovascular and microvascular complications of diabetes. However,the conditions for testing the effect of constant high glucose levels compared to normal glucose levels on HUVECs varied widely in studies that have been conducted to date[343, 371-376] . The effects of 7mM glucose concentration increasing network formation observed in this present study have not been reported in the literature to the best of our knowledge although there are studies on effects of glucose on HUVECs that have categorised 7mM glucose concentration as normal glucose and 30mM considered as high glucose [376, 377].

Thus, the results presented in these published studies could be affected not only by high and variable glucose levels, but also by varied conditions of experiments. As endothelial cell dysfunction is associated with vascular abnormalities in diabetes, hyperglycaemia-induced apoptosis of vascular endothelial cells via various pathways and mechanisms observed in *in vitro* angiogenesis, with confirmed destructive effects of high glucose on endothelial function at the cellular level [369], could relate to the aberrant fetoplacental microvascular phenotypes proposed to result from dysregulated angiogenesis in diabetic women with poor glycaemic control.

4.6.3 Effects of fluctuation in glucose concentrations on angiogenesis; can glycaemic control rescue effects of impaired angiogenesis?

To simulate unstable glucose concentrations in diabetic mothers, HUVECs were exposed to glucose concentration fluctuating between control and pathophysiological raised level of glucose (5-18mM) and between control and high glucose concentrations (5mM to 25mM). This investigation demonstrated that the endothelial cells were not capable of regaining their cellular network like -forming ability once switched to high glucose concentration. At all time points, measured variables of cellular network formation were greatest in 5mM

glucose concentrations. After 16h 5mM had the highest number of meshes of cellular network formed. There was no effect on master segments in 18mM over the time course and slight changes to other variables (meshes, master junctions and all segments and branches) in 18mM. In 5 to 18mM switch experiments, there was an increase in master junctions but no effects on the other variables at the endpoint of the experiments. HUVEC cellular networks were evident at each 4h time interval in 5mM glucose controls but networks were diminished in 18mM glucose and did not recover following return to medium with 5mM glucose. 18mM glucose inhibited all network variables by 12 hours and this inhibition was not reversed by switching to 5mM glucose.

In fluctuating experiments, cellular network formation was visibly inhibited in wells that switched 5mM to 25mM and stayed in similar structure even after being switched back to 5mM with spotted segment regressed branches. Hence after a switch from high glucose concentrations, the HUVECS were not responsive to subsequent changes of glucose concentrations.

The reason for this is unclear; in contrast to the effects of high glucose levels *in vitro* on HUVECs that have been quite extensively studied, there are few research results documenting the effect of varying glucose concentrations in culture medium on HUVECs. The effects of blood glucose fluctuations reported in the literature on vascular complications in diabetes by Risso et al. (2001) demonstrated that after 7 and 14 days of HUVECs culturing in normal glucose level of 5mM, high glucose level of 20 mM and glucose levels varying every 24 h from 5mM to 20mM and vice versa, (H/N) the viability of HUVECs was significantly affected [344]. After 14 days, high glucose levels significantly affected cell viability compared to normal culture conditions, but the switch from high (20mM) to normal (5mM) glucose concentration resulted in the death of far more cells than in continuous normal and continuous high glucose concentrations. The authors concluded using various research methods (cell viability, cytometry analysis, DNA fragmentation and Bcl-2 and Bax expression) that both variable and high glucose levels stimulate HUVECs apoptosis, with varying glycaemic conditions being more unfavorable to cells than constant high glycaemic conditions [344].

Quagliaro et al. (2003) also reported that the blood vessel endothelium was damaged to a greater extent by blood glucose fluctuation than by chronic persistent hyperglycaemia using HUVECs [319]. They continued the Risso et al. 2001 study to demonstrate that the

increase in apoptosis of cells cultured in high and high to normal glucose conditions is associated with the production of free radicals and oxidative stress via a possible contribution of protein kinase C (PKC) in the activation of nicotinamide adenine dinucleotide phosphate oxidase (NADPH oxidase) [319]. Increased PKC activity was observed after the 7^{th} and 14^{th} days of culture under high and high to normal glucose conditions, with the increase being higher on the 14^{th} day and higher for cells cultured under high to normal glucose conditions compared to high glucose levels [319]. Other studies have also demonstrated that acute and chronic fluctuations in blood glucose levels can increase oxidative stress in type 2 diabetes mellitus patients [320] which results in cell dysfunction and tissue injury [378]. This has also been confirmed by studies that reported intraday glycemic variability is associated with the presence and severity of coronorary artery disease in patients with T2DM [379, 380].

Piconi et al. (2006) also confirmed that a stable high glucose level (20mM) caused an increase in apoptosis and the generation of oxidative stress, and that intermittent glucose levels (5mM-20mM) had a greater proapoptotic effect than stable high glucose level and therefore increased the oxidative stress [345]. Therefore, the reponses observed in the *in vitro* model in this study may be an indication of endothelial cell dysfunction under exposure to high glucose.The protocols for studies on fluctuating glucose concentrations on HUVECs varied especially with number of days (ranging from 7-14 days in studies compared to the duration used in our study) , different culture times and cells were also cultured in different media. A study by Kuricová et al. (2016) proposed a new research methodology to explore the effect of glucose concentration on HUVECs behavior by creating culture conditions more similar to the prevailing conditions in the body of individuals with diabetes or healthy individuals [346]. In earlier systems, the culture medium was replaced once or twice a day.

Kuricová et al. (2016) proposed 8 different daily glucose concentration variability(GV) profiles mimicking glycaemic profiles in the human body[(i) high GV(9.75,10.17,10.75 mmol/L) (ii) low GV(7,7.33, 8 mmol/L), (iii) GV of healthy subjects without diabetes(5.50 mmol/L), (iv) continuous normoglycaemia (5.5 mmol/L glucose) and (v) continuous hyperglycaemia (25 mmol/L glucose)]. Cell cultures were carried out only for 24 h and the medium was changed every 2 h. However, the proposed model resulted in an extremely labour-intensive experiment, but this was concluded as the most realistic approach to study *in vitro* the effect of glucose concentration fluctuations on HUVECs viability. Our

present study incorporated a 4h interval medium change to allow for feasibility and also used concentations that could mimic glucose variability during pregnancy (5mM normoglycaemia, 18mM raised glucose concentration and 25mM as high glucose concentration (hyperglycaemia). Nonetheless, Kuricova et al. (2016) failed to establish any differences in HUVECs viability in cultures using 8 different daily glucose concentration variability profiles probably due to too short culture time (24h and quick 2h changes). Perhaps quantification of cellular network structures in their study could offer insights to differences between glucose concentration method. Overall the literature supports the conclusion that a better understanding of the effect of chronic hyperglycaemia and the blood glucose concentration variability on endothelial cells will help reveal mechanisms underlying the late vascular complications of diabetes.

4.6.4 Effects of varying glucose concentrations, insulin and metformin on endothelial cells behaviour

In this study, the next step of investigation involved using different glucose concentrations (5mM, 18mM, 25mM) +/- physiological/pathophysiological concentrations of insulin to investigate the effects of varying levels of glucose in combination with therapies (metformin) on angiogenesis.

HUVECS were assessed in medium containing 5mM glucose concentration to represent normoglycaemic conditions, 18mM to simulated elevated glucose concentrations in pregnancy and 25mM to represent high glucose concentration(hyperglycaemia). These glucose concentrations were also examined in conjunction with insulin to mimic maternal hyperglycaemia environment which increases fetal plasma glucose and induces fetal hyperinsulinaemia. Insulin is pro-angiogenic and mediated through insulin receptors on fetoplacental endothelial cells. 3 insulin concentrations were used to cover a range of physiological to pathophysiological levels of insulin in relation to fetal levels of insulin in maternal normoglycaemia and hyperglycaemia. In accord with the earlier data (**Figure 4.3**, **Figure 4.4**), qualitative and quantitative assessment of images indicated that all network variables were greatest in 5mM glucose and inhibited in 18 and 25mM glucose.

Elevated glucose (18mM) and high glucose (25mM) significantly reduced a number of network variables (meshes, all segments and branches, master segments and master junctions) consistent with reduced angiogenesis. The addition of insulin (serum contained

insulin and culture medium was prepared by adding sufficient insulin to account for final desired conconcentrations) in raised glucose concentration (18 and 25mM) vs 5mM glucose (control) on each network variable had 5mM concentration with the highest numbers in measured network variables. None of the concentrations of insulin altered network variables in 5mM glucose. However, all 3 concentrations of insulin improved mesh formation in raised glucose (i.e did not have potentially detrimental effects). Insulin at 100pmol/L appeared to improve network formation in 25mM (high) glucose (**Figure 4.18**). Reports have also shown evidence of insulin causing human umbilical vein endothelium-dependent dilation and increase of hCAT-1 expression caused by elevated SLC7A1 (encoding hCAT-1) transcriptional activity and NO synthesis [381, 382] . Additionally, it has been reported in studies that insulin reverses the gestational diabetes mellitus (GDM) or high D-glucose-associated stimulation of the L-arginine/NO pathway in HUVECs and therefore suggest that glucose-increased oxidative stress and vascular dysfunction are attenuated by insulin [372]. In terms of tube formation or *in vitro* angiogenesis, studies showed that insulin enhanced *in vitro* angiogenesis and caused actin reorganisation by reversing the high -glucose-associated increase in ROS generation [231, 383]. Lassance et al. (2013) showed that insulin enhanced *in vitro* angiogenesis and caused actin reorganisation. This effect was associated with phosphorylation of IR and IRS-1, as well as Akt, glycogen-synthase kinase-β3 and endothelial NOS (eNOS). This in turn caused increased nitric oxide (NO) production and activation of Rac1.To test whether insulin stimulates angiogenesis in primary human fetoplacental ECs, the studies used a 2D *in vitro* network formation assay using VEGF as a positive control. They reported network formation 6 hours after seeding on Matrigel (BD Biosciences). To analyse *in vitro* network formation, cellular network length and branching points were quantified. It was reported that insulin increased the tube length of the network (+21%; $P < .05$) comparable with VEGF. Similar effects were found when the number of branching points (+29%; $P < .05$) or meshes were counted (+31% from 73.0 ± 7.6 in the controls to 95.7 ± 7.4 in the insulin treatment; $P < .05$).

In the current study, the addition of insulin in the different glucose concentrations appeared to reduce the formation of colonies of cells in wells and contributed to the development of a more stable network formation. Conversely other reports suggests that insulin at physiological concentrations is not preventive but may even contribute to the vascular impairment of endothelial phenotype previously damaged by high glucose, due to

an increased pro-atherogenic pathway observed by an up-regulation of ERK1/2,p38 and JNK phosphorylation [348]. Studies using diabetic retinopathy rat models have also suggested that fetal insulin is involved in the control of placental angiogenesis and permeability of the vasculature as evidence points to the enhancement of VEGF protein expression and secretion by insulin [41, 230]. The reported mechanistic action of insulin involves activation of endothelial nitric oxide synthase (eNOS) which further activates hypoxia inducible factor 1 (HIF-1). This HIF-1 factor is implicated in up-regulated expression of vascular endothelial growth factor A (VEGF-A). The expression of VEGF facilitates angiogenesis. It is important to also note that human endothelial cells represent a heterogeneous cell type with significant differences among vascular beds [384] and pathways shown in one endothelial cell type are not necessarily the same for others It is yet to be determined whether the above mechanism (eNOS/HIF/VEGF pathway) is operative in the human placenta; however it is most likely as VEGFR2, a notably important receptor for VEGF is abundantly expressed on the placental vasculature, particularly on the arterial endothelial cells [385].

Metformin has been shown to improve both endothelial function and insulin resistance in patients with metabolic syndromes [386]. Metformin is absorbed via the duodenum and jejunum and can freely cross the placenta from the mother to fetus unlike insulin. The absorbed metformin is not metabolised, and is excreted unchanged via the kidney and the bile, with a circulating half-life of approximately 6h [387]. In the second and third trimester , renal clearance of metformin increased due to the physiological increase in glomerular filtration, however this returned to pre-pregnancy levels after delivery [388]. As such metformin doses during pregnancy often require adjustment with changes in the glomerular filtration rate [387].

A systemic review [333] found that the therapeutic concentration of plasma metformin is widely varied with over 120 publications listing about 65 different therapeutic ranges for plasma concentration.

Kajbaf et al. (2016) reported that the average values range from 0.129 to 90 mg/L with lowest and highest boundaries found around 0 and 1800 mg/L respectively [333]. In other studies from a review on metformin use during pregnancy, administered doses varies from between studies, ranging from 500 mg/day to 2500 mg/day [278]. *In vitro* studies on the use of metformin in pregnancy have been reported to use at supratherapeutic

concentrations (~2-10 mM). In treatment of T2DM patients, it has been established that high concentrations of metformin (up to 1800 mg/L, or approximately 13 mM) can occur in their circulation [333].

Following addition of metformin at a therapeutically relevant concentration (100nmol/L), the abillity of endothelial cells to form stable cellular network structures was assesed in 5, 18 and 25mM glucose concentrations to determine whether this treatment could rescue cellular network formation in high glucose concentrations. Cellular network formation was visibly improved in wells containing insulin and metformin treated cells in high glucose concentrations (25mM) (**Figure 4.18** and **Figure 4.19**). Metformin appeared to enhance networks formed by HUVECs maintained in medium containing 25mM glucose with insulin at all three concentrations .The effects of metformin on the network variables at each glucose concentration+insulin was noticeable in the mean number of meshes and master junctions with 25mM glucose. This is consistent with studies that have reported that metformin prevents high-glucose–induced endothelial cell death through a mitochondrial permeability transition-dependent process [389]. Additionally, it was demonstrated that metformin modulated high glucose-incubated HUVECs proliferation and apoptosis through AMPK/CREB/BDNF pathway [373].

Furthermore, some studies *in vitro* and *in vivo* have also demonstrated that metformin directly attenuates endothelial dysfunction by decreasing TNF-α-induced gene expression of proinflammatory and cell adhesion molecules to inhibit endothelial cell inflammation in HUVECs [390]. Likewise, it also inhibits high glucose-dependent reactive oxygen species (ROS) overproduction by reducing NADPH oxidase activity in aortic endothelial cells [391].

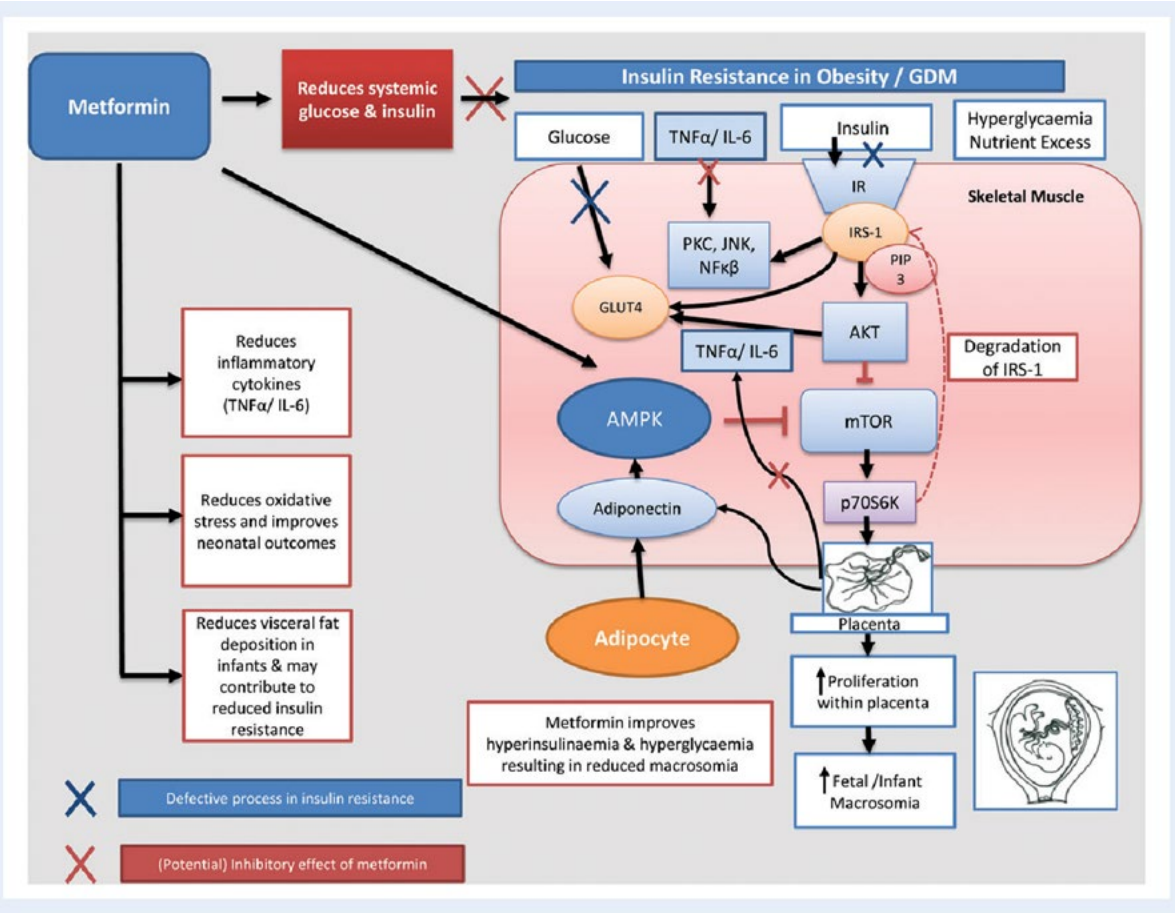

Figure 4.20 Putative mechanisms of action of metformin in pregnancy
Schematic outlining different proposed mechanistic actions of metformin in pregnancy taking into consideration insulin resistance in obesity or gestational diabetes. Different pathways highlighted showing metformin treatment action in reducing systemic hyperglycaemia and hyperinsulinaemia as well as upstream activation of AMPK, resulting in inhibition of the Mtor pathway. Metformin is also shown to have anti-inflammatory actions suggested to improve pregnancy outcomes via exerting this role in placental development and function. Schematic Image taken from Sivalingam, Myers et al. (2014) [331]

Thus, the studies above illustrate different putative mechanisms in which metformin affects angiogenesis in high glucose environments during pregnancy and in the presence insulin . This current study does not investigate mechanisms that underlie the effects of only metformin on cellular network formation and thus can not confirm operative mechanisms of metformin in pregnancies complicated by maternal diabetes. It could be any of the proposed mechanisms highlighted in **Figure 4.20**. However, the observed effects of high glucose on angiogenesis *in vitro* contribute to understanding the mechanism/s that might underlie hypo and hyper fetoplacental vascularisation (proposed to arise from

aberrant angiogenesis) that has been described in the placentas of diabetic women. The data on the effects of metformin +insulin on restored cellular network formation in high glucose conditions support metformin as a therapy for vasular complications in pregnancies complicated by maternal diabetes.

4.6.5 Strength and Study Limitations

To our knowledge, this study is the first to show the effects of varying glucose concentrations + physiological/pathophysiological concentrations of insulin in combination with metformin. Also this study shows novel information that human placental endothelial cells(HUVECs) in high glucose (25mM) can recover from inhibited cellular network fomation with the addition of insulin +metformin.

The interpretations of these findings should take into consideration factors that might have limited the investigations. Factors such as culture handling and transport between experiments could affect their behaviour *in vitro*.

In addition, human umbilical vein endothelial cells (HUVECs), which are most widely used for *in vitro* angiogenesis assays due to ease in isolation by perfusion of the umbilical vein with trypsin or collagenase are not as ideal. Angiogenesis commonly involves the microvasculature rather than the macrovasculature, thus these are not ideal as there are differences between the lineage of these, which may lead to inconclusive or inaccurate responses. HUVECs are derived from the umbilical vein, and so are representative of umbilical cord rather than placental vessels. It is very possible that these endothelial cells may behave differently from endothelial cells derived from placental vessels. In the same organ, the endothelium of small and large vessels, veins and arteries, exhibits significant heterogeneity and therefore differences of responsiveness among ECs are expected, since the endothelium has a high degree of molecular, biochemical, and functional heterogeneity according to the organ's origin and the microenvironment [392-394].

In the human body, adverse changes in endothelial cells due to high or variable blood glucose concentration occur over a much longer period of time, the time of experiments in this study could be increased to give an accurate reflection of this. In addition,it is notable that in studies assessing effects of variable glucose concentrations, cell viability assays are usually performed.

Future experiments from this study could incorporate cell viability assays/apoptosis assays to confirm high glucose toxicity to the cells, proliferation /differentiation assays to assess the formation of colonies in some of the wells and investigate 3D- microvascular visualisation model of tubes formed in matrigel to confirm lumen formation in networks from experiments as shown in other studies [354, 355]. Furthermore, in the literature with the exception of using similar stimulus in the form of high or variable glucose concentration, many other experimental conditions were not unified and in most cases differed between individual studies in terms of the cells used, composition of the culture medium, the size and material of the culture vessel surface and the culture time. Studies show that different culturing substrates modulate the effect of glucose concentration on HUVECs viability in *in vitro* cultures [343]. The literaturate also suggests more general conclusion that the effect of glucose concentration on endothelial cells viability *in vitro* should be interpreted in conjunction with effects of other factors defining the experimental environment including growth factors as they may amplify or attenuate observed differences.

In addition, isolating these cells from placentas from normal pregnancies and pregnancies complicated by maternal diabetes could reflect altered phenotypes or angiogenic potential resulting from exposure to the different environments *in utero.* Thus any assays using endothelial cells alone, while likely to be reproducible, readily quantifiable and rapid, will not permit the study of the more complex physiological interactions that occur *in vivo*, including the assessment of any indirect effects of agents and therefore care should be taken with interpretation of findings.

Although *in vitro* models do have limitations, they are still valuable as *in vitro* assays are able to demonstrate direct effects on endothelial cell function and are also relatively inexpensive compared to *in vivo* assays and are generally more reproducible and quantified more easily. The cells used in this study formed appropriate cellular networks and were capable of eliciting the relevant responses and differences we aimed to investigate in this project.

4.6.6 Summary

In summary, this study to our knowledge has shown novel effects of high glucose concentration +insulin and metformin on endothelial cells (HUVECs). The study demonstrates that the ability of HUVECs to form cellular network structures was inhibited under a high glucose environment (25mM). Fluctuating levels of glucose concentrations affected endothelial cell behaviour by hindering their ability to form cellular network structures even after switching back to control glucose concentration (5mM) from high glucose concentrations. Furthermore, the addition of insulin promoted the number of cellular networks in raised and high glucose concentration and the addition of metformin further enhanced this promotion thus the combination of insulin at the highest concentration and metformin almost restored the number of meshes in high glucose (25mM) to control levels. The addition of physiological concentrations of insulin in the different glucose concentrations appeared to reduce the formation of colonies of cells in wells and contributed to more stable network formation in control concentrations whereas the addition of therapeutically relevant concentration of metformin to cells improved cellular network structures in cells exposed to high glucose concentrations. The findings from this study, confirm the hypothesis by establishing the relationship between glucose concentrations and fluctuating glucose concentrations on the development of cellular networks by HUVECs. Elevated glucose concentrations inhibited network formation which could not be rescued by transient return to normal glucose concentrations. The findings from this study also highlight the modulation of this relationship by physiological/pathophysiological concentrations of insulin and therapeutically relevant concentrations of metformin. Pathophysiological concentrations of insulin enhanced network formation in high glucose concentration and this was further enhanced by addition of a therapeutic concentration of metformin.

Understanding the effect of glucose concentration on endothelial cells and how it manifests as aberrant angiogenesis in pregnancies complicated maternal diabetes is very important as it may become a starting point to develop new treatments slowing down progression of the late vascular complications of diabetes. Therapies may aim not to reduce glucose variability, but to protect or immunize endothelial cells from negative effects of hyperglycaemia, acting not on the cause but on the effects of glucose levels variability. This could be done by blocking signalling pathways that are adversely affected by fluctuating

glucose levels as highlighted in the proposed mechanistic actions of metformin in pregnancy and how it may regulate fetoplacental angiogenesis.

In future, the use of Human placental arterial endothelial cells (HPAECs) and Human placental vein endothelial cells (HPVECs) to reproduce these experiments would be more reflective of events within the placenta.

5 Chapter Five: General Discussion

5.1 Overview

The growing number of pregnancies that are complicated by maternal diabetes is likely to increase the demand on healthcare provision from the adverse complications associated with these pregnancies. Reasons for the increased risk of stillbirth, FGR and LGA in women with pregestational diabetes remain unknown and a better understanding of the pathophysiology underlying these disparate outcomes could lead to targeted therapy. Fetal growth disorders arise from placental dysfunction; abnormal vascular development/function underlies inadequate blood flow in "idiopathic" FGR but whether altered blood flow contributes to LGA remains unclear. Diabetes in non-pregnant individuals is associated with organ specific increased or decreased angiogenesis, leading to hyper or hypo vascularisation respectively, with associated macro and microvascular dysfunction that leads to the clinical complications of disease [36].

Evidence for altered fetoplacental angiogenesis in diabetic women is conflicting with reports of changes in angiogenesis occurring exclusively via longitudinal growth without a change in the cross-sectional calibre or shape of the capillaries using a design based stereological analysis [46, 79].

Other reports have also shown increased branching angiogenesis, hypovascular and hypervascular villi in placentas from women with diabetes[77]. Additionally, changed structure of the villous stroma and enhanced capillary surface areas in terminal villi of placentas affected by maternal T1DM with good glycaemic control have been reported using immunohistochemistry, confocal microscopy, topological schemes and 3D reconstruction techniques [77, 91].

In contrast, little is understood of vascular development of the larger calibre macrovasculature in maternal diabetes. This study tested the hypotheses that placental artery and venous networks would be different in pregnancies complicated by pregestational diabetes compared to normal pregnancies and related to fetal outcome, maternal glycaemic control and maternal levels of angiogenic factors (PlGF).

In summary, the experiments presented within this thesis were designed to address 3 major research questions in order to fill gaps in knowledge:

1. To determine whether there are differences in placental macrovascular networks at term in women with pregestational diabetes compared with normal pregnancy
2. To determine whether metrics of the placental macrovascular network at term are related to fetal growth, maternal glycaemic control and maternal plasma PIGF concentrations in women with pregestational diabetes
3. To determine whether hyperglycaemia +/-insulin and metformin have potential to regulate fetoplacental angiogenesis using human umbilical vein endothelial cells *in vitro*

The findings and main points from each study are brought together for a concluding discussion in this final chapter.

5.2 Reduced measured vascular volume at term in women with pregestational diabetes compared with normal pregnancy

The study has shown using vascular casting that both fetoplacental artery and venous networks assessed at delivery are significantly different in diabetic women. Differences demonstrated in vascular structure in fetoplacental vessels of placenta from pregnancies complicated by maternal diabetes were first observed by the mean number of vessel segments which was significantly higher in arterial casts across radius bins in pregestational diabetes. There was also significantly fewer mean number of vessel segments in venous pregestational diabetes casts across radius bins. The differences were observed within the microcirculation (vessels with radii 150-400µm) between groups, and not in the larger vessels of the chorionic plate. Overall arteries and veins were affected similarly in that both showed shorter mean length, total length and decreased total vascular volume although arteries had lower mean volume but veins had a higher mean volume. Arteries and veins had lower total volume normalised to PW with increasing vessel diameter in diabetes compared to normal pregnancies, and shorter vessel lengths. Gestational age at delivery was significantly lower in women with diabetes, and as such the vascular networks could

be immature vs normal pregnancies at term: however, data were adjusted for placenta weight and gestation at delivery. There was no relationship between gestation and total vascular volume when corrected for placental weight in arterial casts.

It is unclear how these observations of altered vessel networks (i.e. lower length/ reduced vascular volume) of vessels relate to function. It is probable that the shorter length of larger calibre vessels might have implications on nutrient exchange. Given that placental veins convey oxygenated blood and nutrients to the fetus, it may be that shorter venous return path in pregestational diabetes increases efficiency of materno-fetal nutrient and gas transfer, such that fetus is at risk of macrosomia or LGA (increased fetal growth velocity). The placenta may also respond to enhanced fetal oxygen demand by enlarging the surface area of exchange as seen in increased placenta weight and surface area in pregestational diabetes especially in poorly controlled pregestational diabetes.

In an attempt to elucidate the functional significance of the decreased vessel length/volume in diabetes, the umbilical artery RIs/PIs, measured with Doppler ultrasound to give an indication of blood flow velocity, were related to the maximum arterial and venous volume normalised to PW (**Appendix 3(II)**)**.** The measured maximum vascular volume in arterial and venous casts was unrelated to the resistance indices. However, venous resistance might better be reflected in umbilical vein Doppler resistance indices which were not measured and there is evidence that altered resistance in arteries downstream of the cord is not always reflected in altered blood flow velocity measured in the umbilical artery by Doppler [395, 396]. It is therefore unclear whether altered vessel length/volume affects blood flow to and from the sites of placental nutrient exchange.

Abnormalities in larger calibre blood vessel development have been reported in fetal growth restriction, showing longer venous and shorter arterial vasculature in FGR placentas [58]. Previous investigations have also demonstrated the presence of fewer chorionic plate arteries and sparse capillaries in FGR placentas [83]. Similarly, previous vascular corrosion studies have reported that placental vascular volume in severe pre-eclampsia is significantly lower compared with normal placentas; however, the vascular volumes in normal placentas compared with mild pre-eclampsia placentas did not differ significantly and these findings were not related to fetal outcome [300]. However, reduced vascular volumes are commonly associated with poor fetal growth [397, 398].

The significant reduction in the length and total volume of the larger calibre fetoplacental

arteries and veins in women with diabetes were insufficient alone to induce disordered fetal growth in the study cohort in this thesis. However, it is probable that altered macrovascular networks predispose to placental dysfunction and other factors coincident with reduced vascularity are required to trigger fetal growth restriction/overgrowth.

In principle, vessel length discrepancies could be because of altered angiogenesis; however, the exact implications of these alterations on placenta function remains unknown or poorly understood.

5.2.1 Are vascular structure differences between normal and pregestational diabetes pregnancies related to maternal glycaemic control and/or growth factors?

The pregestational diabetic group was split into women with good and poor glycaemic control as dichotomized into groups with overall good control (most measurements <48 mmol/mol) versus overall poor control (most measurements <HbA1c ≥48 mmol/mol) to test whether reduced total vascular volume normalised to PW in the diabetic women was related to glycaemic control.

The poor control group had worse pregnancy outcomes compared to good control: a total of 55% had abnormal growth in poor control and a total of ~22.7% in good control. The incidence of LGA in the poor glucose control group was ~3x that of good control group; but SGA babies were only delivered to diabetic women with good glycaemic control. Two out 3 women with SGA babies were type 2 and on metformin and the other was type 1 diabetic on Seratide. This implies that another facet of diabetes not directly related to maternal hyperglycaemia (or by connection, fetal hyperinsulinemia) predisposes to SGA.

Overall BW, PW and IBC was significantly greater in the diabetic women with poor control vs good control and the number of earlier deliveries (before 37 weeks) was significantly higher in the poor control group.

The study demonstrated a significant reduction in total arterial volume normalised to PW in poorly controlled diabetes compared to normal pregnancy (the control no diabetes group), but total arterial volume was similar in normal pregnancy and in diabetics with good glycaemic control. In contrast, a significant reduction in venous volume normalised to PW

was evident in diabetics with good control vs normal pregnancy; in poorly controlled diabetes, venous volume was lower than in normal pregnancy up to vessels in radius size bin 28 (1700-1750µm).

These data imply that hyperglycaemia (+/- fetal hyperinsulinemia) is associated with reduced arterial volume but that reduced venous volume can occur in the absence of chronically elevated maternal blood glucose and must be secondary to other characteristic features of diabetes: there could be fluctuations in maternal glucose concentrations that affect venous (but not arterial) development in the good control group as defined and in this regard continuous glucose monitoring would be informative in further investigations. However, strategies to lower maternal plasma glucose might not be effective in preventing abnormalities of fetoplacental venous development in diabetes but rather therapies that aim to protect against the effects of variable/ fluctuating maternal blood glucose concentrations might be effective (i.e. blocking signalling pathways affected by glucose variability[343]).

Overall, measured maximum vascular volume normalised to PW was related to pregnancy outcome as assessed by BW. There was a relationship between measured venous vascular volume and BW but not with arterial vascular volume. This study adds to the growing body of knowledge on the association of maternal hyperglycaemia and altered placenta structure. In relation to the hypothesis it confirms that although hyperglycaemia might be related to the reduction in arterial volume, other driving components in the diabetic environment contribute to altered placenta structure and dysfunction as evidenced by reduced venous vascular volumes observed in diabetic women with both good and poor glycaemic control.

5.2.2 Placenta growth factor: marker for aberrant fetoplacental vascular development?

PlGF concentrations in maternal serum rise during pregnancy, peaking at the end of the mid trimester of pregnancy. Low PlGF concentrations during pregnancy are associated with pregnancy complications including recognized later-life cardiovascular risk [121]. Low plasma levels of PlGF, a pro angiogenic factor, has been associated with placental disease and maternal plasma PlGF concentration is used clinically as a biomarker of placental

dysfunction. If reduced maternal plasma PlGF concentrations relate to abnormal vascularity as assessed at term in in pregestational diabetes compared to normal pregnancy, this could be mechanistically relevant as well as a biomarker of disease.

The pregestational diabetes group was split into two sub-groups based on clinical details of the women classified with either normal or lower plasma PlGF concentration in the third trimester. A plasma PlGF of ≥100pg/L was classified as normal and <100 pg/L was considered low.

Demographics comparing diabetic women with low and normal PlGF did not show any differences: the BW/IBC, PW were similar. However, a greater proportion of the normal PlGF group had good glycaemic control (75%) compared to the low PlGF group (58%) consistent with a relationship between hyperglycaemia and placental dysfunction.

There were significant differences in the relationship between total vascular volume and radius size between the normal PlGF group and the lower PlGF group in pregestational diabetes with factored in adjustments for maternal glycaemic status of women using their first and last HbA1c measurements during pregnancy. There was a linear relationship between total venous vascular volume and radius size bins with vascular volume decreasing across increasing radius size in both normal and lower PlGF groups. There was a non-linear relationship between arterial total vascular volume and radius size bin with increasing arterial vascular volume across increasing radius size in lower PlGF group but decreasing arterial vascular volume across increasing radius size in normal PlGF group. In the group used to assess venous volume, BW was lower in the lower PlGF group compared to normal PlGF group suggesting that placental function was may not have been improved. This could imply that low maternal serum PlGF does not relate to the reduced arterial and venous volumes observed in diabetes or perhaps measured maternal plasma PlGF levels may not reflect local placental concentrations.

In relation to the original hypotheses, the total volume of fetoplacental arteries and veins (300-4000μm diameter) was reduced in pre-gestational diabetes compared to normal pregnancies. There was no relationship between vascular volumes and umbilical artery Doppler resistance indices. There was also no relationship between measured vascular volumes and birthweight when considering BW as a continuous variable: there were insufficient numbers to assess whether volumes were different in AGA vs LGA and SGA. Poor glycaemic control could contribute to reduced arterial and venous volume in diabetes,

but venous volume was also reduced in women with good glycaemic control. Although numbers were small, reduced vascular volumes in pregestational diabetes were not related to low maternal serum PlGF concentration in the third trimester.

5.3 The role of Insulin and Metformin on placental angiogenesis

Factors underlying aberrant angiogenesis in maternal diabetes are unknown and we tested the hypotheses that (a) high glucose concentration, to mimic levels achieved in poorly controlled maternal diabetes (b) insulin, at concentrations approximating those in fetal cord blood in maternal diabetes (c) insulin plus metformin at a therapeutically appropriate concentration could regulate angiogenesis using human umbilical vein endothelial cells (HUVECS) *in vitro*.

Our findings showed that compared to 5mM glucose, 7mM (approximating post-prandial levels) increased the ability of HUVECS to develop cellular networks consistent with stimulation of angiogenesis but higher glucose concentrations associated with poor glycaemic control (15-25mM) inhibited network formation. The mechanisms were not explored in this study but similar studies have shown high glucose levels caused an increase in apoptosis and the generation of oxidative stress and toxicity to HUVECs hindering their ability to form cellular networks [319, 344, 345, 348, 370, 371]. In elevated levels of glucose cellular networks seemed to form at earlier time points and regress as time went on. This *in vitro* observation, albeit on umbilical vein ECs, which are not representative of ECs in the fetoplacental vasculature, if reproduced *in vivo* is consistent with the reduction in vascular volume of the lager calibre vessels observed in women with pregestational diabetes in the current study; however, mechanisms that regulate the expansion of the vasculature and formation of the larger vessels are poorly/ incompletely understood.

The current study also demonstrated that transient exposure to elevated glucose can reduce network formation by HUVECS and that this is not reversed by restoring glucose levels to normal. The clinical impact of glucose variability on the development of diabetes complications remains controversial; however, a review of studies has shown that fluctuating glucose levels may have a more deleterious effect on cells compared to constant high glucose concentrations [323, 345, 346] [343]. Reports on the effects of exposure to high glucose concentrations have also been well documented with consequences on

endothelial cell dysfunction and aberrant angiogenesis [318, 362, 364, 365]. Studies on intermittent fluctuating blood glucose levels have also reported an increase in free radicals and endothelial dysfunction, which link hyperglycaemia with the activation of pathological pathways that lead to tissue damage [320, 322, 323]. Numerous studies have shown that macrosomia and congenital malformations relate to glycaemic control and hence reports on fluctuating hyperglycaemic spikes in pregnancies complicated by maternal diabetes could relate to a higher incidence of fetal overweight, via a mechanism at least partly independent of chronic hyperglycaemia [399, 400].

In vivo examinations with placenta casts at term showed a reduction in venous volume even in pregestational diabetes women with good glycaemic control and this might have arisen due to fluctuating glucose levels and could possibly be explored by continuous glucose monitoring.

Elevated maternal plasma glucose in diabetes can lead to fetal hyperinsulinaemia ([186, 279] [185, 187] and this could modulate angiogenesis through insulin receptors expressed by the fetal endothelium[190, 401, 402]. Studies have also reported that a decrease in circulating IGFBP-1 and to a lesser extent an increase in circulating IGF-1 is associated with higher birth weight in maternal diabetes [187]. The current study showed that insulin at 1nmol/L concentration did not alter the ability of HUVECs to form networks at 5mM glucose, but restored network formation in higher concentrations of glucose. This suggests that hyperinsulinemia might be protective against impoverished angiogenesis in maternal diabetes with poor glycaemic control. Studies have shown that insulin stimulates network formation but not proliferation *in vitro* involving the IRS1/PI3K/Akt signalling pathway and downstream eNOS and Rac1 activation and insulin also induces actin rearrangements involving PI3K, eNOS, and Rac1 signalling[231, 372]. This may also explain excessive placental vascularisation in conditions of fetal hyperinsulinemia [383]. Additionally, it has been reported that insulin reverses the gestational diabetes mellitus (GDM) or high D-glucose-associated stimulation of the L-arginine/NO pathway in HUVECs which implies that glucose-increased oxidative stress and vascular dysfunction are attenuated by insulin [372]. Other studies using diabetic retinopathy rat models have suggested that fetal insulin is involved in the control of placental angiogenesis and permeability of the vasculature as evidence points to the enhancement of VEGF protein expression and secretion by insulin [41, 230]. Clinical trials have shown that acute intensive insulin therapy exacerbates

diabetic blood retinal barrier(BRB) breakdown via activation of the hypoxia inducible factor-1alpha (HIF-1α)/VEGF pathway [230]. Retinal HIF-1α levels increase as a result of intensive insulin therapy and this promotes HIF-1α translocation into the nucleus, which in turn increases VEGF mRNA expression and protein synthesis via the PI3-kinase and mitogen activated protein kinase (MAPK) pathways. These two studies confirm a report from Poulaki et al. (2002) which reiterates that hyperglycaemia-induced upregulation of VEGF differs from the insulin-induced upregulation of VEGF [230].

Women with diabetes often take metformin to improve glycaemic control. Metformin can both promote and inhibit angiogenesis in diabetes and as it can cross the human placenta, metformin could potentially influence fetoplacental angiogenesis. Studies have shown the transfer of metformin across the human placental using the dual perfused placental cotyledon model and pharmacokinetic models [403-406].

Studies have also demonstrated the passage of metformin through placental tissues using isolated placental syncytiotrophoblast apical membranes [350], Wharton's jelly mesenchymal stem cells (MSCs) [351]and HUVECs [352].
In vitro, metformin at a therapeutic concentration, given in combination with insulin, restored the ability of HUVECS to form cellular networks in response to elevated glucose concentration. The specific mechanistic action of metformin still remains unclear; however the overall consensus is that metformin exerts its effects via activation of the AMPK signalling pathway [407]. The AMPK signalling pathway is a regulator of cellular energy homeostasis. It is known to be activated by falling cellular energy status i.e. increasing ratio of ADP/ATP and AMP/ATP and thus has been hypothesised to be a possible glucose sensing mechanism. It has been reported that metformin activates the AMPK signalling pathway by increasing phosphorylation of the Thr172 site in AMPK alpha subunit in primary hepatocytes [340]. In a recent review, it is suggested that metformin exerts its effects via its influence on endothelial function and its ability to decrease reactive oxygen species and has been found to increase the number of endothelial progenitor cells hence reducing endothelial dysfunction [408].

A study on a human first trimester trophoblast cell line (Sw.71) treated with glucose concentrations at 5mM, 10mM, 25mM and 50mM, in the presence and absence of metformin demonstrated that metformin partially reduced the glucose-induced inflammatory response, but had no effect on the anti-angiogenic or anti-migratory response [409]. Similarly, a study on the effects of metformin on HUVECs isolated from pregnant women with GDM reported that metformin ameliorated GDM-induced endothelial dysfunction via downregulation of p65 and upregulation of Nrf2 to improve endothelial cell function. This protective effect of metformin on GDM/high glucose-induced impairment of angiogenesis capability was reportedly via Nrf2 [337]. In addition, animal studies have shown the positive effects of metformin treatment on placental dysfunction and insulin demand in pregnant rats with a high fructose-fed diet [410, 411].

In maternal diabetes , studies report that metformin (alone or with supplemental insulin) is not associated with increased perinatal complications as compared with insulin[265].
The studies in this thesis demonstrated reduced placenta vascular volumes in diabetes compared to normal pregnancies despite women receiving metformin (The majority of women with type 2 diabetes from the Velocity study will have been on metformin (>90%)). SGA infants were also recorded in good control diabetes. A meta-analysis study on the effects of metformin in gestational diabetes reported reduced birth weight and incidence of macrosomia in infants born to mothers on metformin and other interventions such as dietary therapy, exercise, oral hypoglycaemic agents and insulin compared to women who had received routine care suggesting the importance of these other therapies in reducing the complications [332].

The majority of evidence supports pro-angiogenic effects of metformin although in placental tissues both hyper and hypo vascularisation are reported in diabetes and it is not possible to predict which effects metformin will exert on fetoplacental angiogenesis. However, in the current study, metformin in combination with insulin was shown to exert pro-angiogenic effects in high glucose concentrations.

5.4 Conclusion

The observations from the current study have identified evidence for structural changes within the patient groups studied, particularly those pregnancies that are complicated by maternal diabetes. In particular, morphometric analysis of placentas from pregnancies complicated by maternal diabetes revealed reduced vessel length and vascular volumes of placenta with associations to maternal glycaemic control.

This thesis has advanced our understanding of the development and structure of fetoplacental vasculature in pregnancies complicated by maternal diabetes. The most significant results from this project may be summarised as follows:

1. Placenta network structure at term is different in pregestational diabetes pregnancies compared to normal pregnancies.
    (a) Shorter arterial and venous length of vessels in placentas from pregestational diabetes pregnancies compared to normal pregnancies.
    (b) Decreased arterial vascular volume in placentas from pregestational diabetes.
    (c) Overall decreased total venous vascular volume in placentas from pregestational diabetes.
    (d) Shorter arterial and venous vessel length in placentas from poor glycaemic control pregestational diabetes.
    (e) Decreased arterial vascular volume in placentas from poor glycaemic control pregestational diabetes.
    (f) Decreased venous vascular volume in placentas from poor as well as good glycaemic control groups in pregestational diabetes compared to normal pregnancies.
    (g) Reduced vascular volumes in placentas from pregestational diabetes pregnancies were not related to low maternal serum PlGF concentration in the third trimester.

2. The analysis of cellular networks formed by HUVECs data showed that over 18h, several variables (mean number of meshes, segments, master junctions, all segments and branches) were significantly affected by glucose concentration.

(a) In comparison to 5mM glucose (normogylcaemia), 7mM significantly increased the number of segments + branches, master segments and nodes, and increased the total mesh area, consistent with a promotion of cellular networks.

(b) HUVEC cellular network formation was diminished in higher glucose concentrations and the number of master segments, master junctions, segments + branches and meshes was significantly lower in 18mM and 25mM glucose compared to normogylcaemia (5mM)

(c) Experiments exploring effects of fluctuating glucose concentrations to simulate unstable maternal plasma glucose in diabetes, showed that HUVEC cellular network variables (meshes, master segments, segments + branches) were significantly inhibited by higher glucose concentrations(25mM) and did not fully recover when normogylcaemia was restored.

(d) The addition of insulin (100pmol/L, 1nmol/L and 10nmol/L) +/- metformin at a therapeutically relevant concentration (100nmol/L), did not alter cellular network variables formed by HUVECs maintained in 5mM glucose. However, insulin at 100pmol/L appeared to improve network formation in raised glucose concentrations particularly at 25mM

(e) Metformin also appeared to enhance networks formed by HUVECs maintained in medium containing 25mM glucose with insulin at all three concentrations ((100pmol/L, 1nmol/L and 10nmol/L).

The structural abnormalities in the fetoplacental vasculature evident at delivery will possibly reflect earlier events in vessel development; this suggests that, investigations relating fetoplacental vascular structure at term with fetal growth, maternal glycaemic control and other biomarkers that could modulate placental vascular development in diabetes throughout pregnancy could contribute to more effective targeted and timely

interventions. The possibility of improving vascularity with maternal therapies (metformin) regulating angiogenesis in a diseased placenta signifies the potential of improving placental blood flow and, by extension, normalising nutrient and oxygen delivery to the fetus to support normal growth. It will be necessary to investigate the specific impact of structural abnormalities observed in the pregestational diabetes feto-placental vasculature on placental function. Investigations on early/second trimester placentas could also contribute in ascertaining ideal timing of therapeutic interventions and understanding the origins of disparate poor pregnancy outcomes in diabetes as it will no doubt place a significant burden on obstetric healthcare.

5.5 Recommendations for future work

There are a number of opportunities for future investigations that would complement and add to the findings of the current study, and would also fill identified scientific gaps in the literature to provide further evidence for the clinical and physiological implications of placenta vascular development in pregnancies complicated by maternal diabetes.

Fetoplacental vascular structure

Limitations encountered in this investigation were that in using this casting technique, arterial and venous networks could not be examined simultaneously in the same placenta. Commercially available coloured pigments added to casting material addresses the issue of creating casts with both arterial and venous network in the same placenta but render Micro-CT imaging futile. It would be interesting to develop a technique that accounts for this limitation and allows for scanning of placenta casts containing both arterial and venous networks and development of placenta specific software for analysis.

In future it would be beneficial to use a scanner with higher resolution to fully examine the smaller diameter fetoplacental vessel networks in an intact cast state. The techniques and software analysis used in this study only permitted a near-full account without having to break casts into smaller sections for higher resolution of smaller vessels. This necessitated imposing a threshold diameter of ≥300μm for vessel analyses. The smaller capillaries could not be seen, ruining the ability to examine the vasculature in its entirety and in continuity. It may be possible to overcome this by applying multiple multiscale imaging approaches to

the same sample, allowing additional data to be collected overcoming the limitations of a single technique. The usage of other three-dimensional imaging approaches including confocal, super resolution, light-sheet, and serial block-face scanning electron microscopy can provide insight into placental structure and function [412]. These approaches when used together, will allow three-dimensional imaging of the placenta across the scales at which different processes occur such as spatial relationships between structures and visualisation of structures that are not clearly apparent in two-dimensions.

Investigations using early and second trimester placentas from normal and pregestational diabetes pregnancies, when large calibre vessel network on the chorionic plate are being developed, could further our understanding on specific window for intervention therapies.

In comparisons of study populations of women whose placenta were used, investigations using longitudinal changes in maternal glycaemia via CGM data could offer a more accurate reflection of maternal glycaemic control instead of first and last HbA1c measurements.
In addition, PIGF measurements in normal pregnancy would enable complete comparisons between women with normal PIGF levels and no diabetes and women with normal PIGF in pregestational diabetes and women with lower PIGF in pregestational diabetes. The sFlt-1/PlGF ratio has been reported to have the highest accuracy for the diagnosis of PE patients from normal pregnant women in comparison to its power for the diagnosis of severe or early-onset forms of the disease[413]. It will also be important to measure the fetal regulation of placental vascular development, by measuring fetal (cord venous/arterial blood) PlGF levels. Future investigations will also aim to incorporate fetal cord PlGF measurements as fetal PlGF is most likely to be influential in regulating development of the fetoplacental vasculature.
Future studies conducted in pregnancies complicated by maternal diabetes must also consider the influence of obesity and other components of the diabetic environment *in utero* (i.e. oxidative stress, AGEs, inflammation, hypoxia). Future work will also aim to also relate vascular abnormalities to BW/IBR and try to relate structure to function i.e. venous Doppler.
Further work could also investigate cord insertion in diabetes in relation to poor outcomes as cord insertion could have a major influence on the pattern of fetoplacental blood vessel branching on the chorionic plate [56].

Histological Studies

Further histological analysis of placenta from normal pregnancies and diabetic pregnancies could be carried out on samples already collected and stored. The assumption is that pathological manifestations in placenta vasculature in pregnancies complicated by gestational diabetes will be the same in pregestational diabetes. However, a holistic view of placental vascular casts from pregnancies complicated by gestational diabetes indicate differences in number of vessel segments per total area to that of placentas from pregnancies complicated by pregestational diabetes. Further histological studies will be conducted in placentas from the different types of diabetes with the hope of relating the 2D histopathological findings to 3D volume structural findings from vascular casts.

For further analysis of vascular structure, the morphometric measurements of the vasculature should consider a number of features such as studies on vessel wall thickness and structure to provide insights on the effects of vascular dysfunction on vessel reactivity in pregnancies complicated by diabetes. There are some challenges in determining if the placental structural alterations in pregnancies complicated by pregestational diabetes can be translated into documented aberrations to placental flow, as studies are sparse. The ratio of lumen area to vessel wall will give insights on vessel adaptations and inform on their ability to respond to demand for changes in blood flow in placentas from normotensive pregnancies compared to pregnancies complicated by pregestational diabetes.

Immunohistochemistry vascular markers can be used in morphometric studies of placental vascularity. Vessel number and size are best quantified using a suitably specific marker such as CD31. CD31, also known as platelet endothelial cell adhesion molecule (PECAM-1), is a 130 kDa protein largely expressed by the endothelium, and thus is used as an endothelial marker in histological and cytological applications when investigating vascular structures [414, 415].

Vascular smooth muscle (VSM) differentiation can also be investigated in placenta samples from the two clinical patient groups (normotensive pregnancies and pregnancies complicated by pregestational diabetes). The VSM appear later in pregnancy compared to the endothelium, and emerge during angiogenesis and the development of stem villi [416] and is denoted by the expression of protein markers of their differentiation from about ten weeks of gestation [417]. The proteins expressed have contractile properties that give the

VSM their ability to vascular tone, blood flow and pressure [274, 418], and from an absence of placental neural networks, their contractile function is entirely modulated by both autocrine and paracrine functions, as well as oxygen levels. Some reports have described alterations to the VSM within pregnancies complicated by either GDM [419] or obesity [420], but have not been explored as of yet in pregestational diabetes. There have been no studies conducted to assess the expression of the VSM markers in placentas from pregnancies complicated by pregestational diabetes. The VSM cells play a role in maintaining the placental vascular structure, therefore it is hypothesized that any alterations to their expression in pregnancies complicated by the diabetes may match with alterations in vascular morphometry which could be assessed by measurements of changes in vascular profiles of structures as reported in the literature [421].

To also address the need for a robust classification of placental lesions in pathologies, an alternative approach to 2D classifications could be used by isolating villous trees and assessing them using 3D quantitative microscopy analysis. Evidence for pathologic findings on altered fetoplacental vasculature have differed among studies with variation in definitions of placental abnormalities.

The different definitions of the placental abnormalities as stated earlier could potentially reflect differences in the type of diabetes, study methodology, or approaches to assess fetoplacental vascular development and glycaemic control of study participants. Future research will aim to address this by exploring the use of quantitative 3D microscopic analysis of isolated placental villous trees. Training for this technique has been undertaken at The University of Munich and villous trees have been successfully isolated. The aim for this will be to isolate villous trees of placenta from both groups and start analysis using the neurolucida software. This technique will provide records of topology, hierarchy and quantitative data of villous tree that could be correlated to 2D classifications of pathological sections e.g. distal villous hypoplasia. This will be done through the isolation of peripheral villous trees from whole mounts of placenta tissues from normal pregnancies and pregnancies complicated by maternal diabetes. The whole mounts from which the villous trees are isolated will also be subsequently fixed in formalin and embedded in paraffin for histological sectioning and staining. The aim will be to correlate quantitative analysis of the isolated villous structures such as surface area, diameters volumes and topology to observed 2D histological placental properties and variables within the same tissue section.

Further *in vitro* studies

In this study HUVECs were used to examine the effects of high glucose concentrations on cellular network formation; however, chorionic and villous blood vessels differ in origin and function, there is a need to compare effects of glucose concentrations in chorionic vessel endothelial cells (HPAECs and HPVECs) and endothelial cells from villous vessels. Future *in vitro* studies could include isolating these cells from placentas from normal pregnancies and pregnancies complicated by maternal diabetes to distinguish the cell-intrinsic effects of diabetes from the effect of a skewed *in utero* environment.

A repeat of experiments of fluctuating glucose levels with insulin and metformin may be useful in accurately mimicking relevant physiological/pathophysiological environment in maternal diabetes.

Future experiments from this study could incorporate cell viability assays/apoptosis assays to confirm high glucose toxicity to the cells, proliferation /differentiation assays to assess the formation of colonies in some of the wells, gene expression studies e.g. single RNA-sequencing and investigate 3D-microvascular visualisation model of tubes formed in matrigel to confirm lumen formation in networks from experiments as shown in other studies[354, 355].

Recovery studies could also be implemented to explore the phenomenon of regressing networks and establishing markers to identify restored ability of cells to form networks after switching from high glucose concentration to normal concentrations in the presence of metformin from cell plates that have been fixed.

In addition, *in vitro studies* can also be conducted to investigate the role of hyperglycaemia in the regulation of PlGF production in endothelial cells isolated from normal pregnancies and pregnancies complicated by maternal diabetes. A recent study has reported that, hyperglycaemia up-regulates placental growth factor (PlGF) expression and secretion in endothelial cells (HUVECs) via suppression of PI3 kinase-Akt signalling and activation of FOXO1[422]. Future studies can explore this investigations using isolated HPAECs from normal pregnancies and pregnancies complicated by pregestational diabetes in the presence of physiological/pathophysiological insulin and with metformin.

Bibliography

1. Virjee, S., S. Robinson, and D. Johnston, *Screening for diabetes in pregnancy.* Journal of the Royal Society of Medicine, 2001. **94**(10): p. 502-509.
2. WHO, *Global Report on Diabetes*, Publications, Editor. 2016, World Health Organization.
3. Federation, I.D., *IDF diabetes atlas.* Brussels: International Diabetes Federation, 2013.
4. Mathers, C.D. and D. Loncar, *Projections of global mortality and burden of disease from 2002 to 2030.* Plos med, 2006. **3**(11): p. e442.
5. Federation., I.D. *IDF Diabetes Atlas*. 2019; 9TH:[Available from: https://www.diabetesatlas.org/.
6. NICE, *Diabetes in pregnancy: Management of daibetes and its complications from pre-conception to the postnatal period National institute for health and care excellence,*. 2015.
7. Kulshrestha, V. and N. Agarwal, *Maternal complications in pregnancy with diabetes.* JPMA. The Journal of the Pakistan Medical Association, 2016. **66**(9 Suppl 1): p. S74.
8. Rubarth, L.B., *Infants of diabetic mothers.* Neonatal Network, 2013. **32**(6): p. 416-418.
9. Umesawa, M. and G. Kobashi, *Epidemiology of hypertensive disorders in pregnancy: prevalence, risk factors, predictors and prognosis.* Hypertension Research, 2016. **40(3)**: p. 213-220.
10. Khalak, R., J. Cummings, and S. Dexter, *Maternal obesity: significance on the preterm neonate.* International Journal of Obesity, 2015. **39**(10): p. 1433-1436.
11. Kate Fitzsimons, A.S., *Maternal obesity in the UK: Findings from a national project*, C.f.M.a.C.E. (CMACE). Editor. 2010, CMACE: London. p. 37-40.
12. Persson, M., M. Norman, and U. Hanson, *Obstetric and perinatal outcomes in type 1 diabetic pregnancies: a large, population-based study.* Diabetes care, 2009. **32**(11): p. 2005-2009.
13. Domanski, G., et al., *Evaluation of neonatal and maternal morbidity in mothers with gestational diabetes: a population-based study.* BMC Pregnancy and Childbirth, 2018. **18**(1): p. 367.
14. Persson, M., et al., *Association of Maternal Diabetes With Neonatal Outcomes of Very Preterm and Very Low-Birth-Weight Infants: An International Cohort Study.* JAMA pediatrics, 2018. **172**(9): p. 867-875.
15. Chen, L., et al., *Diabetes in pregnancy in associations with perinatal and postneonatal mortality in First Nations and non-Indigenous populations in Quebec, Canada: population-based linked birth cohort study.* BMJ Open, 2019. **9**(4): p. e025084.
16. Metcalfe, A., et al., *Trends in obstetric intervention and pregnancy outcomes of Canadian women with diabetes in pregnancy from 2004 to 2015.* Journal of the Endocrine Society, 2017. **1**(12): p. 1540-1549.
17. López-de-Andrés, A., et al., *A population-based study of diabetes during pregnancy in Spain (2009–2015): trends in incidence, obstetric interventions, and pregnancy outcomes.* Journal of clinical medicine, 2020. **9**(2): p. 582.
18. Hotu, S., et al., *Increasing prevalence of type 2 diabetes in adolescents.* Journal of

paediatrics and child health, 2004. **40**(4): p. 201-204.
19. Kitzmiller, J.L., et al., *Pre-conception care of diabetes, congenital malformations, and spontaneous abortions.* Diabetes care, 1996. **19**(5): p. 514-541.
20. Ozumba, B.C., S.N. Obi, and J.M. Oli, *Diabetes mellitus in pregnancy in an African population.* International Journal of Gynecology & Obstetrics, 2004. **84**(2): p. 114-119.
21. Randhawa, M.S., S. Moin, and F. Shoaib, *Diabetes mellitus during pregnancy: a study of fifty cases.* Pakistan Journal of Medical Sciences, 2003. **19**(4): p. 277-282.
22. Senanayake, M.P. and M.K.S. Gunawardene, *Neonatal morbidity following control of maternal diabetes with human insulin.* Sri Lanka Journal of Child Health, 2000. **29**: p. 11-14.
23. Kheir, A.E.M., et al., *Morbidity and mortality amongst infants of diabetic mothers admitted into Soba university hospital, Khartoum, Sudan.* Sudanese journal of paediatrics, 2012. **12**(1): p. 49-55.
24. Langer, O., et al., *Gestational diabetes: the consequences of not treating.* Am J Obstet Gynecol, 2005. **192**(4): p. 989-97.
25. Catalano, P.M. and S. Hauguel-De Mouzon, *Is it time to revisit the Pedersen hypothesis in the face of the obesity epidemic?* American journal of obstetrics and gynecology, 2011. **204**(6): p. 479-487.
26. Aman, J., et al., *Increased fat mass and cardiac septal hypertrophy in newborn infants of mothers with well-controlled diabetes during pregnancy.* Neonatology, 2011. **100**(2): p. 147-54.
27. Chen, D.b. and J. Zheng, *Regulation of placental angiogenesis.* Microcirculation, 2014. **21**(1): p. 15-25.
28. Osol, G. and M. Mandala, *Maternal uterine vascular remodeling during pregnancy.* Physiology, 2009. **24**(1): p. 58-71.
29. Ategbo, J.-M., et al., *Modulation of adipokines and cytokines in gestational diabetes and macrosomia.* The Journal of Clinical Endocrinology & Metabolism, 2006. **91**(10): p. 4137-4143.
30. Flamme, I., T. Frölich, and W. Risau, *Molecular mechanisms of vasculogenesis and embryonic angiogenesis.* Journal of cellular physiology, 1997. **173**(2): p. 206-210.
31. Heil, M., et al., *Arteriogenesis versus angiogenesis: similarities and differences.* J Cell Mol Med, 2006. **10**(1): p. 45-55.
32. Burton, G.J., D. Charnock-Jones, and E. Jauniaux, *Regulation of vascular growth and function in the human placenta.* Reproduction, 2009. **138**(6): p. 895-902.
33. Wang, Y. *Vascular biology of the placenta*. in *Colloquium Series on Integrated Systems Physiology: From Molecule to Function*. 2010. Morgan & Claypool Life Sciences.
34. Education, P., *Classification of Blood Vessel in Systemic Circulation.* 2017.
35. Tahergorabi, Z. and M. Khazaei, *Imbalance of Angiogenesis in Diabetic Complications: The Mechanisms.* International Journal of Preventive Medicine, 2012. **3**(12): p. 827-838.
36. Fadini, G.P., et al., *Angiogenic Abnormalities in Diabetes Mellitus: Mechanistic and Clinical Aspects.* J Clin Endocrinol Metab, 2019. **104**(11): p. 5431-5444.
37. Benirschke, K., G.J. Burton, and R.N. Baergen, *Early development of the human placenta*, in *Pathology of the human placenta*. 2012, Springer. p. 41-53.
38. Aplin, J., *Maternal influences on placental development.* Semin Cell Dev Biol, 2000. **11**(2): p. 115-25.
39. Benirschke, K., G.J. Burton, and R.N. Baergen, *Architecture of normal villous trees*,

in *Pathology of the human placenta*. 2012, Springer. p. 101-144.
40. Leach, L., A. Taylor, and F. Sciota, *Vascular dysfunction in the diabetic placenta: causes and consequences.* Journal of anatomy, 2009. **215**(1): p. 69-76.
41. Leach, L., *Placental vascular dysfunction in diabetic pregnancies: intimations of fetal cardiovascular disease?* Microcirculation, 2011. **18**(4): p. 263-269.
42. Jansson, N., et al., *Down-regulation of placental transport of amino acids precedes the development of intrauterine growth restriction in rats fed a low protein diet.* The Journal of physiology, 2006. **576**(3): p. 935-946.
43. Jauniaux, E. and G. Burton, *Villous histomorphometry and placental bed biopsy investigation in Type I diabetic pregnancies.* Placenta, 2006. **27**(4): p. 468-474.
44. Kaufmann, P., *Basic morphology of the fetal and maternal circuits in the human placenta*, in *In vitro perfusion of human placental tissue*. 1985, Karger Publishers. p. 5-17.
45. Leach, L., et al., *Vascular endothelial cadherin and β-catenin in human fetoplacental vessels of pregnancies complicated by Type 1 diabetes: associations with angiogenesis and perturbed barrier function.* Diabetologia, 2004. **47**(4): p. 695-709.
46. Mayhew, T., *Enhanced fetoplacental angiogenesis in pre-gestational diabetes mellitus: the extra growth is exclusively longitudinal and not accompanied by microvascular remodelling.* Diabetologia, 2002. **45**(10): p. 1434-1439.
47. Gupta, R.K. and R.C. Gupta, *Placental toxicity*, in *Reproductive and developmental toxicology*. 2022, Elsevier. p. 1373-1397.
48. Huppertz, B., *Human Placentation*, in *Encyclopedia of Reproduction (Second Edition)*, M.K. Skinner, Editor. 2018, Academic Press: Oxford. p. 431-439.
49. Stanisław, W., P. Artur, and K. Marcin, *Active and passive transport of drugs in the human placenta.* Ginekol Pol, 2009. **80**: p. 772-777.
50. Pacifici, G.M. and R. Nottoli, *Placental transfer of drugs administered to the mother.* Clinical pharmacokinetics, 1995. **28**(3): p. 235-269.
51. Gordon, Z., et al., *Anthropometry of fetal vasculature in the chorionic plate.* Journal of anatomy, 2007. **211**(6): p. 698-706.
52. Gordon, Z., et al., *Fetal blood flow in branching models of the chorionic arterial vasculature.* Annals of the New York Academy of Sciences, 2007. **1101**(1): p. 250-265.
53. Ullberg, U., B. Sandstedt, and G. Lingman, *Hyrtl's anastomosis, the only connection between the two umbilical arteries. A study in full term placentas from AGA infants with normal umbilical artery blood flow.* Acta obstetricia et gynecologica Scandinavica, 2001. **80**(1): p. 1-6.
54. Raio, L., et al., *In-utero characterization of the blood flow in the Hyrtl anastomosis.* Placenta, 2001. **22**(6): p. 597-601.
55. Benirschke, K., G.J. Burton, and R.N. Baergen, *Macroscopic features of the delivered placenta*, in *Pathology of the Human Placenta*. 2012, Springer. p. 13-15.
56. Ismail, K.I., et al., *Abnormal placental cord insertion and adverse pregnancy outcomes: a systematic review and meta-analysis.* Systematic Reviews, 2017. **6**(1): p. 242-254.
57. Fox, H., *Pathology of the placenta in maternal diabetes mellitus.* Obstetrics & Gynecology, 1969. **34**(6): p. 792-798.
58. Junaid, T.O., et al., *Whole organ vascular casting and microCT examination of the human placental vascular tree reveals novel alterations associated with pregnancy disease.* Scientific Reports, 2017. **7**(1): p. Article No. 4144.

59. Maly, A., et al., *Histomorphometric study of placental villi vascular volume in toxemia and diabetes.* Human pathology, 2005. **36**(10): p. 1074-1079.
60. Björk, O. and B. Persson, *Placental changes in relation to the degree of metabolic control in diabetes mellitus.* Placenta, 1982. **3**(4): p. 367-378.
61. Redline, R.W., *Distal villous immaturity.* Diagnostic Histopathology, 2012. **18**(5): p. 189-194.
62. Turowski, G. and M. Vogel, *Re-view and view on maturation disorders in the placenta.* APMIS, 2018. **126**(7): p. 602-612.
63. Jaiman, S., et al., *Disorders of placental villous maturation in fetal death.* Journal of Perinatal Medicine, 2020. **48**(4): p. 345-368.
64. Mukherjee, A., et al., *The Placental Distal Villous Hypoplasia Pattern: Interobserver Agreement and Automated Fractal Dimension as an Objective Metric.* Pediatr Dev Pathol, 2016. **19**(1): p. 31-6.
65. Redline, R.W., *Placental pathology: a systematic approach with clinical correlations.* Placenta, 2008. **29**: p. 86-91.
66. Evers, I., et al., *Placental pathology in women with type 1 diabetes and in a control group with normal and large-for-gestational-age infants.* Placenta, 2003. **24**(8): p. 819-825.
67. Dicke, J.M., *Placenta: chronicle of intrauterine growth restriction.* F1000 medicine reports, 2010. **2**: p. 69.
68. Tennant, P.W., et al., *Pre-existing diabetes, maternal glycated haemoglobin, and the risks of fetal and infant death: a population-based study.* Diabetologia, 2014. **57**(2): p. 285-294.
69. Higgins, M.F., et al., *Clinical and ultrasound features of placental maturation in pre-gestational diabetic pregnancy.* Early human development, 2012. **88**(10): p. 817-821.
70. Boyd, P.A., A. Scott, and J.W. Keeling, *Quantitative structural studies on placentas from pregnancies complicated by diabetes mellitus.* BJOG: An International Journal of Obstetrics & Gynaecology, 1986. **93**(1): p. 31-35.
71. Teasdale, F., *Histomorphometry of the human placenta in class B diabetes mellitus.* Placenta, 1983. **4**(1): p. 1-12.
72. Teasdale, F., *Histomorphometry of the human placenta in class C diabetes mellitus.* Placenta, 1985. **6**(1): p. 69-81.
73. Aherne, W. and M.S. Dunnill, *Quantitative aspects of placental structure.* The Journal of pathology and bacteriology, 1966. **91**(1): p. 123-139.
74. Aherne, W. and M. Dunnill, *Quantitative aspects of placental structure.* The Journal of pathology and bacteriology, 1966. **91**(1): p. 123-139.
75. Taricco, E., et al., *Foetal and placental weights in relation to maternal characteristics in gestational diabetes.* Placenta, 2003. **24**(4): p. 343-347.
76. Jirkovska, M., *Comparison of the thickness of the capillary basement membrane of the human placenta under normal conditions and in type 1 diabetes.* Functional and developmental morphology, 1990. **1**(3): p. 9-16.
77. Jirkovská, M., et al., *The branching pattern of villous capillaries and structural changes of placental terminal villi in type 1 diabetes mellitus.* Placenta, 2012. **33**(5): p. 343-351.
78. Teasdale, F., *Histomorphometry of the placenta of the diabetic woman: class A diabetes mellitus.* Placenta, 1981. **2**(3): p. 241-251.
79. Mayhew, T.M. and I.C. Jairam, *Stereological comparison of 3D spatial relationships involving villi and intervillous pores in human placentas from control and diabetic*

pregnancies. Journal of anatomy, 2000. **197**(02): p. 263-274.
80. Huynh, J., et al., *A systematic review of placental pathology in maternal diabetes mellitus.* Placenta, 2015. **36**(2): p. 101-114.
81. Björk, O. and B. Persson, *Villous structure in different parts of the cotyledon in placentas of insulin-dependent diabetic women: a morphometric study.* Acta obstetricia et gynecologica Scandinavica, 1984. **63**(1): p. 37-43.
82. Haeussner, E., et al., *Does 2D-Histologic identification of villous types of human placentas at birth enable sensitive and reliable interpretation of 3D structure?* Placenta, 2015. **36**(12): p. 1425-1432.
83. Junaid, T., et al., *Fetoplacental vascular alterations associated with fetal growth restriction.* Placenta, 2014. **35**(10): p. 808-815.
84. Mayhew, T.M., et al., *The effects of mode of delivery and sex of newborn on placental morphology in control and diabetic pregnancies.* Journal of anatomy, 1993. **183**(Pt 3): p. 545.
85. Nelson, S.M., et al., *Placental structure in type 1 diabetes: relation to fetal insulin, leptin, and IGF-I.* Diabetes, 2009. **58**(11): p. 2634-2641.
86. Lao, T., C.-P. Lee, and W.-M. Wong, *Placental weight to birthweight ratio is increased in mild gestational glucose intolerance.* Placenta, 1997. **18**(2): p. 227-230.
87. Ashfaq, M., M.Z. Janjua, and M.A. Channa, *Effect of gestational diabetes and maternal hypertension on gross morphology of placenta.* J Ayub Med Coll Abbottabad, 2005. **17**(1): p. 44-7.
88. Daskalakis, G., et al., *Placental pathology in women with gestational diabetes.* Acta obstetricia et gynecologica Scandinavica, 2008. **87**(4): p. 403-407.
89. Madazlı, R., et al., *The incidence of placental abnormalities, maternal and cord plasma malondialdehyde and vascular endothelial growth factor levels in women with gestational diabetes mellitus and nondiabetic controls.* Gynecologic and obstetric investigation, 2008. **65**(4): p. 227-232.
90. Asmussen, I., *Ultrastructure of the villi and fetal capillaries of the placentas delivered by nonsmoking diabetic women (White group D).* Acta Pathologica Microbiologica Scandinavica Series A: Pathology, 1982. **90**(1-6): p. 95-101.
91. Jirkovská, M., et al., *Topological properties and spatial organization of villous capillaries in normal and diabetic placentas.* J Vasc Res, 2002. **39**(3): p. 268-78.
92. Kingdom, J., et al., *Development of the placental villous tree and its consequences for fetal growth.* European Journal of Obstetrics & Gynecology and Reproductive Biology, 2000. **92**(1): p. 35-43.
93. Burton, G.J., D.S. Charnock-Jones, and E. Jauniaux, *Regulation of vascular growth and function in the human placenta.* Reproduction, 2009. **138**(6): p. 895-902.
94. Charnock-Jones, D., P. Kaufmann, and T. Mayhew, *Aspects of human fetoplacental vasculogenesis and angiogenesis. I. Molecular regulation.* Placenta, 2004. **25**(2-3): p. 103-113.
95. Zygmunt, M., et al., *Angiogenesis and vasculogenesis in pregnancy.* European Journal of Obstetrics & Gynecology and Reproductive Biology, 2003. **110**: p. S10-S18.
96. Aplin, J.D., et al., *Hemangioblastic foci in human first trimester placenta: distribution and gestational profile.* Placenta, 2015. **36**(10): p. 1069-1077.
97. Arroyo, J.A. and V.D. Winn. *Vasculogenesis and angiogenesis in the IUGR placenta*. in *Seminars in perinatology*. 2008. Elsevier.
98. Castellucci, M., et al., *The development of the human placental villous tree.*

Anatomy and embryology, 1990. **181**(2): p. 117-128.
99. Baron, M.H., *Embryonic origins of mammalian hematopoiesis.* Experimental hematology, 2003. **31**(12): p. 1160-1169.
100. Luckhardt, M., et al., *Effect of physiologic perfusion-fixation on the morphometrically evaluated dimensions of the term placental cotyledon.* The Journal of the Society for Gynecologic Investigation: JSGI, 1996. **3**(4): p. 166-171.
101. Baergen, R.N., *Chorionic Villi: Histology and Villous Development*, in *Manual of Pathology of the Human Placenta*. 2011, Springer. p. 69-83.
102. Pepper, M.S., et al., *Vascular endothelial growth-factor (VEGF) induces plasminogen activators and plasminogen-activator inhibitor-1 in microvascular endothelial-cells.* Biochemical and Biophysical Research Communications, 1991. **181**(2): p. 902-906.
103. Unemori, E.N., et al., *Vascular endothelial growth-factor induces interstitial collagenase expression in human endothelial-cells.* Journal of cellular physiology, 1992. **153**(3): p. 557-562.
104. Vuorela, P., et al., *Expression of vascular endothelial growth factor and placenta growth factor in human placenta.* Biol Reprod, 1997. **56**(2): p. 489-94.
105. Kalkunte, S.S., et al., *Vascular endothelial growth factor C facilitates immune tolerance and endovascular activity of human uterine NK cells at the maternal-fetal interface.* J Immunol, 2009. **182**(7): p. 4085-92.
106. Clark, D., et al., *Comparison of expression patterns for placenta growth factor, vascular endothelial growth factor (VEGF), VEGF-B and VEGF-C in the human placenta throughout gestation.* Journal of Endocrinology, 1998. **159**(3): p. 459-468.
107. Shams, M. and A. Ahmed, *Localization of mRNA for basic fibroblast growth factor in human placenta.* Growth Factors, 1994. **11**(2): p. 105-11.
108. Ferriani, R.A., et al., *Colocalization of acidic and basic fibroblast growth factor (FGF) in human placenta and the cellular effects of bFGF in trophoblast cell line JEG-3.* Growth factors, 1994. **10**(4): p. 259-268.
109. Usuki, K., et al., *Localization of platelet-derived endothelial cell growth factor in human placenta and purification of an alternatively processed form.* Cell Regul, 1990. **1**(8): p. 577-84.
110. Simpson, H., et al., *Transforming growth factor β expression in human placenta and placental bed during early pregnancy.* Placenta, 2002. **23**(1): p. 44-58.
111. Forbes, K., et al., *Transforming Growth Factor-β (TGFβ) Receptors I/II Differentially Regulate TGFβ1 and IGF-Binding Protein-3 Mitogenic Effects in the Human Placenta.* Endocrinology, 2010. **151**(4): p. 1723-1731.
112. Anteby, E.Y., et al., *Fibroblast growth factor-10 and fibroblast growth factor receptors 1–4: expression and peptide localization in human decidua and placenta.* European Journal of Obstetrics and Gynecology and Reproductive Biology, 2005. **119**(1): p. 27-35.
113. Baczyk, D., et al., *Bi-potential behaviour of cytotrophoblasts in first trimester chorionic villi.* Placenta, 2006. **27**(4-5): p. 367-374.
114. Kita, N., et al., *Expression and Activation of MAP Kinases, ERK1/2, in the Human Villous Trophoblasts.* Placenta, 2003. **24**(2): p. 164-172.
115. Xuan, Y.H., et al., *Expression of TGF-beta signaling proteins in normal placenta and gestational trophoblastic disease.* Histol Histopathol, 2007. **22**(3): p. 227-34.
116. Senger, D.R., et al., *Tumor cells secrete a vascular permeability factor that promotes accumulation of ascites fluid.* Science, 1983. **219**(4587): p. 983-985.
117. Maglione, D., et al., *Isolation of a human placenta cDNA coding for a protein*

related to the vascular permeability factor. Proceedings of the National Academy of Sciences of the United States of America, 1991. **88**(20): p. 9267-9271.
118. Achen, M.G., et al., *Placenta growth factor and vascular endothelial growth factor are co-expressed during early embryonic development.* Growth Factors, 1997. **15**(1): p. 69-80.
119. Wang Y, Z.S., *Angiogenic Factors*, in *Vascular Biology of the Placenta.* 2010, Morgan & Claypool Life Sciences;: San Rafael (CA). p. Chapter 7.
120. Carmeliet, P., et al., *Synergism between vascular endothelial growth factor and placental growth factor contributes to angiogenesis and plasma extravasation in pathological conditions.* Nature medicine, 2001. **7**(5): p. 575-583.
121. Benschop, L., et al., *Placental Growth Factor as an Indicator of Maternal Cardiovascular Risk After Pregnancy.* Circulation, 2019. **139**(14): p. 1698-1709.
122. Taylor, R.N., et al., *Longitudinal serum concentrations of placental growth factor: evidence for abnormal placental angiogenesis in pathologic pregnancies.* American journal of obstetrics and gynecology, 2003. **188**(1): p. 177-182.
123. Powers, R.W., et al., *Low placental growth factor across pregnancy identifies a subset of women with preterm preeclampsia: type 1 versus type 2 preeclampsia?* Hypertension, 2012. **60**(1): p. 239-246.
124. Chappell, L.C., et al., *Diagnostic accuracy of placental growth factor in women with suspected preeclampsia: a prospective multicenter study.* Circulation, 2013. **128**(19): p. 2121-2131.
125. Benton, S.J., et al., *Placental growth factor as a marker of fetal growth restriction caused by placental dysfunction.* Placenta, 2016. **42**: p. 1-8.
126. Nguyen, Q., et al., *Placental growth factor and its potential role in diabetic retinopathy and other ocular neovascular diseases.* Acta Ophthalmologica, 2016. **96**: p. e1-e9.
127. Shibuya, M., *Vascular endothelial growth factor (VEGF) and its receptor (VEGFR) signaling in angiogenesis: a crucial target for anti-and pro-angiogenic therapies.* Genes & cancer, 2011. **2**(12): p. 1097-1105.
128. Ferrara, N. and T. Davis-Smyth, *The biology of vascular endothelial growth factor.* Endocrine reviews, 1997. **18**(1): p. 4-25.
129. Cebe-Suarez, S., A. Zehnder-Fjällman, and K. Ballmer-Hofer, *The role of VEGF receptors in angiogenesis; complex partnerships.* Cellular and molecular life sciences, 2006. **63**(5): p. 601-615.
130. Ishida, A., et al., *Expression of vascular endothelial growth factor receptors in smooth muscle cells.* Journal of cellular physiology, 2001. **188**(3): p. 359-368.
131. Tischer, E., et al., *The human gene for vascular endothelial growth factor. Multiple protein forms are encoded through alternative exon splicing.* Journal of Biological Chemistry, 1991. **266**(18): p. 11947-11954.
132. Burgess, W.H. and T. Maciag, *The heparin-binding (fibroblast) growth factor family of proteins.* Annual review of biochemistry, 1989. **58**(1): p. 575-602.
133. Ornitz, D.M. and N. Itoh, *Fibroblast growth factors.* Genome biology, 2001. **2**(3): p. 1-12.
134. Hamai, Y., et al., *Evidence for basic fibroblast growth factor as a crucial angiogenic growth factor, released from human trophoblasts during early gestation.* Placenta, 1998. **19**(2-3): p. 149-155.
135. Davis, S., et al., *Isolation of angiopoietin-1, a ligand for the TIE2 receptor, by secretion-trap expression cloning.* Cell, 1996. **87**(7): p. 1161-1169.
136. Davis, S., et al., *Angiopoietins have distinct modular domains essential for receptor*

binding, dimerization and superclustering. Nature structural biology, 2003. **10**(1): p. 38-44.
137. Eklund, L. and B.R. Olsen, *Tie receptors and their angiopoietin ligands are context-dependent regulators of vascular remodeling.* Experimental cell research, 2006. **312**(5): p. 630-641.
138. Dunk, C., et al., *Angiopoietin-1 and angiopoietin-2 activate trophoblast Tie-2 to promote growth and migration during placental development.* The American journal of pathology, 2000. **156**(6): p. 2185-2199.
139. Myatt, L., *Role of placenta in preeclampsia.* Endocrine, 2002. **19**(1): p. 103-111.
140. Milner, C.S., et al., *Roles of the receptor tyrosine kinases Tie1 and Tie2 in mediating the effects of angiopoietin-1 on endothelial permeability and apoptosis.* Microvascular research, 2009. **77**(2): p. 187-191.
141. Holmes, K., et al., *Vascular endothelial growth factor receptor-2: structure, function, intracellular signalling and therapeutic inhibition.* Cellular signalling, 2007. **19**(10): p. 2003-2012.
142. Karkkainen, M.J. and T.V. Petrova, *Vascular endothelial growth factor receptors in the regulation of angiogenesis and lymphangiogenesis.* Oncogene, 2000. **19**(49): p. 5598-5605.
143. Ishikawa, F., et al., *Identification of angiogenic activity and the cloning and expression of platelet-derived endothelial cell growth factor.* Nature, 1989. **338**(6216): p. 557-562.
144. Hellberg, C., A. Östman, and C.H. Heldin, *PDGF and vessel maturation.* Angiogenesis inhibition, 2010: p. 103-114.
145. Bouïs, D., et al., *A review on pro-and anti-angiogenic factors as targets of clinical intervention.* Pharmacological Research, 2006. **53**(2): p. 89-103.
146. Bertolino, P., et al., *Transforming growth factor-β signal transduction in angiogenesis and vascular disorders.* Chest, 2005. **128**(6): p. 585S-590S.
147. Huang, S.S. and J.S. Huang, *TGF-β control of cell proliferation.* Journal of cellular biochemistry, 2005. **96**(3): p. 447-462.
148. Jones, R.L., et al., *TGF-β superfamily expression and actions in the endometrium and placenta.* Reproduction, 2006. **132**(2): p. 217-232.
149. Cvitic, S., G. Desoye, and U. Hiden, *Glucose, insulin, and oxygen interplay in placental hypervascularisation in diabetes mellitus.* BioMed research international, 2014. **2014**.
150. Huang, D., et al., *Macrovascular Complications in Patients with Diabetes and Prediabetes.* BioMed Research International, 2017. **2017**: p. 7839101.
151. Chawla, A., R. Chawla, and S. Jaggi, *Microvasular and macrovascular complications in diabetes mellitus: Distinct or continuum?* Indian journal of endocrinology and metabolism, 2016. **20**(4): p. 546-551.
152. Cade, W.T., *Diabetes-related microvascular and macrovascular diseases in the physical therapy setting.* Physical therapy, 2008. **88**(11): p. 1322-1335.
153. Crawford, T.N., et al., *Diabetic retinopathy and angiogenesis.* Current diabetes reviews, 2009. **5**(1): p. 8-13.
154. Houston, E.P.o.N., *Diabetic Retinopathy.* 2017.
155. Wirostko, B., T.Y. Wong, and R. Simó, *Vascular endothelial growth factor and diabetic complications.* Progress in Retinal and Eye Research, 2008. **27**(6): p. 608-621.
156. Aiello, L.P., et al., *Vascular endothelial growth factor in ocular fluid of patients with diabetic retinopathy and other retinal disorders.* New England Journal of Medicine,

1994. **331**(22): p. 1480-1487.
157. Bai, Y., et al., *Müller cell-derived VEGF is a significant contributor to retinal neovascularization.* The Journal of pathology, 2009. **219**(4): p. 446-454.
158. Wang, J., et al., *Müller Cell-Derived VEGF Is Essential for Diabetes-Induced Retinal Inflammation and Vascular Leakage.* Diabetes, 2010. **59**(9): p. 2297-2305.
159. Khaliq, A., et al., *Increased expression of placenta growth factor in proliferative diabetic retinopathy.* Laboratory investigation; a journal of technical methods and pathology, 1998. **78**(1): p. 109-116.
160. Nakagawa, T., et al., *Abnormal angiogenesis in diabetic nephropathy.* Diabetes, 2009. **58**(7): p. 1471-1478.
161. Min, W. and N. Yamanaka, *Three-dimensional analysis of increased vasculature around the glomerular vascular pole in diabetic nephropathy.* Virchows Archiv A, 1993. **423**(3): p. 201-207.
162. Nyengaard, J. and R. Rasch, *The impact of experimental diabetes mellitus in rats on glomerular capillary number and sizes.* Diabetologia, 1993. **36**(3): p. 189-194.
163. Gnudi, L., *Angiopoietins and diabetic nephropathy.* Diabetologia, 2016. **59**(8): p. 1616-1620.
164. Lygnos, M., et al., *Changes in maternal plasma levels of VEGF, bFGF, TGF-β1, ET-1 and sKL during uncomplicated pregnancy, hypertensive pregnancy and gestational diabetes.* In Vivo, 2006. **20**(1): p. 157-163.
165. Lassus, P., et al., *Vascular endothelial growth factor and angiogenin levels during fetal development and in maternal diabetes.* Neonatology, 2003. **84**(4): p. 287-292.
166. Hill, D., et al., *Fibroblast growth factor 2 is elevated in term maternal and cord serum and amniotic fluid in pregnancies complicated by diabetes: relationship to fetal and placental size.* The Journal of Clinical Endocrinology & Metabolism, 1995. **80**(9): p. 2626-2632.
167. Barton, W.A., et al., *Crystal structures of the Tie2 receptor ectodomain and the angiopoietin-2–Tie2 complex.* Nature structural & molecular biology, 2006. **13**(6): p. 524-532.
168. Lea, R., et al., *Placental leptin in normal, diabetic and fetal growth-retarded pregnancies.* Molecular human reproduction, 2000. **6**(8): p. 763-769.
169. Gelato, M., et al., *The serum insulin-like growth factor-II/mannose-6-phosphate receptor in normal and diabetic pregnancy.* Metabolism, 1993. **42**(8): p. 1031-1038.
170. Pietro, L., et al., *Vascular endothelial growth factor (VEGF) and VEGF-receptor expression in placenta of hyperglycemic pregnant women.* Placenta, 2010. **31**(9): p. 770-780.
171. Janota, J., et al., *Expression of angiopoietic factors in normal and type-I diabetes human placenta: a pilot study.* European Journal of Obstetrics & Gynecology and Reproductive Biology, 2003. **111**(2): p. 153-156.
172. Grissa, O., et al., *Growth factor concentrations and their placental mRNA expression are modulated in gestational diabetes mellitus: possible interactions with macrosomia.* BMC Pregnancy and Childbirth, 2010. **10**(1): p. Article No. 7.
173. Arany, E. and D. Hill, *Fibroblast growth factor-2 and fibroblast growth factor receptor-1 mRNA expression and peptide localization in placentae from normal and diabetic pregnancies.* Placenta, 1998. **19**(2-3): p. 133-142.
174. Di Blasio, A., et al., *Basic fibroblast growth factor messenger ribonucleic acid levels in human placentas from normal and pathological pregnancies.* Molecular human

reproduction, 1997. **3**(12): p. 1119-1123.
175. Burleigh, D., et al., *Influence of maternal diabetes on placental fibroblast growth factor-2 expression, proliferation, and apoptosis.* Journal of the Society for Gynecologic Investigation, 2004. **11**(1): p. 36-41.
176. Radaelli, T., et al., *Gestational diabetes induces placental genes for chronic stress and inflammatory pathways.* Diabetes, 2003. **52**(12): p. 2951-2958.
177. Shan, Z., et al., *Enhanced PDGF signaling in gestational diabetes mellitus is involved in pancreatic β-cell dysfunction.* Biochem Biophys Res Commun, 2019. **516**(2): p. 402-407.
178. Escobar, J., et al., *Amniotic fluid oxidative and nitrosative stress biomarkers correlate with fetal chronic hypoxia in diabetic pregnancies.* Neonatology, 2013. **103**(3): p. 193-198.
179. Teramo, K., et al., *High amniotic fluid erythropoietin levels are associated with an increased frequency of fetal and neonatal morbidity in type 1 diabetic pregnancies.* Diabetologia, 2004. **47**(10): p. 1695-1703.
180. Kleiblova, P., et al., *Expression of adipokines and estrogen receptors in adipose tissue and placenta of patients with gestational diabetes mellitus.* Molecular and cellular endocrinology, 2010. **314**(1): p. 150-156.
181. Moreli, J.B., et al., *Influence of maternal hyperglycemia on IL-10 and TNF-α production: the relationship with perinatal outcomes.* Journal of Clinical Immunology, 2012. **32**(3): p. 604-610.
182. Lapolla, A., et al., *Lymphocyte subsets and cytokines in women with gestational diabetes mellitus and their newborn.* Cytokine, 2005. **31**(4): p. 280-287.
183. Jahan, S., et al., *Influence of maternal diabetes on serum leptinemic and insulinemic status of the offspring: a case study of selected patients in a tertiary care hospital in Bangladesh.* Diabetes & Metabolic Syndrome: Clinical Research & Reviews, 2011. **5**(1): p. 33-37.
184. Persson, B., et al., *Leptin concentrations in cord blood in normal newborn infants and offspring of diabetic mothers.* Hormone and Metabolic Research, 1999. **31**(08): p. 467-471.
185. Vela-Huerta, M.M., et al., *Insulin and leptin levels in appropriate-for-gestational-age infants of diabetic mother.* Iranian journal of pediatrics, 2012. **22**(4): p. 475.
186. Westgate, J.A., et al., *Hyperinsulinemia in cord blood in mothers with type 2 diabetes and gestational diabetes mellitus in New Zealand.* Diabetes care, 2006. **29**(6): p. 1345-1350.
187. Lindsay, R.S., et al., *Inverse changes in fetal insulin-like growth factor (IGF)-1 and IGF binding protein-1 in association with higher birth weight in maternal diabetes.* Clinical endocrinology, 2007. **66**(3): p. 322-328.
188. Luo, Z.-C., et al., *Maternal and fetal IGF-I and IGF-II levels, fetal growth, and gestational diabetes.* The Journal of Clinical Endocrinology, 2012. **97**(5): p. 1720-1728.
189. LIU, Y.-J., et al., *Insulin-like growth factors (IGFs) and IGF-binding proteins (IGFBP-1,-2 and-3) in diabetic pregnancy: relationship to macrosomia.* Endocrine journal, 1996. **43**(2): p. 221-231.
190. Roth, S., et al., *Insulin-like growth factors I and II peptide and messenger RNA levels in macrosomic infants of diabetic pregnancies.* Journal of the Society for Gynecologic Investigation, 1996. **3**(2): p. 78-84.
191. Desoye, G., M. Gauster, and C. Wadsack, *Placental transport in pregnancy pathologies.* The American Journal of Clinical Nutrition, 2011. **94**(suppl_6): p.

1896S-1902S.
192. Gaccioli, F., et al., *Placental transport in response to altered maternal nutrition.* Journal of developmental origins of health and disease, 2013. **4**(2): p. 101-115.
193. Garner, P.R., et al., *Preeclampsia in diabetic pregnancies.* American journal of obstetrics and gynecology, 1990. **163**(2): p. 505-508.
194. Moore, T.R., *Fetal growth in diabetic pregnancy.* Clinical obstetrics and gynecology, 1997. **40**(4): p. 771-786.
195. Vambergue, A. and I. Fajardy, *Consequences of gestational and pregestational diabetes on placental function and birth weight.* World J Diabetes, 2011. **2**(11): p. 196-203.
196. Nylund, L., et al., *Uteroplacental blood flow in diabetic pregnancy: measurements with indium 113m and a computer-linked gamma camera.* Am J Obstet Gynecol, 1982. **144**(3): p. 298-302.
197. Kitzmiller, J.L., N. Watt, and S.G. Driscoll, *Decidual arteriopathy in hypertension and diabetes in pregnancy: immunofluorescent studies.* American journal of obstetrics and gynecology, 1981. **141**(7): p. 773-779.
198. Barth Jr, W.H., et al., *Uterine arcuate artery Doppler and decidual microvascular pathology in pregnancies complicated by type I diabetes mellitus.* Ultrasound in Obstetrics and Gynecology: The Official Journal of the International Society of Ultrasound in Obstetrics and Gynecology, 1996. **8**(2): p. 98-103.
199. Pietryga, M., et al., *Abnormal uterine Doppler is related to vasculopathy in pregestational diabetes mellitus.* Circulation, 2005. **112**(16): p. 2496-500.
200. Bennett, S.N., et al., *Assessing White's classification of pregestational diabetes in a contemporary diabetic population.* Obstet Gynecol, 2015. **125**(5): p. 1217-1223.
201. Gutaj, P. and E. Wender-Ozegowska, *Diagnosis and Management of IUGR in Pregnancy Complicated by Type 1 Diabetes Mellitus.* Current diabetes reports, 2016. **16**(5): p. 39-39.
202. Benirschke, K. and P. Kaufmann, *Nonvillous parts of the placenta*, in *Pathology of the human placenta*. 1995, Springer. p. 182-267.
203. Kami, K. and T. Mitsui, *Ultrastructural observations of chorionic villi at term in diabetic women.* The Tokai Journal of Experimental and Clinical Medicine, 1984. **9**(1): p. 53-67.
204. Pedersen, J., *The pregnant diabetic and her newborn: problems and management*. 1967: Williams & Wilkins Company.
205. Group, H.S.C.R., *The hyperglycemia and adverse pregnancy outcome (HAPO) study.* International Journal of Gynecology & Obstetrics, 2002. **78**(1): p. 69-77.
206. Inoguchi, T., et al., *Preferential elevation of protein kinase C isoform beta II and diacylglycerol levels in the aorta and heart of diabetic rats: differential reversibility to glycemic control by islet cell transplantation.* Proceedings of the National Academy of Sciences of the United States of America, 1992. **89**(22): p. 11059-11063.
207. Craven, P.A., C.M. Davidson, and F.R. DeRubertis, *Increase in Diacylglycerol Mass in Isolated Glomeruli by Glucose From De Novo Synthesis of Glycerolipids.* Diabetes, 1990. **39**(6): p. 667-674.
208. Shiba, T., et al., *Correlation of diacylglycerol level and protein kinase C activity in rat retina to retinal circulation.* American Journal of Physiology-Endocrinology and Metabolism, 1993. **265**(5): p. E783-E793.
209. Derubertis, F.R. and P.A. Craven, *Activation of Protein Kinase C in Glomerular Cells in Diabetes: Mechanisms and Potential Links to the Pathogenesis of Diabetic*

Glomerulopathy. Diabetes, 1994. **43**(1): p. 1-8.
210. Kelly, D.J., et al., *Effects on protein kinase C-β inhibition on glomerular vascular endothelial growth factor expression and endothelial cells in advanced experimental diabetic nephropathy.* American Journal of Physiology-Renal Physiology, 2007. **293**(2): p. F565-F574.
211. Xia, L., et al., *Reactive oxygen species, PKC-β1, and PKC-ζ mediate high-glucose-induced vascular endothelial growth factor expression in mesangial cells.* American Journal of Physiology-Endocrinology and Metabolism, 2007. **293**(5): p. E1280-E1288.
212. Desoye, G., H.H. Hofmann, and P.A. Weiss, *Insulin binding to trophoblast plasma membranes and placental glycogen content in well-controlled gestational diabetic women treated with diet or insulin, in well-controlled overt diabetic patients and in healthy control subjects.* Diabetologia, 1992. **35**(1): p. 45-55.
213. Ruiz-Palacios, M., et al., *Role of Insulin in Placental Transport of Nutrients in Gestational Diabetes Mellitus.* Annals of Nutrition and Metabolism, 2017. **70**(1): p. 16-25.
214. Tumminia, A., et al., *Maternal Diabetes Impairs Insulin and IGF-1 Receptor Expression and Signaling in Human Placenta.* Frontiers in Endocrinology, 2021. **12**.
215. Illsley, N.P., *Current topic: glucose transporters in the human placenta.* Placenta, 2000. **21**(1): p. 14-22.
216. Hauguel, S., V. Desmaizieres, and J.C. Challier, *Glucose uptake, utilization, and transfer by the human placenta as functions of maternal glucose concentration.* Pediatric research, 1986. **20**(3): p. 269-273.
217. Illsley, N.P. and M.U. Baumann, *Human placental glucose transport in fetoplacental growth and metabolism.* Biochimica et biophysica acta. Molecular basis of disease, 2020. **1866**(2): p. 165359-165359.
218. Jansson, T., E.A. Cowley, and N.P. Illsley, *Cellular localization of glucose transporter messenger RNA in human placenta.* Reproduction, fertility and development, 1995. **7**(6): p. 1425-1430.
219. Jansson, T., M. Wennergren, and N.P. Illsley, *Glucose transporter protein expression in human placenta throughout gestation and in intrauterine growth retardation.* The Journal of Clinical Endocrinology & Metabolism, 1993. **77**(6): p. 1554-1562.
220. Hauguel-de Mouzon, S., et al., *The GLUT3 glucose transporter isoform is differentially expressed within human placental cell types.* The Journal of Clinical Endocrinology & Metabolism, 1997. **82**(8): p. 2689-2694.
221. Xing, A.Y., et al., *Unexpected expression of glucose transporter 4 in villous stromal cells of human placenta.* The Journal of Clinical Endocrinology & Metabolism, 1998. **83**(11): p. 4097-4101.
222. Castillo-Castrejon, M. and T.L. Powell, *Placental nutrient transport in gestational diabetic pregnancies.* Frontiers in endocrinology, 2017. **8**: p. 306.
223. Hay, W.W., Jr., *Placental-fetal glucose exchange and fetal glucose metabolism.* Transactions of the American Clinical and Climatological Association, 2006. **117**: p. 321-340.
224. Acevedo, C.G., et al., *Insulin and nitric oxide stimulates glucose transport in human placenta.* Life sciences, 2005. **76**(23): p. 2643-2653.
225. Hahn, T., et al., *Hyperglycaemia-induced subcellular redistribution of GLUT1 glucose transporters in cultured human term placental trophoblast cells.* Diabetologia, 2000. **43**(2): p. 173-180.

226. Gordon, M.C., et al., *Insulin and glucose modulate glucose transporter messenger ribonucleic acid expression and glucose uptake in trophoblasts isolated from first-trimester chorionic villi.* American journal of obstetrics and gynecology, 1995. **173**(4): p. 1089-1097.
227. Ericsson, A., et al., *Hormonal regulation of glucose and system A amino acid transport in first trimester placental villous fragments.* American Journal of Physiology-Regulatory, Integrative and Comparative Physiology, 2005. **288**(3): p. R656-R662.
228. Evers, I., et al., *Macrosomia despite good glycaemic control in Type I diabetic pregnancy; results of a nationwide study in The Netherlands.* Diabetologia, 2002. **45**(11): p. 1484-1489.
229. Hiden, U., et al., *Insulin and the IGF system in the human placenta of normal and diabetic pregnancies.* Journal of anatomy, 2009. **215**(1): p. 60-68.
230. Poulaki, V., et al., *Acute intensive insulin therapy exacerbates diabetic blood-retinal barrier breakdown via hypoxia-inducible factor-1α and VEGF.* The Journal of clinical investigation, 2002. **109**(6): p. 805-815.
231. Lassance, L., et al., *Hyperinsulinemia stimulates angiogenesis of human fetoplacental endothelial cells: a possible role of insulin in placental hypervascularization in diabetes mellitus.* The Journal of Clinical Endocrinology & Metabolism, 2013. **98**(9): p. E1438-E1447.
232. Nicholl, I.D., et al., *Increased levels of advanced glycation endproducts in the lenses and blood vessels of cigarette smokers.* Molecular medicine, 1998. **4**(9): p. 594.
233. Goldin, A., et al., *Advanced glycation end products sparking the development of diabetic vascular injury.* Circulation, 2006. **114**(6): p. 597-605.
234. Waltenberger, J., J. Lange, and A. Kranz, *Vascular endothelial growth factor-A–induced chemotaxis of monocytes is attenuated in patients with diabetes mellitus: a potential predictor for the individual capacity to develop collaterals.* Circulation, 2000. **102**(2): p. 185-190.
235. Hernandez, T.L., *Glycemic targets in pregnancies affected by diabetes: historical perspective and future directions.* Current diabetes reports, 2015. **15**(1): p. 1-12.
236. Domingueti, C.P., et al., *Diabetes mellitus: The linkage between oxidative stress, inflammation, hypercoagulability and vascular complications.* Journal of Diabetes and its Complications, 2016. **30**(4): p. 738-745.
237. Coughlan, M., et al., *Altered placental oxidative stress status in gestational diabetes mellitus.* Placenta, 2004. **25**(1): p. 78-84.
238. Kim, Y.-W. and T.V. Byzova, *Oxidative stress in angiogenesis and vascular disease.* Blood, 2014. **123**(5): p. 625-631.
239. Sallam, N.A., et al., *Programming of Vascular Dysfunction in the Intrauterine Milieu of Diabetic Pregnancies.* International Journal of Molecular Sciences, 2018. **19**(11): p. 3665.
240. Kinalski, M., et al., *Lipid peroxidation, antioxidant defence and acid-base status in cord blood at birth: the influence of diabetes.* Hormone and Metabolic Research, 2001. **33**(04): p. 227-231.
241. Biri, A., et al., *Oxidant status in maternal and cord plasma and placental tissue in gestational diabetes.* Placenta, 2006. **27**(2-3): p. 327-332.
242. Gui, J., et al., *Vitamin D rescues dysfunction of fetal endothelial colony forming cells from individuals with gestational diabetes.* Placenta, 2015. **36**(4): p. 410-418.
243. Patel, H., et al., *Hyperglycemia induces differential change in oxidative stress at gene expression and functional levels in HUVEC and HMVEC.* Cardiovascular

diabetology, 2013. **12**(1): p. 1-14.
244. Jebur, A.B., M.H. Mokhamer, and F.M. El-Demerdash, *A review on oxidative stress and role of antioxidants in diabetes mellitus.* Austin Endocrinol Diabetes Case Rep, 2016. **1**(1): p. 1006-1011.
245. Lappas, M., et al., *The role of oxidative stress in the pathophysiology of gestational diabetes mellitus.* Antioxidants & redox signaling, 2011. **15**(12): p. 3061-3100.
246. Karin, M., T. Lawrence, and V. Nizet, *Innate Immunity Gone Awry: Linking Microbial Infections to Chronic Inflammation and Cancer.* Cell, 2006. **124**(4): p. 823-835.
247. Martin, P., *Wound Healing--Aiming for Perfect Skin Regeneration.* Science, 1997. **276**(5309): p. 75-81.
248. Martin, A., M.R. Komada, and D.C. Sane, *Abnormal angiogenesis in diabetes mellitus.* Medicinal research reviews, 2003. **23**(2): p. 117-145.
249. Di Tomo, P., et al., *Liraglutide mitigates TNF-α induced pro-atherogenic changes and microvesicle release in HUVEC from diabetic women.* Diabetes/Metabolism Research and Reviews, 2017. **33**(8): p. e2925.
250. Piconi, L., et al., *Intermittent high glucose enhances ICAM-1, VCAM-1, E-selectin and interleukin-6 expression in human umbilical endothelial cells in culture: the role of poly (ADP-ribose) polymerase.* Journal of Thrombosis and Haemostasis, 2004. **2**(8): p. 1453-1459.
251. Association, A.D., *2. Classification and diagnosis of diabetes: standards of medical care in diabetes—2018.* Diabetes Care, 2018. **41**(Supplement 1): p. S13-S27.
252. Shoelson, S.E., L. Herrero, and A. Naaz, *Obesity, inflammation, and insulin resistance.* Gastroenterology, 2007. **132**(6): p. 2169-2180.
253. Challis, J.R., et al., *Inflammation and pregnancy.* Reproductive sciences, 2009. **16**(2): p. 206-215.
254. Nuamah, M.A., et al., *Significant increase in maternal plasma leptin concentration in induced delivery: a possible contribution of pro-inflammatory cytokines to placental leptin secretion.* Endocrine journal, 2004. **51**(2): p. 177-187.
255. Al-Okail, M.S. and O.S. Al-Attas, *Histological changes in placental syncytiotrophoblasts of poorly controlled gestational diabetic patients.* Endocrine journal, 1994. **41**(4): p. 355-360.
256. Ericsson, A., et al., *Brief hyperglycaemia in the early pregnant rat increases fetal weight at term by stimulating placental growth and affecting placental nutrient transport.* The Journal of physiology, 2007. **581**(3): p. 1323-1332.
257. Robinson, J., et al., *Maternal diabetes in rats: I. Effects on placental growth and protein turnover.* Diabetes, 1988. **37**(12): p. 1665-1670.
258. Siddiqi, T., et al., *Biphasic intrauterine growth in insulin-dependent diabetic pregnancies.* Journal of the American College of Nutrition, 1989. **8**(3): p. 225-234.
259. Brown, J., et al., *Insulin for the treatment of women with gestational diabetes.* Cochrane Database of Systematic Reviews, 2017(11).
260. Briggs, G.G., R.K. Freeman, and S.J. Yaffe, *Drugs in pregnancy and lactation: a reference guide to fetal and neonatal risk*. 2012: Lippincott Williams & Wilkins.
261. Taylor, C., et al., *Implementation of guidelines for multidisciplinary team management of pregnancy in women with pre-existing diabetes or cardiac conditions: results from a UK national survey.* BMC pregnancy and childbirth, 2017. **17**(1): p. 1-9.
262. Simmons, D., *Safety considerations with pharmacological treatment of gestational diabetes mellitus.* Drug safety, 2015. **38**(1): p. 65-78.

263. Kolluru, G.K., S.C. Bir, and C.G. Kevil, *Endothelial Dysfunction and Diabetes: Effects on Angiogenesis, Vascular Remodeling, and Wound Healing.* International Journal of Vascular Medicine, 2012. **2012**: p. 918267.
264. Kelley, K.W., D.G. Carroll, and A. Meyer, *A review of current treatment strategies for gestational diabetes mellitus.* Drugs in context, 2015. **4**: p. 212282-212282.
265. Rowan, J.A., et al., *Metformin versus insulin for the treatment of gestational diabetes.* New England Journal of Medicine, 2008. **358**(19): p. 2003-2015.
266. Hellmuth, E., P. Damm, and L. Mølsted-Pedersen, *Oral hypoglycaemic agents in 118 diabetic pregnancies.* Diabetic Medicine, 2000. **17**(7): p. 507-511.
267. Mather, K.J., S. Verma, and T.J. Anderson, *Improved endothelial function with metformin in type 2 diabetes mellitus.* Journal of the American College of Cardiology, 2001. **37**(5): p. 1344-1350.
268. De Jager, J., et al., *Effects of short-term treatment with metformin on markers of endothelial function and inflammatory activity in type 2 diabetes mellitus: a randomized, placebo-controlled trial.* Journal of internal medicine, 2005. **257**(1): p. 100-109.
269. De Aguiar, L.G.K., et al., *Metformin improves endothelial vascular reactivity in first-degree relatives of type 2 diabetic patients with metabolic syndrome and normal glucose tolerance.* Diabetes care, 2006. **29**(5): p. 1083-1089.
270. Natali, A., et al., *Vascular effects of improving metabolic control with metformin or rosiglitazone in type 2 diabetes.* Diabetes care, 2004. **27**(6): p. 1349-1357.
271. Turner, R.C., et al., *Glycemic control with diet, sulfonylurea, metformin, or insulin in patients with type 2 diabetes mellitus: progressive requirement for multiple therapies (UKPDS 49).* Jama, 1999. **281**(21): p. 2005-2012.
272. Polasek, T.M., M.P. Doogue, and T.R.J. Thynne, *Metformin treatment of type 2 diabetes mellitus in pregnancy: update on safety and efficacy.* Therapeutic advances in drug safety, 2018. **9**(6): p. 287-295.
273. Ren, Y. and H. Luo, *Metformin: The next angiogenesis panacea?* SAGE Open Med, 2021. **9**: p. 20503121211001641.
274. Demir, R., Y. Seval, and B. Huppertz, *Vasculogenesis and angiogenesis in the early human placenta.* Acta histochemica, 2007. **109**(4): p. 257-265.
275. Fowler, M., *Microvascular and Macrovascular Complications of Diabetes.* Clinical Diabetes, 2008. **26**: p. 77-82.
276. Kota, S.K., et al., *Aberrant angiogenesis: The gateway to diabetic complications.* Indian journal of endocrinology and metabolism, 2012. **16**(6): p. 918-930.
277. Nguyen, L., S.-Y. Chan, and A.K.K. Teo, *Metformin from mother to unborn child – Are there unwarranted effects?* EBioMedicine, 2018. **35**: p. 394-404.
278. Butalia, S., et al., *Short-and long-term outcomes of metformin compared with insulin alone in pregnancy: a systematic review and meta-analysis.* Diabetic Medicine, 2017. **34**(1): p. 27-36.
279. Vitoratos, N., et al., *Perinatal mortality in diabetic pregnancy.* Ann N Y Acad Sci, 2010. **1205**: p. 94-8.
280. Leiser, R., et al., *Placental vascular corrosion cast studies: a comparison between ruminants and humans.* Microscopy research and technique, 1997. **38**(1-2): p. 76-87.
281. Gordon, Z., et al., *Hemodynamic analysis of Hyrtl anastomosis in human placenta.* American Journal of Physiology-Regulatory, Integrative and Comparative Physiology, 2007. **292**(2): p. R977-R982.
282. Folkman, J. and C. Haudenschild, *Angiogenesis in vitro.* Nature, 1980. **288**(5791): p.

551-556.
283. Brown, K.J., et al., *A novel in vitro assay for human angiogenesis.* Laboratory investigation; a journal of technical methods and pathology, 1996. **75**(4): p. 539-555.
284. Hippenstiel, S., et al., *VEGF induces hyperpermeability by a direct action on endothelial cells.* American Journal of Physiology-Lung Cellular and Molecular Physiology, 1998. **274**(5): p. L678-L684.
285. Galazios, G., et al., *Umbilical cord serum vascular endothelial growth factor (VEGF) levels in normal pregnancies and in pregnancies complicated by preterm delivery or pre-eclampsia.* International Journal of Gynecology & Obstetrics, 2004. **85**(1): p. 6-11.
286. Kuchroo, P., et al., *Paracrine factors secreted by umbilical cord-derived mesenchymal stem cells induce angiogenesis in vitro by a VEGF-independent pathway.* Stem cells and development, 2015. **24**(4): p. 437-450.
287. Brownbill, P., et al., *Vasoactive and permeability effects of vascular endothelial growth factor-165 in the term in vitro dually perfused human placental lobule.* Endocrinology, 2007. **148**(10): p. 4734-4744.
288. Delbaere, I., et al., *Should we adjust for gestational age when analysing birth weights? The use of z-scores revisited.* Human Reproduction, 2007. **22**(8): p. 2080-2083.
289. Kiserud, T., et al., *The World Health Organization fetal growth charts: a multinational longitudinal study of ultrasound biometric measurements and estimated fetal weight.* PLoS medicine, 2017. **14**(1): p. e1002220.
290. Duhig, K.E., et al., *Placental growth factor testing to assess women with suspected pre-eclampsia: a multicentre, pragmatic, stepped-wedge cluster-randomised controlled trial.* The Lancet, 2019. **393**(10183): p. 1807-1818.
291. Aharinejad, S.H. and A. Lametschwandtner, *Microvascular corrosion casting in scanning electron microscopy: techniques and applications*. 2012: Springer Science & Business Media.
292. Mayhew, T., *Fetoplacental angiogenesis in diabetes mellitus.* Placenta, 2012. **33**(7): p. 589.
293. Aharinejad, S.H. and A. Lametschwandtner, *Corrosion Casting—A Historical Review*, in *Microvascular Corrosion Casting in Scanning Electron Microscopy*. 1992, Springer. p. 3-11.
294. Konerding, M.A., *Scanning electron microscopy of corrosion casting in medicine.* Scanning microscopy, 1991. **5**(3): p. 25.
295. Hossler, F.E. and J.E. Douglas, *Vascular corrosion casting: review of advantages and limitations in the application of some simple quantitative methods.* Microscopy and microanalysis, 2001. **7**(3): p. 253-264.
296. Khimmaktong, W., et al., *Study of curcumin on microvasculature characteristic in diabetic rat's liver as revealed by vascular corrosion cast/scanning electron microscope (SEM) technique.* Journal of the Medical Association of Thailand = Chotmaihet thangphaet, 2012. **95 Suppl 5**: p. S133-41.
297. Amemiya, T. and I.A. Bhutto, *Retinal vascular changes and systemic diseases: corrosion cast demonstration.* Ital J Anat Embryol, 2001. **106**(2 Suppl 1): p. 237-44.
298. Bhutto, I.A., et al., *Retinal and Choroidal Vasculature in Rats with Spontaneous Diabetes Type 2 Treated with the Angiotensin-Converting Enzyme Inhibitor Cilazapril: Corrosion Cast and Electron-Microscopic Study.* Ophthalmic Research, 2002. **34**(4): p. 220-231.

299. Sangiorgi, S., et al., *The cutaneous microvascular architecture of human diabetic toe studied by corrosion casting and scanning electron microscopy analysis.* Anat Rec (Hoboken), 2010. **293**(10): p. 1639-45.
300. Yin, G., et al., *Vascular corrosion casting of normal and pre-eclamptic placentas.* Exp Ther Med, 2017. **14**(6): p. 5535-5539.
301. Peker, T., et al., *Three-dimensional assessment of the morphology of the umbilical artery in normal and pre-eclamptic placentas.* Journal of Obstetrics and Gynaecology Research, 2006. **32**(5): p. 468-474.
302. Robertson, W.B., et al., *The placental bed biopsy: review from three European centers.* American journal of obstetrics and gynecology, 1986. **155**(2): p. 401-412.
303. Kaaja, R., et al., *Serum lipoproteins, insulin, and urinary prostanoid metabolites in normal and hypertensive pregnant women.* Obstetrics & gynecology, 1995. **85**(3): p. 353-356.
304. Abundis, E.M., et al., *Hyperinsulinemia in glucose-tolerant women with preeclampsia A controlled study.* American journal of hypertension, 1996. **9**(6): p. 610-614.
305. Lorentzen, B., et al., *Glucose intolerance in women with preeclampsia.* Acta obstetricia et gynecologica Scandinavica, 1998. **77**(1): p. 22-27.
306. Innes, K. and J. Wimsatt, *Pregnancy-induced hypertension and insulin resistance, evidence for a connection.* Acta obstetricia et gynecologica Scandinavica, 1999. **78**(4): p. 263-284.
307. Villar, J., et al., *Methodological and technical issues related to the diagnosis, screening, prevention, and treatment of pre-eclampsia and eclampsia.* International Journal of Gynecology & Obstetrics, 2004. **85**: p. S28-S41.
308. American College of, O. and Gynecologists, *Diagnosis and management of preeclampsia and eclampsia.* Obstet. Gynecol., 2002. **99**: p. 159-167.
309. Roberts, J.M. and K.Y. Lain, *Recent insights into the pathogenesis of pre-eclampsia.* Placenta, 2002. **23**(5): p. 359-372.
310. Mirbod, P., *Analytical model of the feto-placental vascular system: consideration of placental oxygen transport.* Royal Society open science, 2018. **5**(4): p. 180219.
311. Desoye, G. and J.C.K. Wells, *Pregnancies in Diabetes and Obesity: The Capacity-Load Model of Placental Adaptation.* Diabetes, 2021. **70**(4): p. 823.
312. Nuzzo, A.M., et al., *Placental and maternal sFlt1/PlGF expression in gestational diabetes mellitus.* Scientific Reports, 2021. **11**(1): p. 2312.
313. Leahy, M., et al., *Functional imaging for regenerative medicine.* Stem cell research & therapy, 2016. **7**(1): p. 1-13.
314. Haeussner, E., et al., *Novel 3D light microscopic analysis of IUGR placentas points to a morphological correlate of compensated ischemic placental disease in humans.* Scientific reports, 2016. **6**(1): p. 1-11.
315. Kleinsmith, L.J., et al., *Understanding Angiogenesis.* National Cancer Institute, http://cancer. gov/cancertopics/understandingcancer/angiogenesis, 2010.
316. Umapathy, A., L.W. Chamley, and J.L. James, *Reconciling the distinct roles of angiogenic/anti-angiogenic factors in the placenta and maternal circulation of normal and pathological pregnancies.* Angiogenesis, 2020. **23**(2): p. 105-117.
317. Yang, Z., et al., *Critical effect of VEGF in the process of endothelial cell apoptosis induced by high glucose.* Apoptosis, 2008. **13**(11): p. 1331-1343.
318. Song, F., et al., *High glucose and AGEs inhibit tube formation of vascular endothelial cells by sustained Ang-2 production.* INTERNATIONAL JOURNAL OF CLINICAL AND EXPERIMENTAL PATHOLOGY, 2017. **10**(3): p. 3786-3793.

319. Quagliaro, L., et al., *Intermittent high glucose enhances apoptosis related to oxidative stress in human umbilical vein endothelial cells: the role of protein kinase C and NAD (P) H-oxidase activation.* Diabetes, 2003. **52**(11): p. 2795-2804.
320. Chang, C.-M., et al., *Acute and chronic fluctuations in blood glucose levels can increase oxidative stress in type 2 diabetes mellitus.* Acta diabetologica, 2012. **49**(1): p. 171-177.
321. Hayashi, J.N., et al., *Effects of glucose on migration, proliferation and tube formation by vascular endothelial cells.* Virchows Archiv B, 1991. **60**(1): p. 245-252.
322. Dalfrà, M.G., et al., *Glucose Fluctuations during Gestation: An Additional Tool for Monitoring Pregnancy Complicated by Diabetes.* International Journal of Endocrinology, 2013. **2013**: p. 279021.
323. Ceriello, A. and M.A. Ihnat, *'Glycaemic variability': a new therapeutic challenge in diabetes and the critical care setting.* Diabet Med, 2010. **27**(8): p. 862-7.
324. Desoye, G. and E. Shafrir, *The human placenta in diabetic pregnancy.* Diabetes reviews, 1996. **4**(1): p. 70-89.
325. Reece, E.A., D.R. Coustan, and S.G. Gabbe, *Diabetes in women: adolescence, pregnancy, and menopause*. 2004: Lippincott Williams & Wilkins.
326. Desoye, G., E. Shafrir, and S. Hauguel-de Mouzon, *Textbook of Diabetes and Pregnancy.* The placenta in diabetic pregnancy, 2003.
327. Desoye, G. and S. Hauguel-de Mouzon, *The human placenta in gestational diabetes mellitus. The insulin and cytokine network.* Diabetes Care, 2007. **30 Suppl 2**: p. S120-6.
328. Pereira, R.D., et al., *Angiogenesis in the Placenta: The Role of Reactive Oxygen Species Signaling.* BioMed Research International, 2015. **2015**: p. 814543.
329. Westgate, J.A., et al., *Hyperinsulinemia in cord blood in mothers with type 2 diabetes and gestational diabetes mellitus in New Zealand.* Diabetes Care, 2006. **29**(6): p. 1345-50.
330. Treins, C., et al., *Insulin stimulates hypoxia-inducible factor 1 through a phosphatidylinositol 3-kinase/target of rapamycin-dependent signaling pathway.* J Biol Chem, 2002. **277**(31): p. 27975-81.
331. Sivalingam, V., et al., *Metformin in reproductive health, pregnancy and gynaecological cancer: established and emerging indications.* Human reproduction update, 2014. **20 6**: p. 853-68.
332. Gui, J., Q. Liu, and L. Feng, *Metformin vs insulin in the management of gestational diabetes: a meta-analysis.* PloS one, 2013. **8**(5): p. e64585.
333. Kajbaf, F., M.E. De Broe, and J.-D. Lalau, *Therapeutic concentrations of metformin: a systematic review.* Clinical pharmacokinetics, 2016. **55**(4): p. 439-459.
334. Orecchioni, S., et al., *The biguanides metformin and phenformin inhibit angiogenesis, local and metastatic growth of breast cancer by targeting both neoplastic and microenvironment cells.* International journal of cancer, 2015. **136**(6): p. E534-E544.
335. Moschetta, M.G., et al., *Evaluation of angiogenesis process after metformin and LY294002 treatment in mammary tumor.* Anti-Cancer Agents in Medicinal Chemistry (Formerly Current Medicinal Chemistry-Anti-Cancer Agents), 2019. **19**(5): p. 655-666.
336. Wang, J.-C., et al., *Metformin inhibits metastatic breast cancer progression and improves chemosensitivity by inducing vessel normalization via PDGF-B downregulation.* Journal of Experimental & Clinical Cancer Research, 2019. **38**(1): p. 1-17.

337. Sun, C.C., et al., *Metformin ameliorates gestational diabetes mellitus-induced endothelial dysfunction via downregulation of p65 and upregulation of Nrf2.* Frontiers in pharmacology, 2020. **11**.
338. Ying, Y., et al., *Metformin inhibits ALK1-mediated angiogenesis via activation of AMPK.* Oncotarget, 2017. **8**(20): p. 32794.
339. Dallaglio, K., et al., *Paradoxic effects of metformin on endothelial cells and angiogenesis.* Carcinogenesis, 2014. **35**(5): p. 1055-1066.
340. Zhang, C.-S., et al., *Fructose-1, 6-bisphosphate and aldolase mediate glucose sensing by AMPK.* Nature, 2017. **548**(7665): p. 112-116.
341. He, L. and F.E. Wondisford, *Metformin action: concentrations matter.* Cell metabolism, 2015. **21**(2): p. 159-162.
342. Mills, J.L., et al., *Physiological reduction in fasting plasma glucose concentration in the first trimester of normal pregnancy: the diabetes in early pregnancy study.* Metabolism, 1998. **47**(9): p. 1140-4.
343. Ciechanowska, A., et al., *Effect of glucose concentration and culture substrate on HUVECs viability in in vitro cultures: A literature review and own results.* Biocybernetics and Biomedical Engineering, 2021.
344. Risso, A., et al., *Intermittent high glucose enhances apoptosis in human umbilical vein endothelial cells in culture.* American Journal of Physiology-Endocrinology and Metabolism, 2001. **281**(5): p. E924-E930.
345. Piconi, L., et al., *Constant and intermittent high glucose enhances endothelial cell apoptosis through mitochondrial superoxide overproduction.* Diabetes/metabolism research and reviews, 2006. **22**(3): p. 198-203.
346. Kuricová, K., et al., *Effect of glucose variability on pathways associated with glucotoxicity in diabetes: Evaluation of a novel in vitro experimental approach.* Diabetes research and clinical practice, 2016. **114**: p. 1-8.
347. Yu, W., et al., *A Review of Research Progress on Glycemic Variability and Gestational Diabetes.* Diabetes, metabolic syndrome and obesity : targets and therapy, 2020. **13**: p. 2729-2741.
348. De Nigris, V., et al., *Short-term high glucose exposure impairs insulin signaling in endothelial cells.* Cardiovascular diabetology, 2015. **14**(1): p. 1-7.
349. Montesano, R., L. Orci, and P. Vassalli, *In vitro rapid organization of endothelial cells into capillary-like networks is promoted by collagen matrices.* The Journal of cell biology, 1983. **97**(5): p. 1648-1652.
350. Goodwin, A.M., *In vitro assays of angiogenesis for assessment of angiogenic and anti-angiogenic agents.* Microvascular research, 2007. **74**(2-3): p. 172-183.
351. Arnaoutova, I., et al., *The endothelial cell tube formation assay on basement membrane turns 20: state of the science and the art.* Angiogenesis, 2009. **12**(3): p. 267-274.
352. Bisht, M., D.C. Dhasmana, and S.S. Bist, *Angiogenesis: Future of pharmacological modulation.* Indian journal of pharmacology, 2010. **42**(1): p. 2-8.
353. Staton, C.A., M.W.R. Reed, and N.J. Brown, *A critical analysis of current in vitro and in vivo angiogenesis assays.* International Journal of Experimental Pathology, 2009. **90**(3): p. 195-221.
354. Takahashi, H., et al., *Visualizing dynamics of angiogenic sprouting from a three-dimensional microvasculature model using stage-top optical coherence tomography.* Scientific Reports, 2017. **7**(1): p. 42426.
355. Andrée, B., et al., *Formation of three-dimensional tubular endothelial cell networks under defined serum-free cell culture conditions in human collagen hydrogels.*

Scientific Reports, 2019. **9**(1): p. 5437.
356. Carpentier, G., et al., *Angiogenesis Analyzer for ImageJ — A comparative morphometric analysis of "Endothelial Tube Formation Assay" and "Fibrin Bead Assay".* Scientific Reports, 2020. **10**(1): p. 11568.
357. Carpentier, G., *Contribution: angiogenesis analyzer.* ImageJ News, 2012. **5**: p. 2012.
358. Zheng, Y., et al., *In vitro microvessels for the study of angiogenesis and thrombosis.* Proceedings of the National Academy of Sciences of the United States of America, 2012. **109**(24): p. 9342-9347.
359. DeCicco-Skinner, K.L., et al., *Endothelial cell tube formation assay for the in vitro study of angiogenesis.* Journal of visualized experiments : JoVE, 2014(91): p. e51312-e51312.
360. Korn, C. and H.G. Augustin, *Born to Die.* Circulation, 2012. **125**(25): p. 3063-3065.
361. Lorenzi, M., E. Cagliero, and S. Toledo, *Glucose toxicity for human endothelial cells in culture: delayed replication, disturbed cell cycle, and accelerated death.* Diabetes, 1985. **34**(7): p. 621-627.
362. Lorenzi, M., et al., *High glucose induces DNA damage in cultured human endothelial cells.* The Journal of clinical investigation, 1986. **77**(1): p. 322-325.
363. Peng, H.-Y., H.-P. Li, and M.-Q. Li, *High glucose induces dysfunction of human umbilical vein endothelial cells by upregulating miR-137 in gestational diabetes mellitus.* Microvascular research, 2018. **118**: p. 90-100.
364. Du, X.L., et al., *Induction of apoptosis by high proinsulin and glucose in cultured human umbilical vein endothelial cells is mediated by reactive oxygen species.* Diabetologia, 1998. **41**(3): p. 249-256.
365. Ho, F.M., et al., *High glucose–induced apoptosis in human endothelial cells is mediated by sequential activations of c-Jun NH2-terminal kinase and caspase-3.* Circulation, 2000. **101**(22): p. 2618-2624.
366. Ido, Y., D. Carling, and N. Ruderman, *Hyperglycemia-induced apoptosis in human umbilical vein endothelial cells: inhibition by the AMP-activated protein kinase activation.* Diabetes, 2002. **51**(1): p. 159-167.
367. Ho, F.M., et al., *High glucose-induced apoptosis in human vascular endothelial cells is mediated through NF-κB and c-Jun NH2-terminal kinase pathway and prevented by PI3K/Akt/eNOS pathway.* Cellular signalling, 2006. **18**(3): p. 391-399.
368. Sheu, M.L., et al., *High glucose induces human endothelial cell apoptosis through a phosphoinositide 3-kinase–regulated cyclooxygenase-2 pathway.* Arteriosclerosis, thrombosis, and vascular biology, 2005. **25**(3): p. 539-545.
369. Zhao, X.-Y., et al., *Effects of high glucose on human umbilical vein endothelial cell permeability and myosin light chain phosphorylation.* Diabetology & metabolic syndrome, 2015. **7**(1): p. 1-5.
370. Zhang, J., et al., *High glucose induces apoptosis of HUVECs in a mitochondria-dependent manner by suppressing hexokinase 2 expression.* Experimental and therapeutic medicine, 2019. **18**(1): p. 621-629.
371. Alvarado-Vásquez, N., et al., *HUVECs from newborns with a strong family history of diabetes show diminished ROS synthesis in the presence of high glucose concentrations.* Diabetes/metabolism research and reviews, 2007. **23**(1): p. 71-80.
372. González, M., et al., *Insulin Reverses D-Glucose–Increased Nitric Oxide and Reactive Oxygen Species Generation in Human Umbilical Vein Endothelial Cells.* PLOS ONE, 2015. **10**(4): p. e0122398.
373. Han, X., et al., *Metformin Modulates High Glucose-Incubated Human Umbilical*

Vein Endothelial Cells Proliferation and Apoptosis Through AMPK/CREB/BDNF Pathway. Frontiers in pharmacology, 2018. **9**: p. 1266-1266.
374. Zhang, J., et al., *High glucose induces apoptosis of HUVECs in a mitochondria-dependent manner by suppressing hexokinase 2 expression.* Experimental and therapeutic medicine, 2019. **18**(1): p. 621-629.
375. Chen, Y., et al., *High-glucose treatment regulates biological functions of human umbilical vein endothelial cells via Sirt1/FOXO3 pathway.* Annals of translational medicine, 2019. **7**(9): p. 199-199.
376. Wang, Y., et al., *Ginsenoside Rc Ameliorates Endothelial Insulin Resistance via Upregulation of Angiotensin-Converting Enzyme 2.* Frontiers in Pharmacology, 2021. **12**(69).
377. Boesten, D.M., et al., *Multi-targeted mechanisms underlying the endothelial protective effects of the diabetic-safe sweetener erythritol.* PLoS One, 2013. **8**(6): p. e65741.
378. Piwowar, A., M. Knapik-Kordecka, and M. Warwas, *Oxidative stress and endothelium dysfunction in diabetes mellitus type 2.* Polski merkuriusz lekarski: organ Polskiego Towarzystwa Lekarskiego, 2008. **25**(146): p. 120-123.
379. Su, G., et al., *Association of glycemic variability and the presence and severity of coronary artery disease in patients with type 2 diabetes.* Cardiovascular diabetology, 2011. **10**(1): p. 1-9.
380. Zhang, X., et al., *The effects of glucose fluctuation on the severity of coronary artery disease in type 2 diabetes mellitus.* Journal of diabetes research, 2013. **2013**: p. 576916-576916.
381. González, M., et al., *Insulin-stimulated L-arginine transport requires SLC7A1 gene expression and is associated with human umbilical vein relaxation.* Journal of cellular physiology, 2011. **226**(11): p. 2916-2924.
382. Westermeier, F., et al., *Insulin restores gestational diabetes mellitus–reduced adenosine transport involving differential expression of insulin receptor isoforms in human umbilical vein endothelium.* Diabetes, 2011. **60**(6): p. 1677-1687.
383. Escudero, C.A., et al., *Pro-angiogenic role of insulin: from physiology to pathology.* Frontiers in physiology, 2017. **8**: p. 204.
384. Aird, W.C., *Phenotypic heterogeneity of the endothelium: II. Representative vascular beds.* Circ Res, 2007. **100**(2): p. 174-90.
385. Lang, I., et al., *Human fetal placental endothelial cells have a mature arterial and a juvenile venous phenotype with adipogenic and osteogenic differentiation potential.* Differentiation, 2008. **76**(10): p. 1031-43.
386. Vitale, C., et al., *Metformin improves endothelial function in patients with metabolic syndrome.* Journal of internal medicine, 2005. **258**(3): p. 250-256.
387. Graham, G.G., et al., *Clinical pharmacokinetics of metformin.* Clinical pharmacokinetics, 2011. **50**(2): p. 81-98.
388. Eyal, S., et al., *Pharmacokinetics of metformin during pregnancy.* Drug Metabolism and Disposition, 2010. **38**(5): p. 833-840.
389. Detaille, D., et al., *Metformin Prevents High-Glucose–Induced Endothelial Cell Death Through a Mitochondrial Permeability Transition-Dependent Process.* Diabetes, 2005. **54**(7): p. 2179.
390. Hattori, Y., et al., *Metformin inhibits cytokine-induced nuclear factor kappaB activation via AMP-activated protein kinase activation in vascular endothelial cells.* Hypertension, 2006. **47**(6): p. 1183-8.
391. Batchuluun, B., et al., *Metformin and liraglutide ameliorate high glucose-induced*

oxidative stress via inhibition of PKC-NAD(P)H oxidase pathway in human aortic endothelial cells. Atherosclerosis, 2014. **232**(1): p. 156-64.
392. Garlanda, C. and E. Dejana, *Heterogeneity of endothelial cells: specific markers.* Arteriosclerosis, thrombosis, and vascular biology, 1997. **17**(7): p. 1193-1202.
393. Hewett, P.W., *Vascular endothelial cells from human micro-and macro-vessels: isolation, characterisation and culture*, in *Angiogenesis Protocols*. 2009, Springer. p. 95-111.
394. Trepel, M., W. Arap, and R. Pasqualini, *In vivo phage display and vascular heterogeneity: implications for targeted medicine.* Current opinion in chemical biology, 2002. **6**(3): p. 399-404.
395. Alfirevic, Z., T. Stampalija, and G.M. Gyte, *Fetal and umbilical Doppler ultrasound in high-risk pregnancies.* The Cochrane database of systematic reviews, 2010(1): p. CD007529-CD007529.
396. Cahill, L.S., et al., *Placental vascular abnormalities in the mouse alter umbilical artery wave reflections.* American Journal of Physiology-Heart and Circulatory Physiology, 2019. **316**(3): p. H664-H672.
397. MacDonald, T.M., et al., *Reduced growth velocity across the third trimester is associated with placental insufficiency in fetuses born at a normal birthweight: a prospective cohort study.* BMC Medicine, 2017. **15**(1): p. 164.
398. Burton, G.J. and E. Jauniaux, *Pathophysiology of placental-derived fetal growth restriction.* American Journal of Obstetrics & Gynecology, 2018. **218**(2): p. S745-S761.
399. Langer, O., et al., *Gestational diabetes: the consequences of not treating.* American journal of obstetrics and gynecology, 2005. **192**(4): p. 989-997.
400. Page, R.C.L., et al., *Is macrosomia associated with poor glycaemic control in diabetic pregnancy?* Diabetic medicine, 1996. **13**(2): p. 170-174.
401. Desoye, G., et al., *Insulin receptors in syncytiotrophoblast and fetal endothelium of human placenta. Immunohistochemical evidence for developmental changes in distribution pattern.* Histochemistry, 1994. **101**(4): p. 277-85.
402. Desoye, G., et al., *Location of insulin receptors in the placenta and its progenitor tissues.* Microsc Res Tech, 1997. **38**(1-2): p. 63-75.
403. Kovo, M., et al., *Determination of metformin transfer across the human placenta using a dually perfused ex vivo placental cotyledon model.* Eur J Obstet Gynecol Reprod Biol, 2008. **136**(1): p. 29-33.
404. Kovo, M., et al., *Carrier-mediated transport of metformin across the human placenta determined by using the ex vivo perfusion of the placental cotyledon model.* Prenat Diagn, 2008. **28**(6): p. 544-8.
405. Tertti, K., et al., *The role of organic cation transporters (OCTs) in the transfer of metformin in the dually perfused human placenta.* Eur J Pharm Sci, 2010. **39**(1-3): p. 76-81.
406. Kurosawa, K., et al., *Development of a Pharmacokinetic Model of Transplacental Transfer of Metformin to Predict In Vivo Fetal Exposure.* Drug Metab Dispos, 2020. **48**(12): p. 1293-1302.
407. Hawley, S.A., et al., *The Antidiabetic Drug Metformin Activates the AMP-Activated Protein Kinase Cascade via an Adenine Nucleotide-Independent Mechanism.* Diabetes, 2002. **51**(8): p. 2420.
408. Soobryan, N., et al., *Angiogenic Dysregulation in Pregnancy-Related Hypertension—A Role for Metformin.* Reproductive Sciences, 2018. **25**(11): p. 1531-1539.

409. Han, C.S., et al., *Glucose and metformin modulate human first trimester trophoblast function: a model and potential therapy for diabetes-associated uteroplacental insufficiency.* American journal of reproductive immunology (New York, N.Y. : 1989), 2015. **73**(4): p. 362-371.
410. Alzamendi, A., et al., *Oral metformin treatment prevents enhanced insulin demand and placental dysfunction in the pregnant rat fed a fructose-rich diet.* International Scholarly Research Notices, 2012. **2012**.
411. Shishavan, M.H., et al., *Metformin improves endothelial function and reduces blood pressure in diabetic spontaneously hypertensive rats independent from glycemia control: comparison to vildagliptin.* Scientific reports, 2017. **7**(1): p. 1-12.
412. Lewis, R.M. and J.E. Pearson-Farr, *Multiscale three-dimensional imaging of the placenta.* Placenta, 2020. **102**: p. 55-60.
413. Nikuei, P., et al., *Diagnostic accuracy of sFlt1/PlGF ratio as a marker for preeclampsia.* BMC Pregnancy and Childbirth, 2020. **20**(1): p. 80.
414. Muller, W.A., et al., *A human endothelial cell-restricted, externally disposed plasmalemmal protein enriched in intercellular junctions.* The Journal of experimental medicine, 1989. **170**(2): p. 399-414.
415. Gumina, R.J., et al., *The human PECAM1 gene maps to 17q23.* Genomics, 1996. **34**(2): p. 229-232.
416. Kaufmann, P., T.M. Mayhew, and D.S. Charnock-Jones, *Aspects of human fetoplacental vasculogenesis and angiogenesis. II. Changes during normal pregnancy.* Placenta, 2004. **25**(2-3): p. 114-126.
417. Kohnen, G., et al., *Placental villous stroma as a model system for myofibroblast differentiation.* Histochemistry and cell biology, 1996. **105**(6): p. 415-429.
418. Chiong, M., et al., *Influence of glucose metabolism on vascular smooth muscle cell proliferation.* Vasa, 2013. **42**(1): p. 8-16.
419. Leiva, A., et al., *Fetoplacental vascular endothelial dysfunction as an early phenomenon in the programming of human adult diseases in subjects born from gestational diabetes mellitus or obesity in pregnancy.* Experimental diabetes research, 2011. **2011**.
420. Higgins, L., et al., *Obesity and the placenta: a consideration of nutrient exchange mechanisms in relation to aberrant fetal growth.* Placenta, 2011. **32**(1): p. 1-7.
421. Whittle, S., *Placental vascular smooth muscle cell differentiation in pregnancies complicated by obesity and gestational diabetes*. 2016, University of Manchester.
422. Sissaoui, S., et al., *Hyperglycaemia up-regulates placental growth factor (PlGF) expression and secretion in endothelial cells via suppression of PI3 kinase-Akt signalling and activation of FOXO1.* Scientific reports, 2021. **11**(1): p. 16344-16344.

Appendices

Appendix 1: Velocity Study Protocol

Central Manchester University Hospitals NHS
NHS Foundation Trust

Study Protocol

Investigators: Dr Jenny Myers, Dr Ed Johnstone, Dr Alice Dempsey & Dr Eleanor Scott

VELOCITY: Evaluating fetal growth in pregnancies Complicated by maternal diabetes

Background

The evaluation of fetal growth in pregnancies complicated by maternal diabetes is important in determining not only growth restriction but also fetal macrosomia. The importance of identifying and therefore allowing early intervention is paramount in the setting of antenatal care.

Fetal growth restriction, defined as a pathological restriction of the genetic growth potential (RCOG 2014), causes an increased risk of perinatal morbidity and mortality in particular fetal compromise and stillbirth (RCOG 2014). Fetal macrosomia, defined as fetal growth greater than the 90th centile, has significant implications for both mother and baby. Maternal complications include prolonged labour, operative deliveries and perineal trauma

(Ju 2009). Fetal complications include shoulder dystocia resulting in birth trauma, brachial plexus injuries and admission to neonatal intensive care unit (Esakoff 2009).

The current tools used for the evaluation of fetal growth are:
1. Measuring symphysio-fundal height. This has a poor sensitivity and specificity with detection of abnormalities in growth as low as 30% (Rosenberg 1982).
2. 2D Ultrasound measurements of fetal biometry. Those commonly used are head circumference, abdominal circumference and femur length. Estimated fetal weight is calculated using a formula (Hadlock 1985), which is then plotted on a customised fetal weight growth chart.

Although these practices are widely used, their accuracy is widely debated (Chauhan 2005). In women with diabetes, fetal growth is more difficult to assess as there is often maternal obesity and conflicting mechanisms influencing fetal growth (maternal hyperglycaemia and placental insufficiency). It is therefore evident that more accurate assessments of fetal growth are needed. Based on previous success using 3D ultrasound techniques in small for gestational age infants, we will use fractional thigh volumes (measured by 3D ultrasound) to evaluate and predict fetal growth trajectory. We anticipate that earlier detection of deviations in fetal growth will allow earlier intervention (e.g. earlier delivery or closer monitoring of fetal wellbeing/maternal diabetes) and thereby ameliorate some of the maternal and neonatal morbidity associated with abnormal fetal growth.

Clinic environment:

Women will be seen in a dedicated research clinic run within the clinical suite of the Maternal & Fetal Health Research Centre (5th floor St Mary's Hospital) and as part of the Diabetes Antenatal Clinic at St James' Teaching Hospital. Women will be recruited to this research study by a member of the research team and research samples will be collected and immediately processed.

The study is sponsored by the University of Manchester.

Referral criteria:

Women <20 weeks gestation with pre-existing diabetes

Exclusion criteria

Multiple pregnancies

Women unable to provide written informed consent

Women under 16 years of age

Consent

Women will be consented by trained research staff who are able to assess capacity and who are familiar with the principles underpinning informed consent. Appropriate information will be provided to women who are invited to participate in this research.

Study protocol:

1. Referral at booking from diabetic antenatal services, first visit 10-16 weeks
2. Subsequent visits 4 weekly (or as clinically indicated)

Appointments within the research study will replace a small number of routine antenatal care visits usually performed in the specialist diabetes clinic. Assessments will be performed by clinical staff and documented in the hand-held notes and main hospital notes for all women. Any abnormal findings will be shared with the booking consultant and appropriate follow up arrangements made. Any clinical investigations performed during a research visit (e.g. blood tests) will be followed up by the research team and communicated to the clinical staff as necessary.

Planned research investigations:

1. Collection of demographic data, including obstetric, medical and drug history. Routine blood test results (such as HbA1C) will also be recorded.
2. Uteroplacental assessment: Measurement of uterine artery and umbilical artery Doppler. Fetal biometry will be performed 4 weekly from the first scan with placental volume assessments at 22-24 weeks. 3D fractional thigh measurements will also be obtained where possible during each scan; these measurements will be post processed.
3. Women will be asked to wear a continuous glucose monitor (CGM) three times during their pregnancy (10-16, 22-26 and 30-34 weeks), which will be fitted by trained staff for up to a week at a time. Glucose readings will remain blinded to the participant but a summary of the readings will be provided at the end of each week of measurements. Women will also be asked to complete a short questionnaire detailing their daily activity levels.
4. Vascular assessment (Manchester only): Assessment of blood pressure and vascular compliance using TensioClinic Arteriograph. This device uses an upper arm cuff to detect pulse waves generated from central and peripheral vessels. The arteriograph will provide the following data: Augmentation index, pulse wave velocity, aortic

systolic BP, systolic and diastolic BP. Noninvasive cardiac output monitoring (NICOM) measurements will also be obtained at the same time. Measurements will be taken three times during pregnancy (see table 1).

5. Collection of blood and urine samples (Manchester only): Samples (one EDTA 8 ml, one serum 8 ml) will be collected for measurement of existing placental biomarkers (e.g. Placental growth factor) in addition to novel biomarkers currently under development. Samples will be collected at four time points during pregnancy (see table 1).
6. Collection of pregnancy outcome data: Detailed pregnancy outcome data will be collected including details of delivery and neonatal outcomes.
7. Collection of cord blood for measurement of biochemical parameters (e.g. erythropoietin and C peptide) and placentas for assessment of angiogenesis and morphological abnormalities. Samples will be collected by research staff using in line with existing protocols.
8. Measurement of skin fold thickness will be carried out on the infants (born after 28 weeks) after birth (within 72 hours).

Data storage

All clinical, ultrasound and vascular measurements will be collected and stored using a customized database (e.g., ViewPoint). This database can only be accessed by clinical members of the research team. For data analysis purposes non-identifiable data only will be transferred to encrypted University PCs accessible only by research staff.

Sample storage

All samples will be processed using standard operating procedures within MFHRC. Processed samples will be labelled with date, unique study ID and initials and stored at -80 ºC.

Primary outcome

The correlation of 3D measurements to final birth weight and predicted birthweight (iGAP) in comparison to the performance of 2D biometry

Secondary outcomes

1. Association between continuous glucose monitoring and fetal growth trajectory measured in each trimester throughout pregnancy

2. Utility of longitudinal biochemical measurements and the identification of fetal growth abnormalities

3. Association between 3D fractional thigh volume measurements and neonatal skin fold

thickness

Sample size

250 women with pregestational diabetes recruited over 5 years.

Analysis

At St Mary's Hospital we provide care for 50-70 women with pre-existing diabetes per year. Our experience with similar cohort studies is that recruitment is high (>95%), we would therefore anticipate the recruitment of at least 50 women per year (1 per week) to the study. Leeds Teaching Hospital NHS Trust provide care for a similar number of women with diabetes. Fetal macrosomia complicates 30-40% of pregnancies complicated by maternal diabetes with a further 15-20% being complicated by small for gestational age.

In our previous studies, we have demonstrated an improvement of 0.09-0.13 in the R^2 (correlation between scan measurements and birthweight) using 3D volume measurements in comparison with 2D biometry. Using these estimates, the inclusion of 250 women would give sufficient power to detect a 0.12 change in the regression correlations (α=0.05, β=0.8). Accuracy of the IGAP software using 3D volume measurements will be assessed using standard diagnostic metrics (sensitivity, specificity, positive predictive value etc.) in line with our previous studies, which have demonstrated a significant improvement in the detection of fetal growth restriction with the inclusion of fractional thigh measurements.

The association of blood glucose monitoring and fetal growth trajectory will be investigated using linear regression analysis (outcome variable: fetal growth velocity using iGAP software) incorporating appropriate covariate data including biochemical and biophysical measurements). Detailed analysis of the CGM data (Law et al) will be performed in conjunction with Division of Epidemiology and Biostatistics, Leeds Institute of Cardiovascular and Metabolic Medicine, University of Leeds.

Reporting of clinical information

Observations obtained as part of the research study which would be considered to be part of routine clinical care (blood pressure, urinalysis, fetal biometry etc.) will be reported to the clinical care team and managed according to local clinical protocols. A summary of the blinded CGM measurements will be fed back to participants after each sensor episode, but will not be reported to the clinical team.

Risks, Burdens and Benefits

As this is an observational cohort study, adverse events are not anticipated.

Women referred to VELOCITY will be managed in line with specialist antenatal clinics' care pathways and their care will not be altered by their enrolment in this research study. Women will be offered additional ultrasound scans as part of the study and for women recruited in Manchester additional blood samples and vascular profile measurements will be obtained during the study visits (5 minutes). As women with diabetes in pregnancy attend hospital appointments 2- 4 weekly during their pregnancy, it is not anticipated that additional visits will be necessary for women taking part in the study. Study visits will replace or be incorporated within routine clinical care appointments.

Women will be asked to wear a glucose sensor for a week at a time at three time points during their pregnancy. This can occasionally be associated with minor local skin reactions and there is a small risk of localised infection. Women will be provided with information regarding the sensor and a contact telephone number in case of problems.

We have discussed this study and its long-term goals with our Maternal & Fetal Health user group.

Confidentiality

Data will be collected in accordance with the "Caldicott Principles". All women recruited will be allocated a study number which will be linked to their identifiable information held in a separate file stored within the Maternal & Fetal Health Research Centre. All outcome data will be stored using a password protected database within the Research Centre accessible only to members of the research team. All electronic data will be anonymised and no identifiable data will be stored on this database. All samples will be labelled with the study number and date only. Samples will be monitored and stored in line with the Human Tissue Act guidelines.

	10-16 weeks	16-22 weeks	22-26 weeks	26-30 weeks	30-34 weeks	34-38 weeks	Pregnancy outcome	Post Delivery (<72 hours)
	Baseline visit	Study visit 2	Study visit 2	Study visit 3	Study visit 4	Study visit 5	Delivery	
Patient Information Leaflet	✓							
Inc/Exc Criteria								
Consent Form	✓							
Collection demographic data	✓							
Fit glucose sensor	✓		✓		✓			
Confirm consent/continuation		✓	✓	✓	✓	✓		
Ultrasound scan inc 3D volume	✓	✓[a]	✓	✓[a]	✓	✓[a]		
Blood/urine samples[b]	✓		✓		✓	✓		
Vascular measurements[b]	✓		✓		✓			
Review and record pregnancy complications							✓	
Labour/Delivery Information							✓	
Collection cord blood and placenta							✓	
Measurement of neonatal skin fold thickness								✓

a. Ultrasound scans may be performed at these gestations as part of routine clinical care

b. Manchester only

(Myers et al, "Velocity Study Protocol ", 2016)

Appendix 2: Avizo Micro-CT Data Analysis Protocol

Steps involved in protocol for micro-CT data analysis in Avizo software.

1. **Obtain voxel size of data**
    - Locate the .vgi file of the data e.g. CTB 257.vgi
    - Right click the file
    - Open with notepad
    - Scroll down to resolution, note the value (the 3 values represent the X, Y &
    - Z planes respectively)

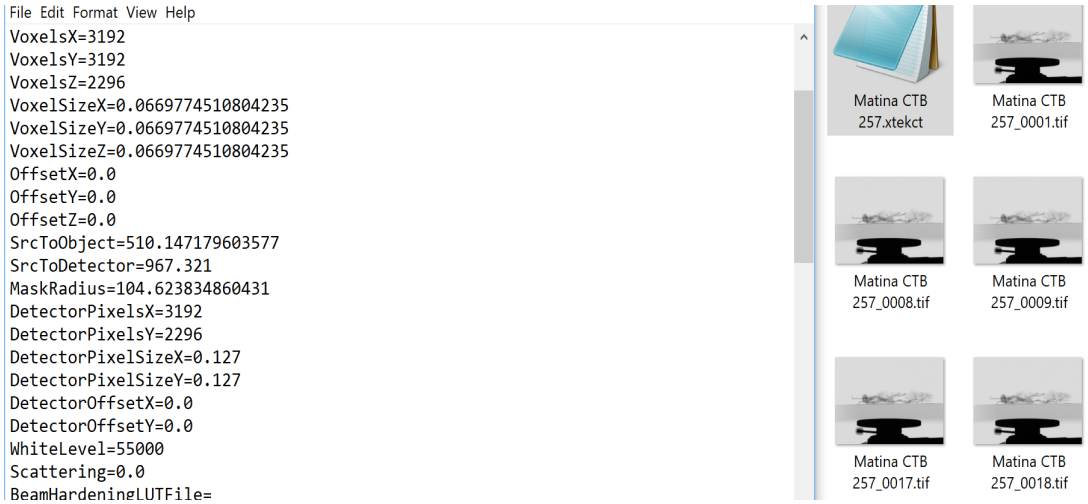

Scroll further down to verify the unit e.g., mm

2. **Open data in Avizo**
    - Start Avizo standard
    - Click “open data” in project view

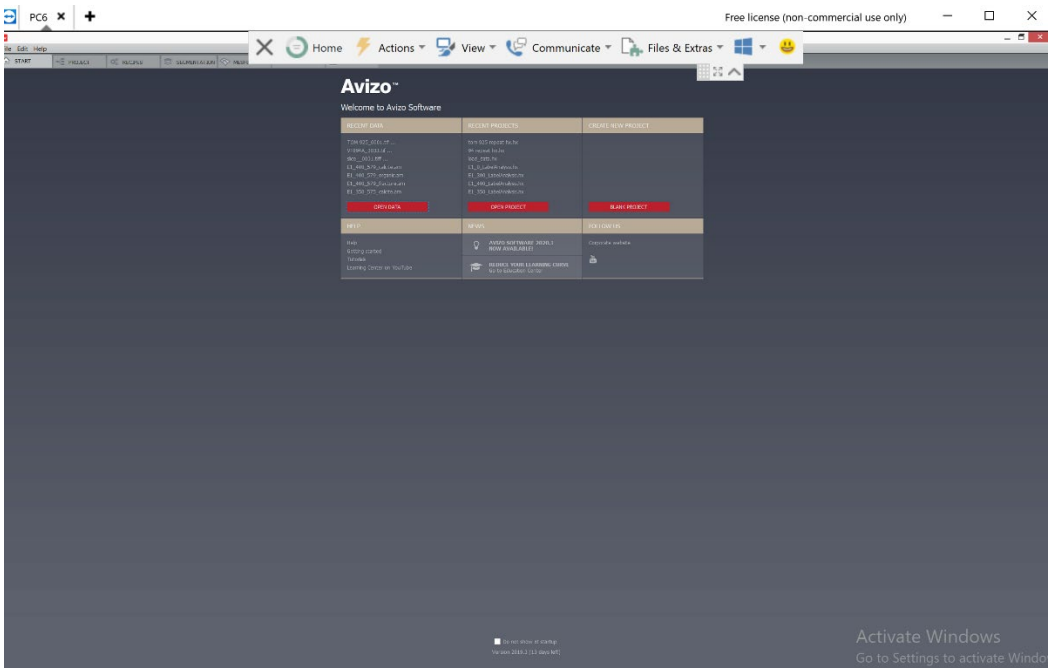

- Locate and open the data stored in .tiff format
- Copy all the .tiff files (Ctrl A), then click open

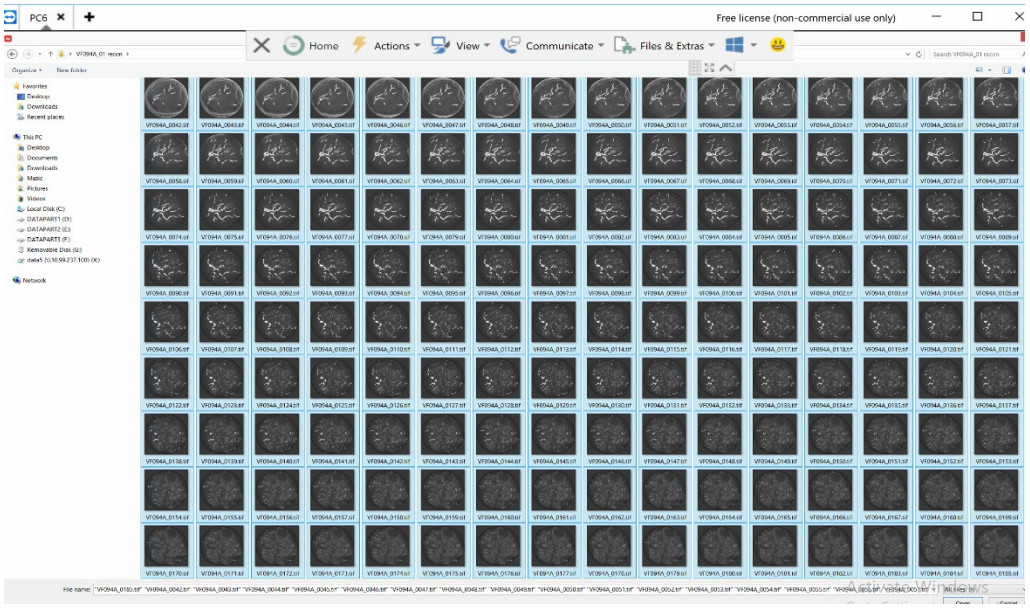

- Type in the voxel size obtained in section 1 above (in the 3 boxes)
- Click ok

3. Volume rendering of data

- Right click the imported data in project view

- Click volume rendering

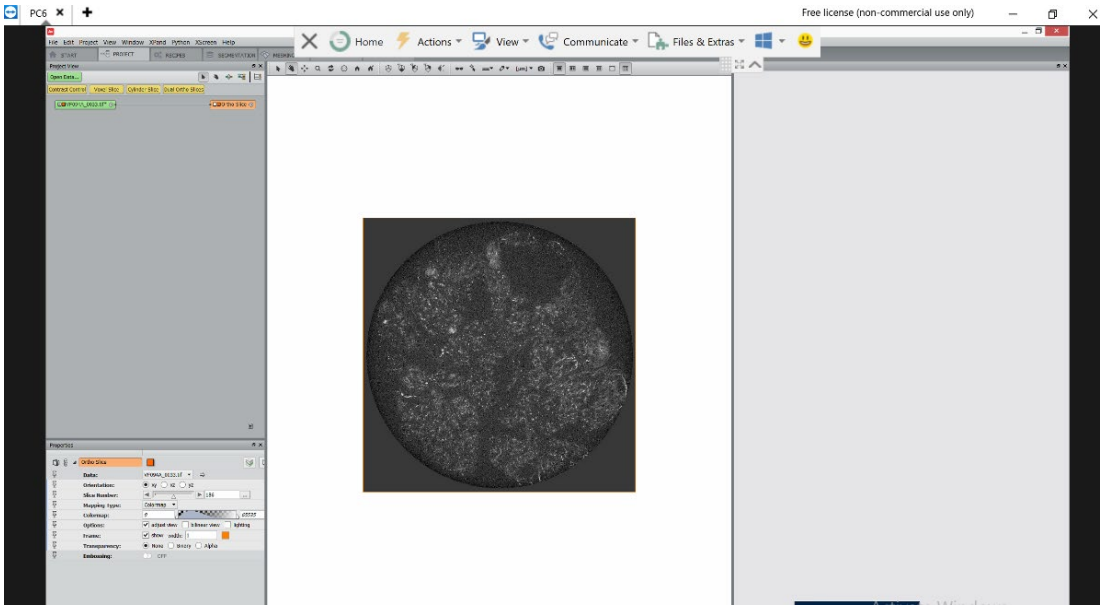

- Adjust the colour map to get rid of background grey scale/noise (change numbers until you achieve a desirable view)

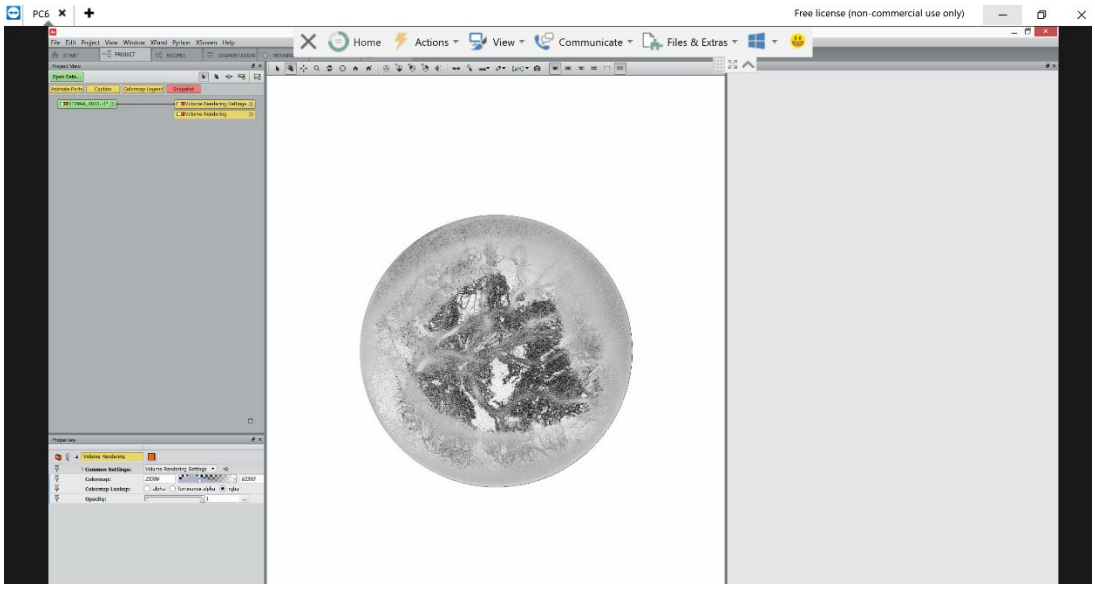

- Click view on the top pane, choose “background”, choose “uniform” and change colour as desired, then click ok

4. Cropping

- Right click the data
- Go to “compute”

- Go to “volume edit”
- Change from “Draw” to “Tadbox”
- Change from “Box” to “Cylinder”
- Change axis to “Z axis”
- Click the “outside” box on “cut”

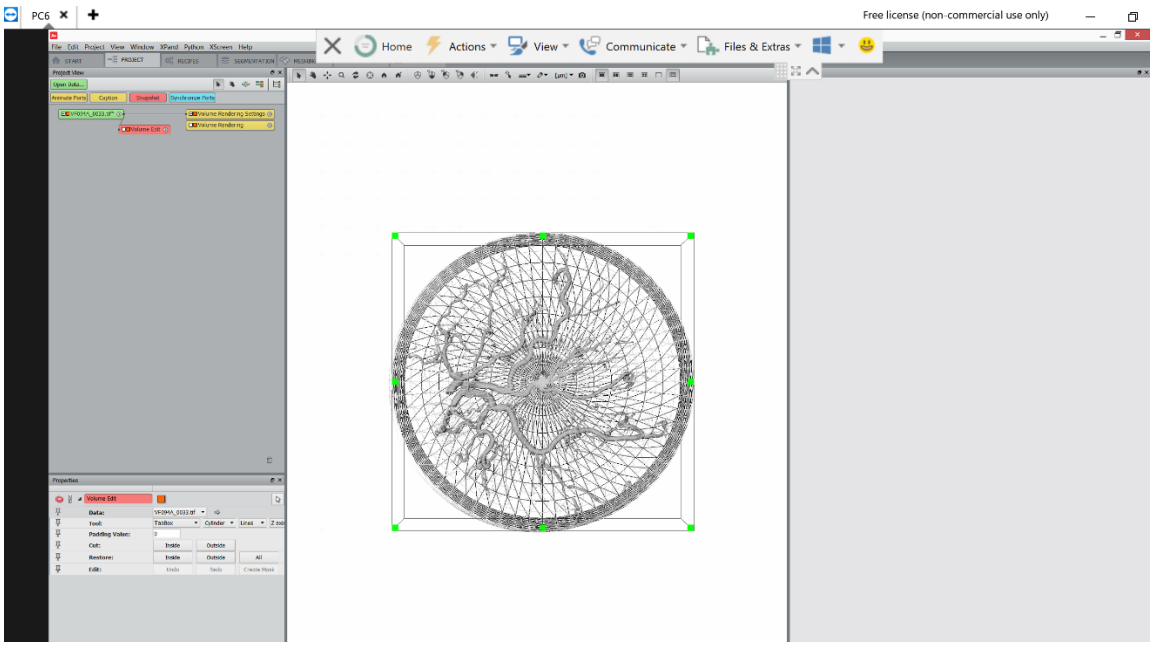

- Click apply
- This creates another data in the project view with the suffix “modif*”
- Deactivate the former data
- Do volume rendering for the new data (as in section 3 above)
- Rotate the new 3D image to view its base/background and crop any background noise as follows:
    - Right click the data, choose orthoslice

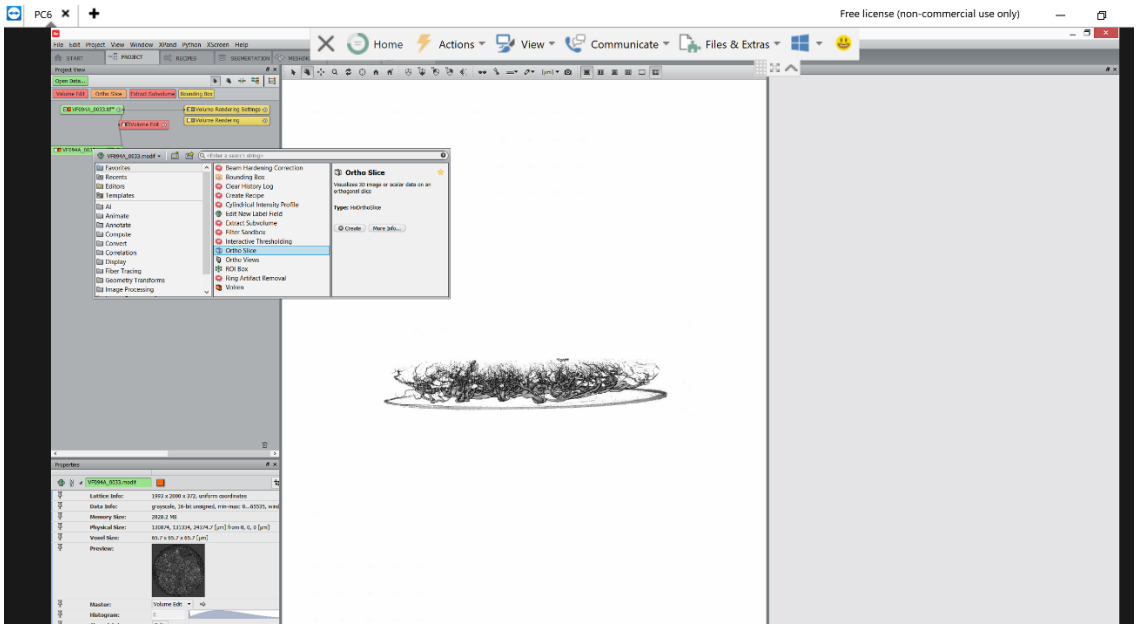

- Move the slice line to separate the data from the background noise (move slice number)

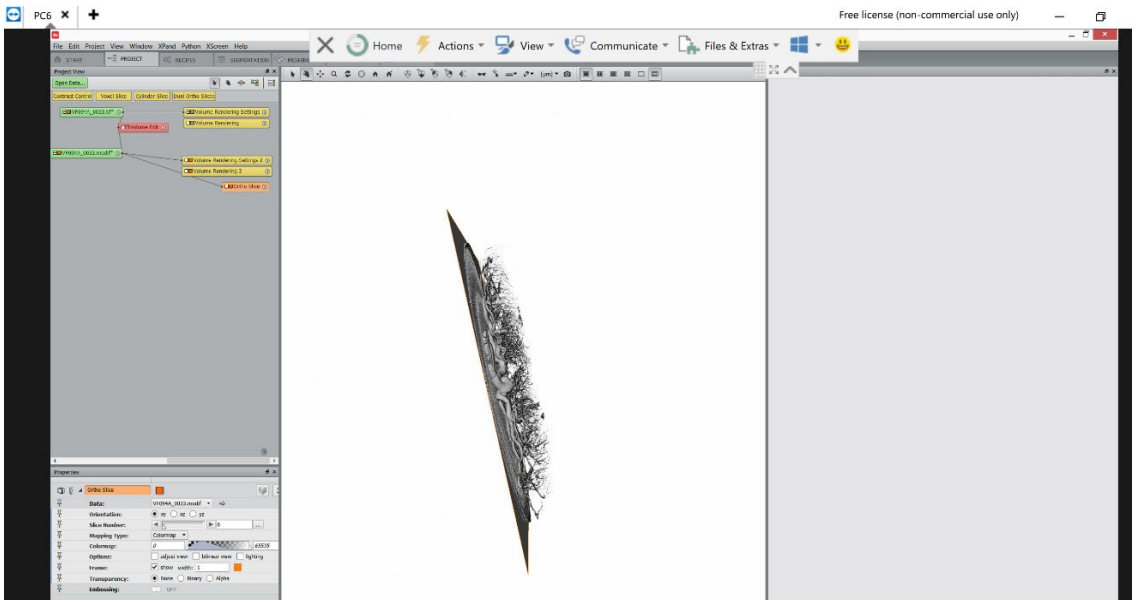

- Click the “clip” tool to crop off the noise
- Deactivate orthoslice

- Rotate the data back to position

5. Apply scale bars & grids

- Right click data

- Click “annotate”
- Choose “scale bars” or “local axis” (whichever is required)

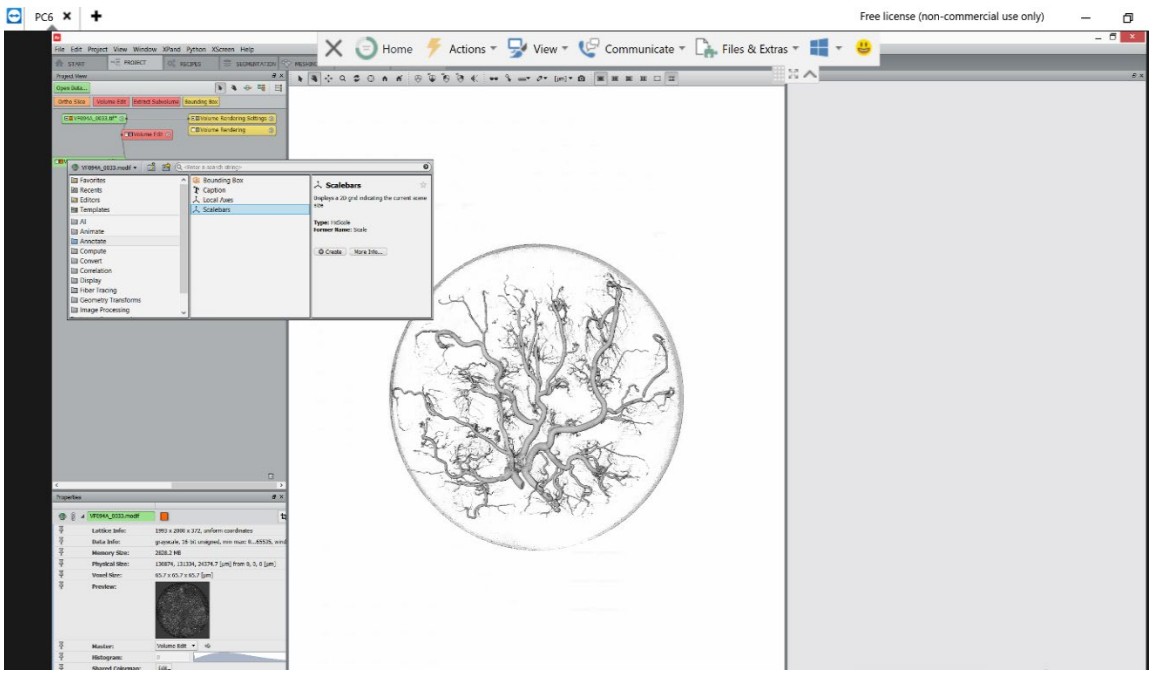

- Change colour from the background/default colour (default is white)
- Change unit to what is desired e.g. mm
- Change font and select its colour as desired
- Adjust scale bars as desired
- Apply grids if necessary

6. Segmentation of data

- Right click data, scroll to “image segmentation”, choose “edit new label field”

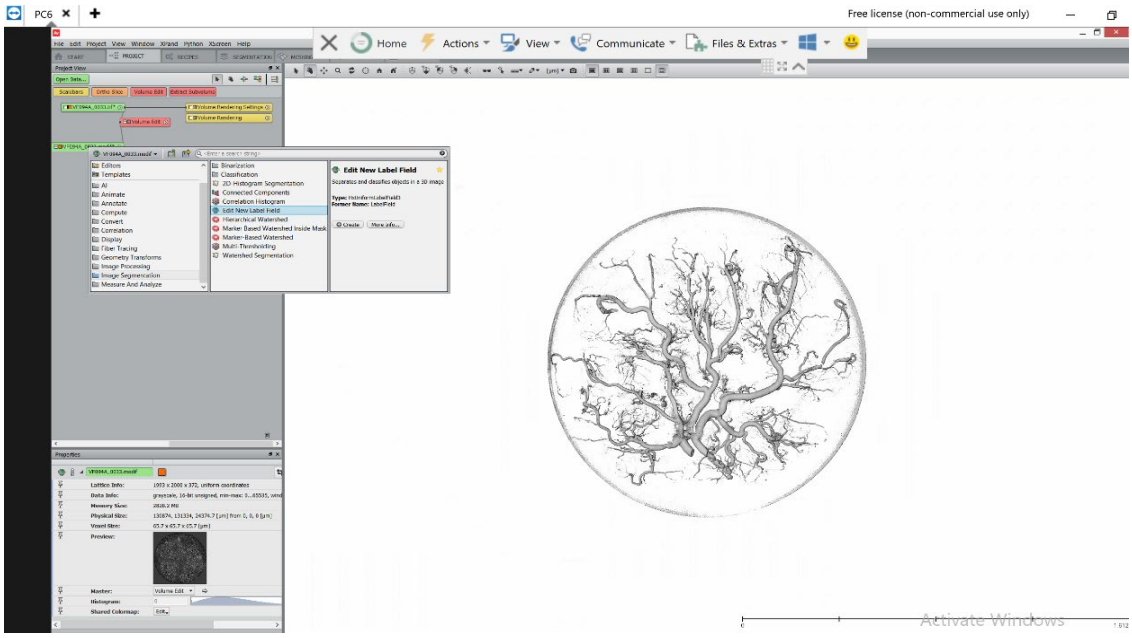

- View in 4 viewers mode (viewers 0, 1, 2 & 3)

0 = 3D view

1 = XY

2 = XZ slice planes

3 = YZ

- Choose the XY slice, change to 2 viewer mode

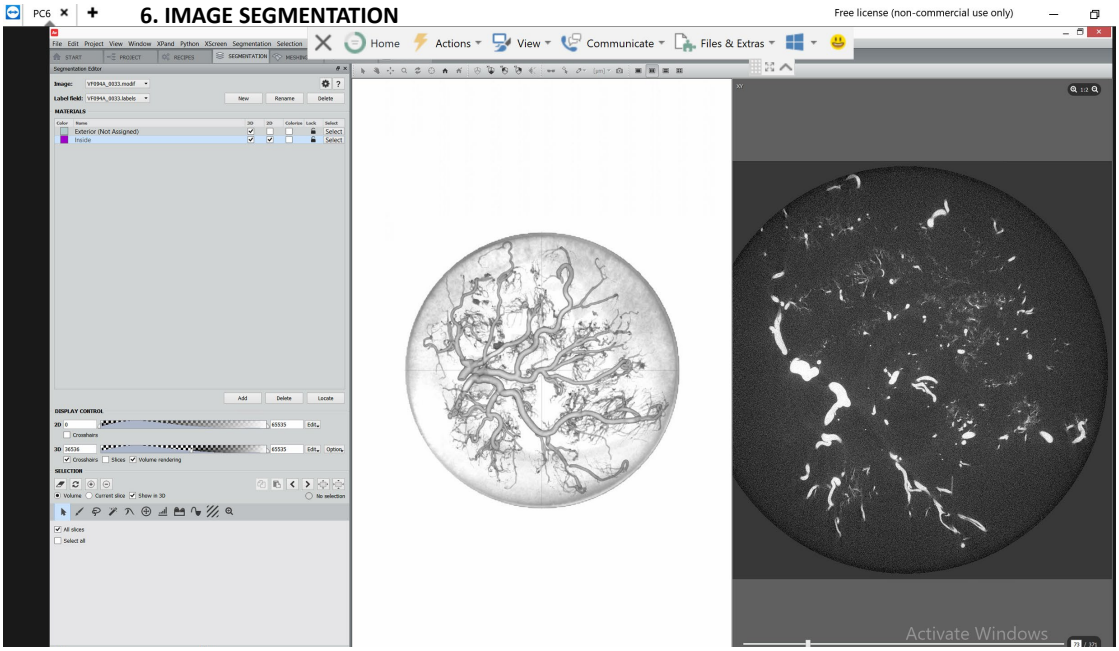

- Tick show in 3D

Tick all slices

- Use zoom tools to zoom in to show a perfect circle of slice XY (whole data in view)
- Set “data window” to 37 & 100 (or whichever values you’ve been working with from the beginning)
- Use magic wand tool or threshold tool to select data to segment
- Selected data turns red, adjust slider to create your selection

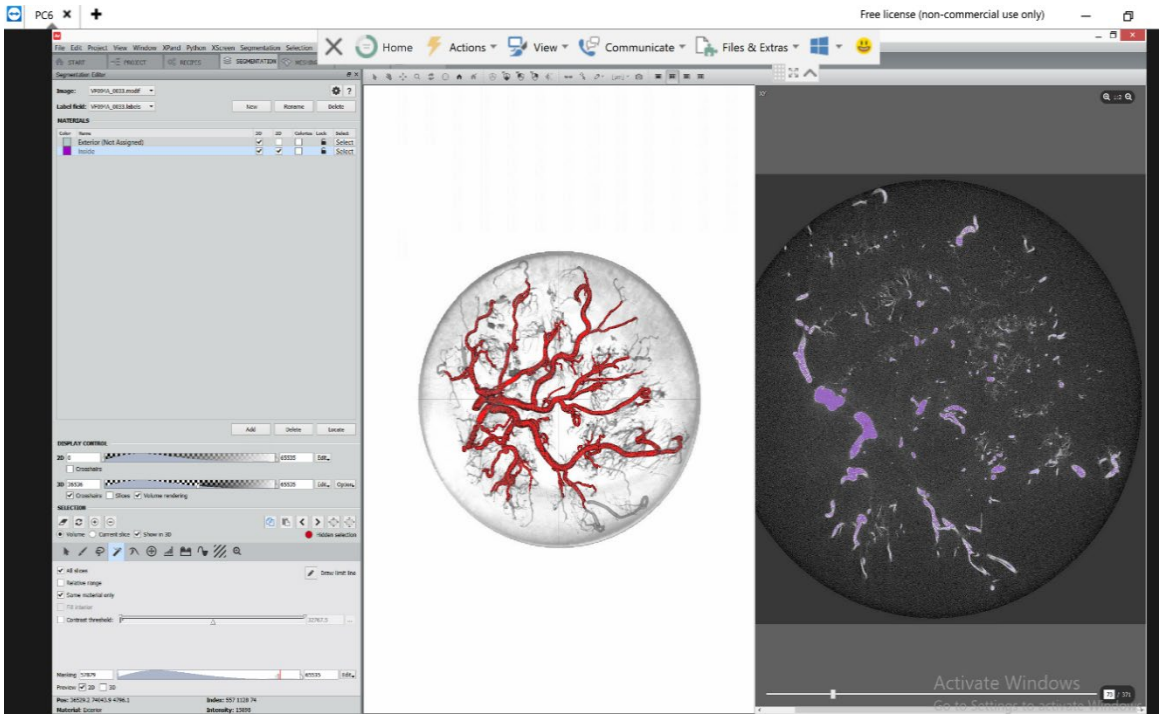

Use eraser tool to clean off errors

- Tick “all slices”
- Click the sign to add the selection for analysis
- You can change the title “inside” to whatever you want to use

7. Measurements 1: volume and area

- Click segmentation at the top pane
- Click material statistics

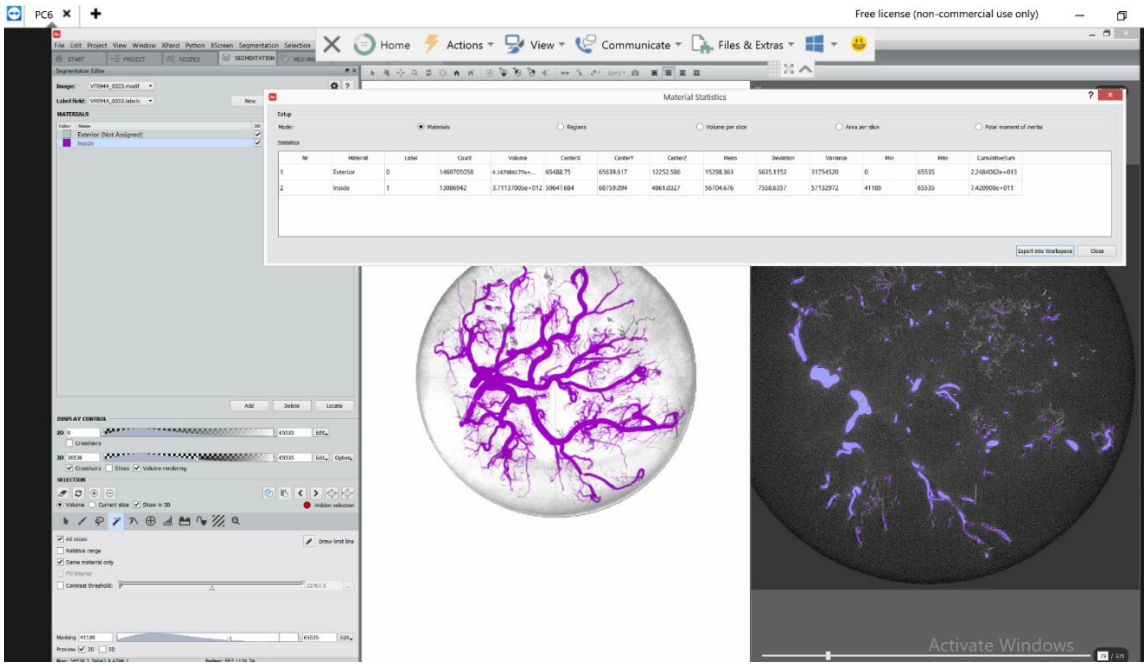

- You will obtain the volume in mm^3 and area in mm^2 (use the inside data, ignore the exterior ones)

8. Skeletonisation

- Right click labels (green in project view)

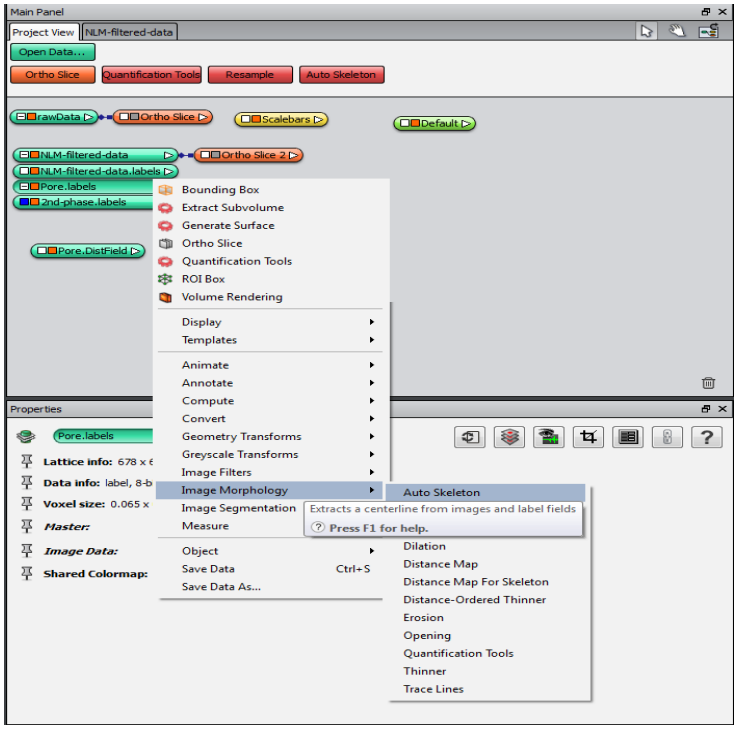

- Scroll down to image morphology

- Click autoskeleton
- Click apply at the bottom of the page

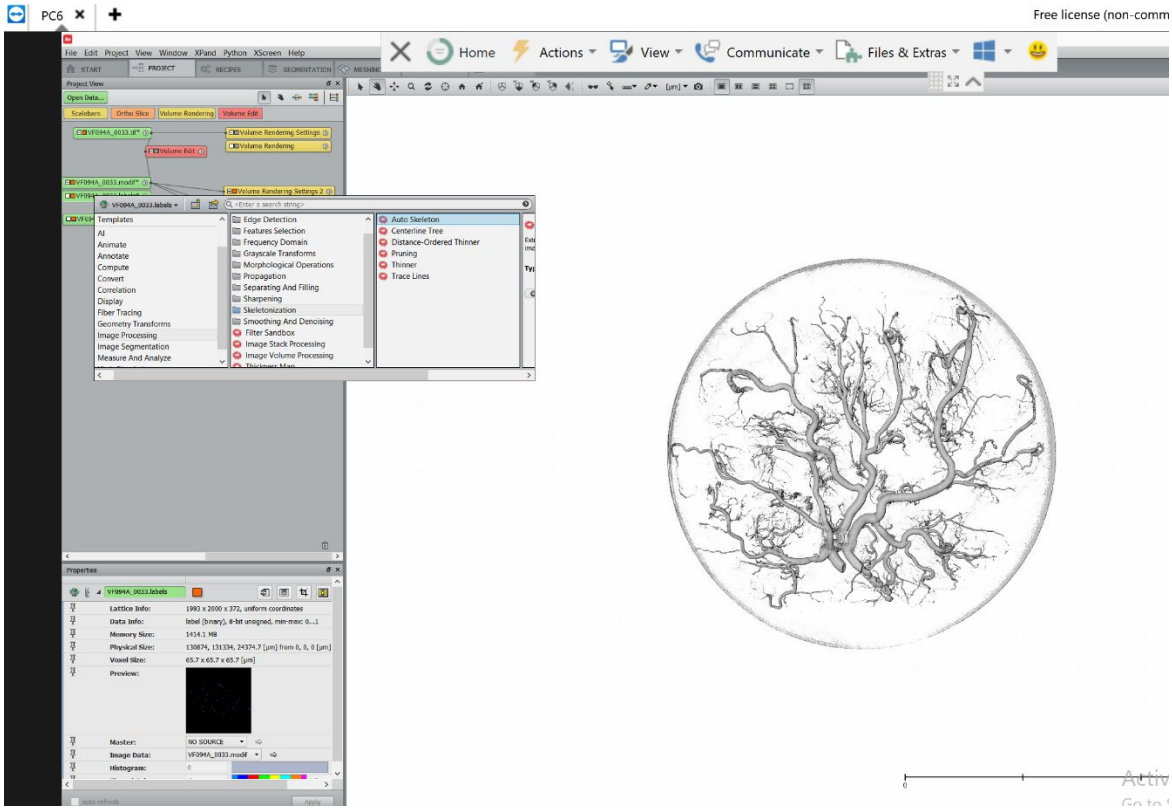

- Click spatial graph view on project view to modify parameters as follows:

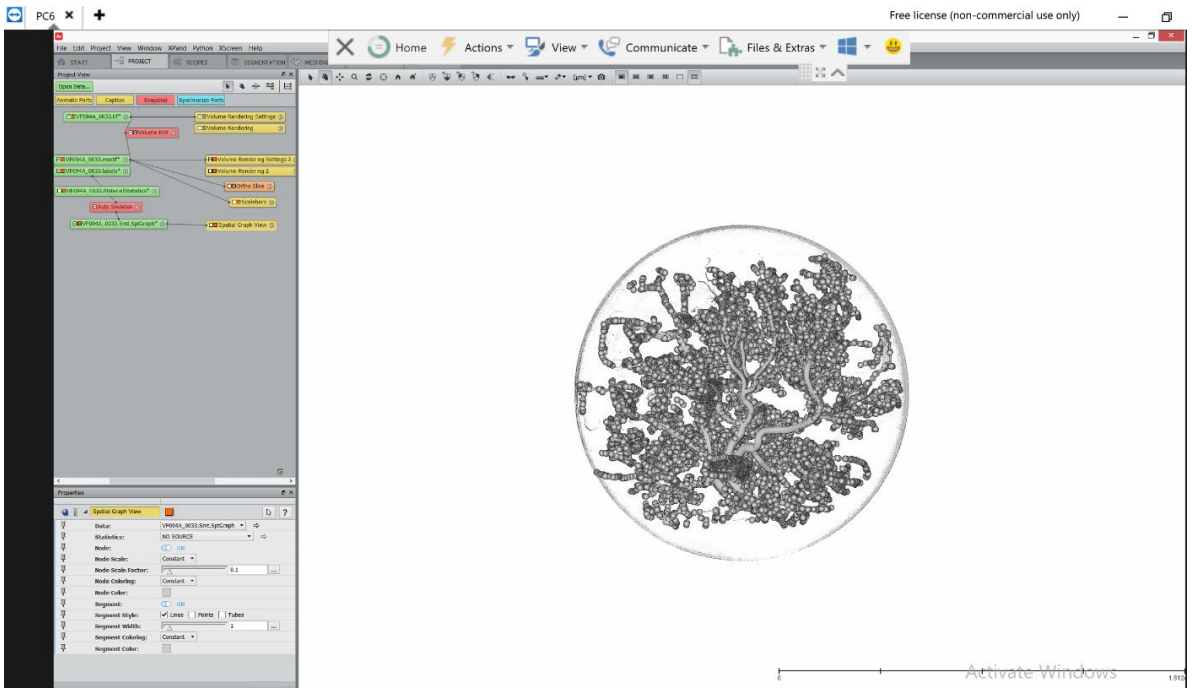

- Turn nodes on or off

- Change node colour

- Change segment styles – choose tubes

- Change colour of segments/tubes

- Change tube scale from “constant” to “thickness”

- Adjust tube scale factor

- Change segment colouring from “constant” to “thickness”

- Change segment colour map to physics.icol (click edit and choose physics.icol)

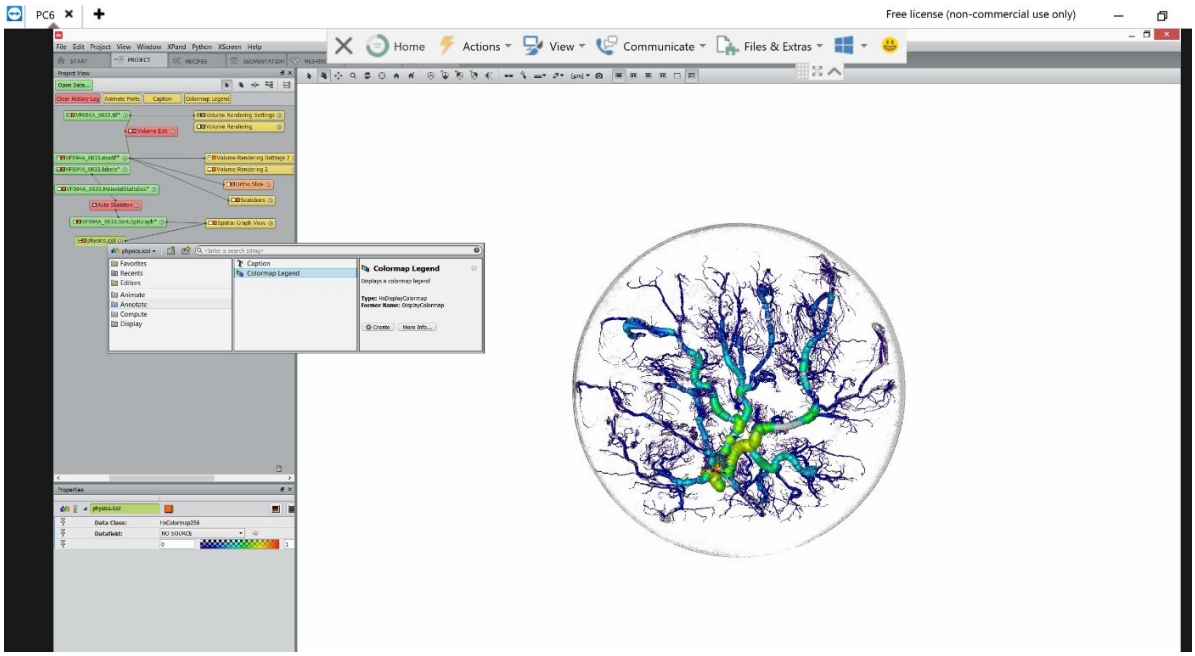

- Double click the colour gradient shown, physics.icol data will appear in project view. Right click the physics.icol data, choose annotate, choose colour map legend

- Tick custom text

- Change font colour to black (default is white)

- Type in values with desired unit in apostrophe e.g. 0/”0 mm” 0.5/”0.5 mm” 1/”1 mm” to replace the low, medium and high in the default settings

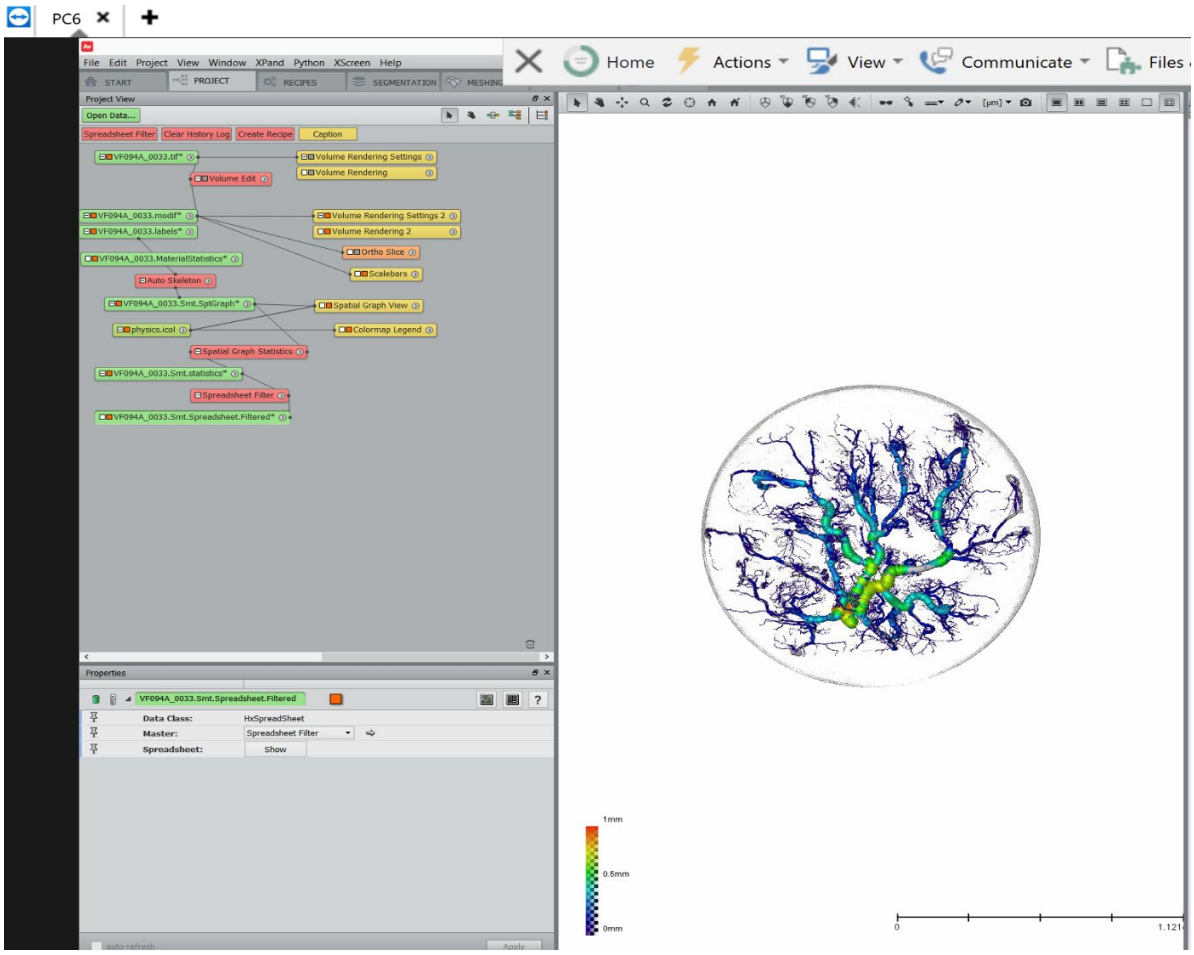

9. Measurements 2: length, number of branch points

- Right click spatial graph data in project view
- Choose measure
- Click spatial graph statistics

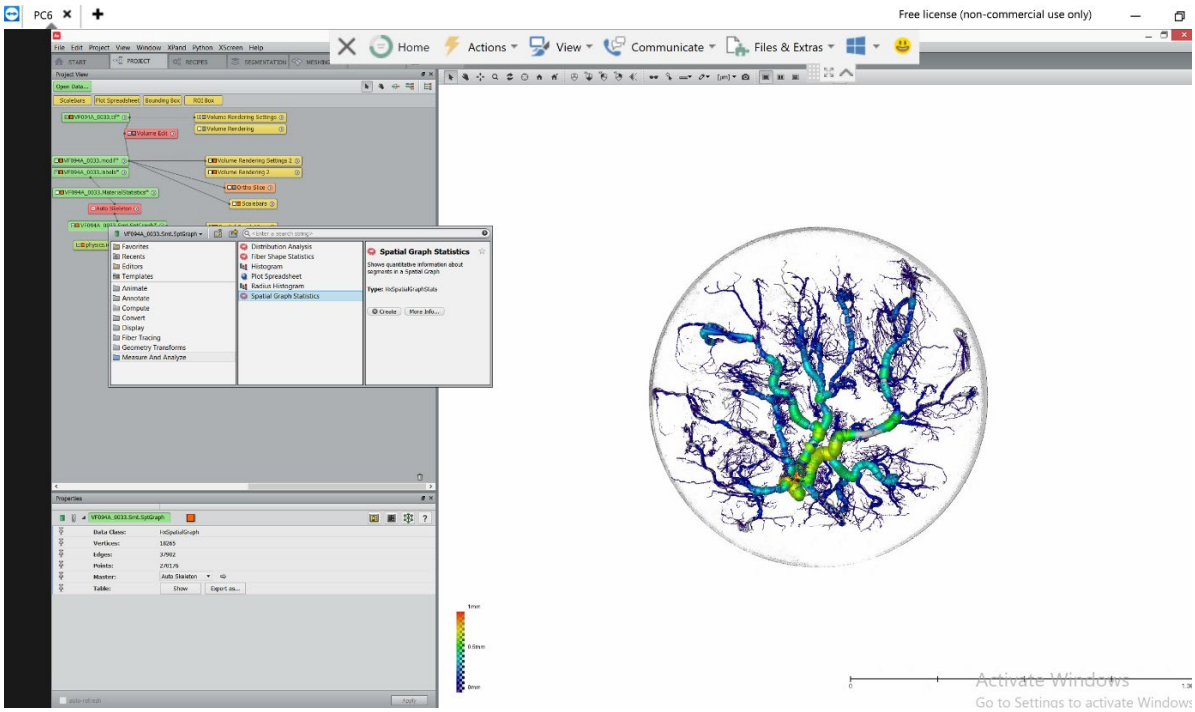

- Click apply
- Right click on the resultant green data “Smt.statistics” in project view
- Scroll to compute and click “spreadsheet filter”
- Click “show spreadsheet”

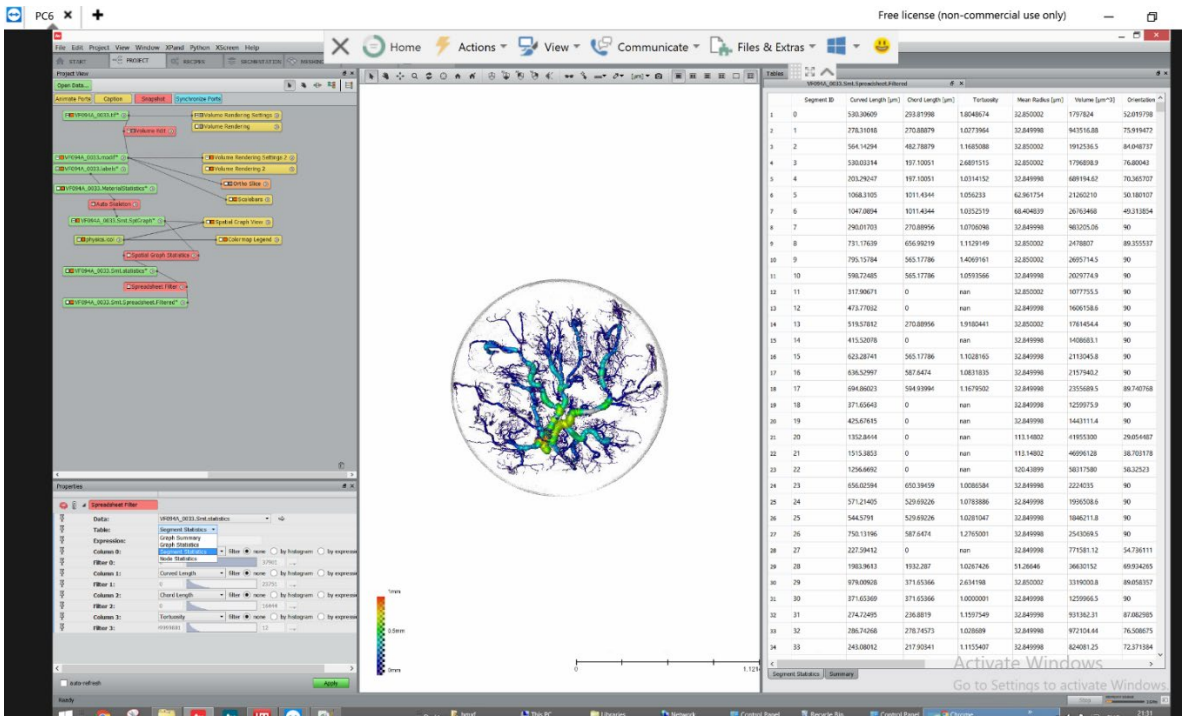

10. Measurements 3: diameter, length, manual measures

- Convert spatial graph to line set

- Right click the Smt.SptGraph data

- Scroll to “convert” and click “spatial graph to line set”
- Click apply
- Click on the resultant data in project view
- Click the ruler icon in the top pane
- Draw line to measure

11. Taking snapshots

- Take snapshots at any point by clicking on the camera icon in the top pane

(put scale bars or colour map legend, as in sections 5 and 8 respectively, before taking snapshot, if necessary)

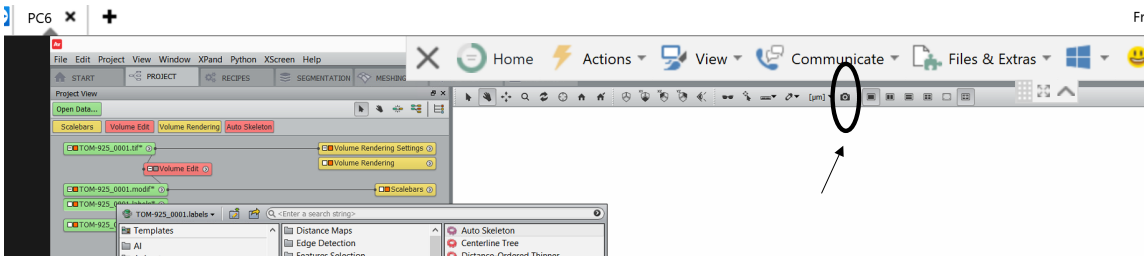

Appendix 2(I): R code Protocol for Cast Data Analysis

1. **Set up R Studio and install following libraries**
   - library(ggplot2)
   - library(dplyr)
   - library(mixOmics)
2. **Set working directory**
   - setwd("R:/<Username>/Placental Vasculature/Data") #set working directory to where your data is
3. **Input following code**
   - file_list<-list.files(pattern = ".*.csv") #list files ending .csv
   - files<-lapply(file_list, read.csv) #read files in list
   - files<-lapply(files,function(x){colnames(x)<-c("Segment_ID","Curved_Length","Chord_Length","Tortuosity","Mean_Radius","Volume","Classification")
   - return(x)}) #make column names uniform
   - data<-do.call(rbind,files) #bind data into one dataset
   - num_rows<-as.numeric(lapply(files,nrow)) #calculate number of rows per file
   - PIDs<-substr(file_list,1,nchar(file_list)-4) #generate unique IDs per participant from file names
   - Grp<-substr(file_list,1,3) #generate a group variable (VF0 vs TOM, 3 characters for ease)
   - Grp[15:24]<-substr(Grp[15:24],1,2) #drop character 3 from VF (VF0 -> VF)
   - data$PIDs<-rep(PIDs,num_rows) #add participant IDs to data
   - data$Group<-rep(Grp,num_rows) #add group IDs to data
   - data$Vessel<-substr(data$PIDs,nchar(data$PIDs)-4,nchar(data$PIDs)-4) #generate new column which specifies vessel type from PIDs
   - data<-data[which(data$Classification!="A1"),] #drop all rows where classification = A1 (774 dropped (472 TOM; 302 VF))
   - data<-data[which(data$Mean_Radius>300),] #drop all rows where radius < 300 (408482 dropped (251461 TOM; 157021 VF))
   - data$Tortuosity<-as.numeric(data$Tortuosity) #convert tortuosity to a numeric variable

- data<-data[which(!is.na(data$Tortuosity)),]#drop all rows where tortuosity = NA (540 NAs (31 '#N/A'; 509 'NaN')(269 TOM; 271 VF))

4. Apply to each dataset accordingly

- TOM<-data[which(data$Group=="TOM"),] #create a new object 'TOM' which is just the TOM samples
- VF<-data[which(data$Group=="VF"),] #create a new object 'VF' which is just the VF samples
- TOM_binned <-TOM %>%
- group_by(PIDs) %>% #New – first group by participant
- mutate(Bins = cut(Mean_Radius, breaks = seq(from = min(Mean_Radius),to = max(Mean_Radius),length.out = 21),include.lowest = T)) %>% #New – generate new column “Bins” separating each placenta into 20 equal groups based on Mean_Radius (21 breaks = 20 groups)
- group_by(PIDs,Bins) %>% #New - Added “PIDs” as a grouping variable as well as Bins which was already there
- summarise(Mean_Chord_Length = mean(Chord_Length),
  Mean_Curved_Length = mean(Curved_Length),
  Mean_Mean_Radius = mean(Mean_Radius),
  Mean_Volume = mean(Volume),
  Mean_Tortuosity = mean(Tortuosity),
  Number_of_segments = length(Bins)) #
- VF_binned<-VF %>%
- group_by(PIDs) %>%
- mutate(Bins = cut(Mean_Radius, breaks = seq(from = min(Mean_Radius),to = max(Mean_Radius),length.out = 21,include.lowest = T))) %>%
- group_by(PIDs,Bins) %>%
- summarise(Mean_Chord_Length = mean(Chord_Length),
- Mean_Curved_Length = mean(Curved_Length),
- Mean_Mean_Radius = mean(Mean_Radius),
- Mean_Volume = mean(Volume),
- Mean_Tortuosity = mean(Tortuosity),
- Number_of_segments = length(Bins))

5. **Save synthesized data**

- write.csv(TOM_binned,"TOM_binned.csv") #save new binned data in working directory
- write.csv(VF_binned,"VF_binned.csv")

6. **Plot graphs showing showcasing data**

- #Plot boxplots for binned data
- ggplot(TOM,aes(y=Tortuosity,group=Bins,col=Bins))+
- geom_boxplot()+
- scale_y_continuous(trans="log2")
- ggplot(VF,aes(y=Volume,group=Bins,col=Bins))+
- geom_boxplot()+
- scale_y_continuous(trans="log2")
- #PCA of binned data, summarizing Tortuosity,Chord Length, Curved Length & Volume
- TOM_pca<-pca(TOM_binned[,c(2,3,5,6)],ncomp = 3)
- plotIndiv(TOM_pca,group=TOM_binned$Bins,ind.names = TOM_binned$Bins,cex=4.5)
- VF_pca<-pca(VF_binned[,c(2,3,5,6)],ncomp = 3)
- plotIndiv(VF_pca,group=VF_binned$Bins,ind.names = VF_binned$Bins,cex=4.5)
- #Linear model to test significance continuously
- ggplot(data,aes(x=Curved_Length,y=Volume,group=Group,col=Group))+
- geom_point(alpha=0.02)+
- scale_x_continuous(trans="log2",breaks = c(1,10,100,1000,10000,100000))+
- scale_y_continuous(trans="log2",breaks = c(1e+7,1e+8,1e+9,1e+10,1e+11,1e+12))+
- geom_smooth(method="lm",size=1,se=TRUE)
- summary(lm(log2(Volume)~log2(Curved_Length)*Group,data))56
- #Linear model to test significance continuously
- ggplot(data,aes(x=Volume,y= Mean_Radius, group=Group,col=Group))+
- geom_point(alpha=0.02)+
- scale_x_continuous(trans="log2",breaks = c(1,10,100,1000,10000,100000))+

- scale_y_continuous(trans="log2",breaks = c(1e+7,1e+8,1e+9,1e+10,1e+11,1e+12))+
- geom_smooth(method="lm",size=1,se=TRUE)
- summary(lm(log2(Volume)~log2(Mean_Radius)*Group,data))

Appendix 3: Chapter 3 Results: Binned size numbers data presentation

Appendix 3(I): Vascular Vessel length in normal and pregestational diabetes

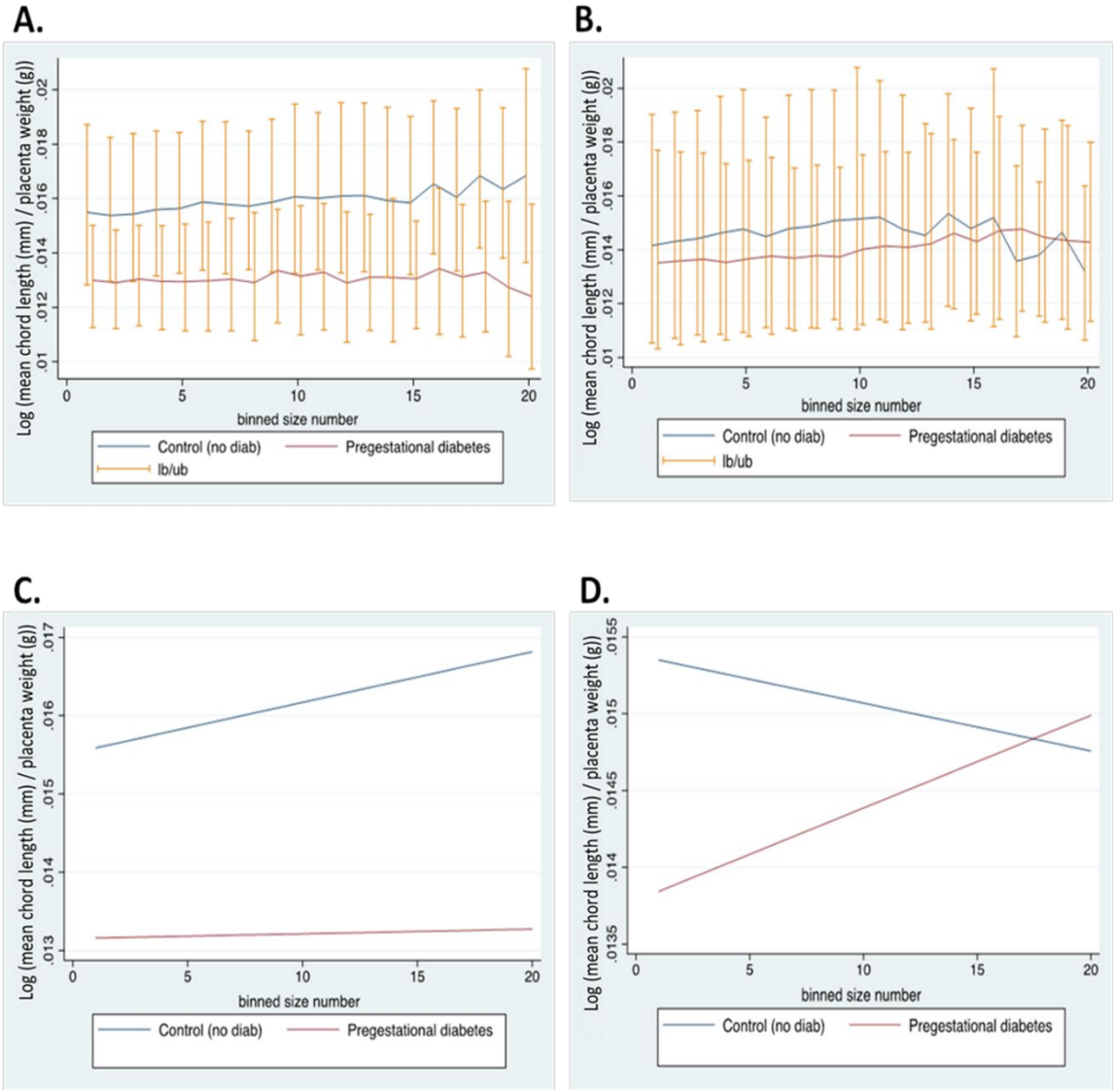

Figure A3.0.1 The length of arteries and veins in normal and pregestational diabetes casts. The mean chord length of vessels segments in arterial and venous placental casts from normal and pregestational diabetes pregnancies. All data are normalised to placental weight. **A (arterial,** p ≤0.0001 control vs diabetes**) and B (venous,** p=0.026 control vs diabetes**)** represent line graphs of mean chord length placenta weight ratio in binned radius size numbers (150 µm-2000 µm) while **C (arterial) and D (venous)** represent linear prediction smooth graphs of **(A) and (B**) respectively. Data presented as (log) geometric mean ± SD. Control (no diabetes) = 16(9 arterial, 7 venous) and Pregestational diabetes = 33 (16 arterial,17 venous). Mixed effects – ML Regression analysis, $p < 0.05$ was taken as significant.

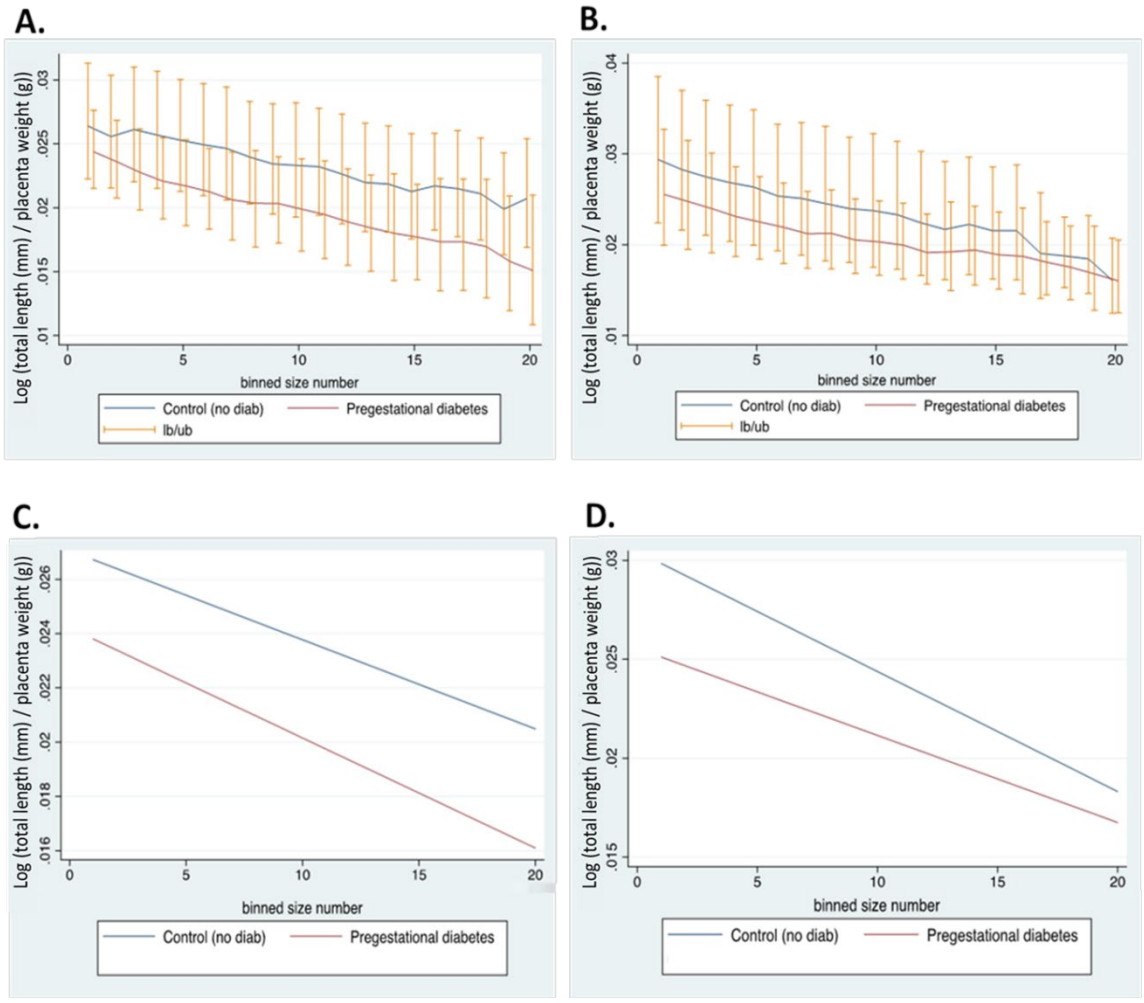

Figure A3.0.2 The total length of arteries and veins in normal and pregestational diabetes casts.

The total length of vessels segments in arterial and venous placental casts from normal and pregestational diabetes pregnancies. All data are normalised to placental weight. **A (arterial,** p ≤0.0001 control vs diabetes**) and B (venous,** p=0.026 control vs diabetes**)** represent line graphs of the total length placenta weight ratio in binned radius size numbers format (150 µm-2000 µm) while **C (arterial) and D (venous)** represent linear prediction smooth graphs of **(A) and (B**) respectively. Data presented as (log) geometric mean ± SD. Control (no diabetes) = 16(9 arterial, 7 venous) and Pregestational diabetes = 33 (16 arterial,17 venous). Mixed effects – ML Regression analysis, $p < 0.05$ was taken as significant.

Appendix 3(II): Vascular volume in normal and pregestational diabetes

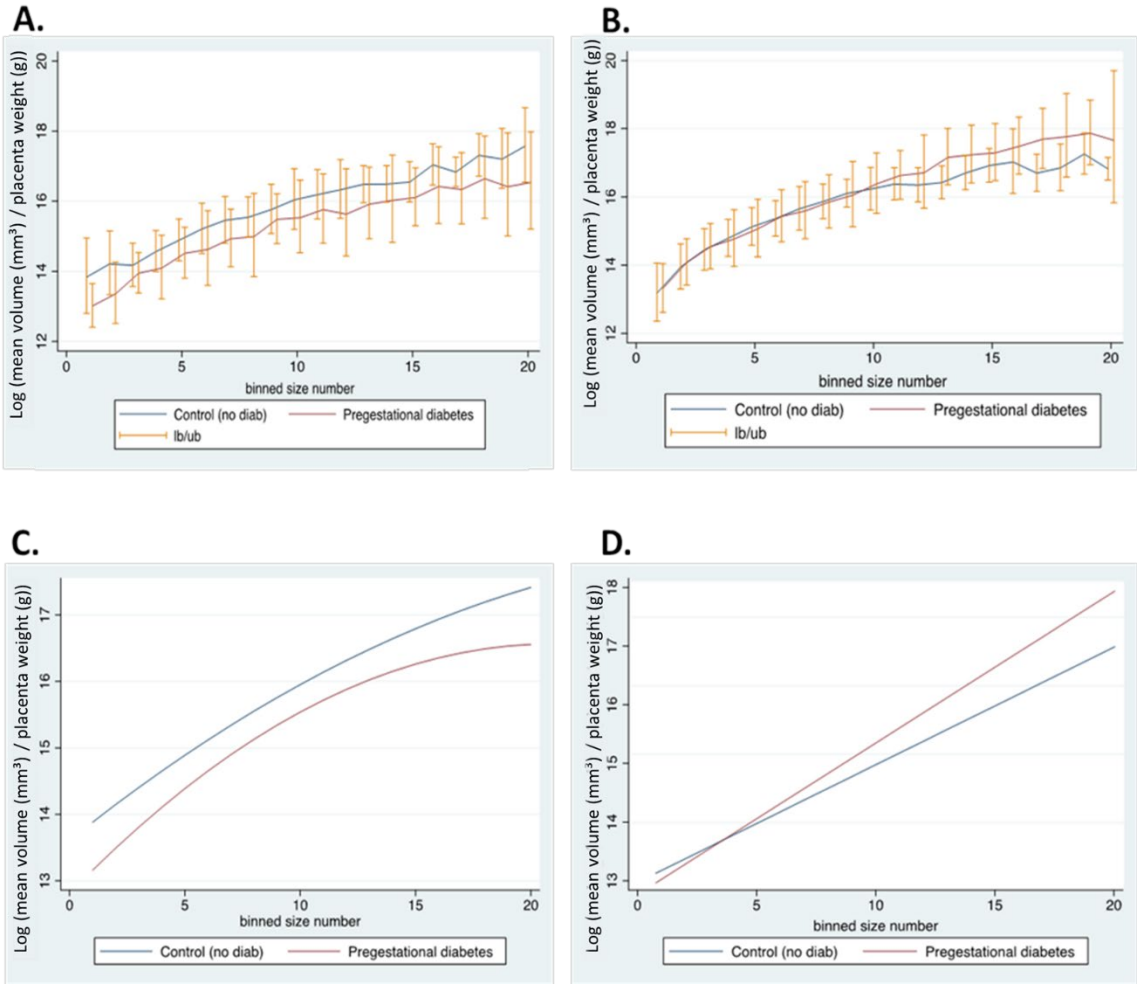

Figure A3.0.3 The mean vascular volume of arteries and veins in normal and pregestational diabetes casts.

The mean measured vascular volume of vessels segments in arterial and venous placental casts from normal and pregestational diabetes pregnancies. All data are normalised to placental weight. **A (arterial,** p=0.004 control vs diabetes**) and B (venous)** represent line graphs of the mean volume placenta weight ratio in binned radius size numbers format (150 µm-2000 µm) while **C (arterial) and D (venous)** represent linear prediction smooth graphs of **(A) and (B**) respectively. Data presented as (log) geometric mean ± SD. Control (no diabetes) = 16(9 arterial,7 venous) and Pregestational diabetes = 33 (16 arterial,17 venous). Mixed effects – ML Regression analysis, $p < 0.05$ was taken as significant.

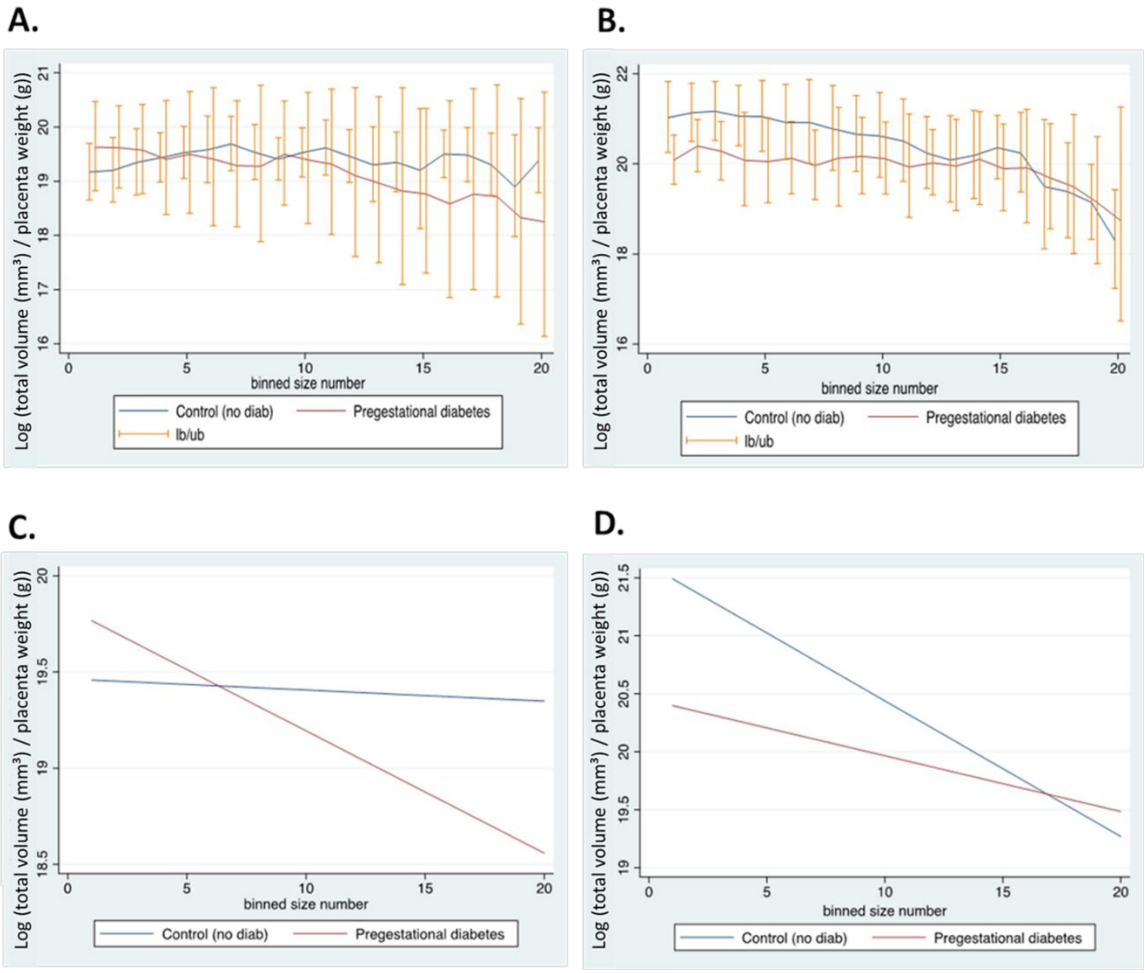

Figure A3.0.4 The total vascular volume of arteries and veins in normal and pregestational diabetes casts.

The total vascular volume of vessels segments in arterial and venous placental casts from normal and pregestational diabetes pregnancies. All data are normalised to placental weight. **A (arterial) and B (venous** p ≤0.0001 control vs diabetes***))*** represent line graphs of the total volume placenta weight ratio in binned radius size numbers format (150 µm-2000 µm) while **C (arterial) and D (venous)** represent linear prediction smooth graphs of **(A) and (B**) respectively. Data presented as (log) geometric mean ± SD. Control (no diabetes) = 16(9 arterial, 7 venous) and Pregestational diabetes = 33 (16 arterial,17 venous). Mixed effects – ML Regression analysis, $p < 0.05$ was taken as significant

Appendix 3(III): Vascular Vessel length in normal and maternal glycaemic control groups in pregestational diabetes

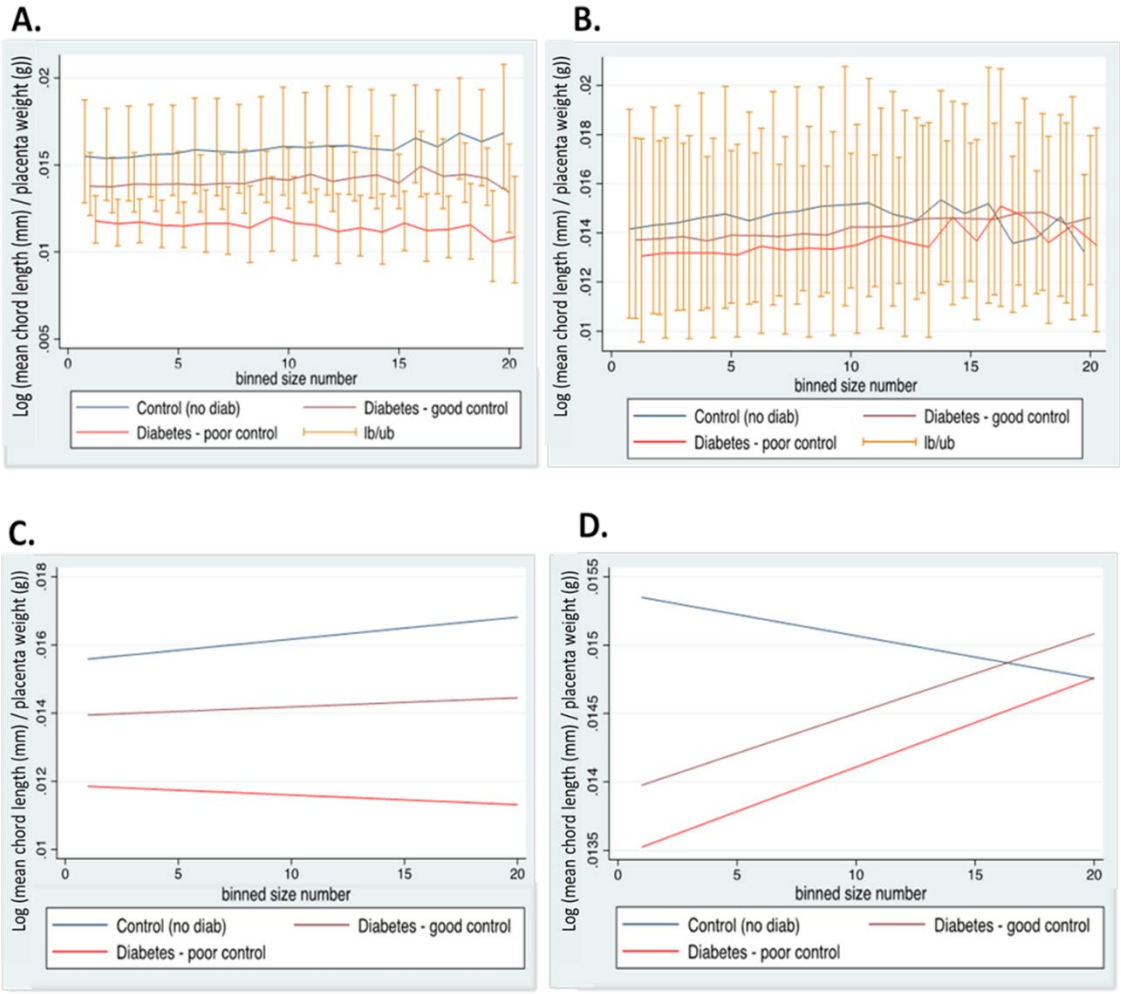

Figure A3.0.5 The length of arteries and veins in normal and maternal glycaemic status groups in pregestational diabetes casts.

The mean chord length of vessels segments in arterial and venous casts of normal and pregestational diabetes categories of glycaemic control over the course of pregnancy. All data are normalised to placental weight. **A (arterial:** control no diab vs Diabetes good control, p≤0.0001, control no diab vs Diabetes poor control, p≤0.0001) **and B (venous:** Control no diab vs Diabetes good control, p=0.05, Control no diab vs Diabetes poor control, p = 0.04**)** represent line graphs of mean chord length placenta weight ratio in binned radius size numbers format (150 µm-2000 µm) while **C (arterial) and D (venous)** represent linear prediction smooth graphs of **(A) and (B**) respectively. Data presented as (log) geometric mean ± SD. Control (no diabetes) = 16(9 arterial, 7 venous and Pregestational diabetes = 33 (16 arterial cast =10 good control ,6 poor control,17 venous casts= 12 good control, 5 poor control). Data presented. Mixed effects – ML Regression analysis, $p < 0.05$ was taken as significant.

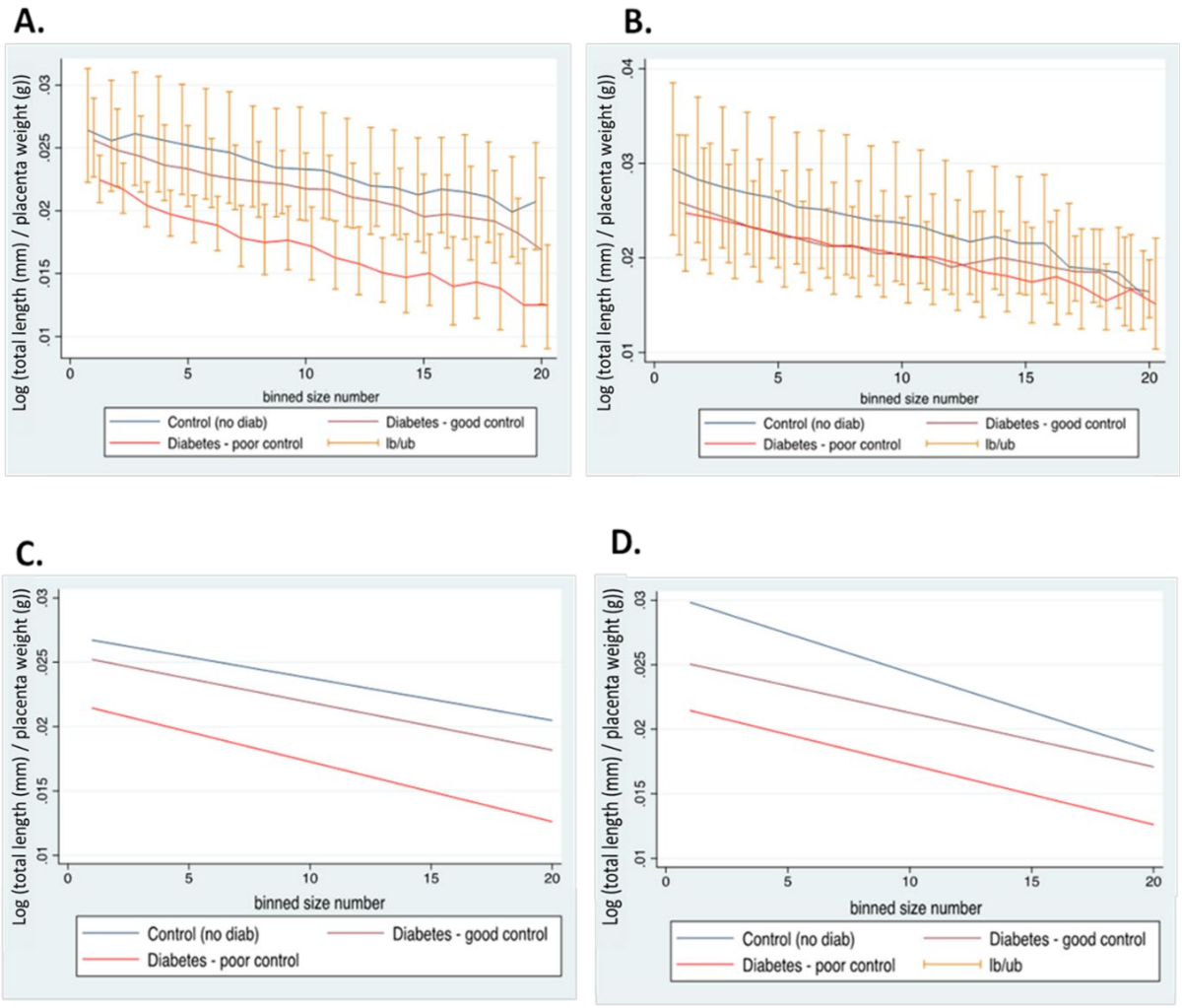

Figure A3.0.6 The total length of arteries and veins in normal and maternal glycaemic status groups in pregestational diabetes casts.

The total length of vessels segments in arterial and venous casts of normal and pregestational diabetes categories of glycaemic control over the course of pregnancy. All data are normalised to placental weight. **A (arterial**: control no diab vs Diabetes good control, p=0.035, control no diab vs Diabetes poor control, p≤0.0001**)** and **B (venous**: Control no diab vs Diabetes good control, p≤0.0001, Control no diab vs Diabetes poor control, p = 0.001**)** represent line graphs of total length placenta weight ratio in binned radius size numbers format (150 µm-2000 µm) while **C (arterial) and D (venous)** represent linear prediction smooth graphs of **(A) and (B**) respectively. Data presented as (log) geometric mean ± SD. Control (no diabetes) = 16(9 arterial, 7 venous and Pregestational diabetes = 33 (16 arterial cast =10 good control ,6 poor control) (17 venous casts= 12 good control, 5 poor control). Data presented. Mixed effects – ML Regression analysis, $p < 0.05$ was taken as significant.

Appendix 3(IV): Vascular volume in normal and maternal glycaemic control groups in pregestational diabetes

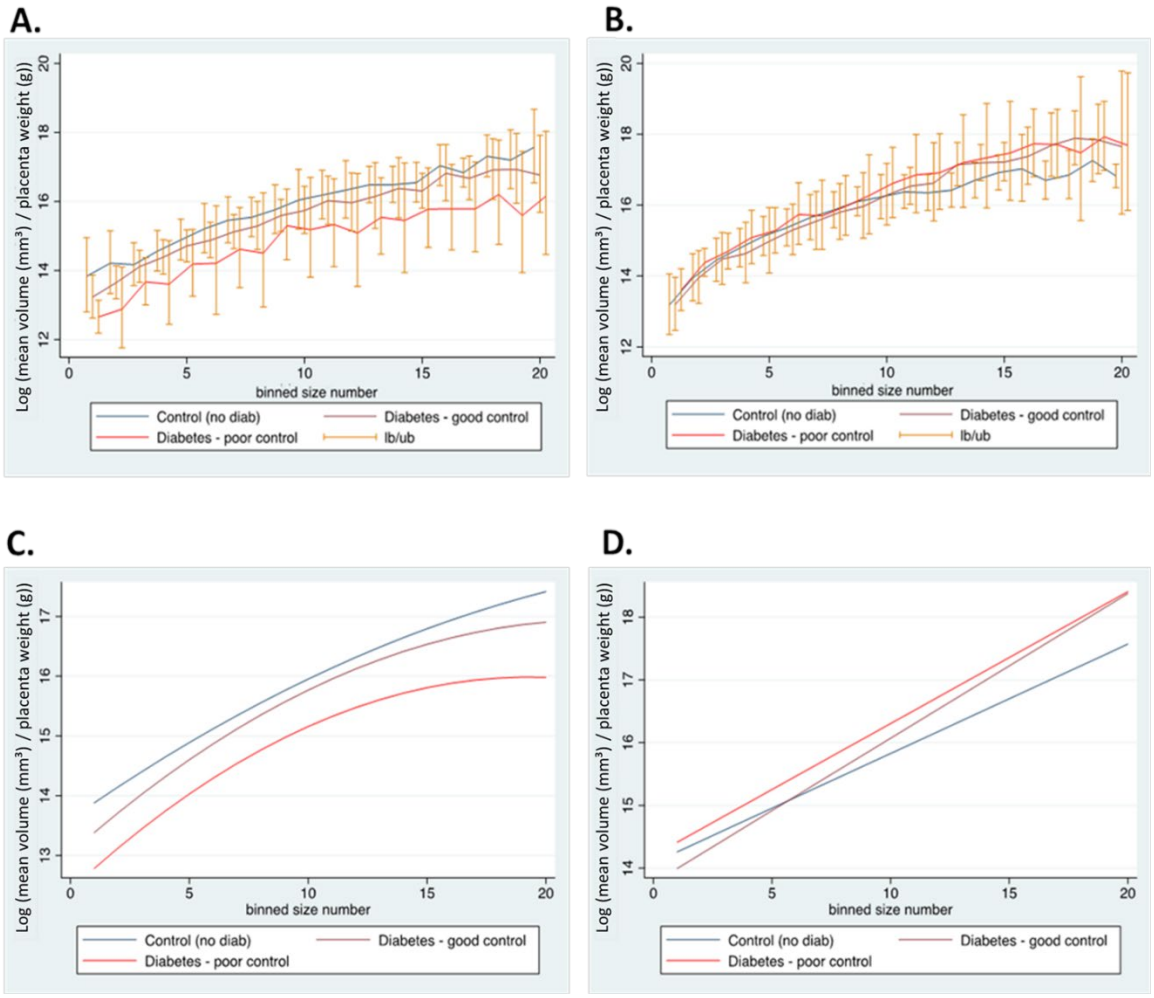

Figure A3.0.7 The mean vascular volume of arteries and veins in normal and maternal glycaemic status groups in pregestational diabetes casts.

The mean measured vascular volume of vessels segments in arterial and venous casts of normal and pregestational diabetes categories of glycaemic control over the course of pregnancy. All data are normalised to placental weight. **A (arterial**: control no diab vs Diabetes good control, p=0.049, control no diab vs Diabetes poor control, p≤0.0001**)** and **B (venous)** represent line graphs of mean volume placenta weight ratio in binned radius size numbers format (150 µm-2000 µm) while **C(arterial) and D(venous)** represent linear prediction smooth graphs of **(A) and (B**) respectively. Data presented as (log) geometric mean ± SD. Control (no diabetes) = 16(9 arterial, 7 venous and Pregestational diabetes = 33 (16 arterial cast =10 good control ,6 poor control) (17 venous casts= 12 good control, 5 poor control). Data presented. Mixed effects – ML Regression analysis, $p < 0.05$ was taken as significant.

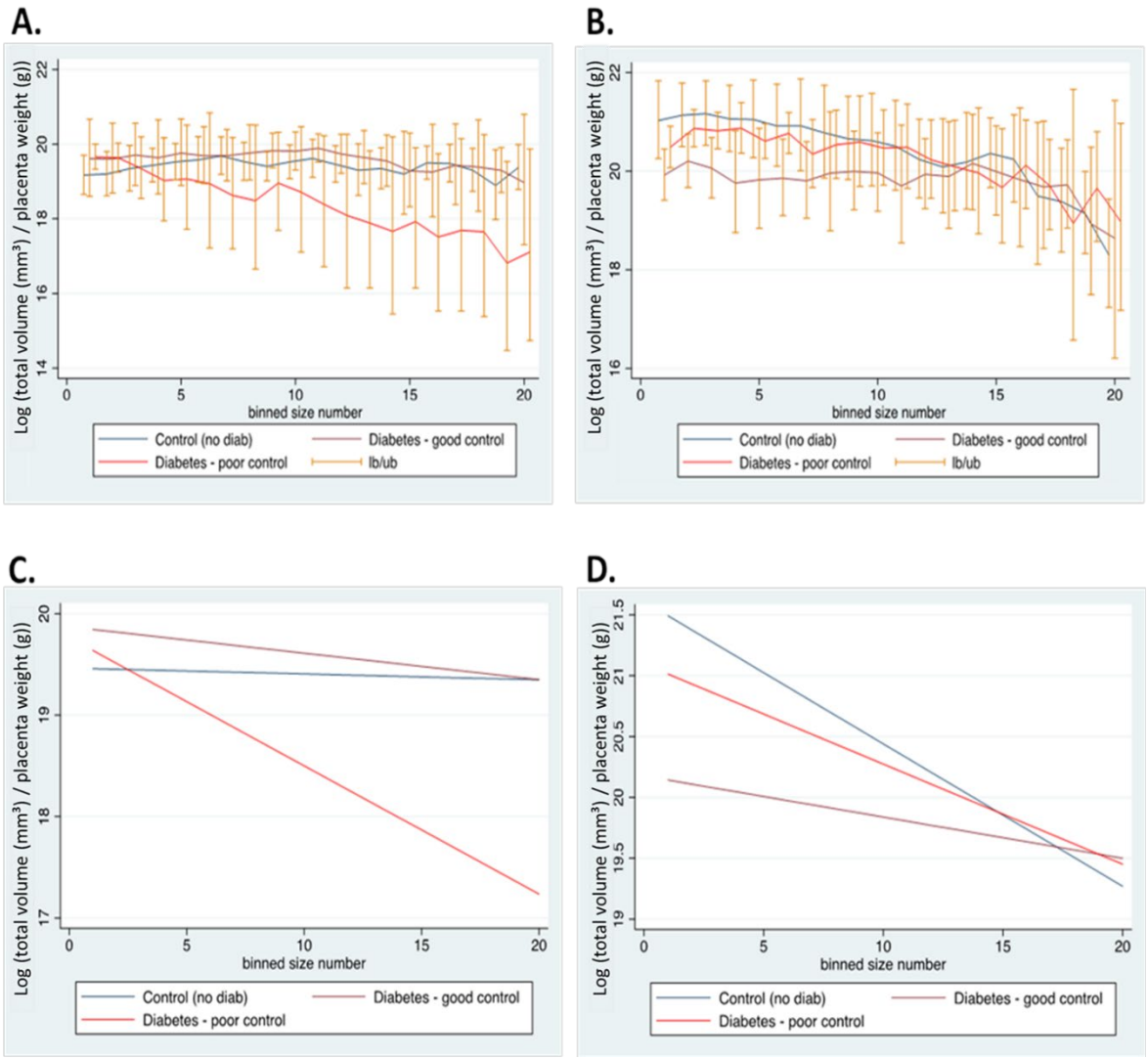

Figure A3.0.8 The total vascular volume of arteries and veins in normal and maternal glycaemic status groups in pregestational diabetes casts.

The total vascular volume of vessel segments in arterial and venous casts of normal and pregestational diabetes categories of glycaemic control over the course of pregnancy. All data are normalised to placental weight. **A (arterial)** and **B (venous**: Control no diab vs Diabetes good control, p≤0.0001, Control no diab vs Diabetes poor control, p = 0.05**)** represent linear prediction smooth graphs of **(A) and (B**) respectively. Data presented as (log) geometric mean ± SD. Control (no diabetes) = 16(9 arterial, 7 venous and Pregestational diabetes = 33 (16 arterial cast =10 good control ,6 poor control) (17 venous casts= 12 good control, 5 poor control). Data presented. Mixed effects – ML Regression analysis, $p < 0.05$ was taken as significant

Appendix 3(V): Vascular vessel length in PIGF profile groups in pregestational diabetes

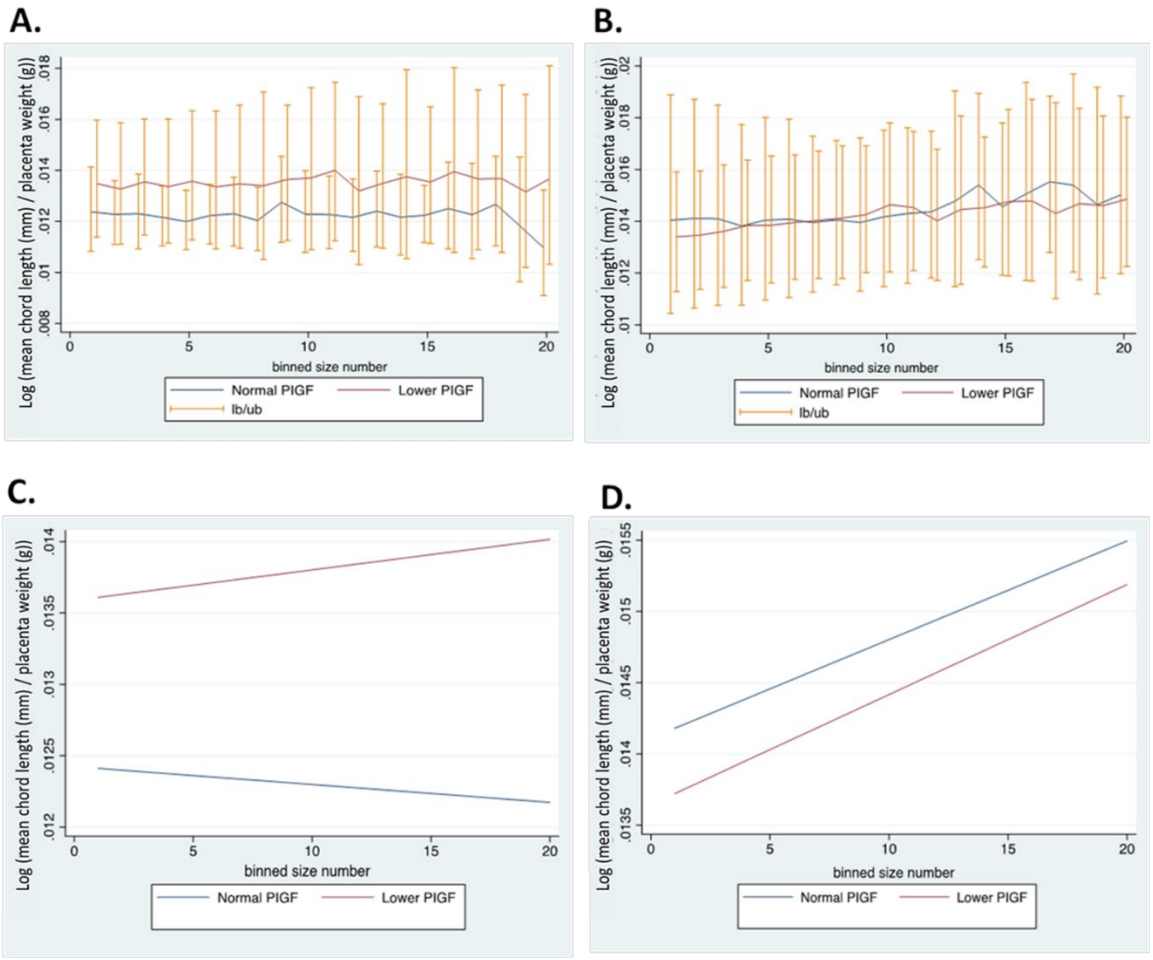

Figure A3.0.9 The length of arteries and veins in maternal PIGF profile groups in pregestational diabetes casts.

The mean chord length of vessel segments in arterial and venous casts of normal and lower PIGF groups in pregestational diabetes**.** All data are normalised to placental weight. **A (arterial:** Normal PlGF vs Lower PlGF p=0.026**) and B (venous)** represent line graphs of mean chord length placenta weight ratio in binned radius size numbers format (150 µm-2000 µm) while **C(arterial) and D(venous)** represent linear prediction smooth graphs of **(A) and (B**) respectively. Data represented as (log) geometric mean ± SD, Normal PIGF group = (7 arterial, 9 venous) casts and Lower PIGF group (7 arterial,5 venous) casts. Mixed effects – ML Regression analysis, $p < 0.05$ was taken as significant

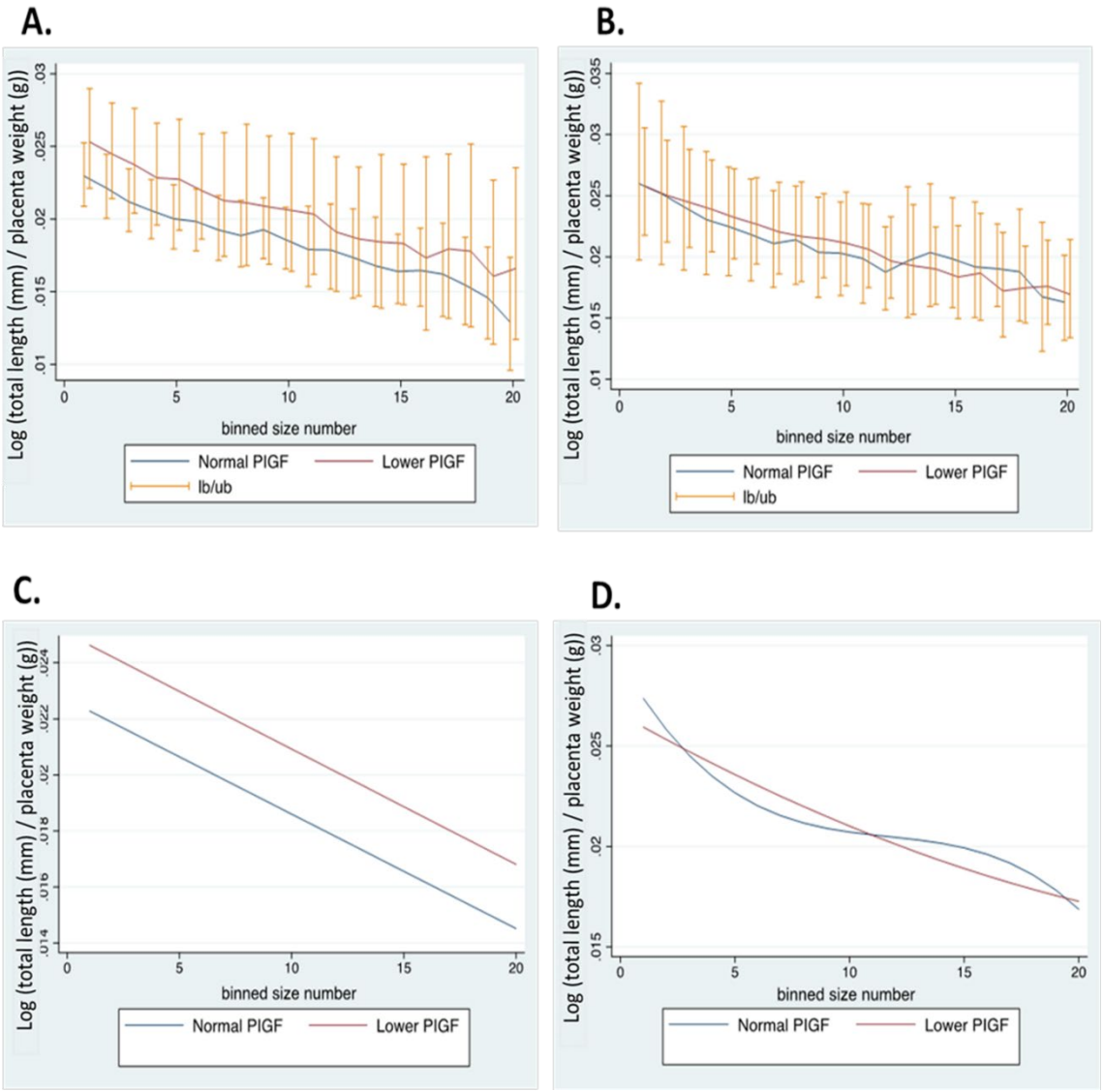

Figure A3.0.10 The total length of arteries and veins in maternal PIGF profile groups in pregestational diabetes casts.

The total length of vessels segments in arterial and venous casts of normal and lower PIGF groups in pregestational diabetes**.** All data are normalised to placental weight. **A (arterial:** Normal PlGF vs Lower PlGF p=0.004**) and B (venous)** represent line graphs of total length placenta weight ratio in binned radius size numbers format (150 µm-2000 µm) while **C (arterial) and D (venous)** represent linear prediction smooth graphs of **(A) and (B**) respectively. Data represented as (log) geometric mean ± SD, Normal PIGF group = (7 arterial, 9 venous) casts and Lower PIGF group (7 arterial,5 venous) casts. Mixed effects – ML Regression analysis, $p < 0.05$ was taken as significant.

Appendix 3(VI): Vascular volume in PIGF profile groups in pregestational diabetes

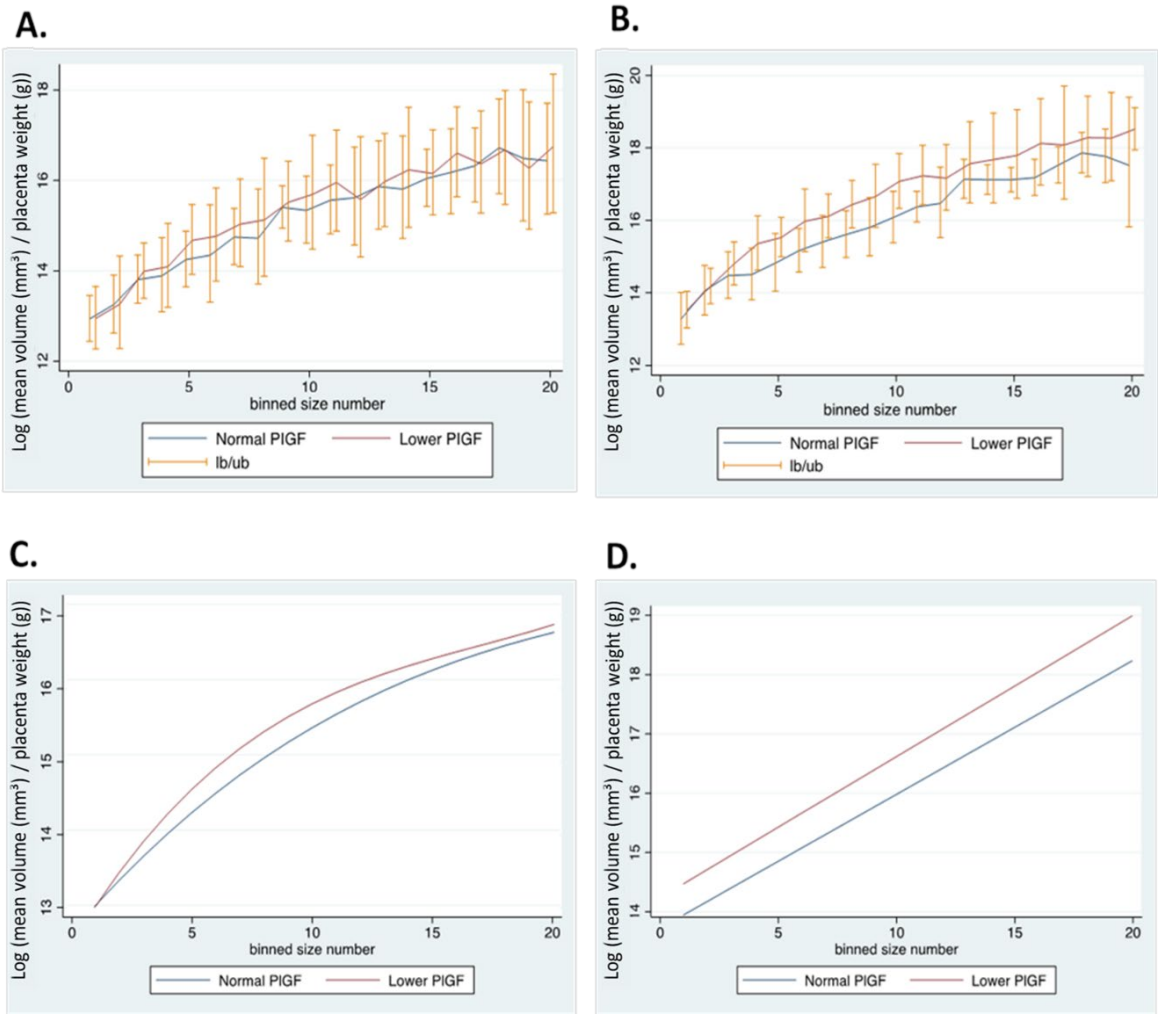

Figure A3.0.11 The mean vascular volume of arteries and veins in maternal PIGF profile groups in pregestational diabetes casts.

The mean vascular volume of vessel segments in arterial and venous casts of normal and lower PIGF groups in pregestational diabetes**.** All data are normalised to placental weight. **A (arterial) and B (venous**: Normal PlGF vs Lower PlGF p=0.024**)** represent line graphs of mean volume placenta weight ratio in binned radius size numbers format (150 µm-2000 µm) while **C(arterial) and D(venous)** represent linear prediction smooth graphs of **(A) and (B**) respectively. Data represented as (log) geometric mean ± SD, Normal PIGF group = (7 arterials, 9 venous) casts and Lower PIGF group (7 arterial,5 venous) casts. Mixed effects – ML Regression analysis, $p < 0.05$ was taken as significant.

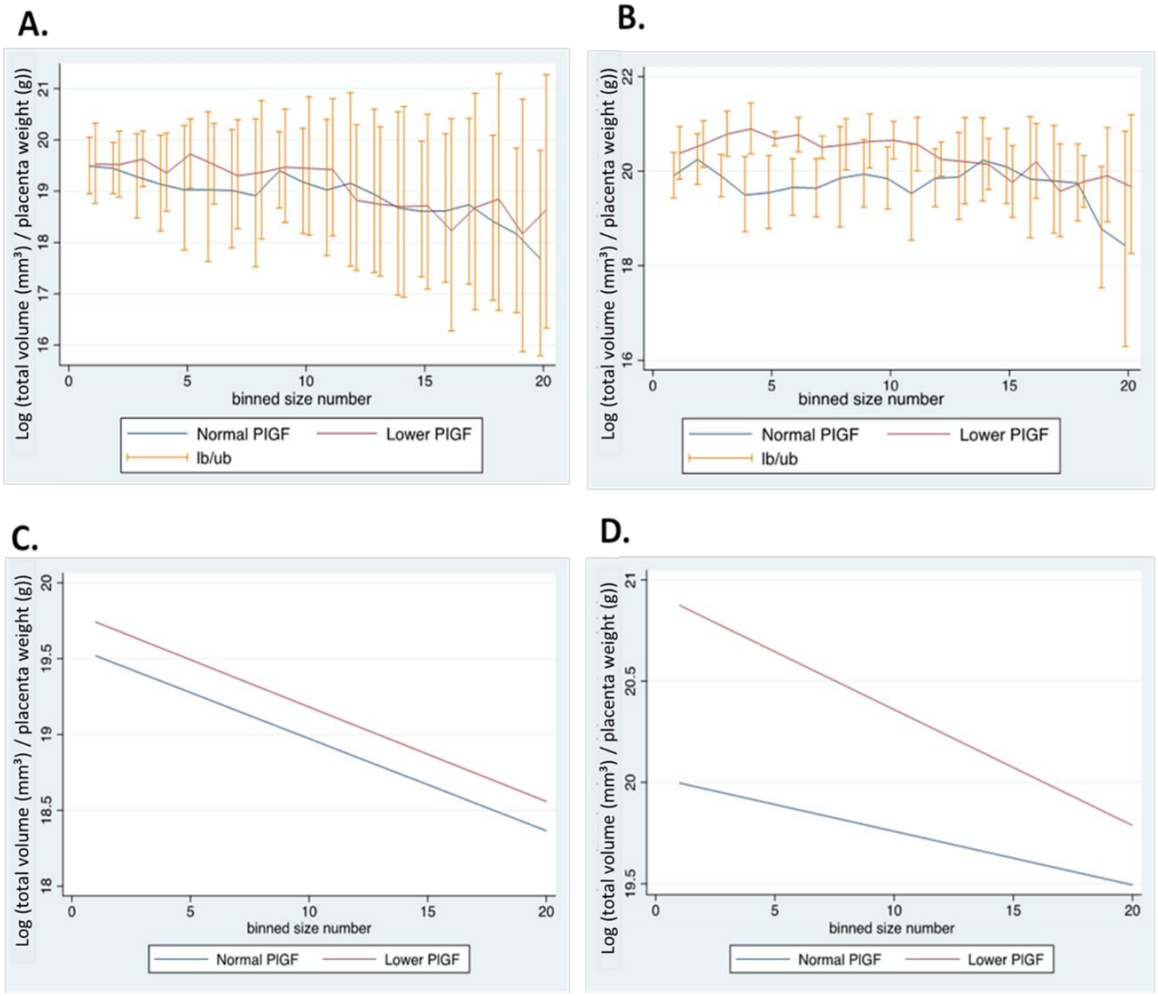

Figure A3.0.12 The total vascular volume of arteries and veins in maternal PIGF profile groups in pregestational diabetes casts.

The total vascular volume of vessel segments in arterial and venous casts of normal and lower PIGF groups in pregestational diabetes**.** All data are normalised to placental weight. **A(arterial) and B (venous**: Normal PlGF vs Lower PlGF p=0.001**)** represent line graphs of total volume placenta weight ratio in binned radius size numbers format (150 µm-2000 µm) while **C(arterial) and D(venous)** represent linear prediction smooth graphs of **(A) and (B**) respectively. Data represented as (log) geometric mean ± SD, Normal PIGF group = (7 arterials, 9 venous) casts and Lower PIGF group (7 arterials,5 venous) casts. Mixed effects – ML Regression analysis, $p < 0.05$ was taken as significant.

Appendix 3(VII): Measured vascular volume and Uterine artery Doppler measurements in pregestational diabetes

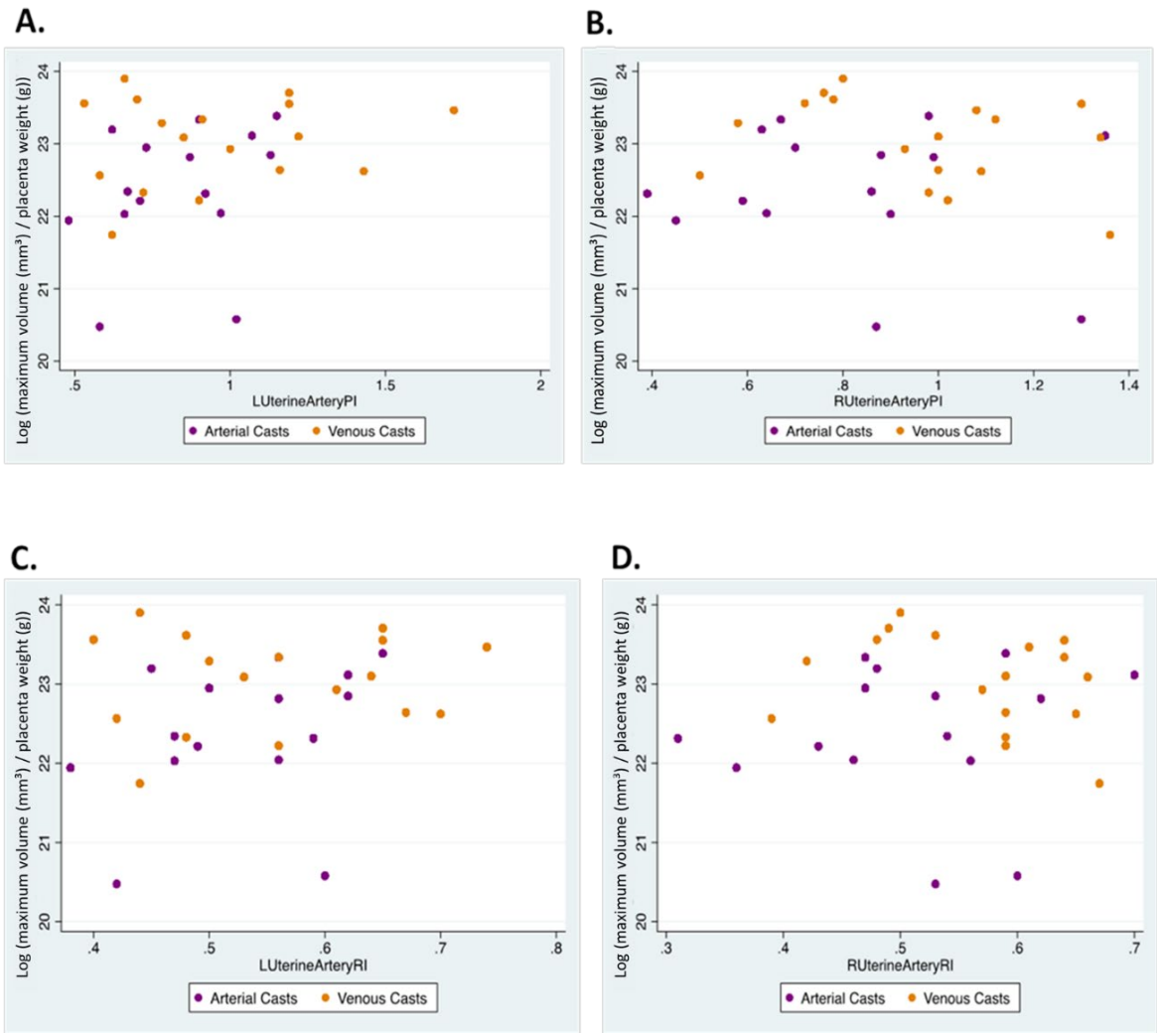

Figure A3.0.13 The distribution of measured maximum vascular volume per placenta weight ratio of venous and arterial placental casts with Uterine Doppler measurements from Pregestational diabetes pregnancies.

(A) logged maximum vascular volume placenta weight ratio against left uterine artery pulsatility index. **(B)** logged maximum vascular volume placenta weight ratio against right uterine artery pulsatility index at term. **(C)** logged maximum vascular volume placenta weight ratio against left uterine artery resistance index. **(D)** logged maximum vascular volume placenta weight ratio against right uterine artery resistance index. Data represented as scatter plots n = 33 Pregestational diabetes (16 arterial,17 venous).

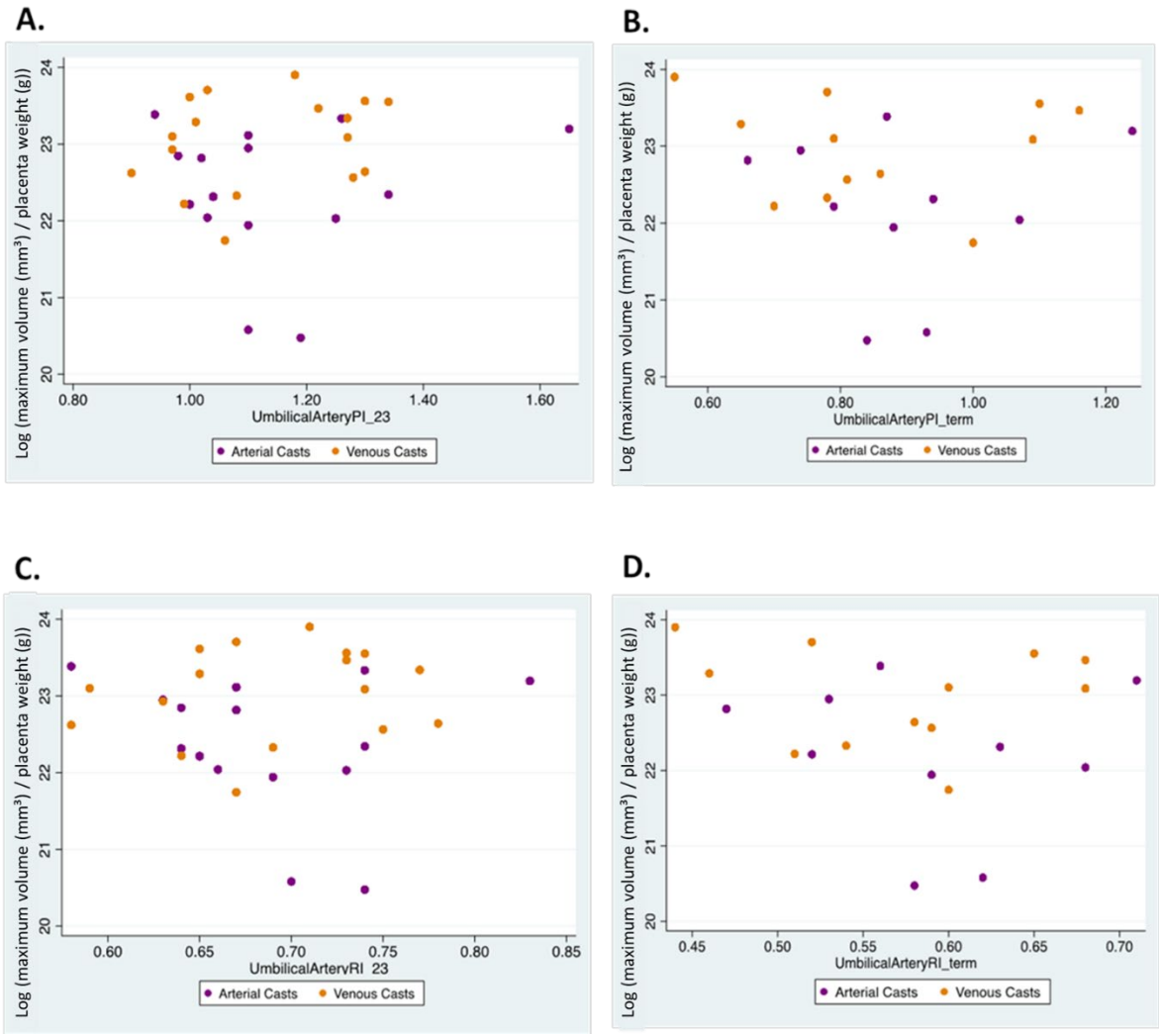

Figure A3.0.14 The distribution of measured maximum vascular volume per placenta weight ratio of venous and arterial placental casts with Umbilical Doppler measurements from pregestational diabetes pregnancies.

(A) logged maximum vascular volume placenta weight ratio against umbilical artery pulsatility index at 23 weeks. **(B)** logged maximum vascular volume placenta weight ratio against umbilical artery pulsatility index at term. **(C)** logged maximum vascular volume placenta weight ratio against umbilical artery resistance index at 23 weeks. **(D)** logged maximum vascular volume placenta weight ratio against umbilical artery resistance index at term. Data represented as scatter plots n = 33 Pregestational diabetes (16 arterial,17 venous)

Appendix 4(I): Angiogenesis Analyzer Protocol (Carpentier ,2012 Image J Plugin)

Angiogenesis Assay Analysis

The Angiogenesis Analyzer plugin on image J allows analysis of cellular networks. This detects and analyses the pseudo vascular organisation of endothelial cells cultured in gel medium. In suitable culture conditions these cells form structures that can branch and mimic a pseudo capillary in vitro formation. At later stage this differentiation can lead to a meshed network from different mesh sizes. Although widely used, the interpretation of this assay still remains a problem, especially to obtain a **quantitative evaluation** of the vessels-like net organisation. The Angiogenesis Analyzer is a simple tool to quantify the experiment images by extracting characteristic information of the network.

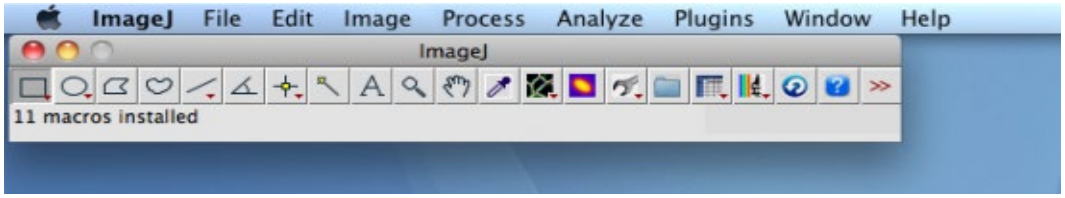

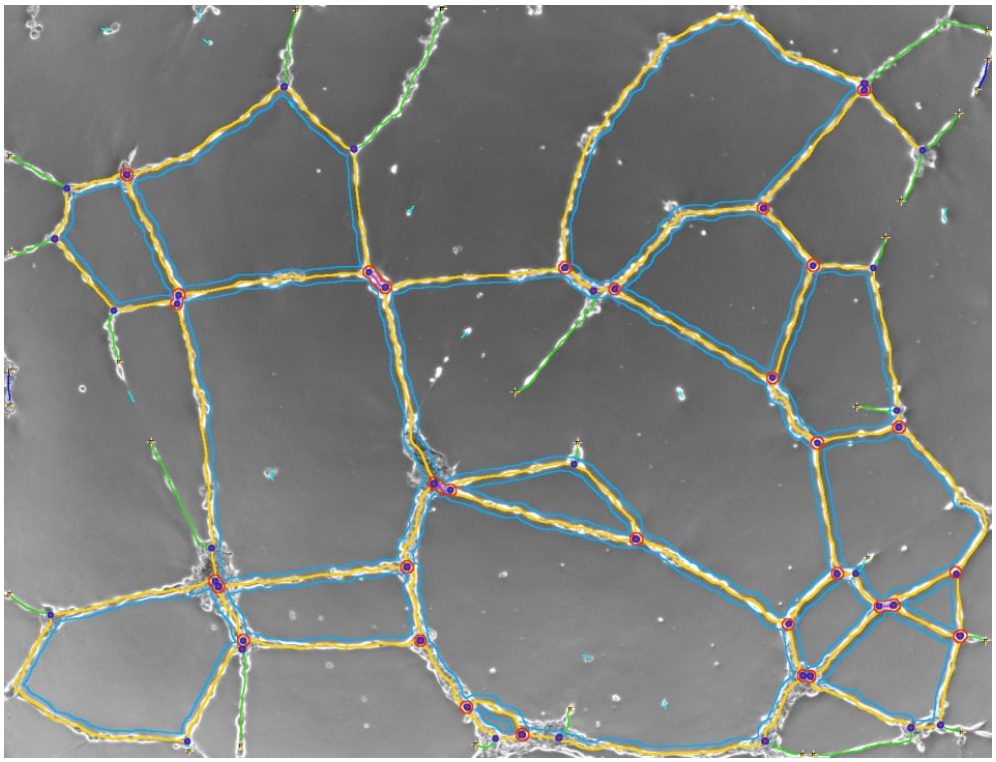

Above: phase contrast image of HUVEC network, analysed by the ***Angiogenesis Analyzer*** for ImageJ.

Network Analysis Menu Tool:

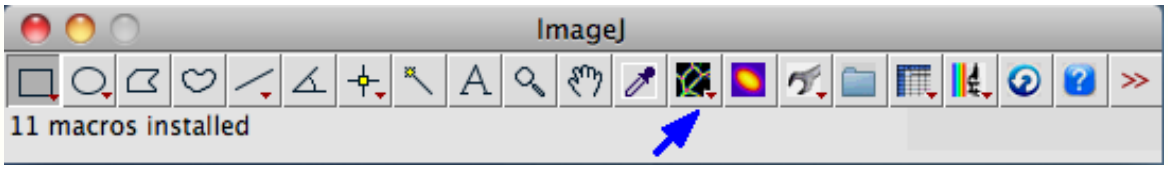

- "**Analyze HUVEC Phase Contrast**" and "**Analyze HUVEC Fluo**" functions, allow the network analysis organisation of individual HUVEC images taken in phase contrast or in fluorescence. The phase contrast images have to be encoded in RGB colour 24 bits and fluorescence images in 8 or 16 bits.

This menu tool regroups several functions and settings to tune the analysis parameters.

1. **Find a Tree:** return a binary skeleton (or tree) of a natural HUVEC image acquired in phase contrast or fluorescence.
2. **Find & Remove Loops:** removes the artifactual loops in a binary tree image on the criteria of the size
3. **"Find Extremities:** detects the extremities in a binary tree. It returns results as overlays and binary map.
4. **Find Nodes and Junctions:** detects nodes (pixels with 3 neighbours) as a circular dot and junctions, which correspond to nodes or group of fusing nodes.
5. **Find Nodes and Branches:** Performs the same of the two precedent functions (detects extremities, nodes and junctions) plus other elements of the ramification:
6. **segments;** elements delimited by two junctions.
7. **branches**; elements delimited by a junction and one extremity.
8. **twigs**; a twig is a branch whose size is lower than a user defined threshold value.
9. **isolated elements** are binary lines which are not branched.
10. **Record the Steps of Limbing** record in a dedicated repertory, the results of every iteration required to get an analysis corresponding to a limbing, including master segments, master junctions and meshes detection.
11. **Master segments** consist in pieces of tree delimited by two junctions none exclusively implicated with one branch, called master junctions.
12. **Master junctions** are junctions linking at least three master segments. Occasionally, two close master junctions can be fused into unique master junction.
13. **Meshes:** are areas enclosed by segments or master segments.

Appendix 4(II): Angiogenesis Pilot Experiments Results

Establishing *in vitro* optimum seeding density and exposure time of endothelial cells

In order to investigate the optimum seeding density and time for formation of endothelial cell network, images of the HUVEC cells seeded at two different densities 15,000 cells/well and 20,000 cells/well were taken at 3 different time points (12hrs, 18hrs, 24 hrs). Although cellular network formation started as early as after 6h, the optimum time point for establishing a defined cellular network was at 18 hrs as shown (**Figure A.4.*0.15***) in both seeding densities. The cells formed in a network around a colony of cells in the middle of the Matrigel. After 24hrs the cellular network formation was not as defined with an appearance of regression of the branches into colonies of cells.

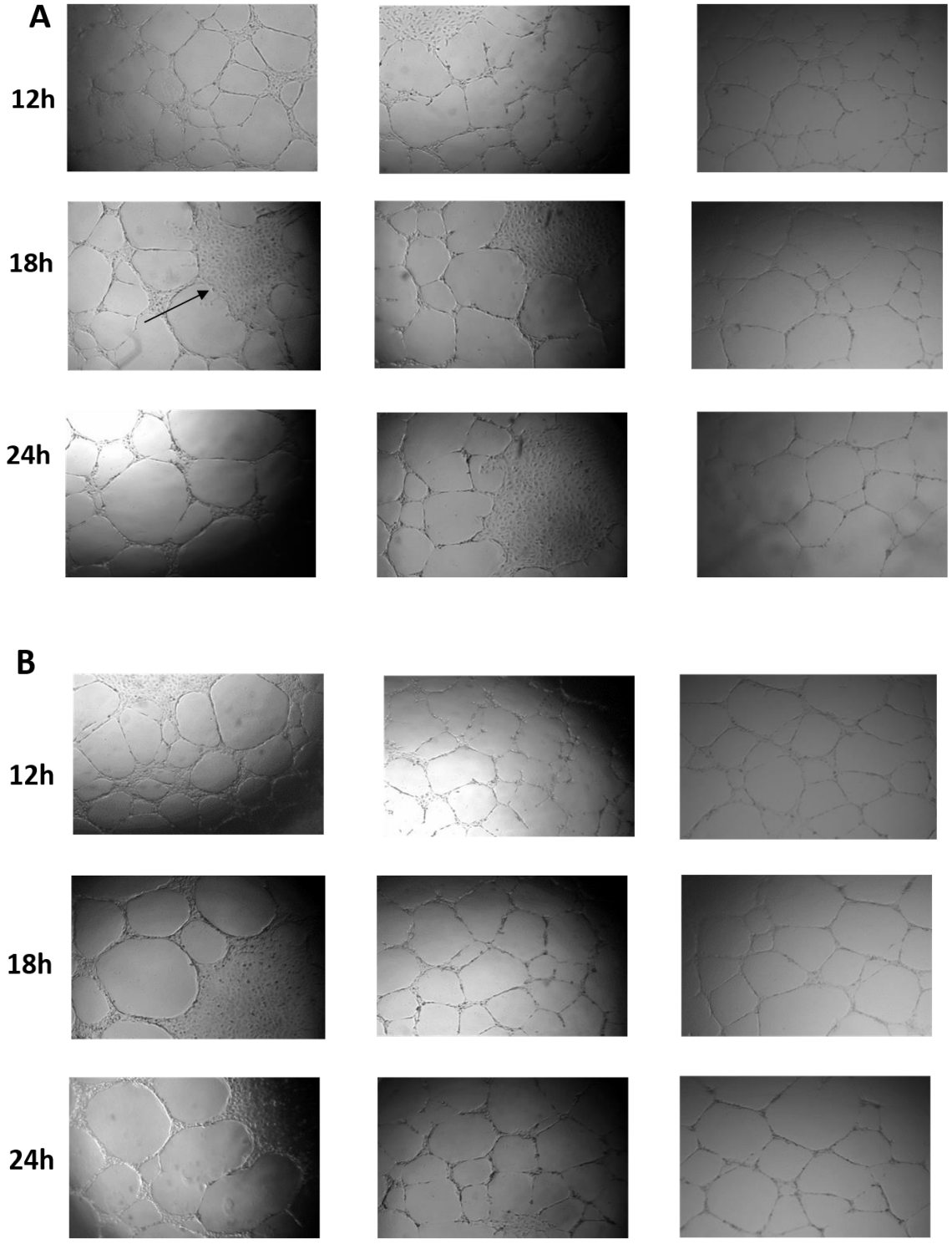

Figure A.4.0.15 Seeding densities of HUVECs on basement membrane substrate
Representative images of Human umbilical vein endothelial cell (HUVEC) cellular network formation on a basement membrane substrate after 12h, 18h and 24 h from 6 different experiments. (A)Cells were seeded at 20,000 cells/well with no VEGF. Black arrows show colony of cells. (B) Representative Human umbilical vein endothelial cell (HUVEC) cellular network formation on a basement membrane substrate after 12h, 18h and 24 h in 6 different experiments. Cells were seeded at 15,000 cells/well with no VEGF. Images under a light microscope (Olympus BX41) at 4× objective

Establishing *in vitro* optimum seeding density and effects of angiogenic factor VEGF on endothelial cells behaviour

To compare the effects of cell density and VEGF on cellular network formation of the HUVEC cells, the cells were seeded at two different densities 15,000 cells/well and 20,000 cells/well with two concentrations of VEGF (Low VEGF = high VEGF 1 in 67 dilution and High VEGF = 6.67ng/ml) and a control. After 18 h cellular network formation could be observed in control cells with no VEGF however low VEGF resulted in sparse formation of cellular networks. On the other hand, high VEGF seemed to promote proliferation of cells as marked by increase in colonies in the cellular network on the matrigel. The differences between 15,000 and 20,000 cells/well densities were less marked on the formation of cellular networks, however in the 20,000cells/well experiments there were more appearances of colonies forming on the matrigel and sparse network formation in wells with low VEGF concentration added as observed in Figure **A4.0.16**

In conclusion, the optimum time point for cellular network formation identified from the experiments was after 18h and the chosen optimum seeding density was 15, 000 cells/well which reflects densities used in published literature.

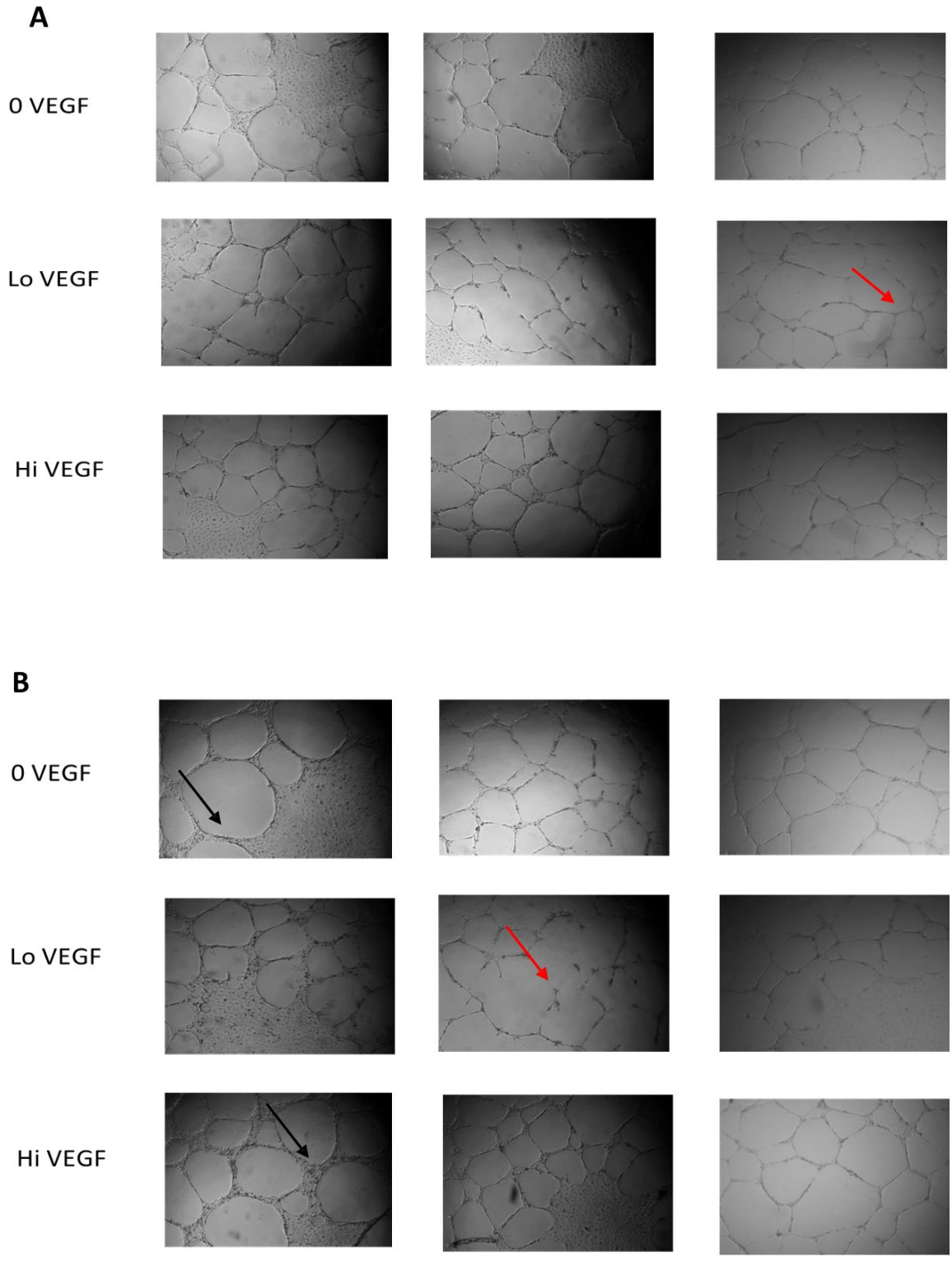

Figure A4.0.16 *In vitro* effects of VEGF concentrations on HUVECs

Representative images of Human umbilical vein endothelial cell (HUVEC) cellular network formation on a basement membrane substrate after 18hrs in 6 different experiments. (A) Cells were seeded at 15,000 cells/well.0 VEGF = Normal control, Low VEGF = (high VEGF 1 in 67 dilution), High VEGF = 6.67ng/ml.(B) Representative Human umbilical vein endothelial cell (HUVEC) cellular network formation on a basement membrane substrate after 18h in 3 different experiments. Cells were seeded at 20,000 cells/well.0 VEGF = Normal control, Low

VEGF=(high VEGF 1 in 67 dilution), High VEGF = 6.67ng/ml. Red arrows show areas of sparse network with no cellular structure formation. Black arrows indicate colonies of cells within the formed cellular networks. Images under a light microscope (Olympus BX41) at 4× objective